THE EFFECTS OF WAVE GROUPING ON THE SLOW DRIFT OSCILLATIONS OF FLOATING MOORED STRUCTURES

JOHN J. MURRAY

THE EFFECTS OF WAVE GROUPING ON THE SLOW DRIFT OSCILLATIONS OF FLOATING MOORED STRUCTURES

BY

JOHN J. MURRAY

A Thesis Submitted in Partial Fullfillment of the
Requirements for the Degree
Doctor of Philosophy
In the Faculty of Engineering and Applied Science
Memorial University of Newfoundland

December 1984

TABLE OF CONTENTS

ACKNOWLEDGEMENT

The author wishes to express his gratitude to Dr. D.B. Muggeridge for his guidance and encouragement during this study. The valuable comments and advice of Dr. M. Booton and Dr. A. Zielinski are also acknowledged.

This study would not have been possible without the financial assistance of a C-CORE Fellowship. Additional funds provided by the Faculty of Engineering and Applied Science arranged by the Dean, Dr. G.R. Peters and his predecessor, Mr. C. diCenzo, are also gratefully acknowledged.

The facility used in the experimental portion of this study was funded by NSERC Grants A4885, A0561 and A4885.

Finally the author would like to sincerely thank Mr. N.E. Jeffrey, Director of The Institute of Marine Dynamics, for the opportunity to complete the work through a Research Associateship at the Institute.

LIST OF FIGURES

LIST OF TABLES

ABSTRACT

An original combined analytical and experimental study of the effects of wave grouping on the slow drift oscillations of floating moored structures has been presented. The work constitutes the first incorporation of existing techniques of simulating wave groups and the slow oscillating response of a moored model of a rectangular barge. The analytical model assumes that each pair of frequencies in a discrete wave spectrum will give rise to a regular wave group. Each of these regular wave groups will produce a low frequency force that is proportional to the product of the wave amplitudes in the group and varies at a frequency equal to the difference in the frequency pair. Furthermore, this low frequency force is related to a modified SIWEH of the regular wave group by a constant phase angle. Therefore the resultant force is determined by superposition of these regular slow-varying forces. Subsequently the ensuing slow oscillating motions can be established and related to the SIWEH spectrum. This relation is expressed in the form of a transfer function. The analytical model is then evaluated by means of a set of detailed experimental tests conducted on a rectangular barge. A JONSWAP spectrum was modelled for a range of grouping characteristics and the results compared to the analytical model. Results indicate that the slow drift motions are highly influenced by free motion effects. An empirical transfer function which included these free motion effects produced good agreement between subsequent predicted and measured slow drift responses. The technique developed in this study shows that the second-order response to linear waves can be related to the wave envelope when the effects of these linear waves are dominant.

NOMENCLATURE

a	incident amplitude
a_r	amplitude of radiated wave
b	damping coefficient
c	restoring coefficient
f	frequency (Hz)
f_b	base frequency
f_e	average wave frequency
f_o	natural frequency
f_{HF}	high frequency cut-off
f_{LF}	low frequency cut-off
g	gravity
h	water depth
$h(\tau)$	impulse response
$\bar{j}_1$	average number of waves in a group
k	wave number, $2\pi/\lambda$
ℓ_1	mean length of wave group
m_a	total mass
m_o	zeroth moment
$m_{\varepsilon o}$	zeroth moment of the SIWEH spectral density
m_2	second moment
m_4	fourth moment
$\bar{n}_1(\ell)$	directional cosine in the longitudinal direction
p_T	total pressure
$p^{(1)}$	first-order pressure term
$p^{(2)}$	second-order pressure term
pr	probability
$pr(H_c)$	probability of exceedence of H_c

u	total velocity
$\bar{u}$	velocity vector (u,v,w)
$u^{(1)}$	first-order velocity
$u^{(2)}$	second-order velocity
v	velocity component
v_r	radial velocity
v_θ	tangential velocity
z	vertical coordinate axis
A_m	complex wave amplitude
B	vessel beam
C_B	block coefficient
D	vessel draft
$\bar{E}$	average value of E(t)
$E(t)$	Smoothed Instantaneous Wave Energy History
F	scaling factor
$\bar{F}_D$	steady drift force
$\bar{F}_m$	mean drift force
$\bar{F}_x$	steady drift force in surge direction
$\bar{F}_y$	steady drift frce in sway direction
F_{dd}	amplitude of slow oscillating drift component
F_{nm}	second-order force transfer function
$F^{(1)}(t)$	first-order force
$F^{(2)}(t)$	second-order force
GF	groupiness factor
G_{nm}	transfer function relating first-order profile to second-order profile
$H(\theta)$	Kochin function
$H_{1/3}$	significant wave height

L	vessel length
$P(h_o)$	probability density function for the value h_o
P_o	mean position of P linked to body surfaces
P	pressure
P_{nm}	real part of low frequency force
Q_1	window filter
Q_{nm}	imaginary part of low frequency force
R_e	real part of complex expression
$R(\omega)$	steady drift coefficient
SIWEH	Smoothed Instantaneous Wave Energy History
$SIWEH_m$	modified SIWEH
S_o	amplitude of sway motion
$S_F(\mu)$	spectrum of slow-drift force
$S_R(\mu)$	spectrum of low frequency response
$S(f)$	wave energy spectrum
T	wave period
T_n	natural period (sec)
T_g	average period of a wave in a group
T_o	length of a finite wave record
T_p	peak period of spectra
T_R	record period to wave group
V_g	variance of a group
V_R	variance of a sample record
W_o	amplitude of heave
$\forall$	volume
$\times$	cross product

ε	phase angle
$\zeta_a(t)$	wave profile
ζ	damping ratio
$\zeta^{(1)}$	first-order free surface term
$\zeta^{(2)}$	second-order free surface term
λ	wave length
ρ	mass density
$\tau(h_o)$	average time duration a wave height stays above a level h_o
τ	lag time (sec)
∇	Del operator
$\phi(t)$	correlation function
ϕ	wave velocity potential
ϕ_B	complex body potential including diffraction and radiation
ϕ_o	incident wave potential
$\phi^{(1)}$	first-order velocity potential
$\phi^{(2)}$	second-order velocity potential
ω	radian frequency
ω_n	radian frequency of wave component n
$\llcorner$	phase angle

CHAPTER 1

INTRODUCTION

The increase in offshore activities which require support from large moored or dynamically positioned structures, has prompted a need for an acute understanding of the physical phenomena related to the mooring of large vessels in open sea conditions. Situations will be further complicated with attempts by the offshore industry to extend its operating season as well as moving into more violent environments. The industrial sector will therefore require safe, accurate and inexpensive techniques of design and analysis of systems to enable it to operate effectively in such environments. One of the problems associated with the mooring of structures in waves is the effect of wave grouping on their slowly oscillating drift response.

A floating structure moored in irregular waves will experience first-order wave forces that are linearly proportional to the heights of the waves and will act at frequencies that are equal to the frequencies of the waves. They also experience smaller, low frequency second-order forces that are proportional to the square of the wave heights. The frequencies of the second-order forces are related to the frequencies of the wave groups contained in the irregular waves. These low frequency second-order forces are commonly referred to as slow drift forces and the structure's response to these drift forces are referred to as slow drift oscillations. The slow drift forces, though relatively small in magnitude, can excite large horizontal motions in moored structures. The group frequences at which these forces act

typically coincide with the resonant frequencies of moored structures. In general the damping that is associated with the horizontal motions of a moored structure is very low. Therefore, when these group frequencies fall near the resonant frequency of the structure the result is large amplitude motion behaviour in the horizontal direction.

The traditional approach to design and analysis of offshore structures is a combination of analytical and scaled prototype modelling. In relation to studying the effects of wave grouping on floating structures both analytical and experimental efforts have only begun in recent years. The earliest observations of these effects were reported by Remery and Hermans (1971) and Hsu and Blenkarn (1972). These authors showed that the drift forces in irregular wave trains are associated with the frequencies of the groups present in the train. Hsu and Blenkarn (1972) and Newman (1974) approximated these forces using coefficients found from regular waves. These methods did not give phase information between the group and the slow varying drift force. This information is important when considering the effect of these slow drift forces on the motion of a structure in terms of the sequence at which wave groups impinge on it. Pinkster (1981) has presented a technique of determining the slow drift forces on structures by direct integration of second-order pressures on the wetted part of the structure. This analytical model does describe a means of determining the phase between the slow drift force and the wave envelope.

Paralleling developments in theories which may be used to predict

second-order forces are studies of wave groups. These began with studies of sequences of wave heights by Goda (1970). Then Nolte and Hsu (1972) studied the statistics of envelopes by observations of time traces. Arhan and Ezraty (1978) and Rye (1981) studied wave heights and envelopes by means of auto correlation functions. Funke and Mansard (1979) and Nelson (1980) analyzed wave groups by squaring and smoothing time traces. Analysis of field data using the techniques of these authors have shown that group characteristics can be unique to a particular region. This suggests that a structure's performance can be optimized for a particular region.

In order to evaluate the theories predicting the influence of slow drift forces caused by particular wave groups on the performance of a structure, the most reliable method available is scaled model testing. Confidence in the accuracy of analytical models will be heightened by agreement with experimentally simulated conditions provided these simulations are controllable and understood. Although Pinkster and van Oortmerssen (1977) has presented a rigorous formulation of his approach to computing the slowly-varying forces caused by irregular waves, experimental verification of these methods is for the most part limited to regular waves. Results of experiments in irregular waves are confined to comparisons between predicted and measured spectral densities of drift forces. Funke and Mansard (1979) have presented a technique to identify the grouping characteristics of waves contained in an irregular wave train by introducing the concept of the SIWEH.

SIWEH is an acronym for the smoothed instantaneous wave energy history. This method is used to indicate the group activity along the time axis by describing wave energy as the square of the water surface elevation averaged over a time period which is a function of the peak frequency. These authors have also presented a method of modelling a wave spectrum containing particular group characteristics but have not attempted to predict the slowly oscillating drift response of a structure to wave groups.

The following study addresses, both analytically and experimentally, the effects of wave grouping on the slowly oscillating drift response of floating moored structures. The thesis is organized as follows:

(i) A review of the pertinent literature is presented and discussed in Chapter 2. This review covers the areas of wave groups, second-order wave forces on structures and prototype modelling. This Chapter identifies an inefficiency in predicting the response of floating moored structures to irregular wave groups.

(ii) Chapter 3 presents an original analytical technique which relates the slow drift response of a floating moored structure to the wave group affecting it. The development integrates a number of techniques found in the literature.

(ii) Chapter 4 describes a method to determine the number of discrete components needed to simulate a wave group. This is done in terms of the characteristics of the structure under investigation.

(iii) Chapter 5 describes the calibration of a 60 m wave tank used to experimentally evaluate the method proposed in Chapter 3. The

calibration procedure implements a number of simulation techniques described in Chapter 4. Subsequently a detailed set of model tests are conducted on a model of a rectangular barge.

(iv) Chapter 6 compares the analytical and experimental results.

(v) Chapter 7 discusses the results of this comparison and presents a number of conclusions.

Work found in the present study which is not available in current literature and thereby contributes to this area of research includes:

(i) The analytical model relating the slow drift response to the wave group.

(ii) Experimental demonstration of the magnitude and phase relationship between the wave group and structure response.

CHAPTER 2

LITERATURE REVIEW

The following Chapter reviews the current literature on two topics. One addresses wave groups and the other reviews developments concerning theories and experiments which may be used to predict the second-order wave forces on moored floating structures. Detailed derivations are not given in this chapter but will be discussed in the Appendix.

2.1 Wave Group Analysis

An extremely detailed review of information on ocean wave groups is given in Rye (1981). A more recent review can also be found in LeBlond(1982). Also a concise review of wave groups can be found in van Vledder (1983a, 1983b). This among other literature that was reviewed for the present work has revealed that there are a number of approaches taken in the study of wave groups contained in ocean spectra. These may be categorized as,

1. Statistical analysis involving sequences of wave heights which may exceed some prescribed threshold.
2. Statistical analysis of wave envelopes created by connecting the crests and troughs of zero-crossing waves.
3. Squaring and smoothing of time histories of wave data.

2.1.1 Analysis Using Sequence of Wave Heights

Goda (1970) studied wave groups using a statistical model based on the assumption that successive wave heights are independent of each other. The probability, pr, that the wave height, H, is greater than

the group level, H_c, is defined as, (2.1)

$$pr(H) = 1 - P(H_c)$$

and the probability that the wave height, H, will be less than H_c is defined as,

$$q(H) = 1 - pr(H) \qquad (2.2)$$

Therefore, $pr(H) + q(H) = 1$.

The probability of a wave group of length, j, is equal to the product of the separate probabilities of each of the wave lengths in the group exceeding the value, H_c, simultaneously. This expression is given as,

$$P1(j) = (1-pr)\ pr^{\,j-1} \qquad (2.3)$$

The mean, j1, and standard deviation, sd (j1), are calculated as follows,

$$\overline{j1} = \frac{1}{(1-pr)} \qquad (2.4)$$

and

$$sd(j1) = \frac{pr^{1/2}}{(1-pr)} \qquad (2.5)$$

The probability of a group of waves of heights less than H_c with a group length, j, is expressed as,

$$P2(j) = (1-pr)^{j-1}\ pr \qquad (2.6)$$

with a mean and standard deviation of,

$$\overline{j2} = \frac{1}{pr} \qquad (2.7)$$

and

$$sd(j2) = \frac{(1-pr)^{\frac{1}{2}}}{pr} \qquad (2.8)$$

The probability of a wave group with a length, j, ($j \geq 2$) is found from,

$$P3(j) = \frac{pr(1-pr)}{2pr-1} \left(p^{j-1} - (1-p)^{j-1}\right) \qquad (2.9)$$

Goda (1970) used computer simulations to investigate the above described model for various spectral forms. These simultations used phase components that were generated from a uniform distribution on the interval 0.2 to π. The simulations showed that the average group length produced from a narrow spectrum are higher than those predicted by his model. Goda's model was also compared to field data by Wilson and Baird (1972), Rye (1974), Goda (1976) and Dattatri et al (1977). Once again all results given clearly indicate that the measured average groups lengths are greater than theoretical values. Based on the findings of these authors it is concluded that successive wave heights are dependent. Therefore the resultant average group lengths are greater than those found under the assumption of independence between the successive wave heights.

The dependency between successive wave heights has been examined by various authors who studied the characteristics of its joint probability density distribution. Rye (1974), Dattatri et al (1977), Arhan and Ezraty (1978) and Su et al (1982) studied the correlations between successive wave heights.

Rye (1974) was the first to calculate the correlation coefficient between successive wave heights. The correlation coefficient, Rhh(k)

is expressed as,

$$Rhh(k) = \frac{1}{sd^2(H)} \frac{1}{N-k} \sum_{i=1}^{N-k} (H_i - \bar{H}) \quad (H_{i+k} - \bar{H}) \qquad (2.10)$$

where,

N = number of wave heights in sample

H = average wave height

sd(H)= standard deviation of wave heights

k = difference in number between successive wave heights.

Rye (1974) reported Rhh(1) values of 0.30 and 0.20 for wave growth and wave decay respectively. Other authors, Dattatri et al (1977) found a mean Rhh(1) value of 0.236 and Arhan and Ezraty (1978) gave an average value of 0.297. The latter two authors did not however, distinguish between growing and decaying sea states. Su et al distinguished between wave growth and wave decay be examining the trend in H. In the case if wave growth they reported Rhh(1) values of 0.374 and for wave decay, Rhh(1) values equal to 0.340. Goda (1983) analyzed wave swell in a very narrow spectrum and found Rhh(1) values of 0.649. It is concluded from the work of these authors that the dependency between successive wave heights decreases as wave lengths increase. Also the value of Rhh(1) is dependent upon the spectrum form, i.e. higher correlations are found from narrow spectra.

Kiruma (1980) derived a theory for group lengths where successive waves are correlated. The model assumes that the joint probability density function of two successive wave heights is given by the two-dimensional Rayleigh distribution. In order to calculate the probalility of a sequence of waves of a height greater than H_c, or lower than H_c Kimura used the conditional probabilities,

$$p11 = \text{Prob}\,[H_{i-1} \quad H_c \quad H_i \quad H_c] \tag{2.11}$$

and

$$p22 = \text{Prob}\,[H_{i+1} \quad H_c \; H_i \quad H_c\,] \tag{2.12}$$

The probability of a sequence of j successive heights greater than H_c is,

$$p1(j) = p22^{\,j-1}\,(1-p22) \tag{2.13}$$

with a mean of,

$$j1 = \frac{1}{(1-p22)} \tag{2.14}$$

and a standard deviation of

$$sd(j2) = \frac{p22^{1/2}}{(1-p22)} \tag{2.15}$$

By analogy, the probability of a sequence of j heights less than H_c is,

$$p2(j) = (1-p11)\; p11^{j-1} \tag{2.16}$$

with a mean of,

$$\overline{j2} = \frac{1}{(1-p11)} \tag{2.17}$$

and a standard deviation of,

$$sd(j2) = \frac{p11^{\frac{1}{2}}}{(1-p11)} \qquad (2.18)$$

Kimura (1980) conducted computer simulations to generate time sequences of wave groups. The simulations were generated for a spectrum of different peakedness characteristics. The phases associated with each of the wave components generated were selected from a uniform distribution on the interval (0.2 to π). Using this model Kimura found good agreement between the measured values and those predicted by his model. When compared to field data the measured average group lengths for group levels above the average wave heights in the group are larger than those predicted by Kimura's model. For group levels above $H_{1/3}$ there was an obvious improvement between the theoretical and measured group lengths.

Kimura'a model for group length distribution considers only the correlation between non-successive wave heights. Van Vledder (1983b) extended this model to include correlations between non-successive wage heights. In the extended version of the model a wave height is correlated not only with the previous wave height, but also with the one previous to that. Van Vledder (1983a)assumed the existance of a joint probability density distribution function for three successive heights H_i, H_{i+1}, H_{i+2}. Kimura's original model and its expanded version were tested using data fron the North Sea as well as that found in published literature. Van Vledder (1983a) found that the original model of Kimura provided a good prediction of the average group length. The model also showed that successive wave heights are dependent. This dependency is particularly noticeable for wave heights

greater than $3\sqrt{m_o}$. Conclusions with regard to the expanded version of the model were not given.

Thompson and Smith (1975) have made a study of wave groups appearing in 20 minute pressure records. The measurements obtained from each group included the maximum, significant and average wave heights and wave group periods. These terms are illustrated in Figure 2.1a. Individual wave heights were measured from the crest elevation to the mean through elevation and individual wave periods were measued between visually estimated "centre of mass" of the adjacent crests. Groups having peak waves of height equal to or less than one-third of the significant height were not detected in the wave records. One advantage of using the crest controid over zero-line crossings is that the former is independent of the mean water level and consequently the presence of long waves in the record, which sometimes effects the results derived from zero-crossing analysis. For the case of narrow band ocean wave spectra, height measures derived from wave groups appearing in 20 minute wave records have well defined statistical distributions that are related to the theoretical Rayleigh wave height distribution developed by Longuet-Higgins (1952).

2.1.2 Analysis of Wave Groups Using Envelope Statistics

Nolte and Hsu (1972) expressed wave groups in terms of wave crests and wave troughs. The wave group is defined as that part of the

amplitude envelope that exceeds a specific level. The length of the wave group is defined as the time duration, L1, the amplitude envelope exceeds this level. These authors assumed that successive crossings of levels of the amplitude envelope form a Poisson process, from which the average time duration between an upcrossing of the amplitude envelope through the specific level has an exponential distribution. The Poisson model gives the probability that the time duration, L1, that the wave envelope will exceed the specified level ,H_c, is smaller than a time duration, t, by the following relationship,

$$Pr(t) = Prob\ [L1 \leq t] = 1-exp\ (-t/L1)] \qquad (2.19)$$

where L1 is the average time duration above the level H_c.
Nolte and Hsu (1972) tested their model from recordings in the Gulf of Mexico. Based on 900 individual waves, they found good agreement between their model and the measured values.

2.1.3 Wave Group Analysis by Squaring and Smoothing of Time Data

Several authors have studied wave group characteristics of wave trains by squaring the time trace and smoothing it with a variety of filtering techniques. Sedivy (1978) found that the use of a moving window with a length of twice the peak spectral period to be an optimum value for identifying modelled wave groups. Figure 2.1b shows a definition of the group boundaries used. Nelson (1980) conducted experiments by varying this window length in fractions and multiples of the spectral peak period. Results indicated that large energy groups were identified by all windows and that the number of waves identified

in a group was seldom affected by window length. However for groups with small energy content the number of groups varied as well as the number of waves in a group, i.e. increasing the window length decreased the number of waves in a group. Nelson (1980) also found by varying the window length from one half to four times the peak period the number of wave groups decreased by 50%. The relationship between the maximum wave height in a group and that of the wave record was found to have an average value of unity.

As a means of estimating the essential parameters of a natural sea state and determining how these parameters change as a function of time and location, Funke and Mansard (1979) have presented the smoothed instantaneous wave energy history (SIWEH) function. This SIWEH is defined as,

$$E(t) = \frac{1}{T_p} \int_{\tau=-T_p}^{T_p} \zeta_a^2(t+\tau) \cdot Q_1(\tau)\, d\tau \qquad (2.20a)$$

for

$$T_p \leq t \leq (T_o - T_p) \qquad (2.20b)$$

where T_o is the length of the finite wave record, T_p is the peak period of the spectrum and Q_1 is a smoothing window. For the beginning and end conditions

$$E(t) = \frac{2}{(T_p+t)} \int_{\tau=-t}^{T_p} \zeta_a^2\,(t+\tau) \cdot Q_1(\tau)\, d\tau, \qquad (2.21a)$$

for $0 \leq t \leq T_p$

and

$$E(t) = \frac{2}{T_p+(T_o-t)} \int_{\tau=-T_p}^{T_o-t} \zeta_a^2\,(t-\tau) \cdot Q_1(\tau) d\tau, \qquad (2.21b)$$

for $(T_o-T_p) \leq t \leq T_o$

with

$$Q_1(\tau) = 1 - |\tau|/T_p, \text{ for } -T_p \leq \tau < T_p \tag{2.21c}$$

$$Q_1 = 0, \text{ everywhere else} \tag{2.21d}$$

Evaluation of the ζ_a^2 term identifies several distinct components, one of which is the difference of frequency pairs. It is this difference term which transfers energy in the lower frequency range and thereby tends to excite the slow drift response of floating structures. Wave group activity in terms of wave energy distribution along the time axis is described by the groupiness factor (GF),

$$GF = [\frac{1}{T_o} \int_0^{T_o} (E(t)-\bar{E})^2 \, dt]^{1/2} / \bar{E} \tag{2.22a}$$

$$= (m_{\varepsilon o})^{1/2} / m_o \tag{2.22b}$$

where $\bar{E}$ is the average value of $E(t)$, $m_{\varepsilon o}$ is the zeroth moment of the SIWEH spectrum and m_o is the zeroth moment of the variance spectrum The groupiness factor is a measure of the deviation of the instantaneous wave energy about its mean. Therefore a GF equal to zero would indicate that the waves are regular, i.e. of constant frequency and amplitude, whereas large groupiness factors would imply that the energy fluctuates greatly about its mean. Different groupiness factors are possible for any particular modelled wave spectrum. Hence, it is believed that a different statistical response could be observed for these conditions.

2.2 Theories to Determine Second-Order Forces on Floating Structure

Theories dealing with second-order drift forces may be categorized into four main areas:

1. Potential theories that determine the steady second-order forces on the basis of conservation of momentum and energy. In this method, changes in momentum of the fluid surrounding the body are equated to the steady force acting on the body in regular waves. This method is commonly referred to as the "far field" approach since it uses knowledge of the fluid potential far from the structure when describing the fluid motions. For the most part, these theories are three dimensional and exact to second-order.

2. Potential theories which determine the steady second-order forces and slow oscillating drift forces by direct integration of the fluid pressure acting on the wetted part of the body. This technique is commonly referred to as the "near field" method. These theories are two-dimensional or three-dimensional and exact to second-order.

3. Potential theories which determine the steady second-order forces by equating the damping energy radiated by the oscillating body to the work done by incoming regular waves. These theories are approximate and use the slender body assumption.

4. Theories which use the Morison's equation approximation. These theories apply mainly to slender member structures such as semisubmersibles.

2.2.1 Historical Background

The second-order effects of waves on floating vessels were first

reported by Suyehiro (1924). Expressions for the steady sway force and steady longitudinal force were given by Watanabe (1938) and Havelock (1942) respectively. Both expressions used the Froude-Kryloff components only and neglected diffraction effects. Maruo (1960) presented expressions for the longitudinal and transverse steady second-order forces on a fixed vessel in regular waves. This method makes use of the "far field" approach, and is valid for two and three-dimensions, exact to second-order. In his expression Maruo includes diffraction and radiation effects. Several authors then used modified verisons of Maruo's expression to calculate steady drift forces. Newman (1967) expanded the theory to include the mean yaw moment. Faltinsen and Michelsen (1974) modified the expression and evaluated their results by means of a distribution of singularities over the body surface.

Salvesen (1974) derived an expression for the total mean and low frequency second-order forces and moments on floating structures. The expansions were derived by integration over the wetted surface of the body. This theory was then used by Dalzell and Kin (1976) to determine the steady forces in regular waves. These steady forces were then used to predict the second-order low frequency forces on a vessel. Pinkster and Hooft (1978) gave an expression based on direct integration of pressure for the mean and low frequency second-order horizontal wave force on a vessel in irregular waves. This technique was extended to compute the mean longitudinal and transverse force as well as the yaw moment on a free floating barge in regular waves. Faltinsen and Loken (1979) gave a two-dimensional method based on potential theory to compute the mean and low frequency components of the second-order

transverse force on cylinders floating in beam seas. The contribution of the second-order non-linear velocity term was expressed in terms of first-order quantities. Pinkster and Van Oortmerssen (1977) extended the method of direct pressure integration to include the low frequency components of second-order forces in floating bodies caused by regular wave groups. Then in Pinkster (1981) the direct integration of pressure was used to determine the low frequency second-order longitudinal force on a semi-submersible. Pinkster (1981) assumed that the irregular wave response could be determined by superposition of the results obtained from regular wave groups.

Apart from the theories described above there are numerous others. These are for the most part extensions of the works of the aforementioned authors. For convenience these theories are summarized in Table 1. It is also difficult to draw conclusions regarding the validity of most of the theories due to their lack of sufficient experimental data and in some cases even numerical results are not presented.

2.2.2 Current Methods of Predicting Second-Order Forces

Most of the work that has been carried out in recent years is directed mainly towards the steady drift forces on vessels in regular waves. Second-order forces have been estimated by means of coefficients found from these regular wave analyses. These coefficients are generally expressed as,

$$R^2(f) = \bar{F}_D / [\tfrac{1}{2} \rho g a^2(f) L] \qquad (2.23)$$

where,

$\bar{F}_D$ = steady drift force

ρ = density

g = gravitational acceleration

L = characteristic length of structure

a = wave amplitude

Figure 2.2 shows these coefficients experimentally determined for a variety of structural shapes. As indicated in the Figure the coefficients are highly dependent on structural shape and wave frequency. Pinkster (1974) suggests that the spectrum of the slow varying force, $S_F(\mu)$, can be determined from the steady drift coefficients by the following expression,

$$S_F(\mu) = 2\,\rho^2\,g^2\,L^2 \int_0^\infty S(f)\,S(f+\mu)\,R^4(f+\tfrac{\mu}{2})\,df \qquad (2.24)$$

where, S(f) is the variance spectral density of the water surface elevation.

Subsequently, the low frequency response spectrum $S_R(\mu)$ is determined for a single degree of freedom system using the expression,

$$S_R(\mu) = S_F(\mu)\left[\frac{1}{(c - m_a\,\mu^2)^2 + (b\mu)^2}\right] \qquad (2.25)$$

where, m_a = equivalent mass

c = restoring coefficient

b = damping coefficient

This expression assumes linear damping and restoring coefficients. Roberts (1981) has presented a theoretical model to handle nonlinear restoring cases.

This technique assumes that the effects of second-order waves caused by the simultaneous existence of two or more regular wave components are neglibible. Choice of a theory to predict steady drift coefficients on a vessel in regular waves is strongly dependent on the type of structure under investigation. These coefficients predicted for the same vessel can vary depending on the choice of theory used. This effect is demonstrated in Figure 2.3. The Figure compares the experimental and analytical results for a Series 60 ship. The method of Faltinsen and Michelsen (1974) does not give good agreement with the experiments. However this particular method does show good agreement with experiments on rectangular barges.

Remery and Hermans (1971) applied Equation (3.10) to determine slow drift oscillations on a rectangular barge in regular wave groups, i.e. groups containing two regular wave components. Rye et al (1975) used the same Equation to determine the slow drift oscillations on a model of a large-volume caisson structure also in regular wave groups. In the case of the rectangular barge, analysis showed good agreement between measured and predicted values but for the caisson model agreement was poor. Referring once again to Figure 2.2 Rye et al found that the coefficients found from regular waves underestimated those required for regular wave groups. This difference is illustrated in the Figure.

Standing et al (1981) suggests that this discrepancy is due to second-order wave effects. Standing et al studied the slow oscillating drift response of a ship shape. In his analysis Standing et al has used the method of Pinkster (1975) to determine steady slow-drift effects related to first-order quantities and extended his analysis to

include second-order wave terms using the method of Bowers (1975). Bowers (1975) neglected all wave diffraction and radiation effects and found zero mean force contribution from the second order wave. Standing et al using this combined method, compared his numerical results to model tests in irregular waves. Only magnitude response spectra were presented and agreement between the two methods was not good.

2.3 Wave Modelling for Slow Drift Oscillation Analysis

The effect of wave modelling on the slow drift response of moored floating structures has been illustrated by a number of authors.

Naess (1978) has presented the results of a model test carried out on a model restricted to heave only. The model was exposed to a continuous spectrum of filtered white noise using random phase information. In addition to this, spectra of a finite number of regular waves were applied. These spectra consisted of eight and sixteen components with equidistant and randomly chosen frequency resolutions. The results of his experiments are summarized in Figure 2.4. It was found that slow drift oscillations of the model when exposed to regular components with equidistant frequencies were highly dependent on the resonant frequency of the model. This was further illustrated by altering the resonant frequency and observing the same phenomenon. Spangenberg (1980) has shown experimentally, by testing a semisubmersible, that representation of the natural sea state solely by means of an energy spectrum is insufficient to predict the response of

a system for mooring and dynamic position control. In his experiments the semisubmersible was tested in three different wave patterns of almost identical energy distribution but having different wave grouping characteristics. The results showed that the slow drift oscillations experienced by the model in the horizontal plane were significantly influenced by the wave grouping. Results for surge from the experiments are summarized in Figure 2.5. As can be seen in these results, the period of the slow drift oscillations corresponds to the wave group period where the wave grouping was pronounced. However, these experiments showed no recognizable effect of grouping on any other motion other than those in the horizontal plane.

Mansard and Pratte (1982) showed that the wave grouping present in irregular waves is an important parameter in the assesment of vessel response . The authors have shown that Bounded Long Wave Components must be correctly produced in order to simulate wave groups that will produce a realistic vessel response.

2.4 Summary

The literature reviewed has revealed an inefficiency in the existing techniques to determine the effects of wave grouping on the slow drift response of floating moored structures.

Existing methods to determine the steady drift forces on structures in regular waves produce good agreement with experimental results. Slowly oscillating drift forces determined from steady drift coefficients were found to accurately predict the slowly oscillating drift response in regular wave groups only and in certain cases the

effects of second-order waves caused by the simultaneous existence of the two wave components have a significant influence on the response. When wave spectra are modelled using a large number of components the method of predicting the slowly oscillating drift response from steady drift coefficients results in poor agreement between experiment and theory.

Experimental work has shown that grouping patterns resulting from wave spectra that are simulated using a constant frequency difference can significantly effect the slowly varying response of the model. Therefore, if these groups are not representative natural wave groups they will not give an accurate prediction of the structure's response. Furthermore when a random superposition of regular wave components is used to model irregular wave spectra they should be arranged to produce wave group characteristics that are observed in real sea-states.

The method of squaring and smoothing the time trace to identify the wave group characteristics has two distinct advantages. One is that it readily identifies the low-frequency components of the group and secondly, it expresses the group characteristics in terms of the square of the wave amplitude. It is the square of the amplitude to which these low frequency forces are proportional.

CHAPTER 3

THE ANALYTICAL MODEL

The following chapter presents a model of a quadratic transfer function relating the slow drift response of a moored floating structure to an irregular wave group. The model utilizes the hydrodynamic models of Pinkster (1981) and Faltinsen and Michelsen (1974) in conjunction with the wave modelling techniques of Funke and Mansard (1979). In the model a magnitude and phase relationship between the slow drift forces and the SIWEH is developed. Subsequently an expression to relate the SIWEH and slow drift oscillation is presented.

3.1 Determination of Slowly-Varying Forces

The basic difference between the methods of Pinkster (1981) and Faltinsen and Michelsen (1974) is the "near field" method of Pinkster and the "far field" method used by Faltinsen. Appendix D gives a detailed description of both methods. Although both methods produce the same results for a rectangular barge, the near-field approach shows more clearly the effects of first-order waves on the drift forces. These effects are described as five components defined by Equations (D.35).

In order to elucidate the relationship between each of these components and the wave group affecting them, consider for example Component I, described by Equation (D.35a) rewritten here as,

$$F_I^{(2)}(t) = -\int_{WL} \frac{1}{2} \rho g \, \zeta_r^{(1)^2} (t,\ell) \, \bar{n}_1 (\ell) \, d\ell \qquad (3.1)$$

where,

$\zeta_r^{(1)}(t,\ell)$ - time dependent relative wave elevation at a point, ℓ, along the waterline of the structure.

$\bar{n}_1(\ell)$ - directional cosine of an elemental length, $d\ell$, in the longitudinal direction.

These terms are schematized in Figure 3.1.

Assume that the group consists of a narrow band of N discrete long-crested waves such that the free surface is given to first-order as,

$$\zeta_a^{(1)}(t) = \sum_{n=1}^{N} a_n \cos (\omega_n \tau + \varepsilon_n) \qquad (3.2)$$

Following this, the first-order relative wave elevation at a point, ℓ, on the waterline of the body can be written as,

$$\zeta_r^{(1)}(t,\ell) = \sum_{n=1}^{N} a_n \, \zeta_{rn}^{(1)} (\ell) \cos (\omega_n t + \varepsilon_n + \varepsilon_{rn}(\ell)) \qquad (3.3)$$

where,

a_n = amplitude of component n

ε_n = phase associated with component a_n

ω_n = radian frequency of component n

$\zeta_{rn}^{(1)}$ = magnitude of transfer function relating the undisturbed first-order wave, a_n, at the center of gravity of the structure to the first-order relative wave elevation $\zeta_r^{(1)}$ at point, ℓ, on the structure's waterline.

ε_{rn} = phase of transfer function associated with magnitude $\zeta_{rn}^{(1)}$.

Substituting Equation (3.3) into (3.1) yields,

$$F_I^{(2)}t = \sum_{n=1}^{N}\sum_{m=1}^{N} a_n a_m \int_{WL} \frac{1}{4} \rho g \zeta_{rn}^{(1)}(\ell)\, \zeta_{rm}^{(1)}(\ell) \cos(\varepsilon_{rn}(\ell) - \varepsilon_{rm}(\ell))$$

$$n_1(\ell)\, d\ell \cos(\Delta\omega_{nm}(t) + \Delta\varepsilon_{nm})$$

$$+ \sum_{n=1}^{N}\sum_{m=1}^{N} a_n a_m \int_{WL} \frac{1}{4} \rho g \zeta_{rn}^{(1)}(\ell)\, \zeta_{rm}^{(1)}(\ell) \sin(\varepsilon_{rn}(\ell) - \varepsilon_{rm}(\ell))$$

$$n_1(\ell) d\ell \sin(\Delta\omega_{nm}(t) + \Delta\varepsilon_{nm}) \qquad (3.4)$$

$$+ \text{high frequency terms}$$

where $\Delta\omega_{nm} = \omega_n - \omega_m$

$\Delta\varepsilon_{nm} = \varepsilon_n - \varepsilon_m$

This expression can be rewritten as,

$$F_I^{(2)}(t) = \sum_{n=1}^{N}\sum_{m=1}^{N} a_n a_m P_{nm} \cos(\Delta\omega_{nm}(t) + \Delta\varepsilon_{nm})$$

$$+ \sum_{n=1}^{N}\sum_{m=1}^{N} a_n a_m Q_{nm} \sin(\Delta\omega_{nm}(t) + \Delta\varepsilon_{nm}) \qquad (3.5)$$

where P_{nm} and Q_{nm} are the quadrature components of the time independent transfer function, relating the relative wave height force component to the wave envelope. Expansion of Equation (3.5) reveals that the second-order force contains n constant components as well as the slow varying components. The resulting quadrature components of the low frequency $\Delta\omega_{nm}$, depends on the sum of P_{nm} and P_{mn} and the difference of Q_{nm} and Q_{mn} terms. These terms can be reformatted so that the following symmetry relations are valid.

$$P_{nm} = P_{mn}$$

and

$$Q_{nm} = -Q_{mn}$$

Thus the slowly varying second-order force given by Equation (3.5) can be rewritten as,

$$F_I^{(2)}(t) = \sum_{n=1}^{N} \sum_{m=1}^{N} a_n a_m F_{nm} \cos (\Delta\omega_{nm} t - \gamma_{nm} - \Delta\varepsilon_{nm}) \qquad (3.6)$$

where $F_{nm} = \sqrt{P_{nm}^2 + Q_{nm}^2}$

$$\gamma_{nm} = \tan^{-1} \left[\frac{Q_{nm}}{P_{nm}}\right]$$

and $\gamma_{nm} = -\gamma_{mn}$

Similar developments are made for the other contributions (II-IV). The total quadrature components are determined by summation of all contributions. The resulting transfer function described by terms F_{nm} and γ_{nm} are independent of both time and the phase components, ε_n, associated with each of the sinusoids comprising the wave spectrum. Therefore, the total second-order effects of first-order waves exerted on a structure by a group of n components is expressed as,

$$F_I^{(2)}(t) = \sum_{n=1}^{N} \sum_{m=1}^{N} a_n a_m F_{nm} \cos (\Delta\omega_{nm} t - \Delta\varepsilon_{nm} - \gamma_{nm}) \qquad (3.7)$$

The general assumption of the above model is that the slowly oscillating drift force is the resultant of all superimposed regular wave groups that can be produced by a wave spectrum. The key factor in relating the amplitude of this slowly oscillating drift force to the amplitude of the regular wave group is the steady drift coefficient found from regular waves. This coefficient "R(ω)" is expressed as,

$$R(\omega) = [\bar{F}_D/(1/2\ \rho g\ L\ a^2(\omega))]^{1/2} \qquad (3.8)$$

where $\bar{F}_D$ - constant drift force

$a(\omega)$ - wave amplitude corresponding to frequency ω

L - structure length

These coefficients are dependent on the wavelength to structural length ratio and are therefore a function of wave frequency. Following this, for small differences in frequency the amplitude of the slow varying force coefficient, F_{nm}, in Equation (3.7) is expressed as,

$$F_{nm} = [\tfrac{1}{2} \rho g L \, R(\omega_n) \, R(\omega_m)] \tag{3.9}$$

Equation (3.7) shows that the time record of any component $F_1^{(2)}(t)$ oscillating at frequency $q\Delta\omega$ is the sum of contributions from components whose difference frequencies are equal to $q\Delta\omega$. The contribution of the sum of each frequency difference to the total slow oscillating force is written as,

$$F_q^{(2)}(t) = \sum_{n=1}^{N-q} a_n \, a_{n+q} \, F_{n,q} \cos(q\Delta\omega t - \Delta\varepsilon_{n,n+q} - \gamma_{n+q}) \tag{3.10a}$$

where,

$$q\Delta\omega = \omega_{n+q} - \omega_n$$

$$a_n = a(\omega_n)$$

$$F_{n,q} = [\tfrac{1}{2} \rho g L \, R(\omega_n) \, R(\omega_{n+q})]$$

$$F_q^{(2)}(t) = \sum_{n=1}^{N-q} a_n \, a_{n+q} F_{n,q} [\cos q\Delta\omega t \cos(\Delta\varepsilon_{n,n+q} - \gamma_{n,n+q}) - \sin q\Delta\omega t \sin(\Delta\varepsilon_{n,n+q} - \gamma_{n,n+q})] \tag{3.10b}$$

$$F_q^{(2)}(t) = [\sum_{n=1}^{N-q} a_n \, a_{n+q} \, F_{n,q} \cos(\Delta\varepsilon_{n,n+q} - \gamma_{n,n+q})]\cos(q\Delta\omega t) - [\sum_{n=1}^{N-q} a_n \, a_{n+q} \, F_{n,q} \sin(\Delta\varepsilon_{n,n+q} - \gamma_{n,n+q})]\sin(q\Delta\omega t) \tag{3.10c}$$

Equivalently this can be written as,

$$F_q(t) = \left[\left[\sum_{n=1}^{N-q} a_n\, a_{n+q}\, F_{n,q}\, \cos(\Delta\varepsilon_{n,n+q} - \gamma_{n,n+q})\right]^2 + \left[\sum_{n=1}^{N-q} a_n\, a_{n+q}\, F_{n,q}\, \sin(\Delta\varepsilon_{n,n+q} - \gamma_{n,m+q})\right]^2\right]^{1/2} \cdot \cos(q\Delta\omega t - \theta_q) \qquad (3.10d)$$

where

$$\theta_q = \tan^{-1}\left|\frac{\sum_{n=1}^{N-q} a_n\, a_{n+q}\, F_{n,q}\, \sin(\Delta\varepsilon_{n,n+q} - \gamma_{n,n+q})}{\sum_{n=1}^{N-q} a_n\, a_{n+q}\, F_{n,q}\, \cos(\Delta\varepsilon_{n,n+q} - \gamma_{n,n+q})}\right| \qquad (3.10e)$$

3.2 The Second-Order Wave Term

In addition to the second-order forces caused by first-order waves, as indicated by Equation (D.35e) there are also second-order forces caused by a second-order wave or "set-down" wave.

The second-order "set down" wave can cause an inertial type drift force associated with the pressure gradient in the set-down wave. Salvensen (1974) has shown that the second-order potential makes no contribution to the horizontal mean drift force or overturning moment. The set-down in an irregular wave group represents a long period second-order wave which is associated with the wave envelope and travels at the group velocity. It is affected by a change in the mean water level due to the irregularity of the wave heights. Other contributions to the set-down are from wave diffraction of the first-order wave caused by the structure and interactions between incident and diffracted waves. There are also two free wave components, namely the diffraction of the incident set-down wave

and reflection of the set-down wave from other boundaries such as those in a wave tank.

Bowers (1975) used a Froude-Kryloff type of approximation for pressures in the set down wave. In his analysis, the total second-order effects of the incident waves were considered on a symmetric flat bottom hulk, moored in head seas. Reflections were considered to be small. This method is easy to evaluate and provides good agreement between the calculated values and those measured in a wave tank. The same method is applied here to a rectangular barge.

3.2.1 Set-down Force on a Rectangular Barge

The second-order pressure caused by the set-down wave is defined as,

$$p^{(2)} = -\rho g \frac{\partial \phi^{(2)}}{\partial t}$$

The expression for $\phi^{(2)}$ given by Equation (C.16a) is rewritten as,

$$\phi^{(2)} = \sum_{m=1}^{N-1} \sum_{n=m+1}^{N} d_{nm} \cosh \Delta k_{nm}(z+h) \sin (\Delta\omega_{nm} t + \Delta k_{nm} x + \Delta\varepsilon_{nm}) \quad (3.11)$$

where,

$$\Delta\omega_{nm} = \omega_n - \omega_m$$

$$\Delta k_{nm} = k_n - k_m$$

$$\Delta\varepsilon_{nm} = \varepsilon_n - \varepsilon_m$$

let, $\sum_{m=1}^{N-1} \sum_{n=m+1}^{N} d_{nm} = \bar{d}_{nm}$

then,

$$\phi^{(2)} = \bar{d}_{nm} \cosh \Delta k_{nm}(z+h) \sin (\Delta\omega_{nm} t + \Delta k_{nm} x + \Delta\varepsilon_{nm})$$

$$\frac{\partial \phi^{(2)}}{\partial t} = \bar{d}_{nm} \cdot \Delta\omega_{nm} \cosh \Delta k_{nm}(z+h) \cos (\Delta\omega_{nm} t + \Delta k_{nm} x + \Delta\varepsilon_{nm})$$

$$\nabla\left(\frac{\partial\phi^{(2)}}{\partial t}\right) \cdot \bar{i} = -\bar{d}_{nm} \cdot \Delta\omega_{nm} \cdot \Delta k_{nm} \cosh\Delta k_{nm}(z+h) \sin(\Delta\omega_{nm} t+\Delta k_{nm} x+\Delta\varepsilon_{nm})$$

$$= -\bar{d}_{nm} \cdot \Delta\omega_{nm} \cdot \Delta k_{nm} \cdot \cosh \Delta k_{nm}(z+h)$$

$$\{\sin \Delta k_{nm} x \cos(\Delta\omega_{nm} t+\Delta\varepsilon_{nm}) + \cos \Delta k_{nm} x \sin(\Delta\omega_{nm} t+\Delta\varepsilon_{nm})\} \quad (3.12)$$

Term 1 vanishes after integration from x = -L/2 to x = L/2.

Therefore,

$$\nabla\left(\frac{\partial\phi^{(2)}}{\partial t}\right) \cdot \bar{i} = -\bar{d}_{nm}\Delta\omega_{nm} \Delta k_{nm} \cosh \Delta k_{nm}(z+h) \cos \Delta k_{nm} x$$

$$\cdot \sin(\Delta\omega_{nm} t+\Delta\varepsilon_{nm}) \quad (3.13)$$

$$\int_{-B/2}^{B/2}\int_{z-D}^{0}\int_{-L/2}^{L/2} -\rho\nabla\left(\frac{\partial\phi^{(2)}}{\partial t}\right)\cdot\bar{i}\cdot dV = B\rho\, \bar{d}_{nm}\, \Delta\omega_{nm} \cdot 2 \sin \frac{\Delta k_{nm} L}{2}$$

$$\cdot \sin (\Delta\omega_{nm} t+\Delta\varepsilon_{nm}) \cdot \int_{z-D}^{0} \cosh \Delta k_{nm}(z+h)dz$$

$$= 2\rho B\bar{d}_{nm} \sin \frac{\Delta k_{nm} L}{2} \cdot \sin(\Delta\omega_{nm} t+\Delta\varepsilon_{nm}) \cdot \frac{\Delta\omega_{nm}}{\Delta k_{nm}}$$

$$\{\sinh \Delta k_{nm} h - \sinh \Delta k_{nm} (h-D)\hat{i} \quad (3.14)$$

Therefore the set-down force on a rectangular barge of dimensions LxBxH submerged to draft, D, is,

$$F_2^{(2)}(t) = \sum_{m=1}^{N-1} \sum_{n=m+1}^{N} 2 \cdot \rho \cdot B \cdot d_{nm} \frac{\Delta\omega_{nm}}{\Delta k_{nm}} \sin \frac{\Delta k_{nm}}{2} L$$

$$\{\sinh \Delta k_{nm} - \sinh \Delta k_{nm} (h-D)\} \sin(\Delta\omega_{nm} t+\Delta\varepsilon_{nm}) \quad (3.15)$$

3.3 Slowly-Oscillating Response Motions

The second-order equation of surge motion of a linear moored floating structure with one degree of freedom is given as,

$$m_a \ddot{X}_1^{(2)} + b\dot{X}_1^{(2)} + cX_1^{(2)} = F_1^{(2)}(t) + F_2^{(2)}(t) = F_T^{(2)}(t) \tag{3.16}$$

where,

$X_1^{(2)}$ - is second-order motion response in longitudinal direction

$F_T^{(2)}(t)$ - total second-order forcing function

m_a - effective mass

b - damping coefficient

c - restoring coefficient

When the damping experienced by the moored structure is light and the restoring coefficient is linear then the solution to Equation (3.16) can be expressed in the frequency domain as,

$$X_1^{(2)}(\Delta\omega_{nm})\underline{\lfloor \alpha(\Delta\omega_{nm})} = TF(\Delta\omega_{nm})\underline{\lfloor \Phi(\Delta\omega_{nm})} \cdot F_1^{(2)}(\Delta\omega_{nm})\underline{\lfloor \Theta(\Delta\omega_{nm})} \tag{3.17}$$

where,

$X_1^{(2)}(\Delta\omega_{nm})\underline{\lfloor \alpha(\Delta\omega_{nm})}$ - is the polar form of the Fourier Transform of the slow drift oscillation $X_1^{(2)}(t)$.

$TF(\Delta\omega_{nm})\underline{\lfloor \Phi(\Delta\omega_{nm})}$ - Magnitude and phase of the Transfer Function relating slow oscillating drift force to slow drift oscillation $X_1^{(2)}(t)$. This is determined from the classical solution of the equation of motion of a single degree of freedom system.

$F_1^{(2)}(\Delta\omega_{nm})\angle\theta(\omega_{nm})$ - Fourier Transform of equation (3.10a)

$$\angle\alpha(\Delta\omega_{nm}) = \angle\phi(\Delta\omega_{nm}) + \angle\theta(\Delta\omega_{nm}) \qquad (3.18)$$

A similar procedure is used for the second-order wave effects, $F_2^{(2)}(t)$, and the total response will be the sum of the two.

However, when the structure is moored with a non-linear mooring system a time domain analysis will be necessary to determine the slow drift response $X_1^{(2)}(t)$. For the present case a linear system is assumed.

3.4 The SIWEH Related to the Slow-Drift Response

The SIWEH for rectangular smoothing is defined as,

$$E(t) = \frac{1}{2}\sum_{n=1}^{N} a_n^2 + \sum_{m=1}^{N-1}\sum_{n=m+1}^{N} a_m a_n \cos[\Delta\omega_{nm}t + \Delta\varepsilon_{nm}] \qquad (3.19)$$

Considering the slow-oscillation part only of Equation (3.19), the slow-drift varying contribution of each component of frequency $q\Delta\omega$ is written as,

$$E_q(t) = \sum_{n=1}^{N-q} a_n a_{n+q}\cos(q\Delta\omega\, t - \Delta\varepsilon_{n,n+q})$$

$$= \cos(q\Delta\omega)t \sum_{n=1}^{N-q} a_n a_{n+q}\cos(\Delta\varepsilon_{n,n+q})$$

$$- \sin(q\Delta\omega)t \sum_{n=1}^{N-q} a_n a_{n+q}\sin(\Delta\varepsilon_{n,n+q}) \qquad (3.20)$$

where,

$$q\,\Delta\omega = \omega_{n+q} - \omega_n$$

$$a_n = a(\omega_n)$$

$$\Delta\varepsilon_{n,n+q} = \varepsilon_{n+q} - \varepsilon_n$$

Therefore,

$$E(q\Delta\omega)=\left[\left[\sum_{n=1}^{N-q} a_n a_{n+q}\cos(\Delta\varepsilon_{n,n+q})\right]^2+\left[\sum_{n=1}^{N-q} a_n a_{n+q}\sin(\Delta\varepsilon_{n,n+q})\right]^2\right]^{1/2} \quad (3.21)$$

where,

$$\sigma(q\Delta\omega) = \tan^{-1}\left|\frac{\sum_{n=1}^{N-q} a_n\, a_{n+q}\sin(\Delta\varepsilon_{n,n+q})}{\sum_{n=1}^{N-q} a_n\, a_{n+q}\cos(\Delta\varepsilon_{n,n+q})}\right| \quad (3.22)$$

Equation (3.9) indicates that the force coefficient is a bi-linear function of $R(\omega_n)$ and $R(\omega_m)$. Obviously the contribution from each frequency difference to the total slow oscillating force described by Equation (3.8) will be dependent on the wave amplitude associated with each of the frequencies comprising the difference $\Delta\omega_{nm}$. Therefore, in order to compensate for this effect, the SIWEH will be modified in the following manner. Each component of the first-order wave spectrum is weighted using the non-dimensional drift coefficient, $R(\omega)$, i.e.

$$a_n' = a(\omega_n)\, R(\omega_n)$$

therefore, $a_n'\, a_{n+q}' = a(\omega_n)\, a(\omega_{n+q})\, R(\omega_n)\, R(\omega_{n+q})$

The final expression for the modified SIWEH, $E_m(q\Delta\omega)$, is determined by substitution of a_n' and a_{n+q}' for a_n and a_m respectively in Equation (3.21). This weighting of the SIWEH is applied only to the magnitude of the resultant spectrum. The associated phase spectrum is the same as that given by Equation (3.22)

The $SIWEH_m$ is now related to the slow drift oscillation, $X_1^{(2)}\Delta\omega_{nm}\,\underline{\lfloor\alpha(\Delta\omega_{nm})}$ as,

$$TF^{(2)}(\Delta\omega_{nm})\,\underline{\lfloor\gamma(\Delta\omega_{nm})} = \frac{X_1^{(2)}(\Delta\omega_{nm})\,\underline{\lfloor\alpha(\Delta\omega_{nm})}}{E_m(\Delta\omega_{nm})\,\underline{\lfloor\sigma(\Delta\omega_{nm})}} \quad (3.23)$$

where $\underline{\lfloor\sigma(\Delta\omega_{nm})}$ is defined by Equation (3.22).

3.5 Summary

An original technique to relate the slow oscillating drift response of a moored floating structure to the wave groups contained in an irregular wave spectrum has been presented. The second-order effects of first-order waves are determined from the constant drift coefficients of the structure in regular waves and the second-order effects of second-order waves are established using a Froude-Kryloff approximation for pressures in the undisturbed incident set down wave.

The model assumes that each pair of frequencies in a discrete wave spectrum will give rise to a regular wave group. Each of these regular wave groups will produce a low frequency force that is proportional to the product of the wave amplitudes in the group and varies at a frequency equal to the difference in the frequency pair. Furthermore, this low frequency force is related to the SIWEH of the regular wave group by a constant phase angle. Therefore the resultant force is determined by superposition of these regular slow-varying forces. Subsequently the ensuing slowly oscillating motions can be established and related to the SIWEH spectrum. This relation is expressed in the form of a transfer function. Once this transfer function is known it can be utilized to determine the slow drift response of the structure to any group characteristics that can be associated with a particular wave spectrum.

This technique can be quite efficacious since by applying Fourier transforms a time history of the response motion is readily available without excessive computational effort.

CHAPTER 4

WAVE SPECTRUM MODELLING AND ITS EFFECTS ON SLOW DRIFT RESPONSE

The following Chapter investigates the effects of varying frequency difference on the slow drift response of a moored structure. The objective is to determine an appropriate resolution to model a spectrum. Gererally sprectra are modelled as a finite sum of regular sinusoidal components used to approximate some analytical expression describing a continuous energy spectrum. The frequency difference between the discrete components will have a very significant effect on the response of the system model. This effect has been demonstrated by Naess (1978). The model response is also critically dependent on the width and sharpness of the response peak at the natural frequency. This is a function of the system's mass (including added mass), damping and restoring coefficients and when considering the response of the system to any modelled spectrum, the frequency difference is important since it can either enhance or suppress grouping characteristics that are close to the resonant frequency of the system being tested.

4.1 Wave Spectra

There are a number of empirically derived expressions describing wave energy spectra, the two most common of which are the Pierson-Moskowitz (P-M) and the Joint North Sea Wave Project (JONSWAP).The P-M spectrum is expressed as,

$$S(\omega) = \frac{\alpha g^2}{\omega^5} \exp\left[-\beta \left(\omega_* / \omega\right)^4\right] \qquad (4.1)$$

where ω is the radial frequency, $\alpha = 0.008$, $\beta=0.74$ and $\omega_* = g/U$ where U is the wind speed in meters per second. This spectrum is applicable only for a fully developed sea. A full account of the derivation and properties of this spectrum may be found in Pierson and Moskowitz (1964). The JONSWAP spectrum was postulated in an attempt to account for the higher peaks of spectra in a storm situation for the same total energy as compared with the (P-M). The functional form of the spectrum is given as,

$$S(\omega) = \frac{\alpha g^2}{\omega^5} \exp\left[-\frac{5}{4}\left(\frac{\omega_m}{\omega}\right)^4\right] \gamma \exp\left(-(\omega - \omega_m)^2/2\sigma^2\omega_m\right) \qquad (4.2)$$

where, ω_m is the peak frequency, $\sigma = 0.07$ for $\omega \leq \omega_m$ and $\sigma = 0.09$ for $\omega > \omega_m$. Also, γ, is a peak enhancement factor, $\gamma = 3.3$ is usually used for North Sea conditions and $\gamma = 1$ would represent a Pierson-Moskowitz spectrum.

The wave group spectrum associated with either of these expressions can be rewritten in discrete form following Equation (3.21) as,

$$E(q\Delta\omega)=\left[\left[\sum_{n=1}^{N-q} a_n a_{n+q} \cos(\Delta\varepsilon_{n,n+q})\right]^2+\left[\sum_{n=1}^{N-q} a_n a_{n+q} \sin(\Delta\varepsilon_{n,n+q})\right]^2\right]^{1/2} \qquad (4.3)$$

where, $a_n = \sqrt{S(\omega_n)\Delta\omega}$, $a_{n+q} = \sqrt{S(\omega_{n+q})\Delta\omega}$, ε, randomly chosen phase component and $\Delta\omega$ is the frequency resolution at which $S(\omega)$ is represented. This group spectrum is in turn related to the forcing spectrum by means of the force coefficents described in Section 3.3. The $\Delta\omega$ value is an important feature in terms of the spectrum representation. If too large, the predicted response may underestimate or possibly not indicate the response at the resonant frequency. It would therefore be convenient to express this value of $\Delta\omega$ in terms of the characteristics of a particular moored system.

4.2 Wave Modelling

The modelling of waves via a spectrum in order to investigate the response of a particular structure must produce the wave heights, slopes and groups that will occur in its natural environment and most influence its response. The usual methods of wave simulation can be classified into two main areas; (1) manipulation of pseudo-random signals by means of transfer functions chosen for specific spectral characteristics and; (2) the generation of a wave train in the time domain under the assumption that the surface elevation is Gaussian distributed and that phase of frequency components form a uniform distribution. An alternate technique belonging to this second category derives its source of random noise from a Gaussin distributed real and imaginary, white spectrum.

The first of these two categories is a 'deterministic' method where a given spectral density is appropriately digitized and square rooted. The spectrum is then paired with random phases selected from a uniform random number source with mean of zero and standard deviation of $\pi/2$. The latter case is a 'probabilistic' method where the square root of the desired spectrum is used as a filter which is multiplied with a Gaussianly distributed real and imaginary white spectrum. The result leads to a randomization of the spectrum which is more like that encountered in nature. If the spectrum is represented by equidistant frequencies the repeat period which is inversely proportional to the frequency difference. This method does not provide any means of controlling the grouping characteristics of the resulting wave train.

In order to control these phase characteristics Funke and Mansard (1979) have presented a means of synthesizing the phase associated with

the energy spectrum such that the resulting wave train will have the desired group characteristics. A brief description of this method is outlined as follows:

i) a desired SIWEH is first determined. The SIWEH is described in Chapter 2.

ii) a phase modulating function is setup such that the higher frequencies are contained in a low group area.

ii) a phase modulated sinusoid is then generated with the frequencies arranged in accordance with the modulating function and containing a frequency range equal to the desired spectrum.

iii) this phase modulated sinusoid is then weighted with the square root of the desired SIWEH and a Fourier transform performed, resulting in a magnitude as well as a phase spectrum.

iv) the resulting phase is then paired with the required magnitude spectrum and an inverse Fourier transformation yields a wave train with the proper grouping characteristics.

A second method of wave simulation presented by Spangenberg (1980) generates a surface elevation $\zeta_a(t)$ at some fixed station as,

$$\zeta_a(t) = \lim_{N\to\infty} \sum_{n=1}^{N} a_n' \cos\left(\omega_n(t) + \varepsilon_n\right) \tag{4.4}$$

where

$$a_n^2 = S(\omega_n)\,\Delta\omega \tag{4.5}$$

$$\omega_n(t) = \omega_n' \pm r_n(t) \tag{4.6}$$

also,

$$-\frac{\omega_n' - \omega_{n-1}'}{2} \leq r_n(t) \leq \frac{\omega_n' - \omega_{n-1}'}{2} \tag{4.7}$$

The introduction of the $r_n(t)$ term in Equation (4.6) overcomes the problem of harmonically relating the spectral components. This value is chosen at random from an assumed uniform distribution and will cause a shift in the frequency difference. The frequency shift can be either regularly or randomly selected during the generation of the time series. Continuity is maintained during a frequency shift if,

$$\omega_{na} t_s + \epsilon_{na} = \omega_{nb} t_s + \epsilon_{nb} \qquad (4.8)$$

where ω_{na} and ω_{nb} are the frequencies and ϵ_{na} and ϵ_{nb} are the phase components before and after the shift taking place at time t_s.

This technique enables the generation of a non-repetitive time series. However, depending on the time of the shift t_s, a portion of the simulated train can be repetitive. Therefore when using this method a sufficiently short shift time should be used.

4.3 Wave Grouping

There is very little information available on the wave group characteristics of prototype wave groups therefore it is not known what a typical group spectrum would be. Group patterns are for the most part chosen at random, however once a particular group is determined the SIWEH technique is very effective in arranging the wave pattern to follow these characteristics. This method can also be used to extend a group repeat period further than the limitations of the finite Fourier transform by first generating the longer required group period, breaking it into segments and using the energy spectrum to fill in each segment. Subsequently, these segmental groups are set together again and the complete train is run.

4.4 Response Spectra

The slow drift response spectrum, $S_R(\mu)$, is related to the forcing spectrum, $S_F(\mu)$, by the expression,

$$S_R(\mu) = TF^2(\mu)\, S_F(\mu) \tag{4.9}$$

where $S_F(\mu)$ includes all forcing contributions described in Appendix D. Consider the equation of motion of a single degree of freedom system,

$$m_a \ddot{x} + b\dot{x} + cx = F(t) \tag{4.10}$$

where m_a = effective mass

b = damping coefficient

c = restoring coefficient

For a lightly damped system with natural frequency, ω_o, given by

$$\omega_o^2 = \frac{c}{m_a} \tag{4.11}$$

The transfer function, $TF(\mu)$, of this system can be written,

$$\left|TF(\mu)\right| = [m_a^2(\omega_o^2 - \mu^2)^2 + b^2\,\mu^2]^{-1/2} \tag{4.12}$$

Writing the force spectrum, $S_F(\mu)$, in discrete form,

$$S_F(m\Delta\omega) = A \sum_{n=1}^{N-m} S(n\Delta\omega)\, S[(n+m)\Delta\omega]\, R^2(n\Delta\omega) R^2[(n+m)\Delta\omega]\Delta\omega \tag{4.13}$$

where,

$A = 2\ \rho^2\ g^2\ L^2$

L = structure length

$R(n\Delta\omega)$ and $R[(n+m)\Delta\omega]$ are force coefficients at frequencies $n\Delta\omega$ and $(n+m)\Delta\omega$ respectively

n and m are integers

Supposing for convenience that the force coefficients, $R^2(n\Delta\omega)R^2[(n+m)\Delta\omega]=1$ then the motion response spectrum can be expressed in discrete form as,

$$S_R(m\Delta\omega) = A \sum_{n=1}^{N-m} [m_a(\omega_o{}^2 - (m\Delta\omega)^2)^2 + b^2(m\Delta\omega)^2]^{-1} S(n\Delta\omega)\ S[(n+m)\Delta\omega]$$

$$= A \sum_{n=1}^{N-m} [m_a(\omega_o{}^2-(m\Delta\omega)^2)^2 + b^2(m\Delta\omega)^2]^{-1}\ S_F(m\Delta\omega) \qquad (4.14)$$

Dividing numerator and denominator of Equation (4.14) by b^2, the Equation can now be expressed in non-dimensional form as,

$$\frac{S_R\ (m\Delta\omega)}{S_F\ (m\Delta\omega)}\ b^2 = \left[\left[1 - \left(\frac{m\Delta\omega}{\omega_o}\right)^2\right]^2 + \left[2\ \zeta\ \left(\frac{m\Delta\omega}{\omega_o}\right)^2\right]^2\right]^{-1} \qquad (4.15)$$

where $\zeta = c/2\ m_a\ \omega_o$

Consider a response spectrum of width $\mu_1 - \mu_2$ such that the response at frequencies μ_1 and μ_2 represent $\frac{1}{2}$ of the peak of the response spectrum. Then, when $m_1\Delta\omega = \mu_1$ or $m_2\ \Delta\omega = \mu_2$

$$S_R(\mu_1) = S_R(\mu_2) = S_R(\omega_o)/2 = \frac{1}{2}\ \frac{S_F(\omega_o)}{b^2\ 2\ \zeta}$$

Substituting these values into Equation (4.15) and rearranging the terms yields,

$$\left(\frac{m\Delta\omega}{\omega_o}\right)^4 - 2(1-2\zeta^2)\ \left(\frac{m\Delta\omega}{\omega_o}\right)^2 + (1-8\zeta^2) = 0 \qquad (4.16)$$

Solving for $(m\Delta\omega/\omega_o)^2$,

$$\left(\frac{m\Delta\omega}{\omega_o}\right)^2 = (1-2\zeta^2) \pm 2\zeta\sqrt{1+\zeta^2} \qquad (4.17)$$

Assuming $\zeta << 1$ the roots of Equation (4.17) are,

$$\frac{(\mu_2^2 - \mu_1^2)}{(\omega_o)^2} = 4\zeta \simeq 2\,\frac{(m_2 - m_1)\,\Delta\omega}{\omega_o} \qquad (4.18)$$

Therefore, the frequency difference $\Delta\omega$ is expressed as,

$$\Delta\omega = \left| \frac{2\,\omega_o\,\zeta}{m_2 - m_1} \right| \qquad (4.19)$$

4.5 Sample Calculations

Sample calculations were used to investigate the effects of varying the frequency difference on the response spectrum. The primary objective of this exercise was to suggest a basis for defining a minimum resolution based on structural response properties such as damping and natural frequency. Figure 4.1 illustrates the effects of the γ factor on the JONSWAP spectrum and subsequently the groupiness associated with these. In the Figure, γ values of 1 to 5 are used. These spectra are assumed to be continuous. However, if these spectra are modelled by means of time series of finite length and containing therefore only a finite number of frequency components, the groupiness spectrum as described can vary depending on the choice of phase.

Figure 4.2 shows the effect of damping on a moored structure. The system used has a mass of 166 kg and a restoring coefficient of 12.90 N/m. Consider also for demonstration purposes that the force coefficients in Equation (4.13) are equal to unity, then the grouping spectra in Figure 4.1 will represent the shape of the second-order forcing spectra. Consequently, varying the resolution of the input wave spectrum will in turn vary the resolution of the input forcing spectrum.

Figure 4.3 shows the response of the systems illustrated in Figure 4.2 for a range of frequency resolutions ranging from continuous to $2\omega_o$, in terms of their RMS values. The input spectrum in this case is a modelled JONSWAP with $\gamma = 3.3$ and a ω_m value of 0.75 Hz. This Figure indicates that for $\Delta\omega/\omega_o$ ratios of less than 0.12 there is very good agreement between the RMS response values predicted by a continuous spectrum and those predicted by the modelled spectrum. The results imply that the necessary resolution can be related to both the natural frequency and the amount of damping in the system. This would indicate that the resolution allowable for any model spectrum would be unique to the system being tested. In view of the results obtained from the present analysis it is recommended that the frequency difference satisfy the following minimum requirements,

$$\Delta\omega < \zeta\ \omega_o \tag{4.20}$$

and

$$\Delta\omega < 0.1\ \omega_o \tag{4.21}$$

CHAPTER 5

Wave Tank Calibration and Model Tests

The following chapter describes the wave tank facility at Memorial University and gives a detailed description of the procedures used to calibrate and generate both regular and irregular waves . A description of the methods used to generate wave groups for model tests is also outlined. Following the tank calibration a series of model tests were run and the results are used to evaluate the model developed in Chapter 3.

5.1 First-Order Wave Generation

Gilbert et al (1971) derived dimensionless expressions which relate waveboard displacement to surface profiles for piston type wave generators. These expressions were presented for both regular and random wave generation. In the case of regular waves the operating conditions are defined by the required wave period, T, and water depth h, at the waveboard. Combining these parameters yields a dimensionless variable,

$$\eta_1 = \frac{h}{gT^2} \tag{5.1}$$

where g is acceleration due to gravity. The amplitude of the board stroke, s, and the wave amplitude, a_m, are given by

$$G = \frac{a_m}{s} \tag{5.2}$$

The waves of a random sea state are irregular in height and period, therefore the board stroke and the forces required for the generation of such a sea are similarly irregular. Thus the waves can

no longer be defined in terms of a height and period; instead the sea state is defined by its energy spectrum and variations in wave height must be considered in statistical terms. The statistical properties of waves depend on the mean square water surface elevation and the spectral width parameter both of which can be calculated from the spectrum.

For random wave generation Gilbert et al (1971) have defined a variable

$$V_1 = \frac{ghF}{U^2} \qquad (5.3)$$

where the prototype wind speed U is to be modelled at a linear scale F in a flume of water depth h. Values of V_1 are related to a dimensionless mean square waveboard stroke H_1,

$$H_1 = \frac{M}{h^2} \qquad (5.4)$$

where M, is the mean square value of the paddle displacement. Once a prototype wind speed and scale factor have been established a nondimensional curve can be used to obtain the mean square value of the board stroke.

5.2 Second-order Wave Generation

Sand (1982) has presented equations to generate second-order control signals to correct for group bounded waves in wave modelling. In the analysis a number of long waves have been identified, one of which is a free long wave caused by first-order local disturbances and a second is due to wave board displacement. Another free second-order wave which originates from group bound long waves is defined as a

parasitic long wave. The extent to which each of these waves dominates is dependent on a number of parameters such as frequency difference, water depth and frequency range.

Appendix E describes the development of the second-order signal used to eliminate free long wave components resulting from first-order wave generation and thereby setting-up correct group bounded long waves. The Appendix indicates that in order to construct a second-order control signal for a spectrum each possible combination consisting of two components must be included. This will obviously require an immense amount of calculations.

An approximation for the control signal is given by Barthel et al (1983) as,

$$X^{(2)}_{nm}(t) = (a_n b_m - a_m b_n)\, F_1 \cos(\Delta\omega_{nm} t) + (a_n a_m + b_n b_m)\, F_1 \sin(\Delta\omega_{nm} t) \qquad (5.5)$$

Values of F_1 can be found in Figure E.1. As indicated in the Figure, F_1 is a function of f_n and f_m where $\Delta\omega_{nm} = 2\pi(f_n - f_m)$. It seems that a further approximation of this method would be to choose a value $F_1(\Delta f, f_p)$ which would give the best representation of the second-order wave spectrum corresponding to the frequency band of the resonant frequency of the system under investigation, thus giving a good representation of the second-order wave spectrum most influencing the slow drift response. Therefore Equation (5.5) can be rewritten as,

$$X^{(2)}_{nm}(t) = F_1(\Delta f, f_p)\,[(a_n b_m - a_m b_n)\cos(\Delta\omega_{nm} t) + (a_n a_m + b_n b_m)\sin(\Delta\omega_{nm} t)] \qquad (5.6a)$$

This expression is easily adapted to the SIWEH as,

$$x^{(2)}_{nm}(t) = F_1(\Delta f, f_p)\, E(t) \qquad (5.6b)$$

where E(t) is defined by Equation (3.21).

In the above expressions Δf is chosen to correspond to the resonant frequency of the system found from still water tests and f_p is the peak frequency of the first-order wave spectrum. Following Equation (5.6b) an estimate of the second-order wave profile can be computed from the SIWEH. Once again from Figure E.2 it can be seen that G_{nm} is a function of both f and Δf. Similar to Equation (5.6a) an approximation for the second-order wave profile is written as,

$$\xi_{nm}(t) = G_{nm}(\Delta f, f_p)\,[(a_n b_m - a_m b_n)\cos(\Delta\omega_{nm}t) + (a_n a_m + b_n b_m)\sin(\Delta\omega_{nm}t)] \qquad (5.7a)$$

Once again this expression is adapted to the SIWEH as,

$$\xi_{nm}(t) = G_{nm}(\Delta f, f_p)\, E(t) \qquad (5.7b)$$

5.3 Calibration Procedure

The preceding sections indicate that the second-order wave spectra are dependent on a good representation of the first-order spectral. There are two methods employed to generate these spectra in the wave tank. These are outlined in Figure 5.1. In the first method a closed-loop system is used. Here the spectrum is smoothed to its desired shape through an iterative process using information obtained from the feedback loop. This method does not consider phase and only spectral magnitudes are matched. In the second method phase is considered and using this method the sequence at which the waves pass a particular station in the tank can be controlled. This is achieved

by dividing the input drive signal with a transter function. This transter function between the input drive signal and the resulting wave profile sets the delay required for each of the lower frequency components. Thus the correct sequence of waves is generated at the test location in the tank.

The wave tank facility used in the model tests is shown in Figure 5.2. The tank is a reinforced concrete structure with inside dimensions of 58.7 m (length) x 4.57 m (width) x 3.0 m (depth) and a maximum operating water depth of 1.83 m. One end of the tank is provided with a hydraulically operated piston-type generator. An aluminum waveboard is driven by a hydraulic actuator having a 48.8 kN force capability over a 50 cm stroke. A water tight seal is maintained by means of a pneumatic sealing gasket. Glass viewing windows along one side of the tank are used for observations at both surface and subsurface elevations. Waves are measured using conductivity type probes and are dissipated by a beach. The beach surface is covered with crosshatched wooden strips supported by a steel frame: slope 1:20. The wave generator is a closed loop servo controlled mechanism controlled by analog signals which are input into the system through a port on the control console. Input signals are generated by means of an on-line Hewlett- Packard 5451 Fourier Analyzer computer.

The performance curves of the wave generator are compared to Equations (5.1) and (5.2) in Figure 5.3. In order to establish the transfer functions required to control the generator the flat noise spectrum shown in Figure 5.4 was input into the wave controller. Figure 5.5 illustrates the transfer function between the input signal and the waveboard displacement. As can be seen from the Figure the

response is very flat with a small fall in on the upper part of the frequency range. The transfer function between the waves generated by the input noise at a station 30 m from the mean position of the waveboard at a water depth of 1.25 m and the input signal itself is ehown in Figure 5.6. Very good coherence was found for frequencies less than 1.0 Hz. This transfer function is actually used in the second method illustrated in Figure 5.1. The drop off in the coherence function at low frequency is attributed to reflections and group bounded waves that are described in a previous section. Reflection coefficients were also determined using the least squares method described by Mansard and Funke (1980). Results of these reflection coefficients are shown in Figure 5.7.

Using the second method outlined in Figure 5.1 employing the transfer function in Figure 5.6, fifteen wave groups were modelled for varying frequency differences at the position which would later correspond to the center of the model. These wave groups were generated to simulate JONSWAP spectra with $\gamma = 3.3$ and an ω_n wave of 0.075Hz using randomly chosen phase components. The details of these spectra are given in Table 3. A sample of a group for each of the frequency differences is illustrated in Figures 5.8 to 5.14. These SIWEH spectra were determined by the technique outlined in Figure 5.15. This method gives essentially a rectangular smoothing but uncouples an overlap between frequencies of the SIWEH spectrum and the first-order wave spectrum. This effect is caused when large frequency differences in the first-order spectrum are equal to frequencies of the SIWEH spectrum, occuring when the minimum frequency of the first-order

spectrum is less than the largest difference produced from the spectrum. Comparisons between target and measured profiles for a sample of the groups are shown in Figures 5.16 and 5.17. Good agreement was found for certain cases. Agreement decreases with increased frequency difference. The second-order profiles of these sample groups are compared in Figure5.18 and 5.19 where the groups were generated with and without second-order control signals. Preliminary tests on the barge indicated that the resonant frequency of the barge was 0.039 Hz. Therefore a Δf value of 0.039 Hz was used with a f_p value of 0.75 Hz. These values were then used with Equation (5.7b), to determine the second-order profiles. The second-order generator signal was established using Equation (5.6b) and the resulting second-order profile was found using a moving window.

5.4 Experimental Set-Up

A set of model tests were carried out on the simple model illustrated in Figures 5.20 and 5.21. The wave absorbers on the sides of the wave tank were constructed of nylon netting hung from the top of the tank walls. They had no apparent effect on wave blockage. The model is a rectangular barge 75 cm x 90 cm x 50 cm submerged to a draft of 25 cm. The barge was moored at a station in the tank approximately 37 m from the mean position of the waveboard in a water depth of 1.25m. The counter weight shown in Figure 5.21 had a mass of 1.0 kg.

This mass is small in comparison with the total mass of the barge and therefore assumed to have negligible effect on the overall response. The damping coefficient used in the equation of motion was determined from the logarithmic decrement found from the model oscillating in still water. This coefficient was checked using the half power method and the resulting damping ratio was found to be 0.35. The mooring line was equipped with a linear spring the restoring coefficents of which are shown in Figure 5.22. The centre of gravity was located at the center of the barge in an attempt to minimize the waves scattered by the barge motion itself. Surge motions were measured by means of a rotary potentiometer located a sufficient distance from the model as not to be influenced by any of the other motions and the anchor was strain gauged to monitor the force in the mooring line during each run. All instrumentation was checked regularly during each testing day to ensure consistant outputs.

The barge was tested in regular waves, regular wave groups, i.e. groups consisting of two frequencies, and a number of wave groups of varying groupiing characteristics and frequency resolutions. Each wave condition was precalibrated at the test location, with and without second-order compensation and the corresponding input signals were stored and played back with the barge in location. In order to correlate the input control signal and the resulting wave pattern, the input signal was recorded simultaneously with the response data. Subsequently the transfer function in Figure 5.6 was used to determine the profile at the time the barge response was recorded thus providing phase information between the wave group and response motion.

5.5 Regular Wave Test

In order to determine the steady drift components, the barge was first subjected to trains of regular waves having an amplitude of 5 cm for all cases of a frequency range between 0.02 Hz to 2.00 Hz at increments of 0.10 Hz. The surge response of the barge was monitored from the start of each wave train for a 4 min. duration with the force being measured by the force transducer shown in Figure 5.21. A sample of a run is shown in Figure 5.23.

5.6 Regular Wave Group Tests

The barge was also subjected to regular wave groups or "beating waves", whose beat frequencies were equal to 0.5 f_o, 1.0 f_o, 1.5 f_o and 2.0 f_o with a constant group amplitude of 5 cm. The waves were generated from base frequencies of 0.7 Hz, 0.9 Hz and 1.5 Hz with and without second-order control compensation. Surge motion and mooring loads were monitored from start to five cycles of steady-state. A sample of the steady state condition for a run is shown in Figure 5.24.

5.7 Irregular Wave Group Tests

The model was also subjected to the fifteen precalibrated wave group described in Section 5.3. Each run had a duration of 20 min., after the first 5 min. a sample was taken for the next 15 min.. The repeat period of each spectrum is indicated by its frequency difference. Transfer functions between the slow drift response and the $SIWEH_m$ spectra were determined for each of the response spectra by

using the method as shown in the following expression,

$$TF(f) = \frac{(x_1^{(2)}(t))}{(E_m(t))}$$

where $x_1^{(2)}(t)$ represents the Fourier transform of the slow drift response and $E_m(t)$ is the Fourier transform of $SIWEH_m$. In each case the wave profile measured during the calibration of the groups was used to generate the $SIWEH_m$.

CHAPTER 6

COMPARISON BETWEEN ANALYTICAL AND EXPERIMENTAL MODELS

The analytical model used to determine the slow drift coefficients described in Equation (3.10) is based on the "far field" approach of Faltinsen and Michelsen (1974). Details of the derivation of the working formula based on Green's Function are described in Appendix D. This technique was chosen over the "near field" field technique of Pinkster primarily on the basis of its reduced computational effort. The output of the program is the steady drift coefficient for regular waves. This information allows only a comparison of the magnitudes of the measured and predicted transfer functions.

A panel schematization of the model is illustrated in Figure 6.1. Advantage was taken of the symmetry about the longitudinal plane and computations were carried out using only 36 panels. Forty values of the steady drift coefficient were established for a frequency range between 0.20 Hz and 2.00 Hz. A cubic spline technique was then used to produce a curve of 400 points. Slowly-varying force contributions from the set-down were determined using the expression given by Equation (3.15). Contributions from the first-order waves were determined using Equations (3.8). These were applied to estimate the second-order forces as per Equation (3.9). A comparison between the two is shown in Figure 6.2. The first-order wave effects are illustrated in a non-dimensional form of the slowly-varying force oscillating at a frequency $\Delta f = \Delta\omega_{nm}/2\pi$ with the two constituent frequencies equal to f and $f+\Delta f$. The second-order wave effects of the "set-down" wave are also shown in the Figure. These values increase

with increased values of $\Delta f/f_o$. The broken line indicates the limit of the force that can be produced from a spectrum with a cut-off frequency of 2.00 Hz by a set-down wave caused by a wave group containing waves of frequencies f and f+Δf. Comparison between the two contributions indicates that the second-order wave effects are very small in relation to the forces caused by first-order waves.

6.1 Results in Regular Waves

The steady drift coefficients determined from the regular wave tests are compared to those predicted by the computer model in Figure 6.3. There is relatively good agreement for the range of frequencies tested. The steady drift effects are small up to a frequency of 0.50 Hz corresponding to a wavelength to barge length ratio of 6:1. Above this value the steady drift effect quickly increases.

6.2 Results in Regular Wave Groups

The response of the barge to regular wave groups is shown in Figure 6.4. As indicated in the Figure the response is dependent on the constituent frequencies of the group. Thus the pairs generated from the base frequency of 0.90 Hz produced the largest response values. The experimental results in the Figure were determined with and without inclusion of the second-order control programs. Negligible difference was found for the two methods. This is predicted by Figures (6.2) and (E.1). As mentioned above Figure (6.2) shows that the second-order wave contributions are much smaller than those of the first-order waves. Also Figure E.1 gives relatively small correction

coefficients, F_1, for the water depth and frequency differences used for these model tests.

In general the results in regular wave group tests agree well with the analytical model for frequencies less than the resonant frequency of the moored barge. Discrepancies increase with increasing group frequency above this level. This large disagreement may be explained as follows. The amplitude of the transfer function for the low frequency drift oscillation is found by dividing the measured height, peak to peak, of the measured low frequency oscillation by $4a_1a_2$, where a_1 and a_2 are the amplitudes of the regular wave components. In wave groups of frequencies larger than surge resonant frequency of the moored model, a free motion condition was excited which caused the model to oscillate at a frequency very close to its resonant frequency. This free motion when superimposed on the response affected by the wave group itself produced a larger oscillating motion than that expected from the wave group alone. This behavior indicates an obvious limitation of the assumption upon which the analytical model described in Section (3.1) is based. This condition will be referred to as a "free motion response".

6.3 Results In Irregular Wave Groups

A sample of the measured slowly oscillating drifts response spectral densities for each of the frequency differences is shown in Figures 6.5 to 6.11. Included in the Figures are the corresponding SIWEH spectral densities. Transfer functions determined from each of the sets of measured results are compared to the analytical model

developed in Chapter 3. Figures 6.12 to 6.18 show this comparison for each of the frequency differences indicated in the Figures. The comparisons indicate that the analytical model underestimates the response of the barge up to the resonant frequency and above this value the analytical model gives an overestimation of the response. This effect is attributed to the fact that the slowly oscillating drift response of the barge contained both steady state and free motion components. A Fourier decomposition of the measured slowly varying drift response will result in low frequency components related to changes in the mean position of the model as described in Section (3.2). When these free motion components are added to the components which are directly related to the SIWEH at these frequencies, the result is larger response components than those predicted by the SIWEH alone. This trend was consistant regardless of the frequency difference or grouping characteristics of the waves. The phase component of the transfer functions show a large lag between the wave group and the response motion. This is due mainly to the large inertial effects of the system.

Since the results of the experimental transfer functions showed consistent trends, not withstanding their deviation from the analytical model, it is assumed that the differences in the free motion response with respect to each wave group are small compared to their total effect. Therefore the experimental data for both real and imaginary components were smoothed using a cubic spline technique in order to determine an experimental transfer function. The result is compared in polar form to the analytical model in Figure 6.19. The Figure shows

the experimentally determined transfer function for the data and the magnitude of the transfer function determined from Equation (3.23). The phase component of the analytical transfer function was not obtainable from the present model since the 'far field' method was used. Therefore, the experimental phase components were associated with the analytical magnitude component to form a semi-empirical transfer function. Both these transfer functions were used to predict the response of the model to six groups not included in the first set of tests. The details of these groups are given in Table 4. A time domain comparison of the measured slow drift response and those predicted by both transfer functions to these six groups are given in Figures 6.20 to 6.26. The results were compared in terms of the RMS value of the slow drift response, the maximum displacement of the barge model and the duration above one-third this maximum value. These values are compared in Table 5. Results indicate the free motion response had an obvious effect on the response of the barge. Each of the measured values was higher than that predicted by the analytical model. However agreement was improved when the experimental transfer function was used.

CHAPTER 7

DISCUSSION AND CONCLUSIONS

The following Chapter discusses the work that has been carried out in the preceding study by reviewing each of the chapters. The discussion is thereby based on the relevance of the topic covered in each chapter to the overall study. Conclusions based on the results found in the present study are presented and finally recommendations for further studies are made.

7.1 Discussion

Chapter 2 gives a review of the literature dealing with both wave grouping and the slowly oscillating drift response of moored floating structures. The review showed that the wave grouping highly influences the slow oscillating response of large floating structures. The disagreement shown between the analytical models and observations of field data suggests that the surface elevation of the sea is not purely random. Therefore studies of wave group loading on structures which are based on Rayleigh statistics may not give an accurate prediction of the worst conditions to be experienced by an offshore structure. Better representations of environmental wave conditions will require more sophisticated techniques of wave simulation. Nevertheless physical model testing is quite effective in evaluating analytical models because even though wave conditions are not completely authentic, their characteristics can be accurately determined and a comparison made on that basis. Methods to analyze wave loading on floating structures have also been reviewed in Chapter 2 and for the

most part have produced consistent results. Techniques to analyze the slow drift response of structures moored in irregular seas with both linear and non linear mooring systems were discussed. One of the inefficiencies identified in existing methods was a technique which relates the slowly oscillating drift response to the wave group causing it.

Chapter 3 proposes a model to show the relationship between the slow drift oscillations of a floating moored structure and a modified form of the SIWEH. This relationship seems to be a plausible approach since both the SIWEH and slow drift forces, including the effects of second-order wave, can be described in terms of first-order quantities. The SIWEH is described as the resultant of all regular wave group components superimposed on each other with reference to the center of gravity of the structure. The primary hypothesis of the model is that the force associated with each regular wave group is proportional to the product of the amplitudes of the waves constituting the group and varies at the same frequency but at a constant phase to that group. The resultant force is therefore the superposition of all regular wave group forces. The slow drift displacement is then determined assuming a single degree of freedom system with a linear restoring coefficient. First-order wave forces were determined using the far-field method and second-order wave forces were determined by integration of an approximated second-order pressure term over the surface of the structure. The approximation of the second-order potential, from which

the second-order pressure term used in the present analysis is established, will be most effective when contributions to the second-order diffracted waves and waves generated by structure motions are negligible. These circumstances are more applicable to the semisubmersible type structure than to large ships or barge shapes. However, increases in diffraction and body generated first-order waves result in increased contributions from the first-order waves to the total second-order drift forces, thus proportionally reducing the relative error introduced by approximations of the second-order potential. Therefore the approximate method is acceptable for purposes of comparison of contributions to the second-order drift forces.

The next step in the study was to determine the number of regular wave components required to approximate an irregular wave group. Chapter 4 illustrates the effects of varying the frequency difference of a modelled wave spectrum. This illustration is done by way of comparing moments of response spectra for a particular system when only the damping characteristics are changed. The results indicate that the number of components increases with decreased damping coefficients. This result means that lower damped systems produce higher and more peaked response spectra and therefore require more points to accurately describe them than does a flatter response spectrum. This peaked effect would be more applicable to a streamlined shape such as a slender ship or semisubmersible than to barge type structures. Since the model tested in the present study did not have a high narrowband response spectrum a critical experimental evaluation of the method was not possible.

However it is suggested that it can be done in the following manner. First recall that the shape of the response spectrum is determined by the SIWEH spectrum which in turn is dependent on the choice of phase paired with the first-order wave spectrum. Set up any moored system with variable damping capability and model the same SIWEH spectrum at different frequency resolutions thus giving the same shape for the response spectra. The rms value of the slow drift response should therefore approach some particular value as the number of components used to describe the SIWEH is increased.

Chapter 5 described the calibration procedures and model tests used to validate the analytical model proposed in Chapter 3. First-order wave generation was shown to be highly controllable especially for large frequency differences. The technique used to generate a particular sequence of waves at a station in the tank worked very effectively. The second-order techniques were less effective in the circumstances of the present model. This was due to the small quantities required to simulate the second-order waves. These second-order waves required large excursions at the low frequencies to generate the required long wave. The board displacements necessary when combined with the first-order wave generator were beyond the mechanical capabilities of the wave generator. This however did not invalidate the analytical model since second-order wave contributions to the slow varying drift force were negligible in comparison to first-order wave effects. Results of the calibrations indicate that the procedures used would enable generation of prototype wave trains for model tests.

Chapter 6 compares the results of the model tests to the analytical model. For the most part reasonable agreement was found. Discrepancies between the analytical and measured transfer functions were due to free motion effects. This discrepancy between the analytical and experimental results indicates an obvious limitation of the proposed model. These effects were observed to be consistant regardless of grouping characteristics or frequency differences. An average of all transfer functions was determined and the result subsequently used to predict the response of the model to a number of wave groups. The predictions of this experimental transfer function were more accurate than those of the semi-empirical transfer function. The primary difference between the two transfer functions is that unlike the semi-empirical function, the experimental version contains the effects of the force motion effects. This suggests the following: (1) free motions associated with the response of wave groups have a significant effect on the overall slow drift oscillations. (2) since those effects could be predicted by means of a transfer function, regardless of the grouping patterns, the differences in the free motions resulting from changes in the group patterns are small in comparison to the overall effect of the free motion. Increasing the frequency difference caused shorter repeat periods and also increased the heights of the waves in the group. Since the experimental transfer function still gave an accurate prediction of the response motion for these larger frequency differences, the result somewhat ratifies the assumption of relating irregular group loading to superimposed regular wave group components. Even for the steeper waves the assumption was upheld. Because agreement was consistent for the range of differences tested an upper limitation on the wave steepness could not be

determined. Also the consistant behavior of the free motions suggests that they can be related to the individual low frequency components of the response motions. It must be conceded however that the observations and use of the transfer functions are applicable only to the situations set up in this case. The barge was linearly moored which is not a practical situation. When non-linear mooring systems are used a time domain analysis is more appropriate. However when moored by a linear system the resulting motion, when uncoupled from free motions, can be used to give an indication of the second-order loading on the model caused by the wave groups.

7.2 Conclusions

Through the preceding study, as a result of the analytical model and experimental tests developed in the work, the following conclusions are made:

- There is a predictable relationship between the slowly oscillating drift motion of a moored floating structure and the SIWEH of the wave group affecting the motion.
- The assumption of superposition of regular wave groups is sufficient to predict the slowly oscillating response of a structure in an irregular wave group when first-order wave effects are dominant.
- The slowly oscillating drift response of a linearly moored floating system to any wave group that can be generated from a particular wave spectrum as a result of random phase selection, can be predicted using the transfer function established from any single group.

- Free motion responses have a significant effect on the slow drift response of a moored floating structure for group frequencies greater than the resonant frequency.

7.3 Recommendations for Further Study

On the basis of the observations and conclusions resulting from this study, the following areas are suggested for further examination:

- First it is suggested that the proposed model be tested using other structural types moored with both linear and non-linear systems.
- Additional model testing should be conducted in conditions where group bounded waves and second-order wave effects are more significant.
- Multidirectional wave grouping is also recommended as an area for further study.
- Further work could be conducted on uncoupling the free motion responses from the total response to the groups.

REFERENCES

1. Arhan, M. and Ezraty, R., 1978, "Statistical Relations between Successive Wave Heights", Oceanologica Acta, Vol. 1, No. 2.

2. Barthel, V., Mansard, E.P.D., Sand, S.E., and Vis, F.C., 1983, "Group Bounded Long waves in Physical Models", Ocean Engng., Vol. 10, No. 4, pp. 261-294.

3. Bendat, J. S., and Piersol, A. G., 1971, "Random Data: Analysis and Measurement Procedures", John Wiley.

4. Black, J. L., and Chou, B. S. J., 1979, "Calculations of Drift Forces on Moored Vessels", Proceedings on Civil Engineering in the Oceans IV, pp. 203-207.

5. Bowers, E. C., 1975, "Long Period Oscillations of Moored Ships Subject to Short Wave Seas", Proc. of the Royal Institute of Naval Architects, pp. 181-191.

6. Bowers, E. C., 1980, "Long Period Disturbances Due to Wave Groups", Proc. XVII Cont. on Coastal Engineering Sydney, Australia.

7. Burcharth, H. F., 1981, "A Comparison of Natural Wave and Model Waves with Special Reference to Wave Grouping", Coastal Engineering, 4, pp. 303-318.

8. Chakrabarti, S. K., 1980, "Steady and Oscillating Drift Forces on Floating Objects", Journal of the Waterway Port Coastal and Ocean Division, Vol. 106, WW2, pp. 205-228.

9. Chey, Y., 1964, "Experimental Determinaion of Wave-Excited Forces and Moments Acting on a Ship Model Running in Oblique Regular Waves", Davidson Laboratory Report 1046, Stevens Institute of Technology.

10. Dattatri, J., Raman, H., Jothishankar, N., 1977, "Wave Groups; Analysis of Run and Run Length", Sixth Australian Hydr. Fluid Mech Cont. Adelaide.

11. Dalzell, J.F. and Kim, C.H., 1976, "Analytical Investigations of the Quadratic Frequency Response for Added Resistance". Report SIT-DL-76-1878, Davidson Laboratory, Stevens Institute of Technology.

12. Dean, R. G., 1970, "Relative Validities of Water Wave Theories", Proc., ASCE, Waterways and Harbors Division, 96, WWI.

13. English, J. W., and Wise, D. A., 1975, "Hydrodynamic Aspects of Dynamic Positioning", Meeting of the Royal Institute of Naval Architects, pp. 53-72.

14. Faltinsen, O.M. and Loken, A.E., 1979a, "Drift Forces and Slowly-Varying Horizontal Forces on a Ship in Waves", Symposium on Applied Mathematics, Deft University Press, pp. 22-41.

15. Faltinsen, O.M. and Loken. A.E., 1979b, "Slow-Drift Oscillations on a Ship in Irregular Seas", Applied Ocean Research, Vol. 1, No. 1. pp. 21-31.

16. Faltinsen, O. M. and Loken, A. E., 1978, "Drift Forces and Slow Varying Forces on Ships and Offshore Structures in Waves", Norwegian Maritime Research, Vol. 6, No. 1, pp. 2-15.

17. Faltinsen, O. M., 1975, "Drift Forces on a Ship in Regular Waves", Research Department Report No. 75-4-5, Det Norske Veritas.

18. Faltinsen, O. M. and Michelsen, F., 1974, "Motions of Large Structures in Waves at Zero Froude Number", Proceedings of International Symposium on the Dynamics of Marine Vehicles and Structures in Waves, London, England.

19. Funke, E. R., and Mansard, E. P. D., 1979, "On the Synthesis of Realistic Sea States in a Laboratory Flume", Report No. LTR-HY-66, NRC, Ottawa, Ontario.

20. Gerritsma, J., and Benkelman, W., 1970, "Analysis of the Resistance Increase in Waves of a Fast Cargo Ship", International Shipbulding Progress, Vol. 19, No. 217, pp. 285-293.

21. Gilbert, G., Thompson, D.M. and Brewer, A.J., 1971, "Design Curves for Regular and Random Wave Generators", Journal of Hydraulic Research, Vol. 9, pp. 163-196.

22. Goda, Y., 1970, "Numerical Experiments on Wave Statistics with Spectral Simulation", Report of the Port and Harbr Res. Inst. Japan, Vol. 9, No. 3, pp. 3-57.

23. Goda, Y., 1976, "On Wave Groups", Proceedings, Conf. on Behaviour of Offshore Structures, Trondheim, Vol. 1, pp. 115-128.

24. Goda, Y., 1983, "Analysis of Wave Grouping and Spectra of Long-Trevelled Swell", Rept. Port and Harbour Res. Inst., March 1983.

25. Gravesen, H. and Ottesen Hansen M. E., 1979, "Long Period Oscillations Generated by Wave Groups", Symposium on Long Waves in the Ocean, Marine Sciences Directorate Manuscript Report, Series No. 53.

26. Harris, L. M., 1972, "An Introduction to Deepwater Floating Drilling Operations", Petroleum Publishing Co., Tulsa, Oklahoma.

27. Havelock, T.H., 1942, "The Drifting Force on a Ship Among Waves", Philosophical Magazine, Series, 7, Vol. 33 pp. 467-475

28. Hsu, F. H., and Blenkarn, K. A., 1972, "Analysis of Peak Mooring Force Caused by Slow Vesel Drift Oscillation in Random Seas", OTC 1159.

29. Huse, E. 1976, "Wave Induced Mean Force of Platform in Direction Opposite to Wave Propagation", Interocean.

30. Johnson, R.R., Mansard, E.P.D., and Ploeg, J., 1978, "Effects of Wave Grouping on Breakwater Stability", Proc. 16th Coastal Engineering Conference, Hamburg, Germany.

31. Kaplan, P. And Sargent, T.P., 1976, "Motions of Offshore Structures as Influenced by Moorings and Positioning Systems", Proceedings of the Conference on the Behaviour of Offshore Structures, pp. 248-262.

32. Kim, C. H., and Chou, F., 1970, "Prediction of Drifting Force and Momentum on an Ocean Platform Floating in Oblique Waves", SIT-OE-70-2, Ocean Engineering Department., Stevens Institute of Technology.

33. Kimura, A., 1980, "Statistical Properties of Random Wave Groups", Proc. Seventeenth Coastal Eng. Conf. Sydney.

34. Kinsman, B., 1965, "Wind Waves: Their Generation and Propagaton on the Ocean Surface", Prentice-Hall.

35. Laitone, E. V., 1961, "Higher Order Approximation to Non-linear Water Waves nd the Limitary Heights of Croidal Solitary and Stokes Waves", Hydraulic Engineering Laboratory, Univ. of California, Berkeley, Technical Report, Series 89, Issue 6.

36. Lalangas, P. A., 1963, "Lateral and Vertical Forces and Moments on a Restrained Series 60 Model in Oblique Regular Waves", Davidson Laboratory Report 920, Stevens Institute of Technology.

37. LeBlond, P. H., 1982, "A Preliminary Review of Nonspectral Wave Properties: Grouping, Wave Breaking and "Freak" Waves", Can. Contract. Rep. Hydrogr. Ocean Sci., 1:66 p.

38. Lim, W. C. and Reed, A. M., 1976, "The Second-Order Steady Force and Moment on a Ship Moving in an Oblifque Seaway", The Office of Naval Research, Proceedings on the 11th Symposium on Naval Hydrodynamics.

39. Longuet-Higgins, M. S. and Stewart, R. W., 1964, "Radiation Stresses in Water Waves; a Physical Discussion with Applications", Deep Sea Res, 529-562.

40. Longuet-Higgins, M. S., 1952, "On the Statistical Distribution of the Heights of Sea Waves", Journal of Marine Research, Volume XI, Number 3.

41. Mansard, E.P. and Pratte, B.D. 1982, "Moored Ship Response in Irregular Waves", Proc. Eighteenth International Conference on Costal Engineering.

42. Mansard, E. P. and Funke, E. R., 1980, "The Measurement of Incident and Reflected Spectra Using a Least Square Method". Proc. Seventeenth International Conference on Coastal Engineering, March 1980

43. Maruo, H., 1960, "Wave Resistance of a Ship in Regular Head Seas", Bulletin of Faculty of Engineering, Yokohoma National University, Vol. 9, pp. 337-345.

44. Molin, B., 1979, "Computations of Wave Drift Forces, 1979", OTC 3627, pp. 2337-2344.

45. Naess, A., 1978, "On Experimental Prediction of Low-Frequency Oscillations of Moored Offshore Structures", Norwegian Maritime Research No. 3.

46. Nath, J.H., 1967, "The Dynamic Response of Fixed Offshore Structures of Periodic and Random Waves", Ph. D Thesis, Massachusetts Institute of Technology.

47. Nelson, A.R., 1980, "Statistical Properties of Ocean Wave Groups", M.Sc. Thesis, Naval Postgraduate School, Monterey, California, U.S.A.

48. Newman, J. N., 1974, "Second-Order Slow-Varying Forces on Vessels Marine Vehicles and Structures in Waves, London, pp. 182-186.

49. Newman, J. N., 1967, "The Drift Force and Moment on Ships in Waves", Journal of Ship Research, Vol. 11, No. 1, pp. 51-60.

50. Nolte, K. G., and Hsu, F. H., 1972, "Statistics of Ocean Wave Groups", OTC 1688, pp. 637-644.

51. O'Dea, J. F., 1974, "Low Frequency Forces on a Body in Random Waves", Ph.D. Thesis, Massachusetts Institute of Technology.

52. Ogawa, A., 1967, The Drifting Force and Moment on a Ship in Oblique Regular Waves", International Shipbuilding Progress, Vol. 14, No. 149.

53. Olsen, O. A., Braathen, A., Loken, A. E., Nyhus, K. A. and Torset, O. P., 1978, "Slow and High Frequency Motions and Loads of Articulated Single Point Mooring Systems for Large Tankers", Norwegian Maritime Research, No. 2, pp. 14-28.

54. Ottensen-Hansen, N. E., 1978, "Long period waves in Natural Wave Trans," Progress Report No. 46, Inst. Hydrodyn. and Hydraulic Eng., Techn. Univ. of Denmark, pp. 13-24.

55. Pierson and Moskowitz, L., 1964, "A Proposed Sprectal Form for Fully Developed Wind Seas Based on the Similarity Theory of S.A. Kitaigorodskii", Journal of Geophysical Research, Vol. 69, No.24.

56. Pijfers, J. G. L. and Brink, A. W., 1977, "Calculated Dri of Two Semisubmersibles Platform Types in Regular and Irr Waves, OTC 2977, pp. 155-164.

57. Pinkster, J. A., 1981, "Mean and Low Frequency Forces on Semisubmersibles", OTC 3951, pp. 9-19.

58. Pinkster, J. A. and Hooft, J. P., 1978, "Low Frequency Drifting Forces on Low Frequencies in Waves", Fifth International Ocean Development Conference, Tokyo.

59. Pinkster, J. A. and van Oortmerssen, 1977, "Computation of the First and Second-Order Wave Forces on Bodies Oscillating in Regular Waves", Proceedings of the Second International Conference on Numerical Ship Hydrodynamics, University of California, pp. 136-156.

60. Pinkster, J.A., 1975, "Low-Frequency Phenomena Associated with Vessels Moored at Sea", Society of Petroleum Enginers, Journal V. 15, pp. 487-494

61. Remery, G. F. M. and van Oortmerssen, G., 1973, "The Mean Wave, Wind and Current Forces on Offshore Structures and Their Role in the Design of Mooring Systems", OTC 1741, pp. 1170-1184.

62. Remery, G. F. M., and Hermans, A. J., 1971, "The Slow Drift Oscillations of a Moored Object in Random Seas", OTC 1500.

63. Roberts, J. B., 1981, "Nonlinear Analysis of Slow Drift Oscillations of Moored Vessels in Random Seas", Journal of Ship Research, Vol. 25, No. 2, pp. 130-140.

64. Rye, H., 1981, "Ocean Wave Group", Ph.D. Thesis, The University of Trondheim, The Norwegian Institute of Technology.

65. Rye H., 1974, "Wave Group Formation Among Storm Waves", Proc. of 14th Coastal Engineering Conference, 1, 1964-183.

66. Rye, H. and Lervik, E., 1980, "Wave Grouping Studies by Means of Correlation Techniques", Norwegian Maritime Research, No. 4, pp 181-190.

67. Rye, H., Rynning, S. and Moshagen, H., 1975, "On the Slow Drift Oscillations of Moored Structures", OTC 2366.

68. Salvesen, N., 1974, "Second-order Steady-state Forces on Surface Ships in Oblique Regular Waves", International Symposium on the Dynamics of Maritime Vehicles and Structures in Waves, University College, London, England, pp. 212-226.

69. Salvesen, N., 1978, "Added Resistance of Ships in Waves", Journal of Hydrodynamics, Vol. 12, No. 1, pp. 24-34.

70. Sand, S. E., 1982, "Long Wave Problems in Laboratory Models", J. 1 Watways, Port, Coastal Ocean Div. Am. Soc. Civ. Engrs. 108, (WW4) 492-503.

71. Sedivy, G., 1978, "Ocean Wave Group Analysis", M.Sc. Thesis, Nava Postgraduate School, Monterey, California, U.S.A.

72. Sibul, O. J., 1971a, "Ship Resistance in Uniform Waves", Report No. NA 71-1, College of Engineering, University of California, Berkeley.

73. Sibul, O. J., 1971b, "Measurements and Calculations of Ship Resistance in Waves", Report No. NA-71-2, Parts I & II, College of Engineering, University of California, Berkeley, and NA-71-3.

74. Spangenberg, S. 1980, "With Effects of Wave Grouping on Slow Drift Oscillations of an Offshore Structure", Danish Ship Research Laboratory, Madelelse Bulletin No. 46.

75. Spens, P. and Lalangas, P., 1962, "Measurements of the Mean Lateral Force and Yawing Moment on a Series 60 Model in Oblique Regular Waves", Davidson Laboratory Report 880, Stevens I of Technology.

76. Spens, P. and Lalangas, P., 1962, "Measurements of the Mean Lateral Force and Yawing Moment on a Series 60 Model in Oblique Regular Waves", Davidson Laboratory Report 880, Stevens Institute of Technology.

77. Standing, R. G. Dacunka, N.M.C., and Matten, R. B, 1981, "Slow Varing Second-Order Wave Forces: Theory and Experiment", National Maritime Institute, Report OT-R-8221.

78. Standing, R. G., Dacunha, N. M. C., and Matten, R. B., 1981, "Mean Wave Drift Forces: Theory and Experiment", National Maritime Institute, Report OT-R-8175.

79. Su, M., Bergin, M.T., and Bales, S.L., 1982, "Characteristics of Wave Groups in Storm Seas", Proc. Ocean Structural Dynamics Symposium.

80. Suyehiro, K., 1924, "The Drift of Ships Caused by Rolling Among Waves", Trans. INA, Vol. 66, pp. 60-76.

81. Thompson, C. W. and Smith, C., 1975, "Wave Groups in Ocean Swell", American Society of Civil Engineers Proceedings of the International Symposium on Ocean Wave Measurements on Analysis, pp. 338-351.

APPENDIX A

Tables 1 to 5

	STEADY OR OSCILLATING	COMPARISON WITH EXPERIMENT	STRUCTURAL TYPE
POTENTIAL THEORIES BASED ON CONSERVATION OF MOMENTUM			
Maruo (1960)	STEADY	NO	SHIP
Newman (1967)	STEADY	NO	SHIP
Faltinsen and Michelsen (1974)	STEADY	YES	SHIP,BARGE
Molin (1979)	STEADY	YES	SHIP
Kim and Chou (1970)	STEADY	YES	SHIP
POTENTIAL THEORIES BASED ON INTEGRATION OF FLUID PRESSURE			
Watanabe (1938)	STEADY	NO	SHIP
Havelock (1942)	STEADY	NO	SHIP
Salvensen (1974)	BOTH	NO	SHIP
Pinkster (1975), (1981)	BOTH	YES	SHIP,BARGE
Bowers (1980)	OSCILLATING	YES	SHIP
Faltinsen and Loken (1979)	BOTH	NO	CYLINDER
POTENTIAL THEORIES USING SLENDER BODY ASSUMPTION			
Gerritsma and Benkleman (1970)	STEADY	NO	SHIP
Kaplan and Sargent (1976)	STEADY	NO	SHIP
MORISON'S EQUATION			
Pijfers and Brink (1977)	STEADY	NO	SEMISUB.
Huse (1976)	STEADY	YES	SEMISUB.

TABLE 1 THEORIES TO PREDICT SECOND-ORDER WAVE FORCES

REFERENCE	STRUCTURE TYPE	STEADY OR OSCILLATING	COMPARISON WITH THEORY	AGREEMENT WITH THEORY
Remery and Hermans (1971)	BARGE	REGULAR GROUPS	YES	GOOD
Rye.et.al (1975)	CAISSON STRUCTURE	REGULAR GROUPS	YES	POOR
Ogawa (1967)	SHIP	STEADY	YES	GOOD
Lalagas (1963)	SHIP	STEADY	YES	GOOD
Naess (1978)	SEMISUB.	OSCILLATING	EXPERIMENT ONLY	
Spangenberg (1980)	SEMISUB.	OSCILLATING	EXPERIMENT ONLY	

TABLE 2 EXPERIMENTAL WORK ON DRIFT FORCES

GROUP No.	Δf (Hz)	RMS (cm)
1	1.22×10^{-3}	
2	2.44×10^{-3}	2.08
3	2.44×10^{-3}	2.17
4	2.44×10^{-3}	2.06
5	2.44×10^{-3}	2.18
6	4.88×10^{-3}	2.07
7	4.88×10^{-3}	2.08
8	7.32×10^{-3}	2.10
9	7.32×10^{-3}	2.12
10	9.76×10^{-3}	2.05
11	9.76×10^{-3}	2.10
12	1.22×10^{-2}	2.00
13	1.22×10^{-2}	2.40
14	1.71×10^{-2}	2.05
15	1.71×10^{-2}	2.08

MODEL OF JONSWAP: $\gamma = 3.3$

$f_m = 0.075$ Hz

$m_o = 4.53\ m^2$

SCALE = 1:100

TABLE 3 MODELLED JONSWAP SPECTRA USED IN MODEL TESTS

GROUP No.	Δf (Hz)	RMS (cm)
1a	1.22×10^{-3}	2.12
2a	2.44×10^{-3}	2.08
3a	4.88×10^{-3}	2.14
4a	7.32×10^{-3}	2.05
5a	9.76×10^{-3}	2.08
6a	1.22×10^{-2}	2.10

MODEL OF JONSWAP: $\gamma = 3.3$

$f_m = 0.075$ Hz

$m_o = 4.53\ m^2$

SCALE = 1:100

TABLE 4 MODELLED JONSWAP SPECTRA USED TO TEST PROPOSED MODEL

	Predicted By Analytical Transfer Function	Predicted By Experimental Transfer Function	Measured Result
RMS (cm)			
$\Delta f/f_o$ = 0.03	21.32	28.92	30.65
0.05	17.24	26.85	31.19
0.10	28.56	33.81	32.66
0.16	12.50	16.93	18.50
0.22	21.58	22.90	21.06
0.27	18.19	23.49	28.00
0.39	15.73	14.28	7.35
X_{DMAX}(cm)			
$\Delta f/f_o$ = 0.03	78.71	124.72	104.87
0.05	70.76	86.77	96.30
0.10	140.58	140.27	140.73
0.16	40.43	63.51	50.91
0.22	70.15	63.20	80.84
0.27	38.62	65.33	50.25
0.39	30.19	30.21	15.48
DURATION ABOVE 1/3 X_{DMAX}(sec)			
$\Delta f/f_o$ = 0.03	95.35	122.11	115.79
0.05	87.31	88.42	92.63
0.10	33.21	33.52	33.68
0.16	129.35	136.51	157.89
0.22	202.31	210.65	231.58
0.27	310.11	325.90	320.63
0.39	305.11	336.67	309.83

TABLE 5 COMPARISON BETWEEN MEASURED RESPONSE VALUES AND THOSE PREDICTED BY PROPOSED MODEL

APPENDIX B

Figures 2.1 to 6.25

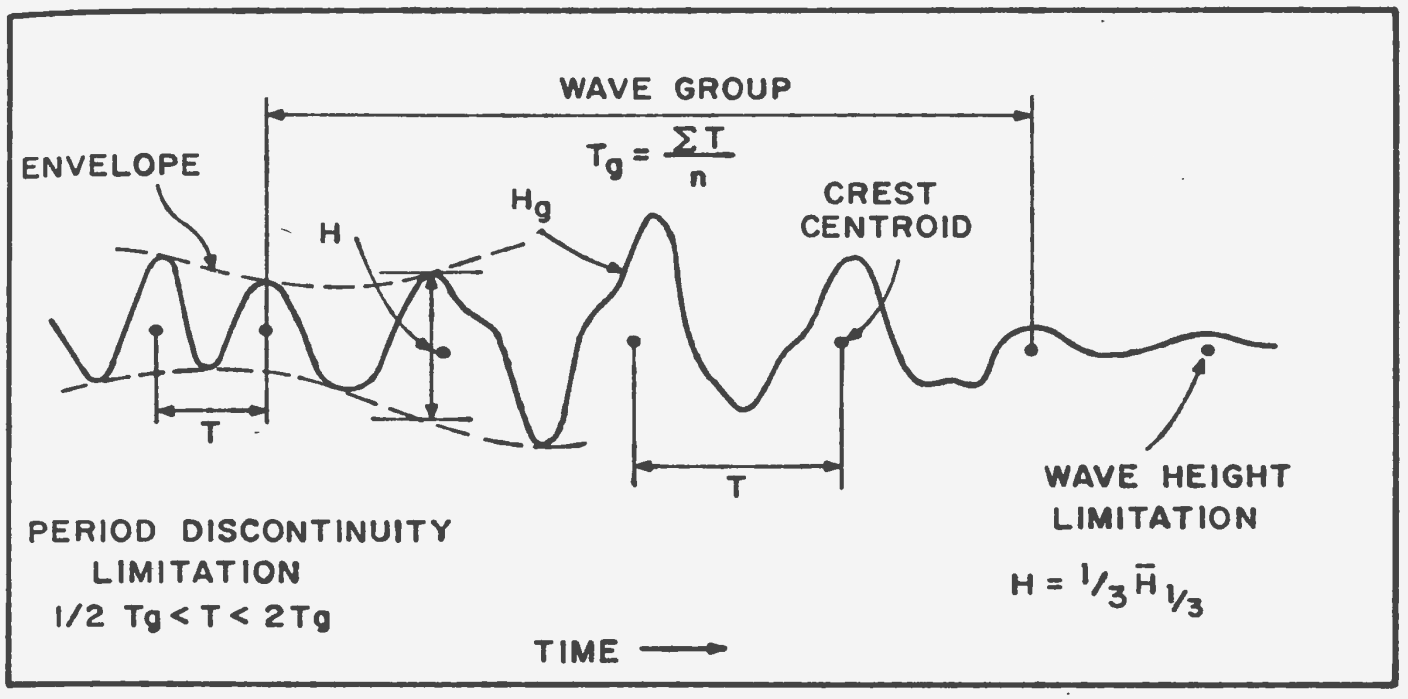

FIG. 2.1a WAVE GROUP DEFINITION AND MEASURES (THOMPSON AND SMITH (1974))

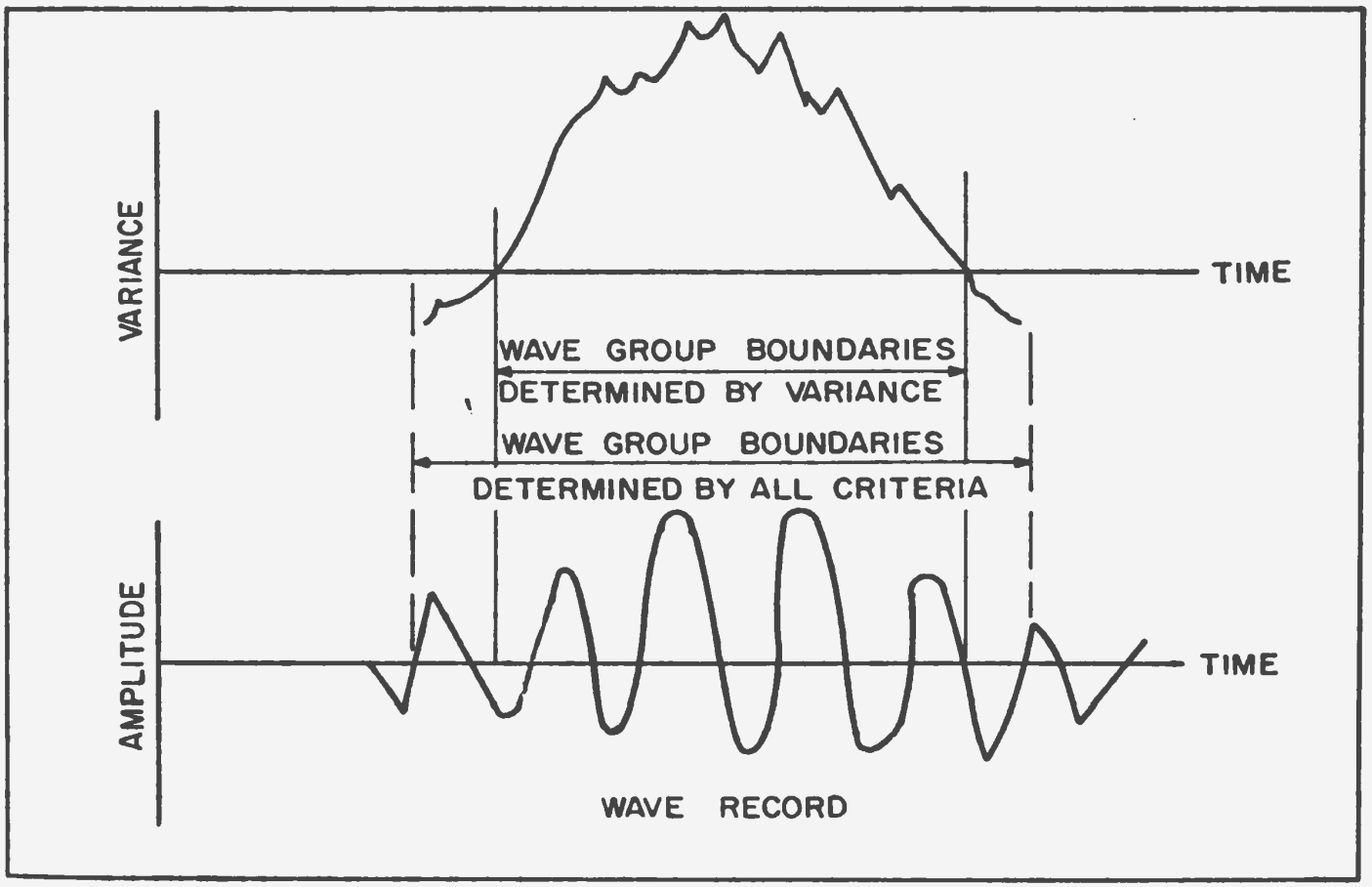

FIG. 2.1b WAVE GROUP BOUNDARY DEFINITION (SEDIVY (1978))

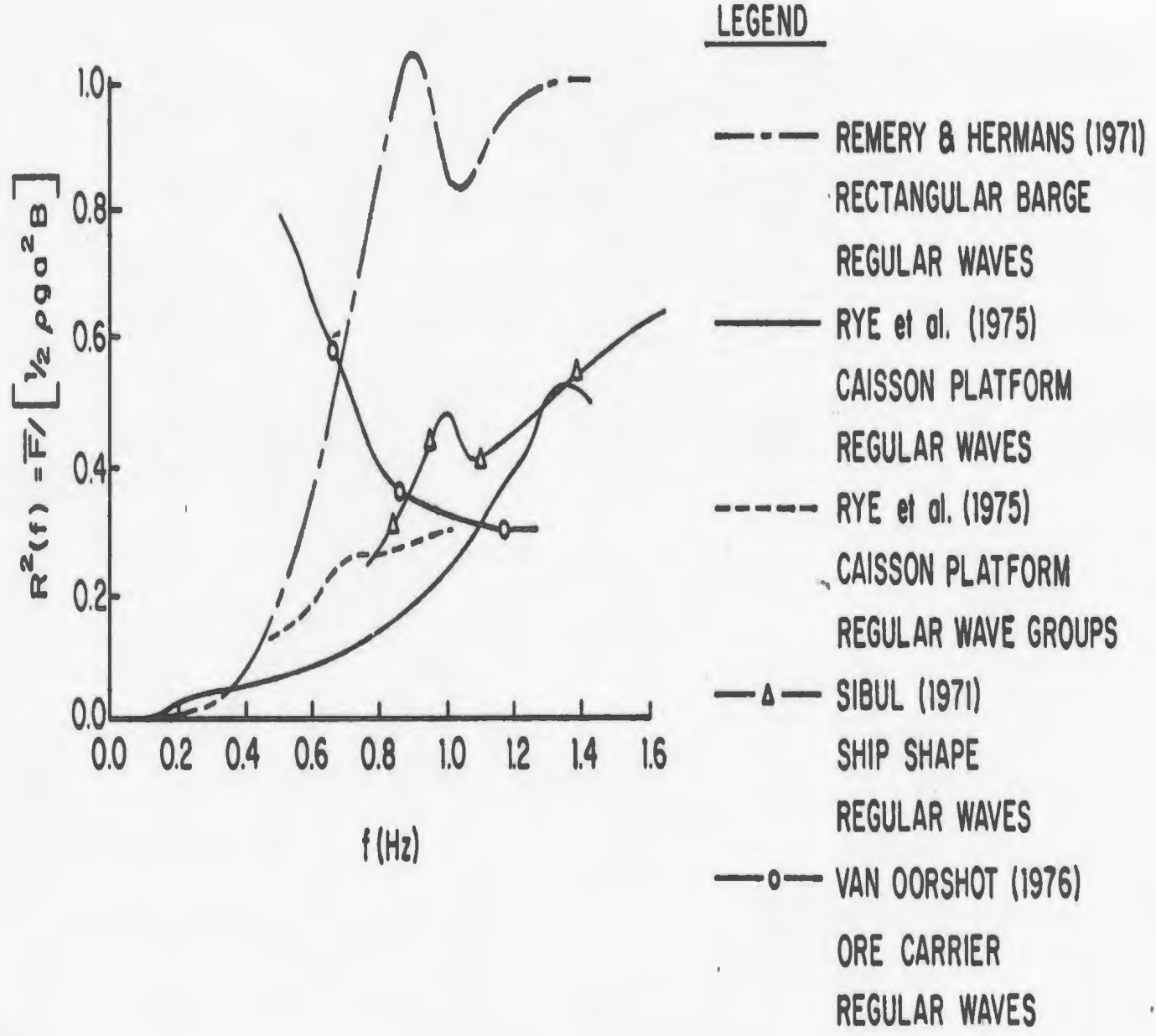

FIG 2.2 STEADY DRIFT COEFFICIENT VERSUS MODEL WAVE FREQUENCY FOR VARIOUS STRUCTURE TYPES

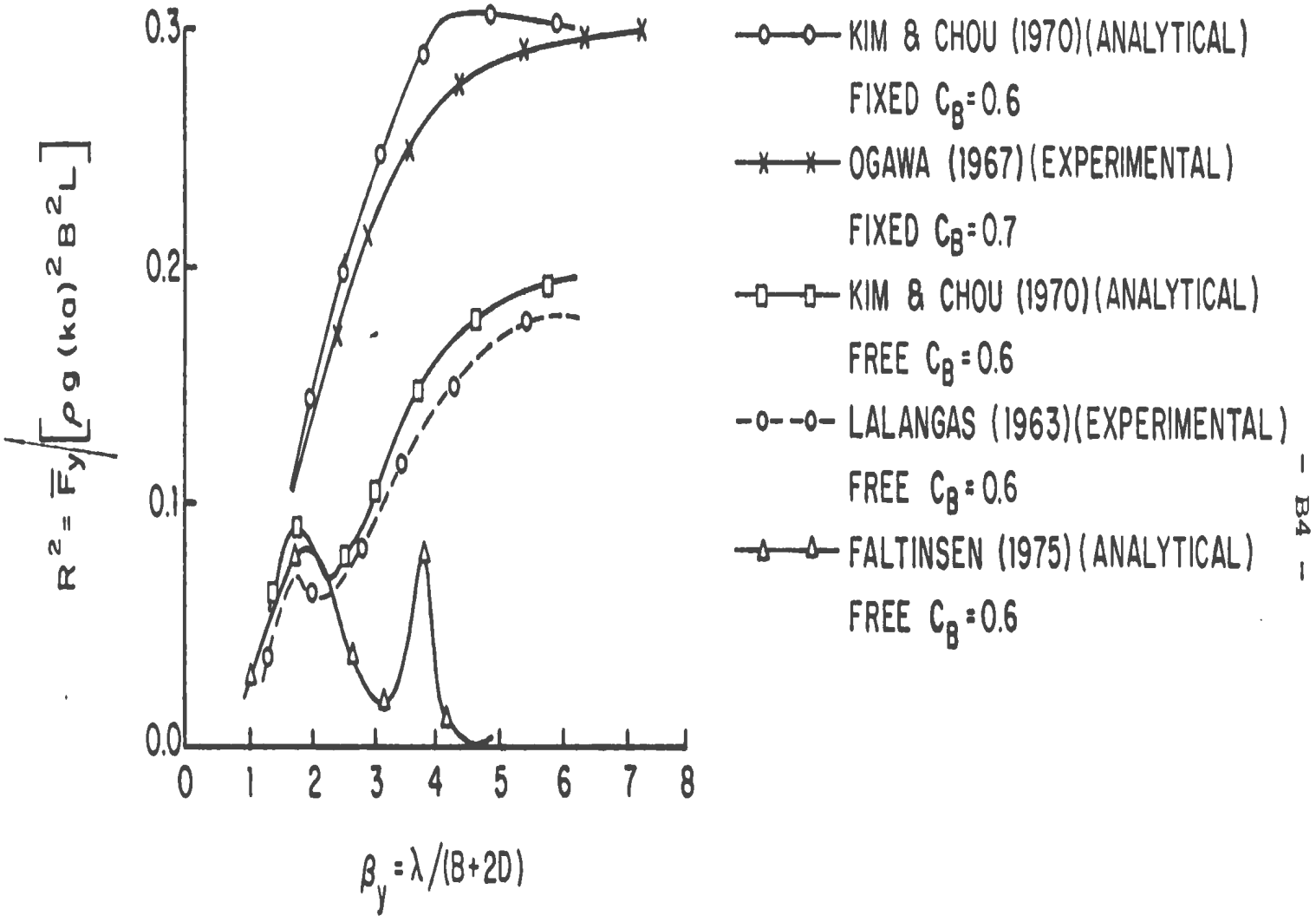

FIG. 2.3 STEADY DRIFT COEFFICIENTS FOR SERIES 60 SHIP MODEL IN BEAM SEAS

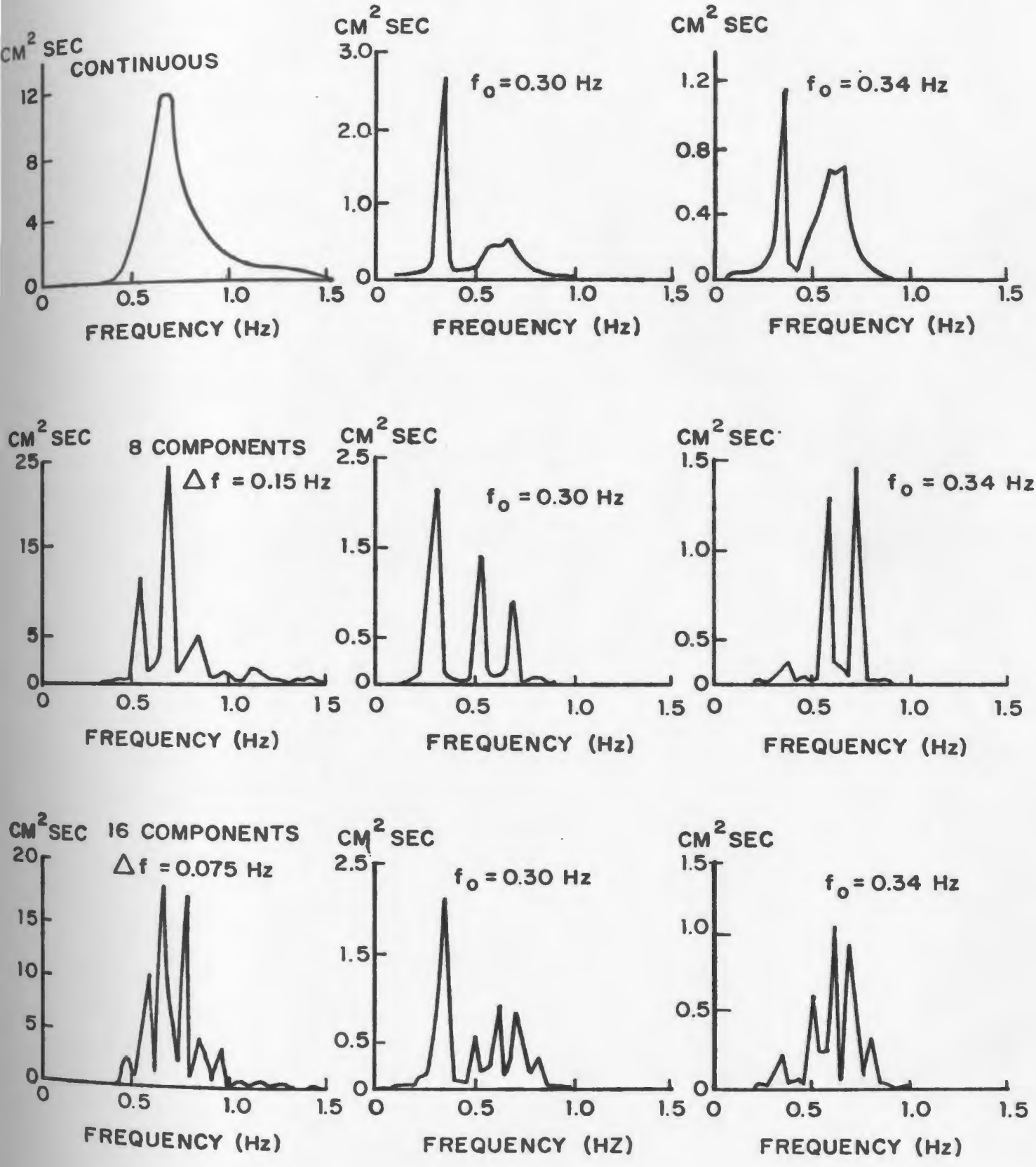

FIG. 2.4 EXPERIMENTAL RESULTS OF NAESS (1978)

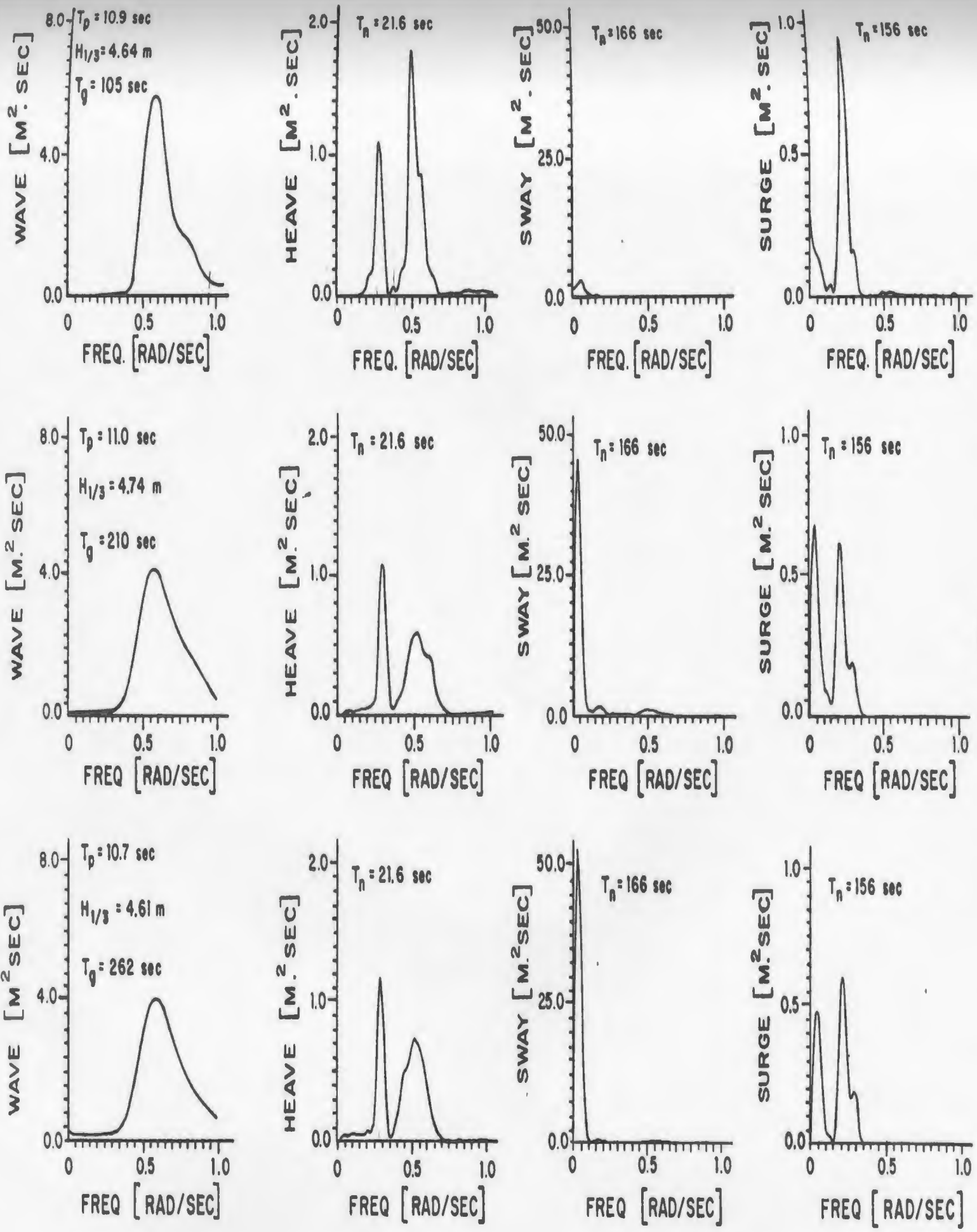

FIG. 2.5a EXPERIMENTAL RESULTS FROM SPANGENBERG (1980)

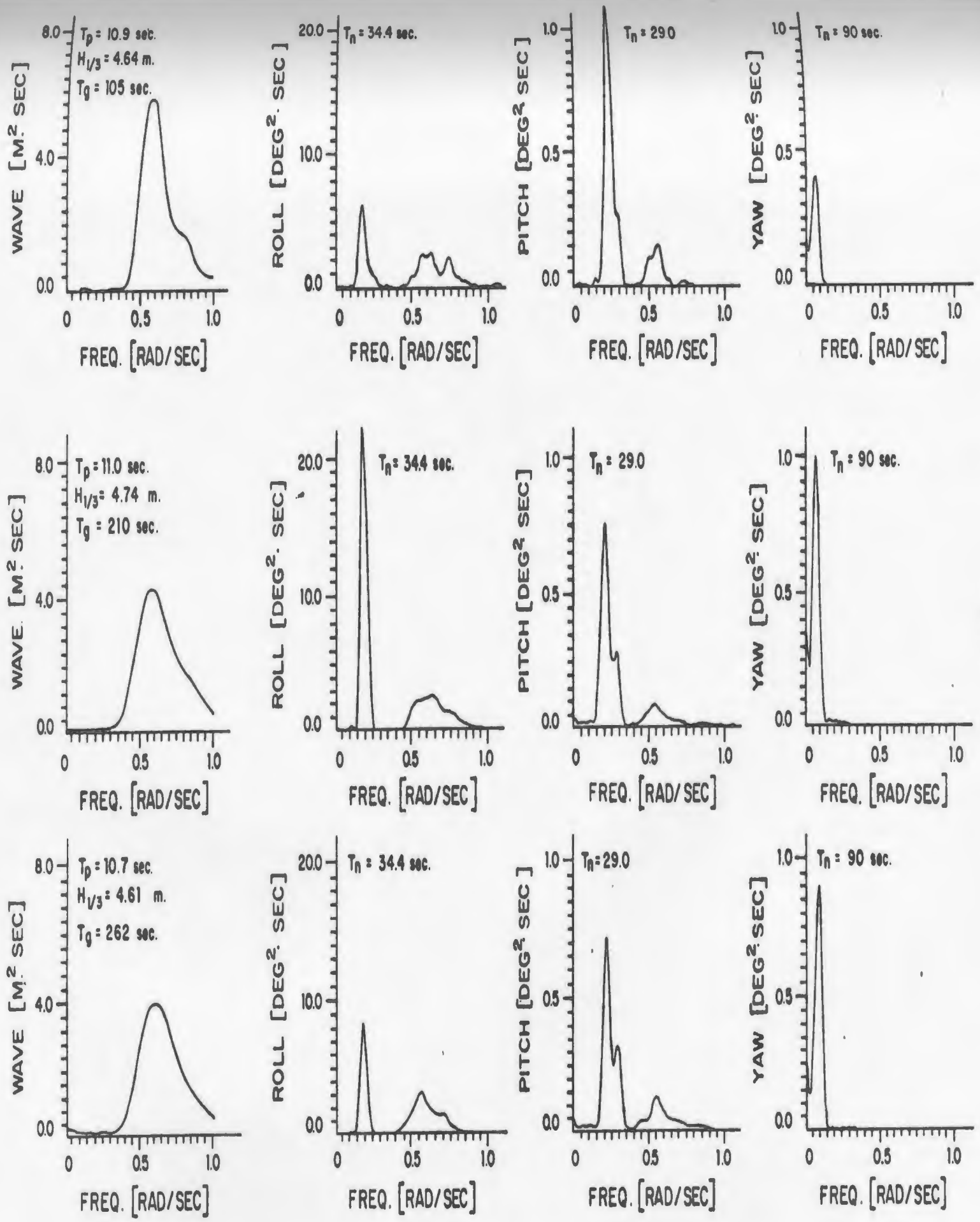

FIG. 2.5b EXPERIMENTAL RESULTS FROM SPANGENBERG (1980).

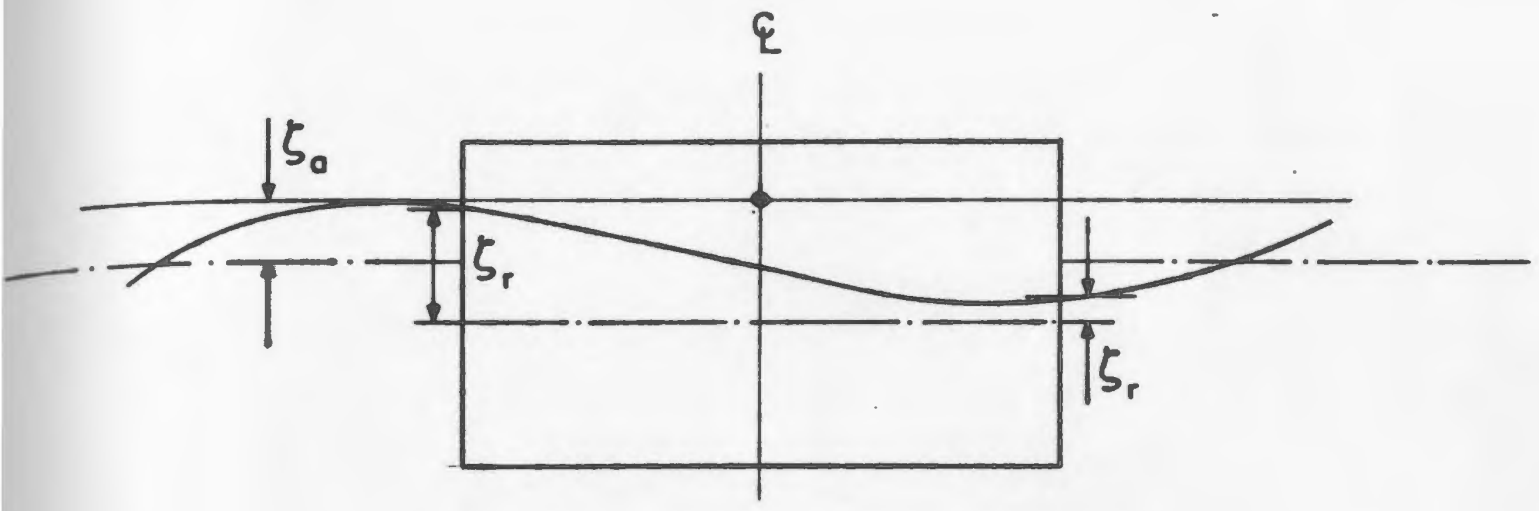

RELATIVE WAVE HEIGHT TERM

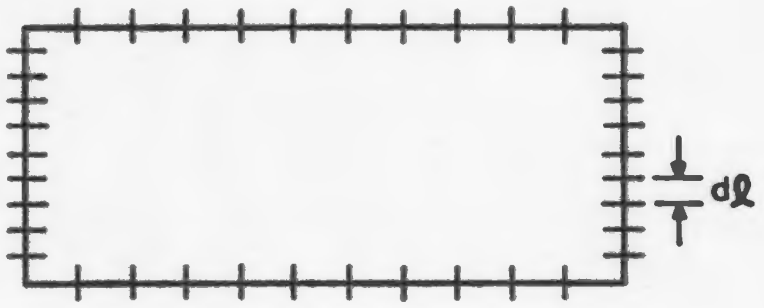

WATER LINE SCHEMATISATION

FIG. 3.1 SCHEMATISATION OF RELATIVE WAVE HEIGHT TERM.

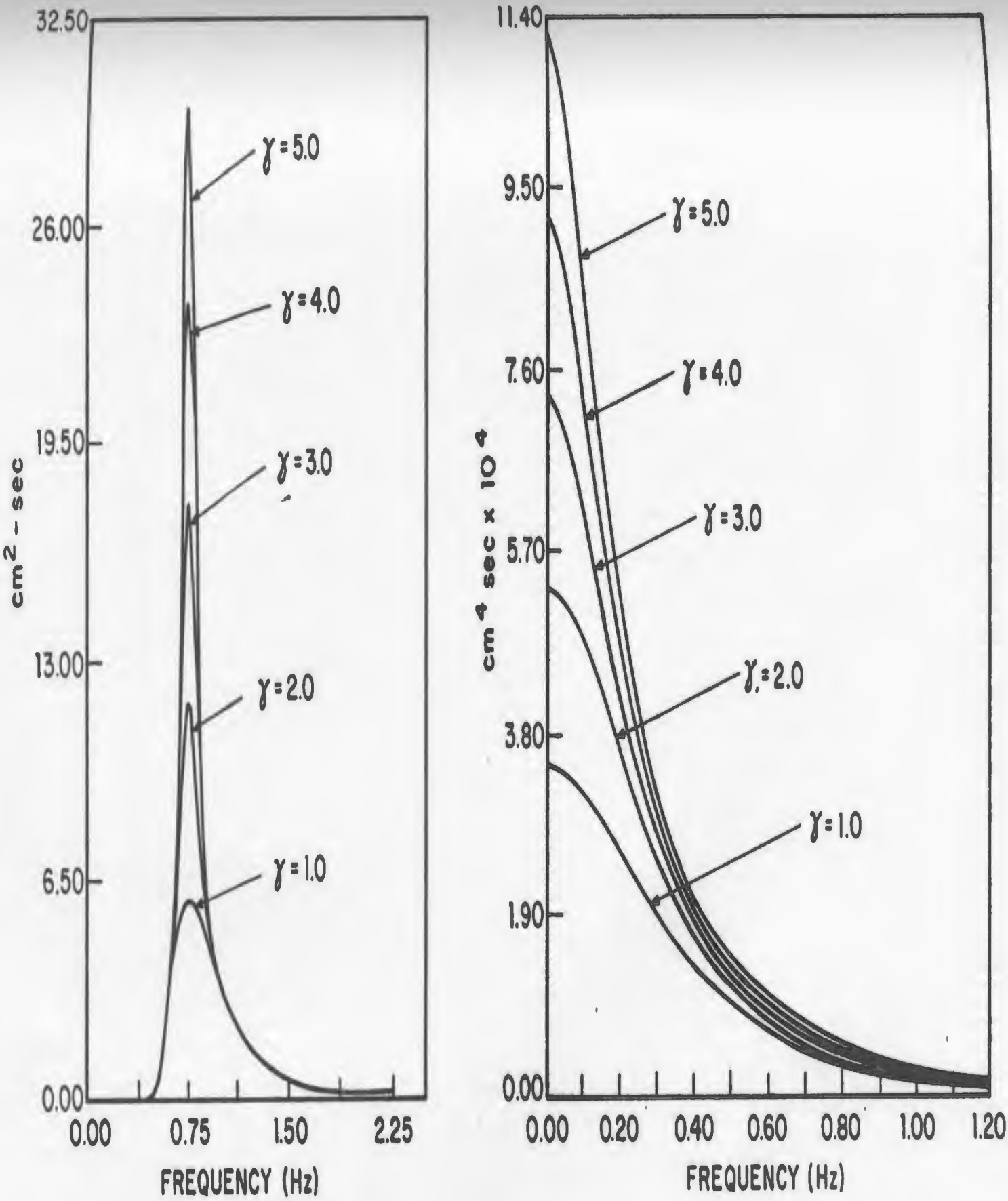

FIG. 4.1 JONSWAP SPECTRA AND ASSOCIATED GROUP SPECTRA

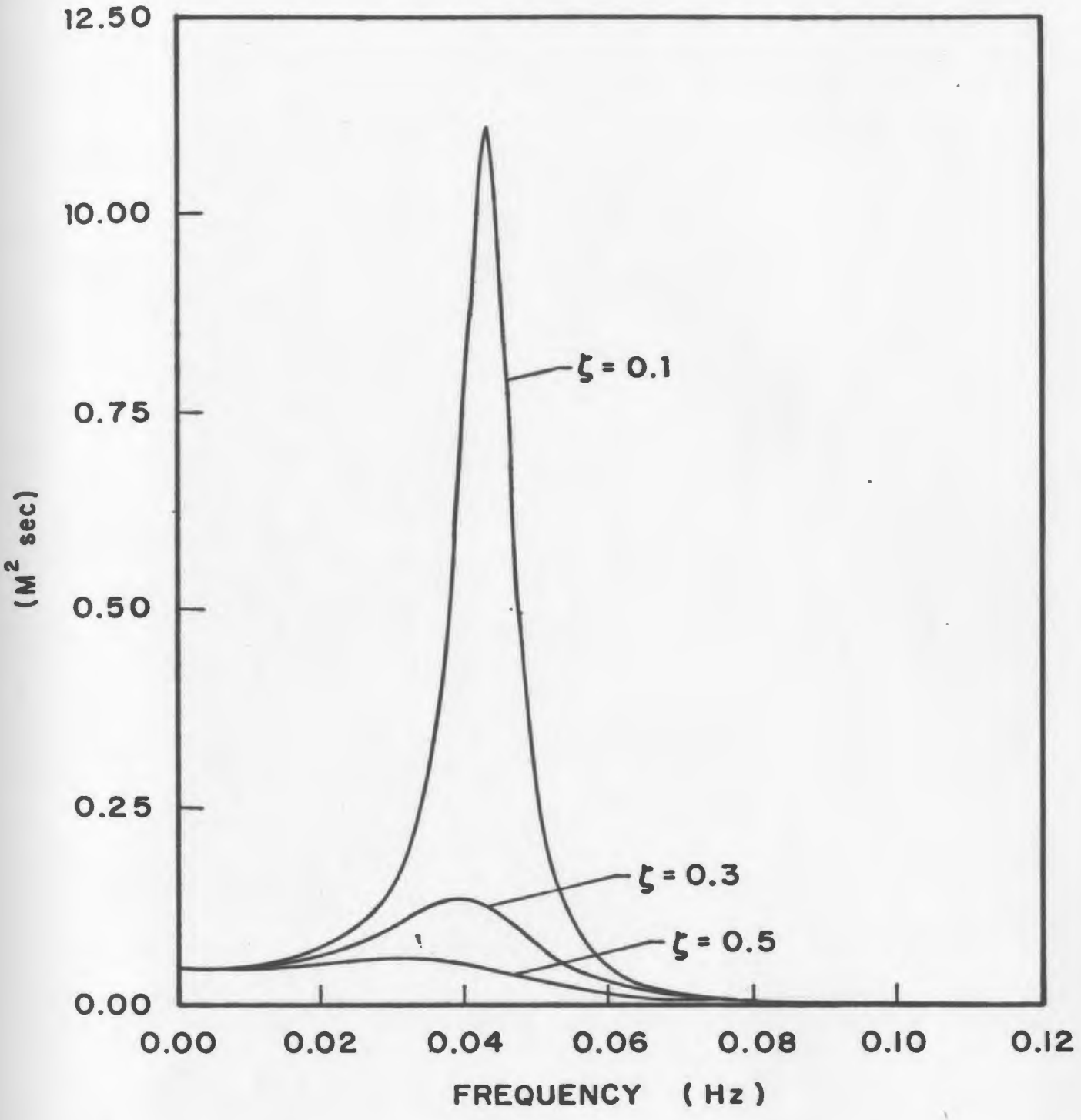

FIG. 4.2 RESPONSE SPECTRA FOR VARIOUS DAMPING COEFFICIENTS

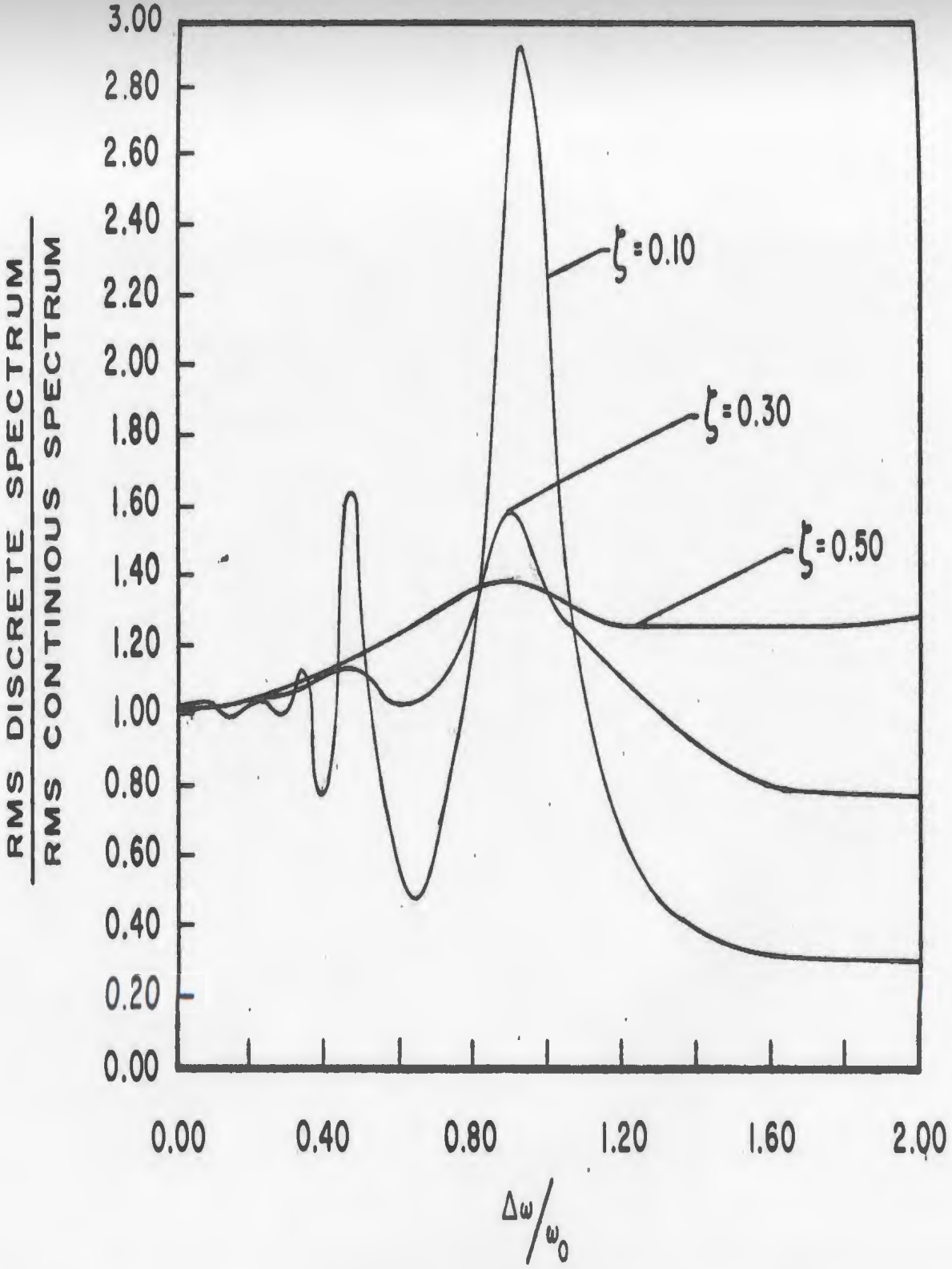

FIG. 4.3 RATIO OF RMS RESPONSE VALUES FOR VARIOUS FREQUENCY RESOLUTIONS

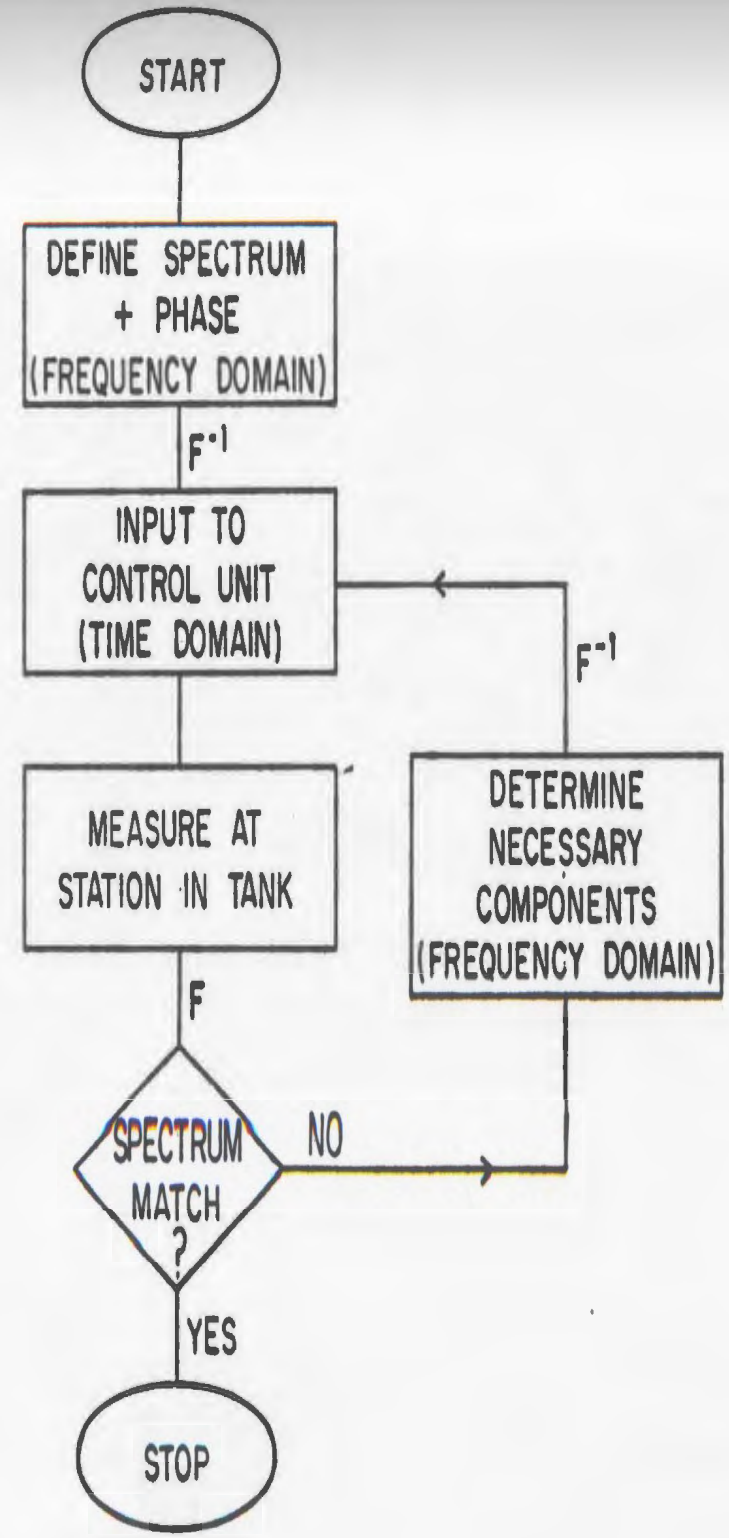

MODEL SPECTRA MATCH

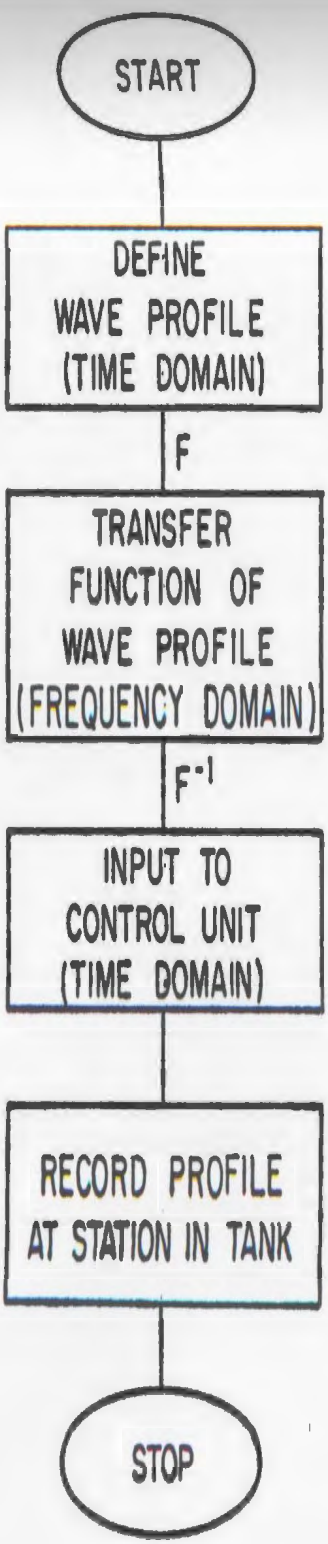

MODEL OF WAVE PROFILE

FIG. 5.1 GENERATION OF WAVES IN WAVE TANK.

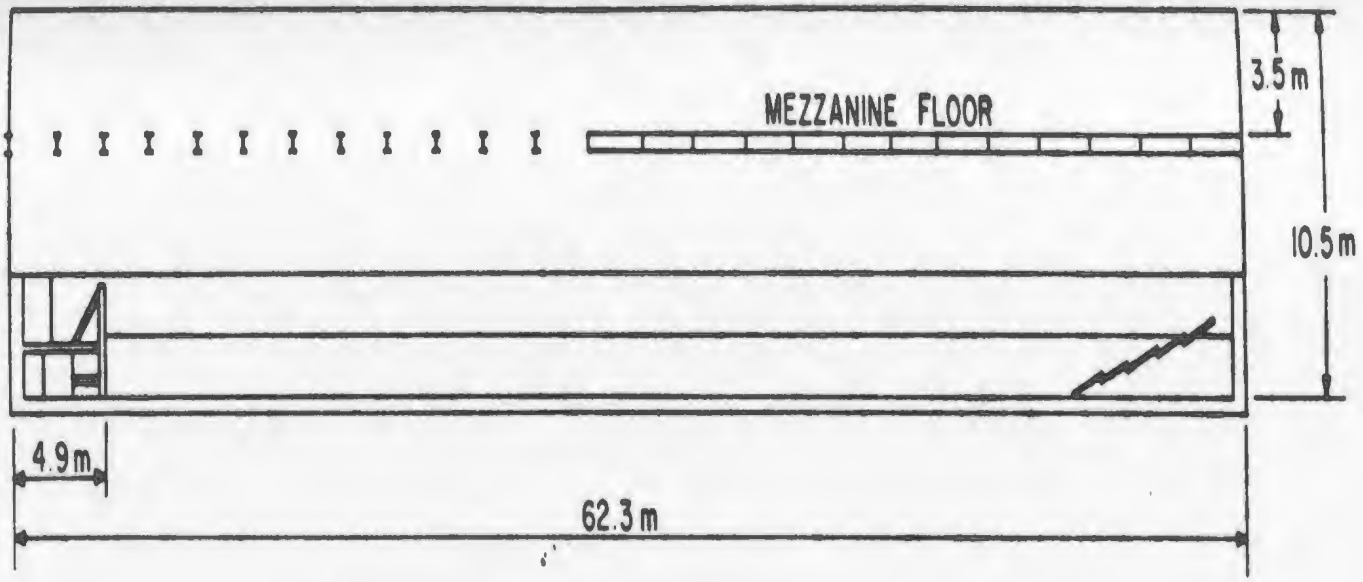

SECTION A-A

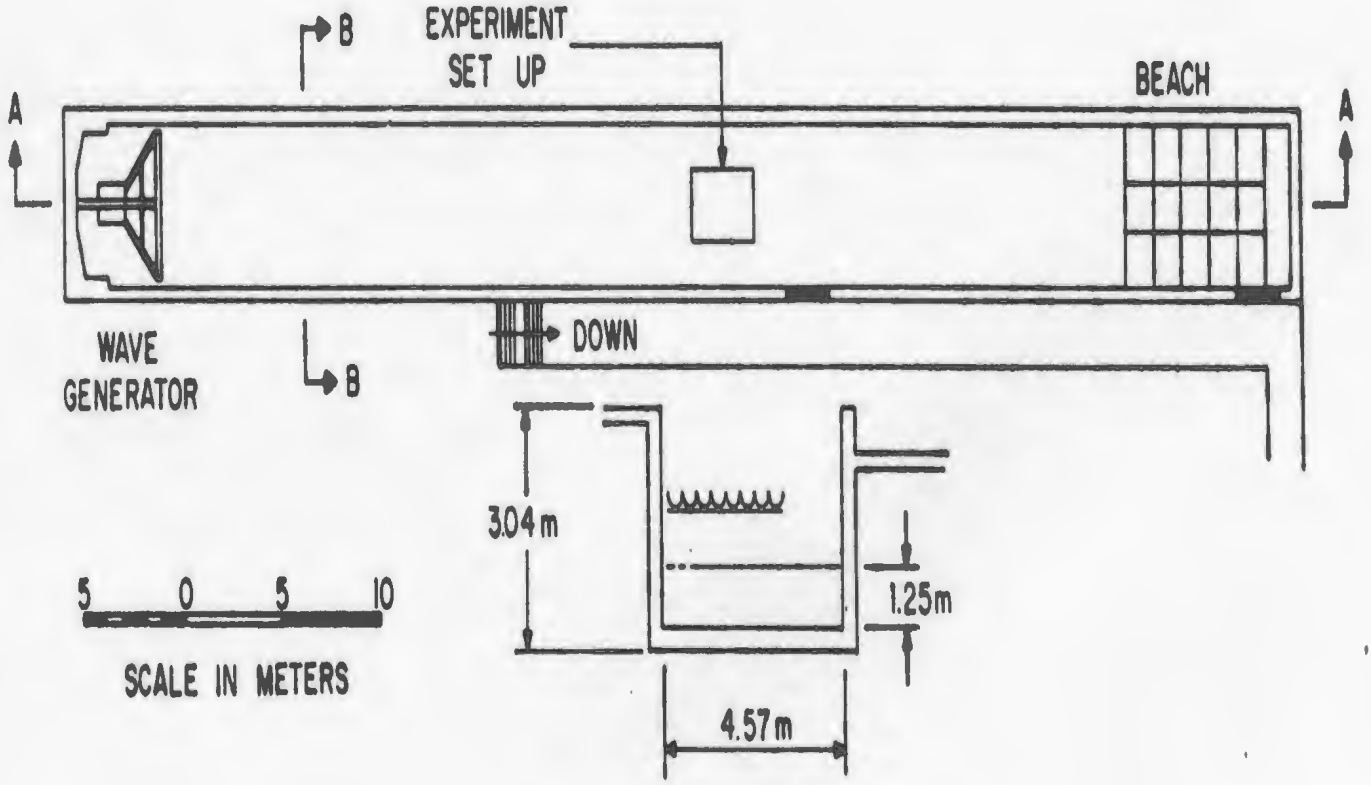

SECTION B-B

PLAN VIEW

FIG. 5.2 WAVE TANK PLAN AND ELEVATION VIEWS

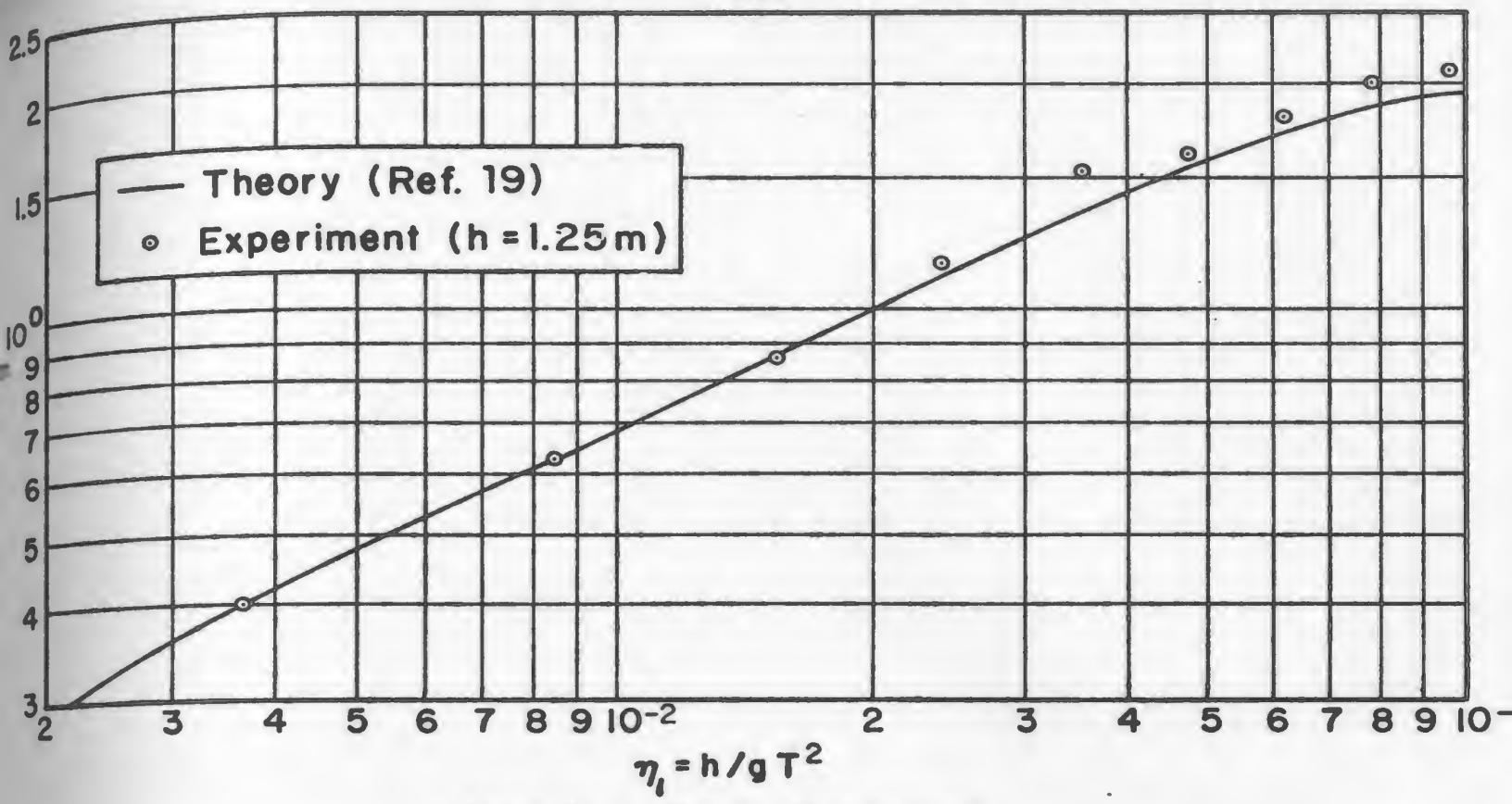

Regular Wave Generator

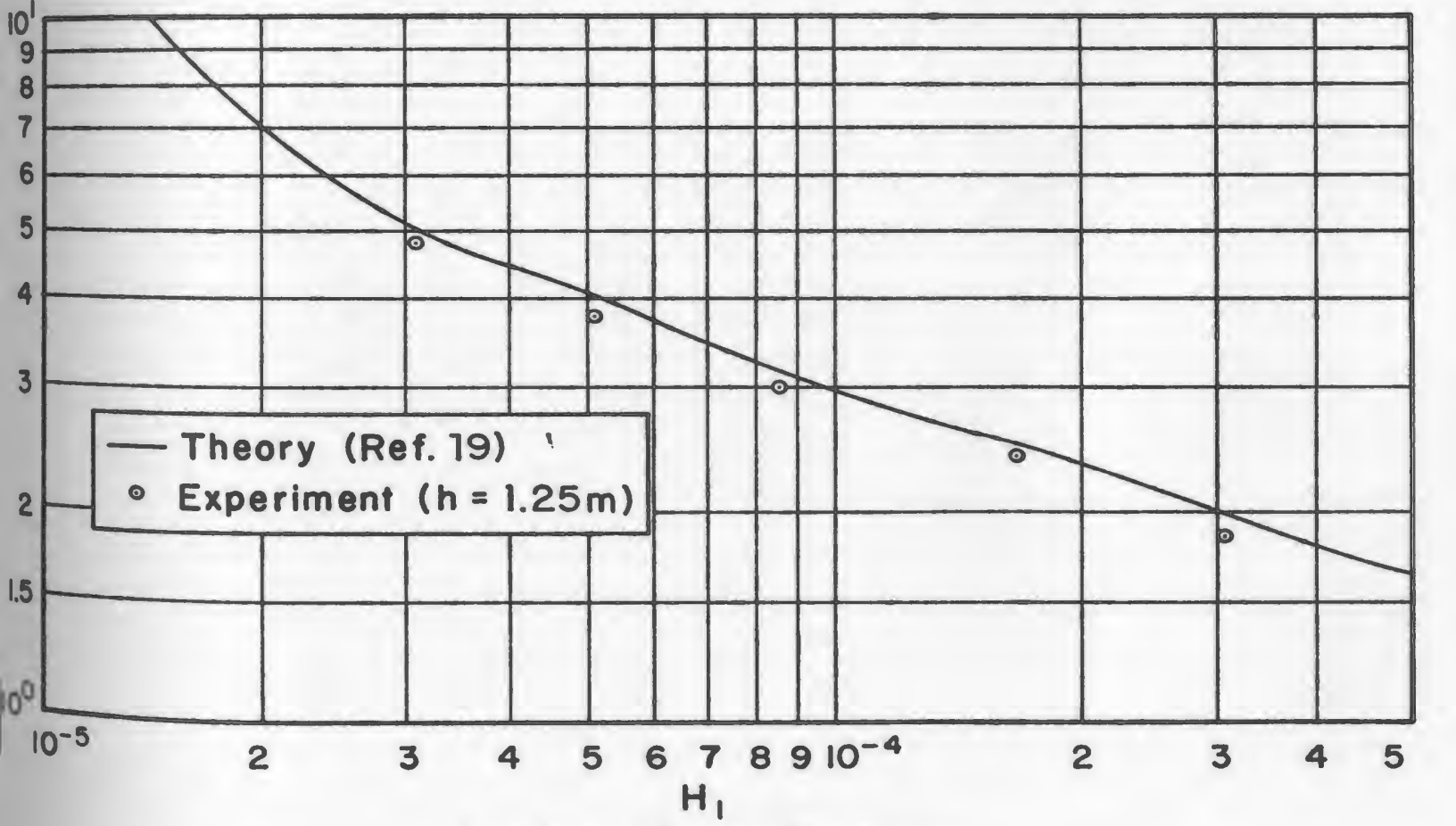

Random Wave Generator

FIG. 5.3 PISTON REGULAR AND RANDOM WAVE GENERATOR PERFORMANCE

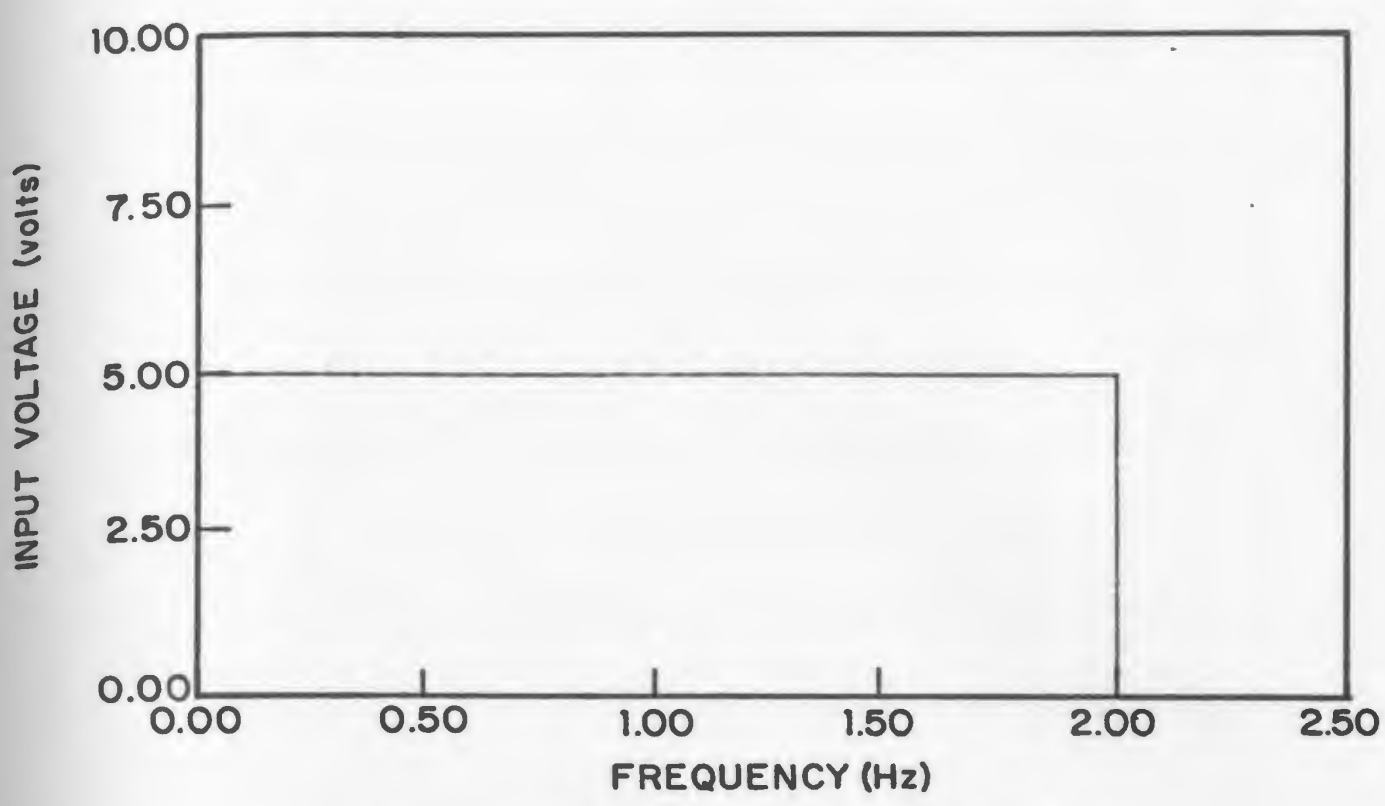

MAGNITUDE OF INPUT SPECTRUM

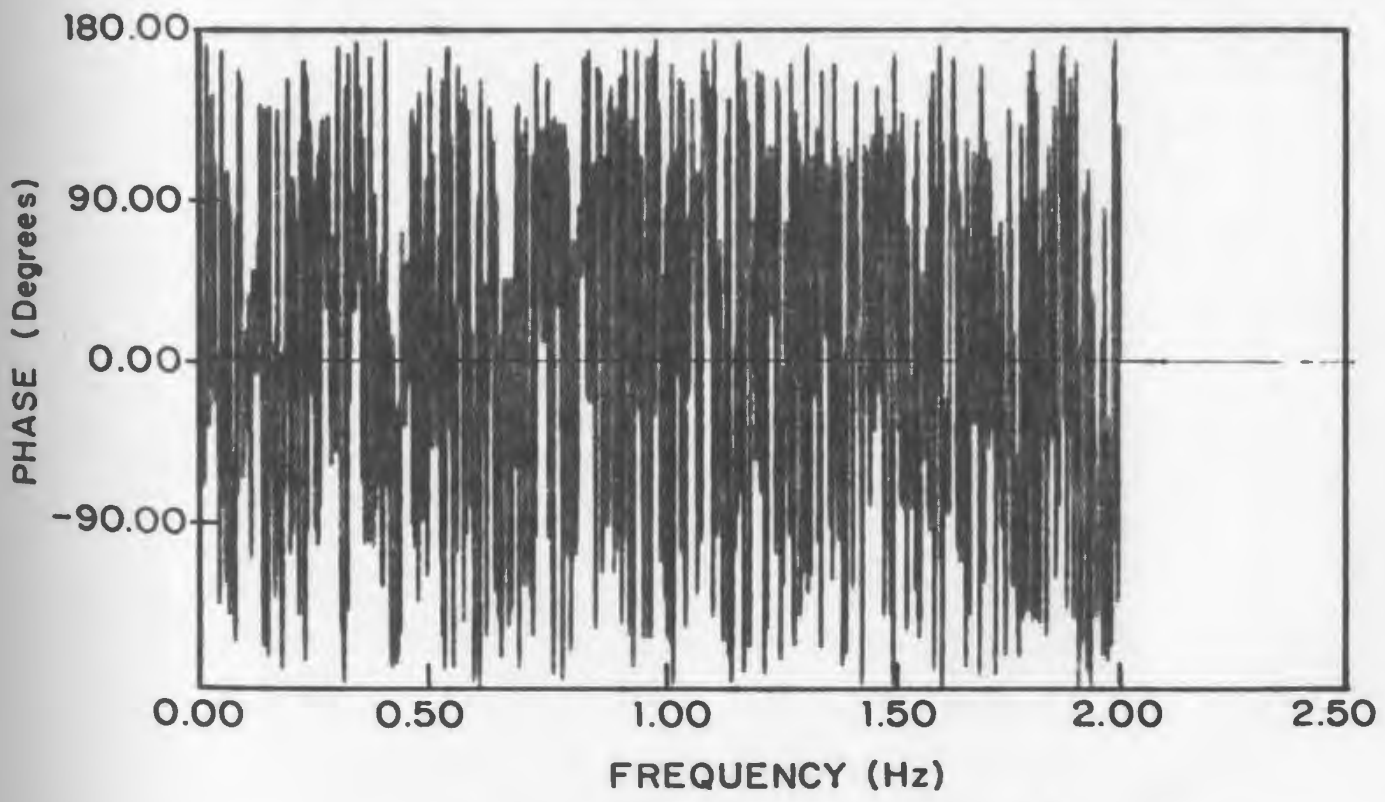

PHASE OF INPUT SPECTRUM

FIG. 5.4 NOISE SPECTRUM INPUT TO WAVE GENERATOR

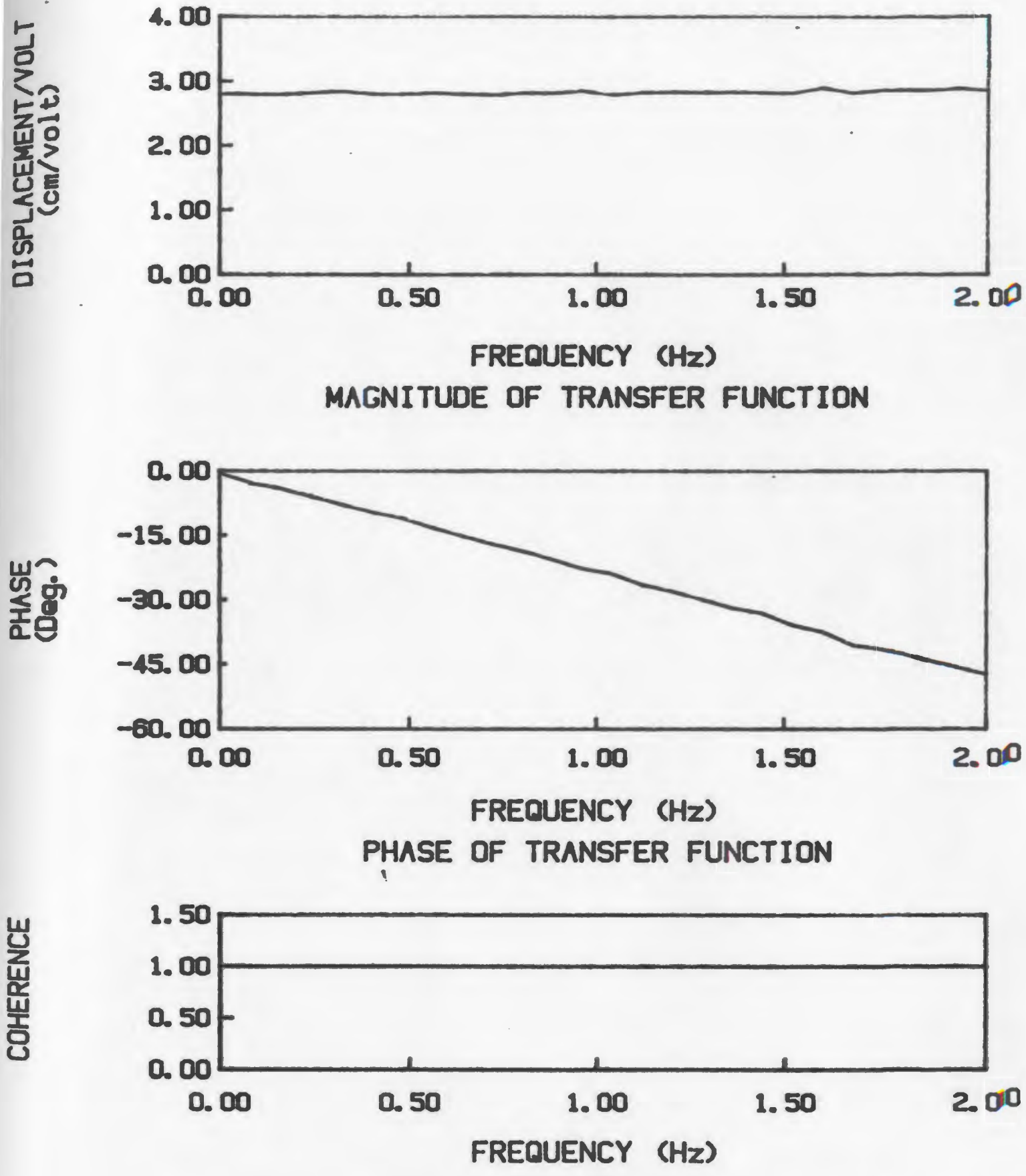

FIG 5.5 TRANSFER FUNCTION BETWEEN INPUT NOISE SPECTRUM AND BOARD DISPLACEMENT

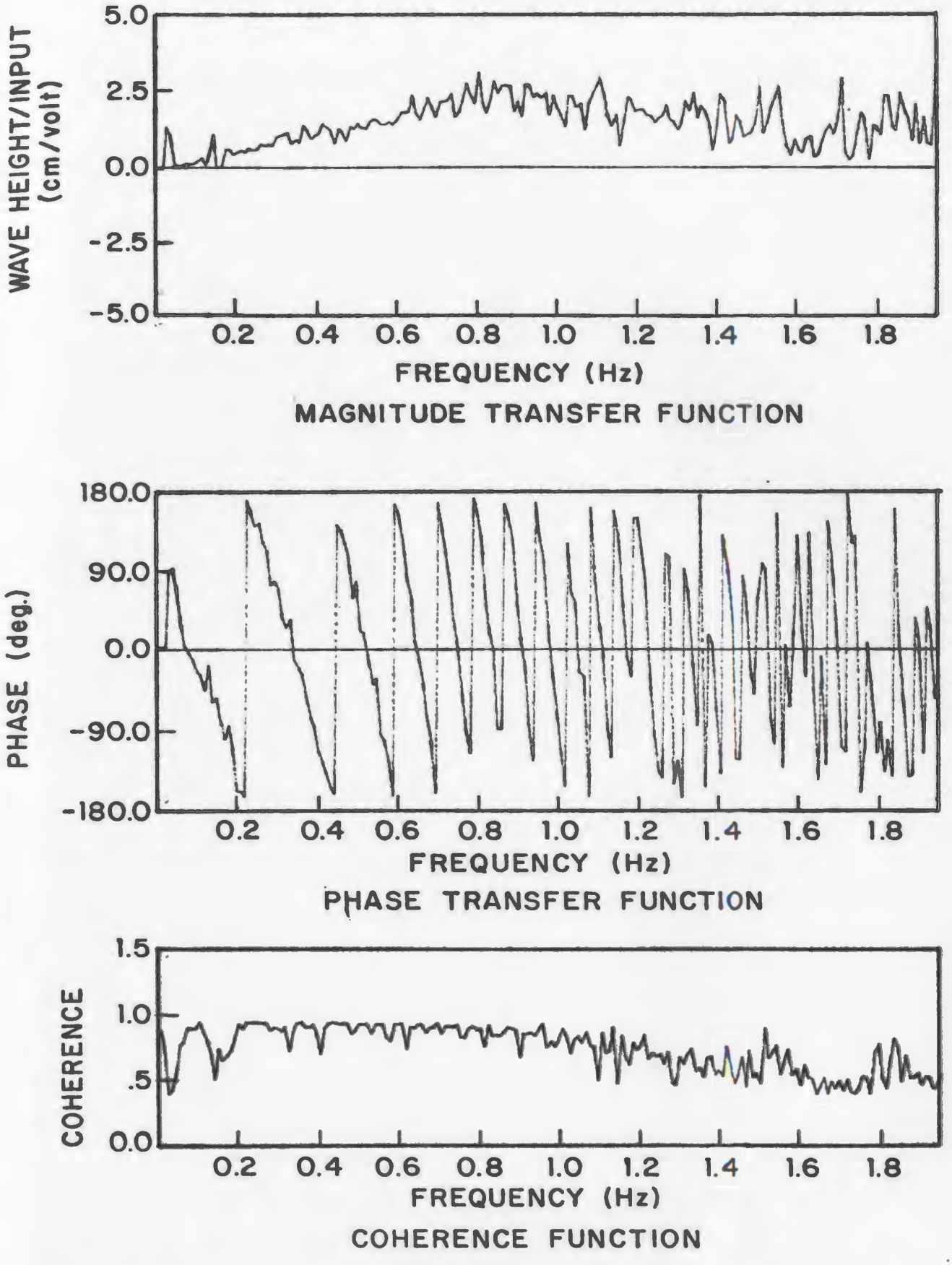

FIG. 5.6 TRANSFER FUNCTION TO STATION AT 30m.

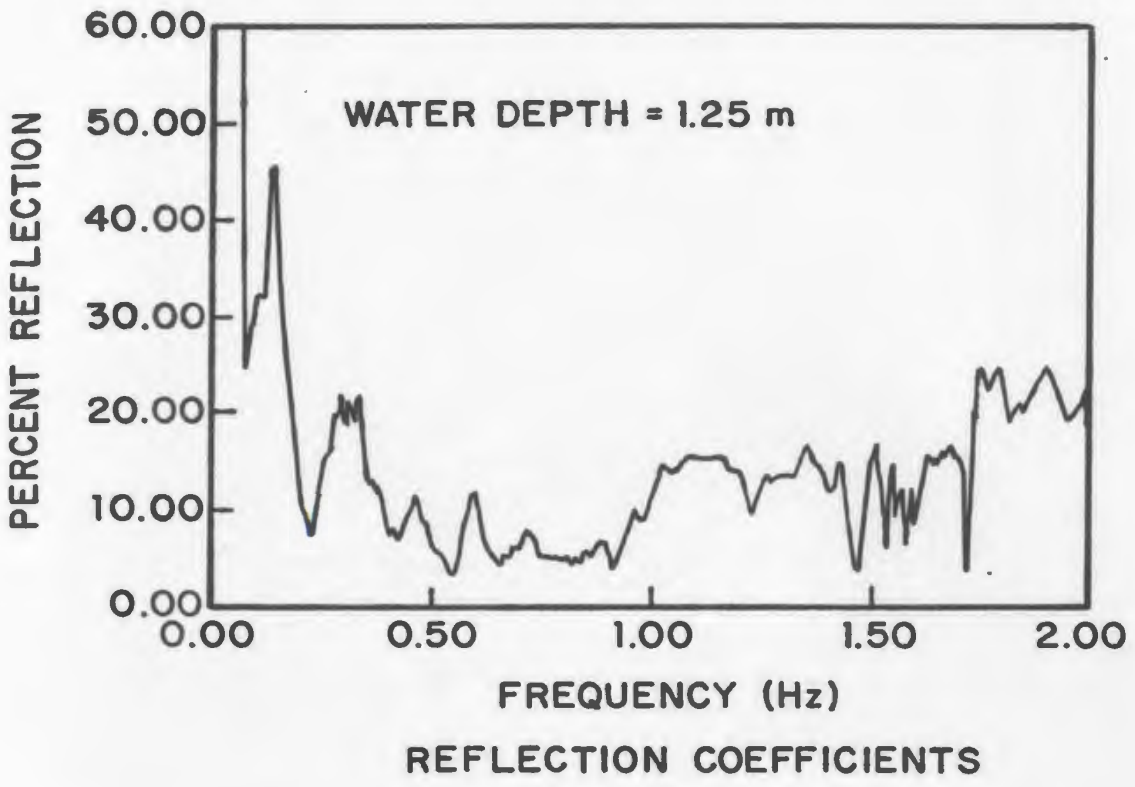

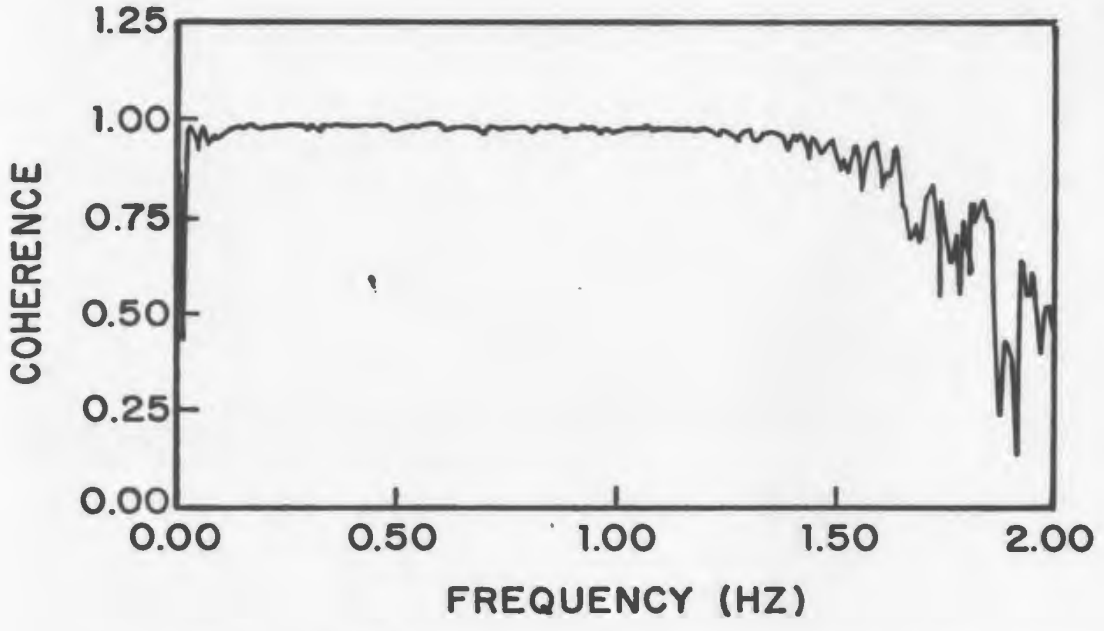

FIG. 5.7 REFLECTION COEFFICIENTS AT TEST LOCATION

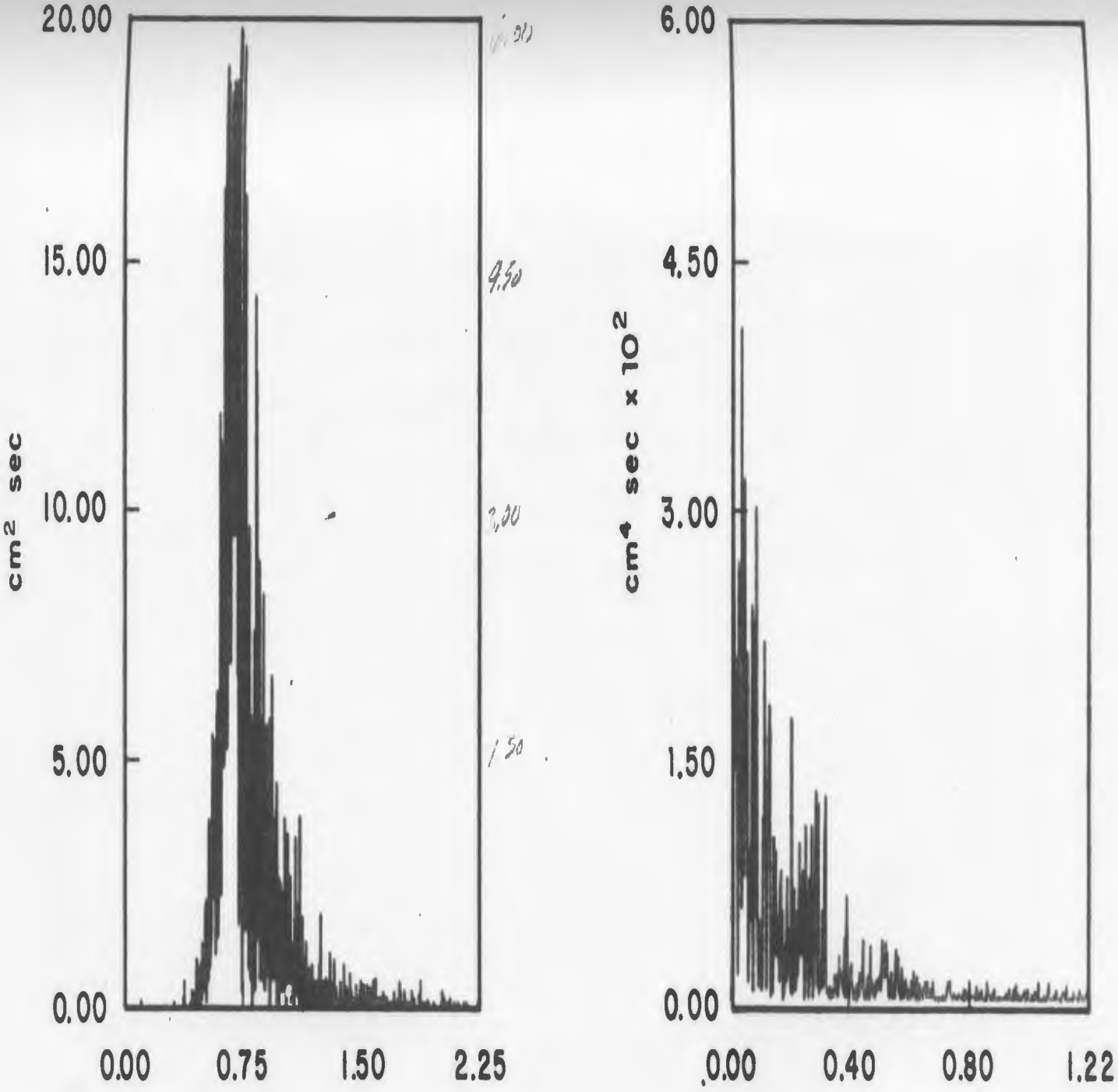

FIG. 5.8 WAVE AND SIWEH SPECTRAL DENSITIES FOR SPECTRUM 1

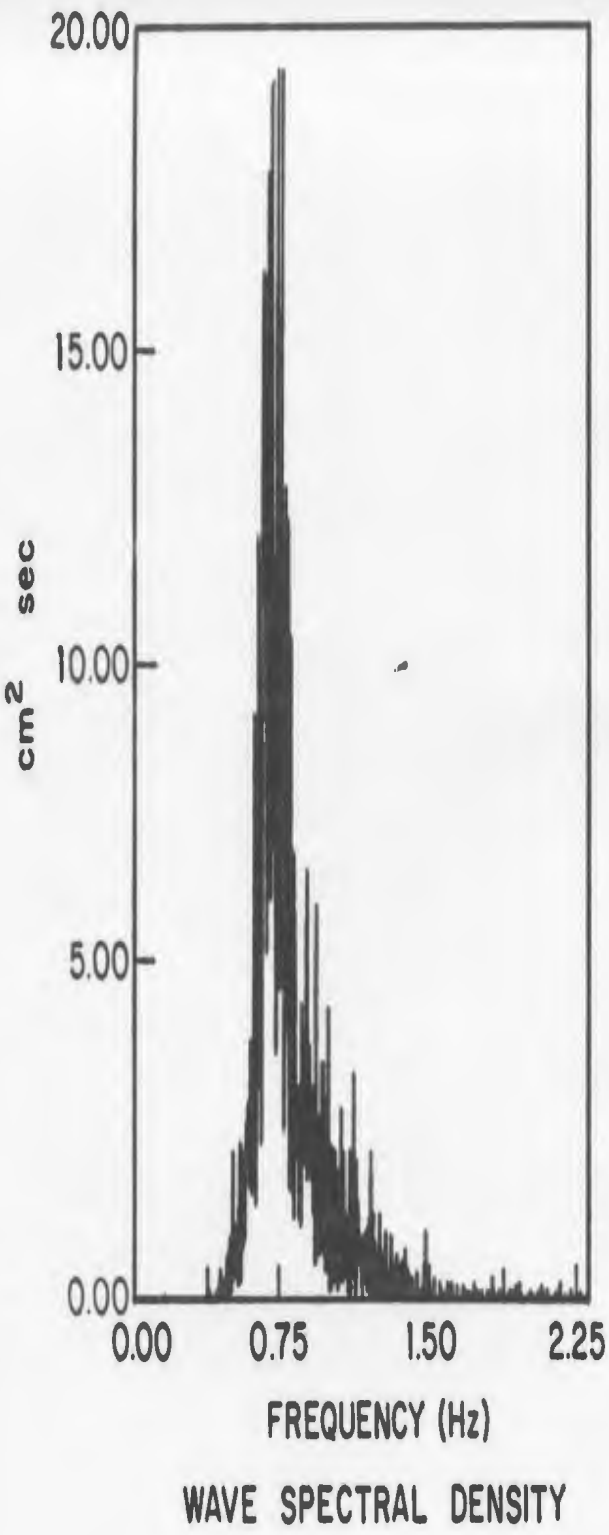

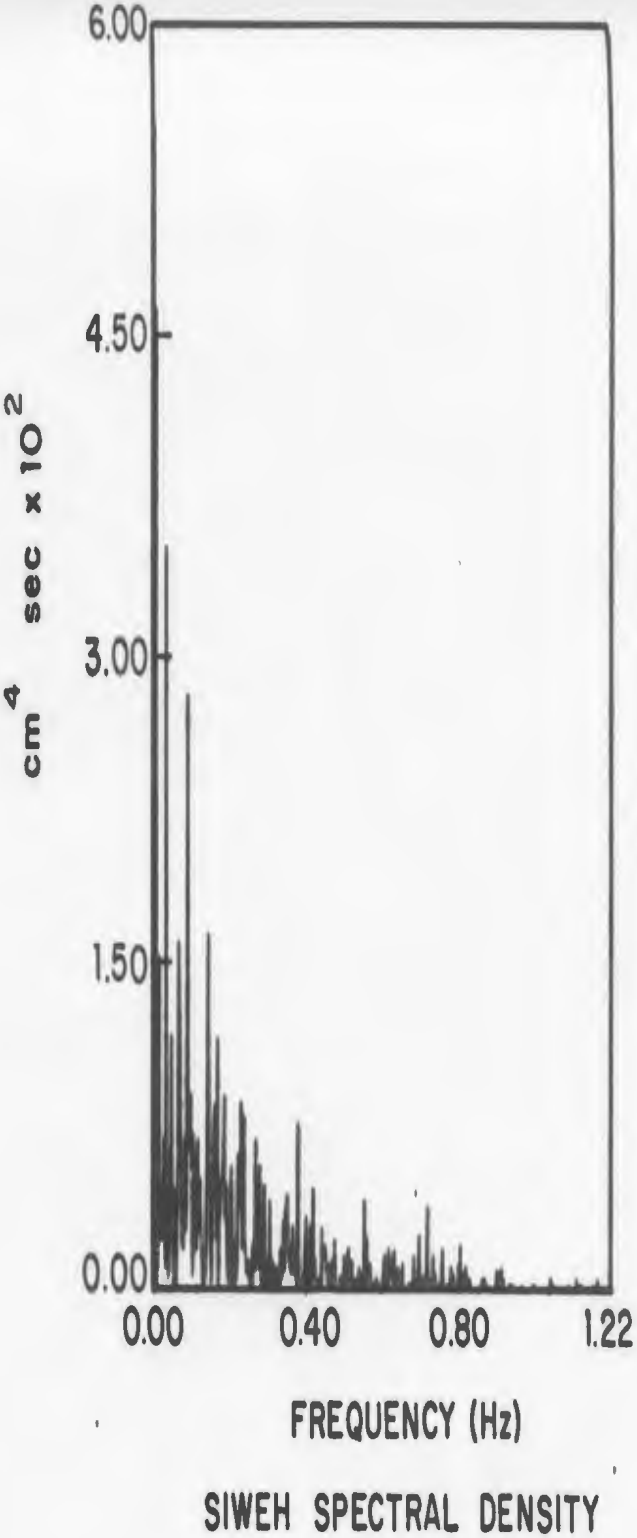

FIG. 5.9 WAVE AND SIWEH SPECTRAL DENSITIES FOR SPECTRUM 2

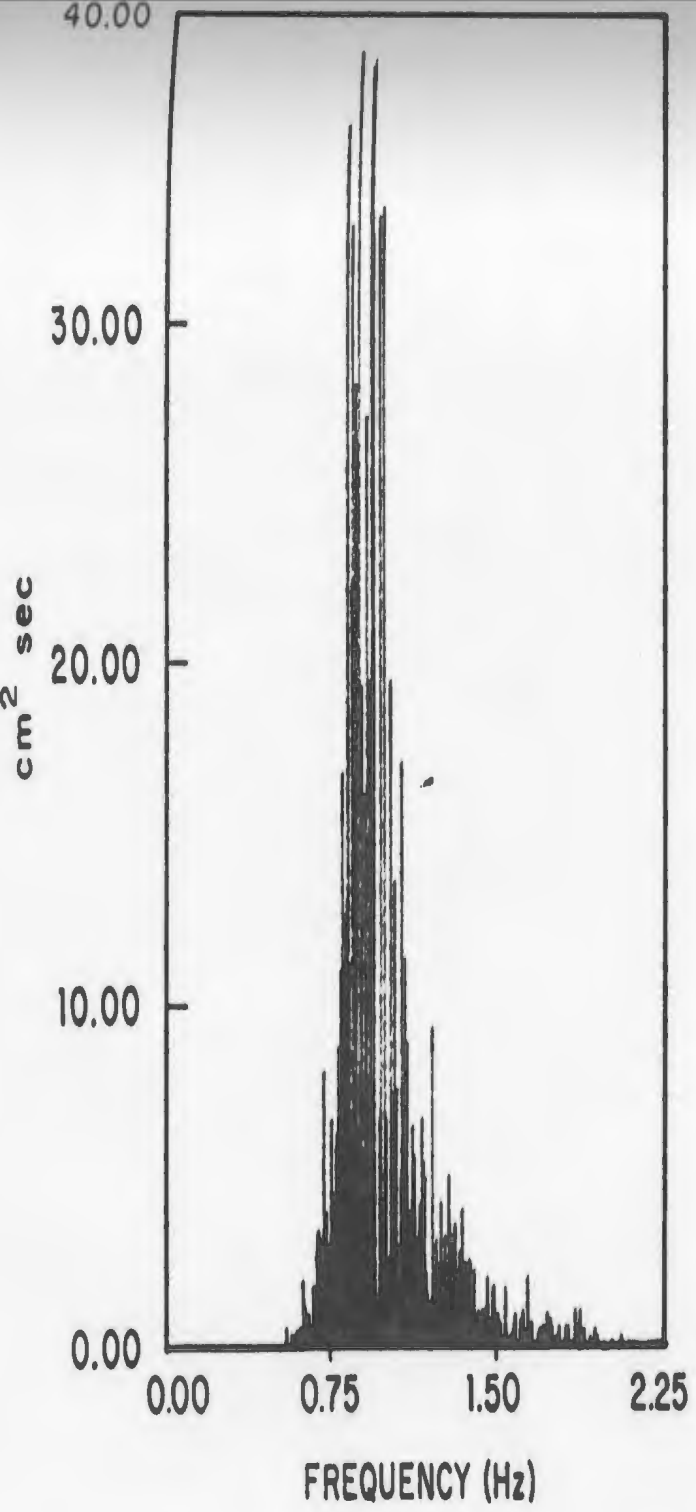

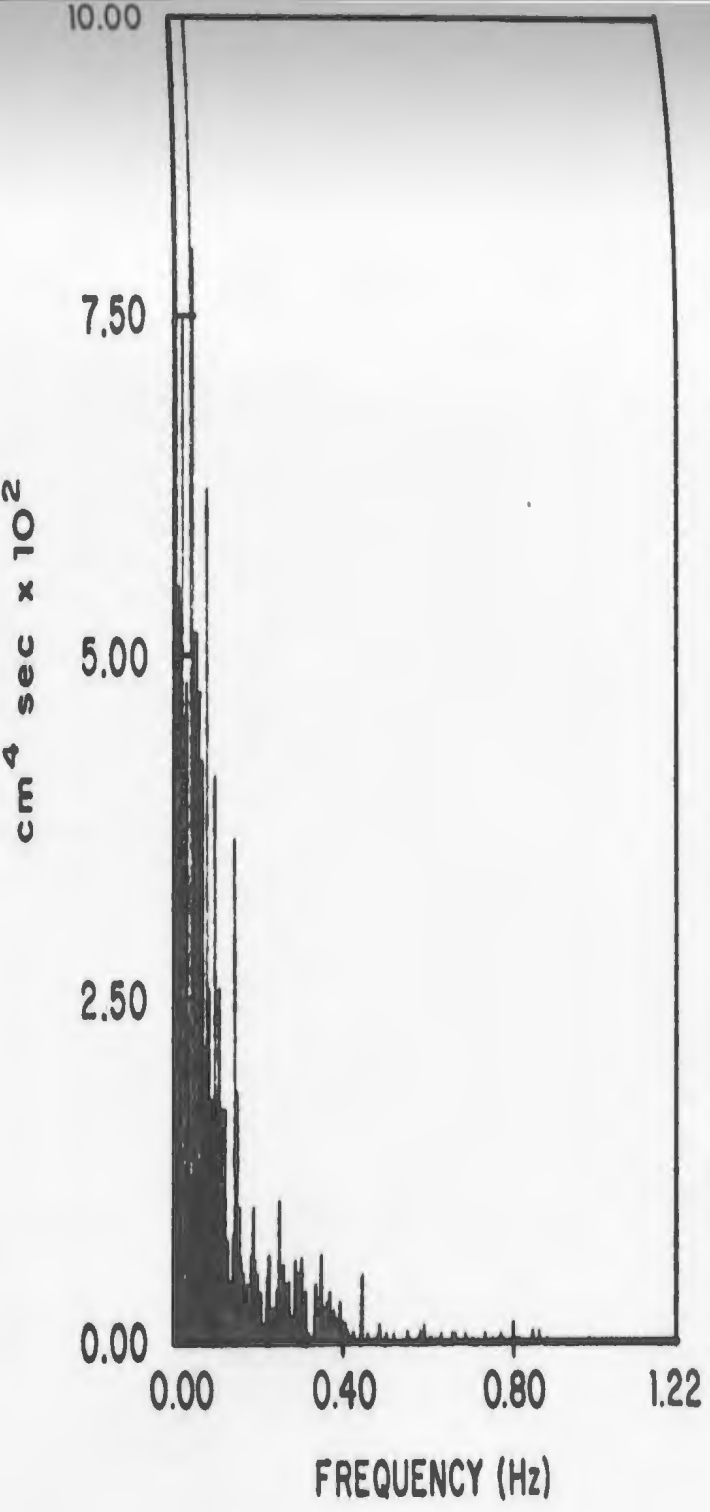

FIG. 5.10 WAVE AND SIWEH SPECTRAL DENSITIES FOR SPECTRUM 6

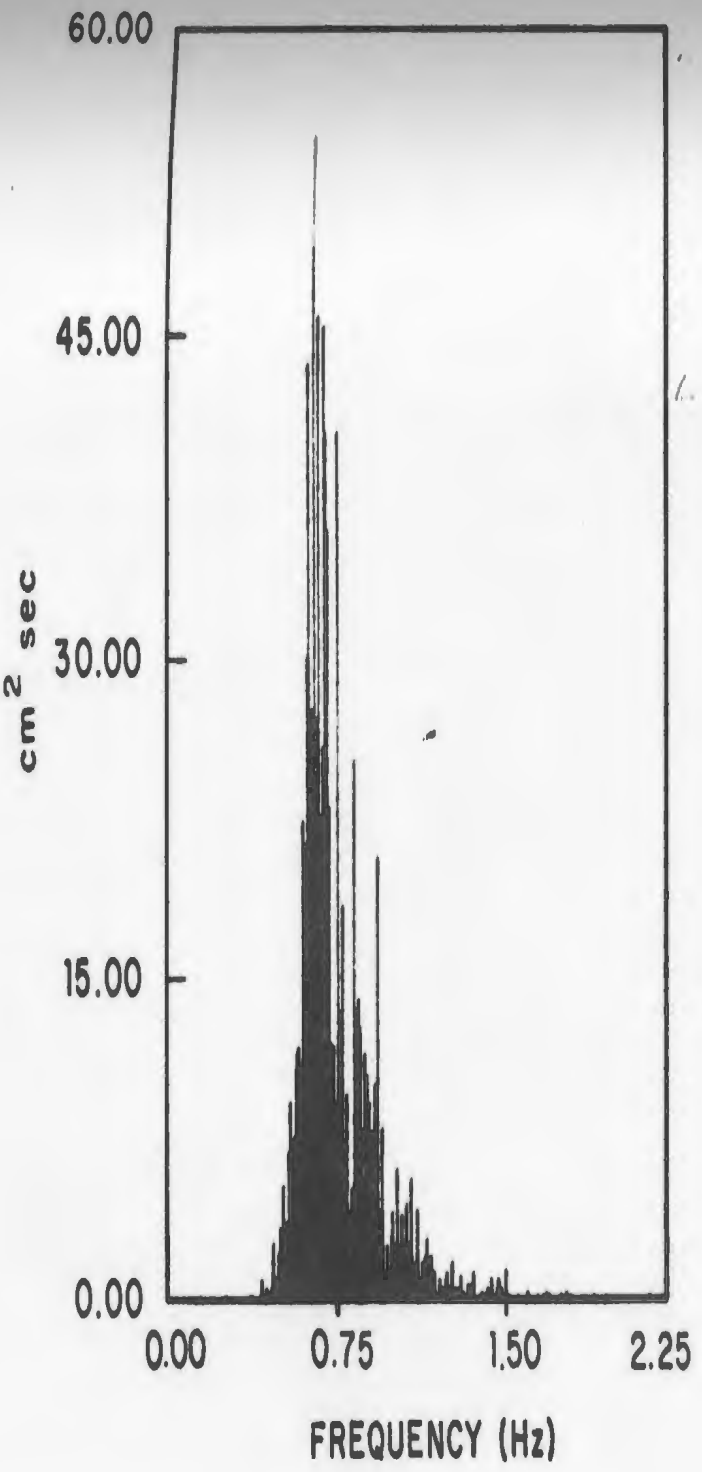

WAVE SPECTRAL DENSITY

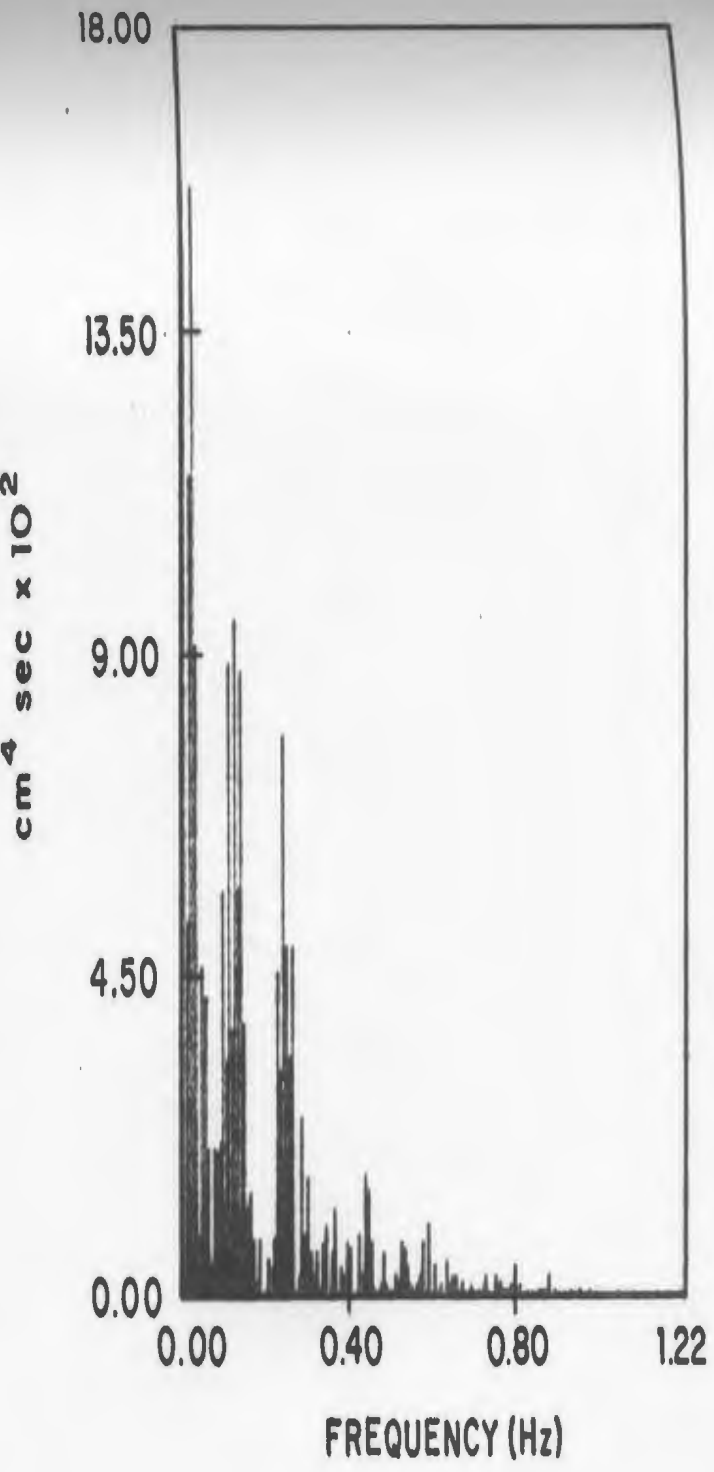

SIWEH SPECTRAL DENSITY

FIG. 5.11 WAVE AND SIWEH SPECTRAL DENSITIES FOR SPECTRUM 8

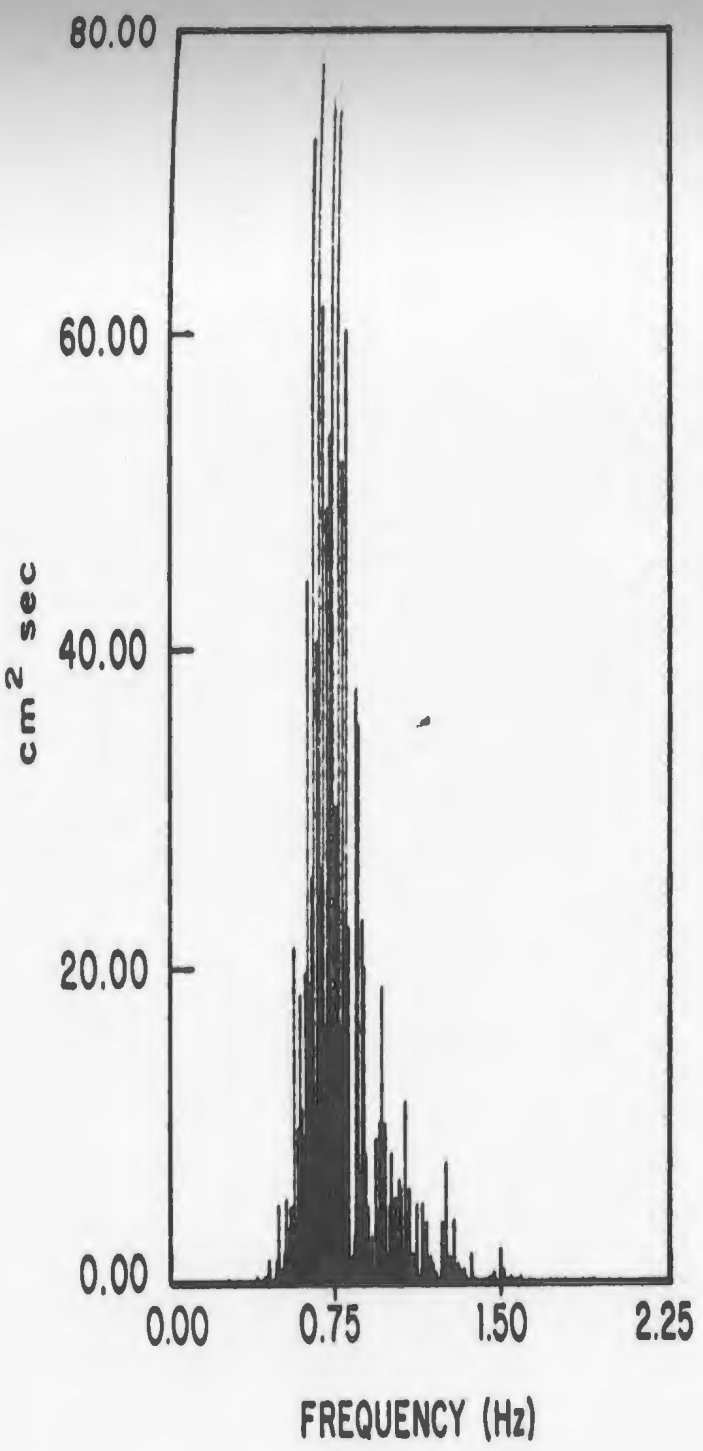

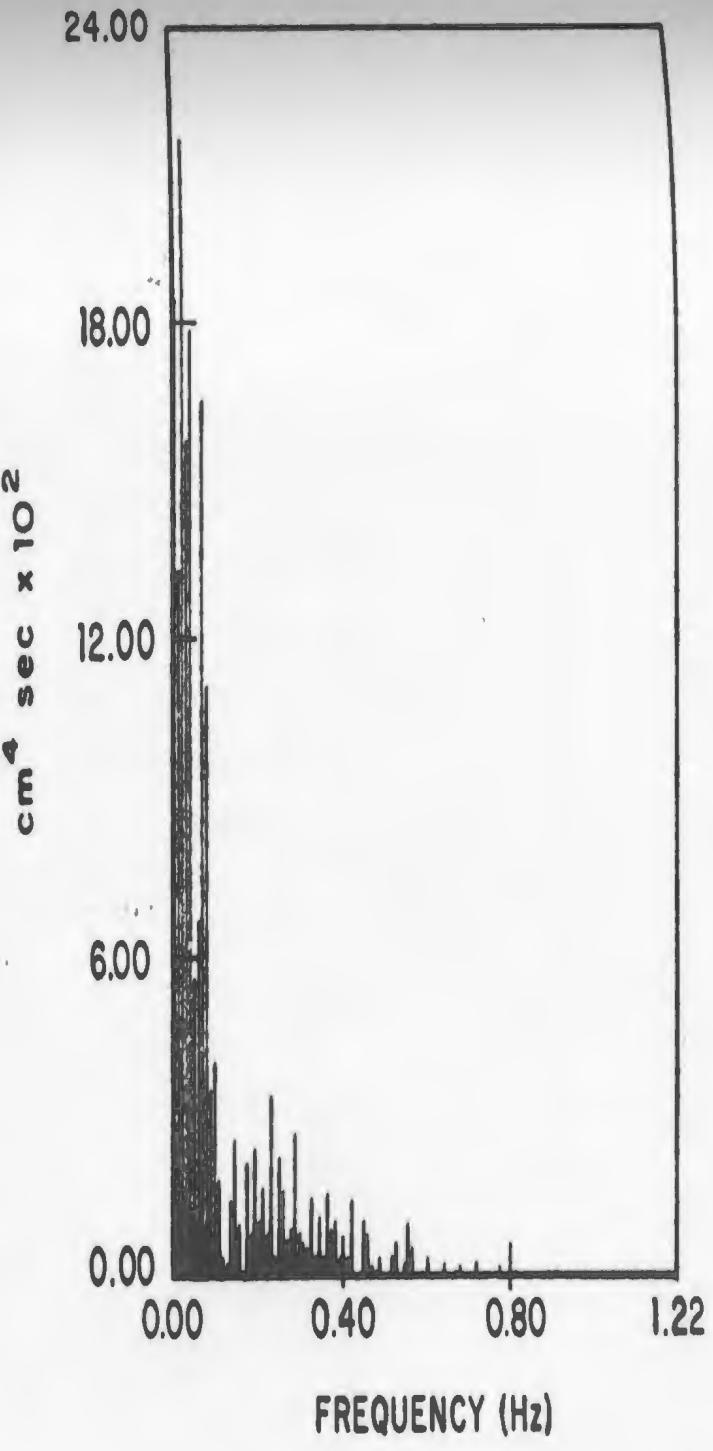

FIG. 5.12 WAVE AND SIWEH SPECTRAL DENSITIES FOR SPECTRUM 10

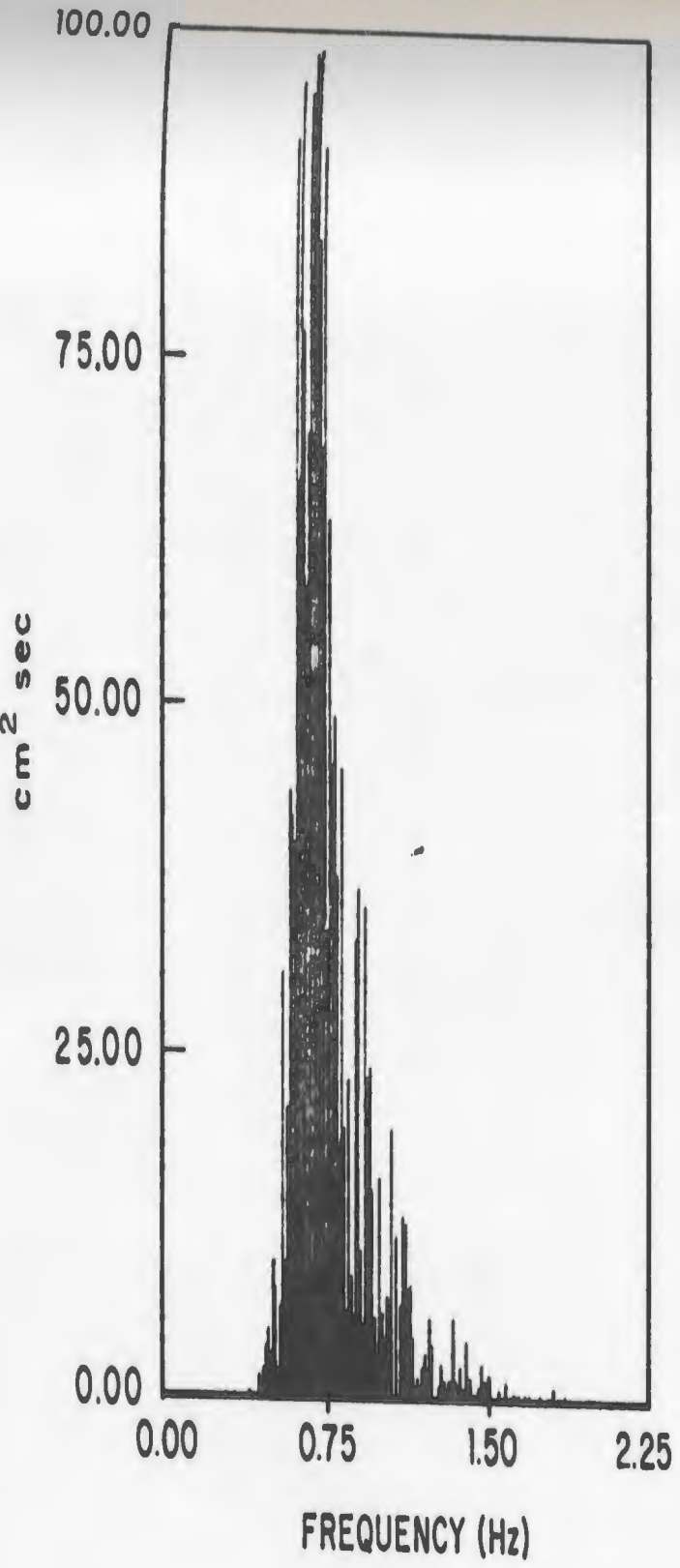

WAVE SPECTRAL DENSITY

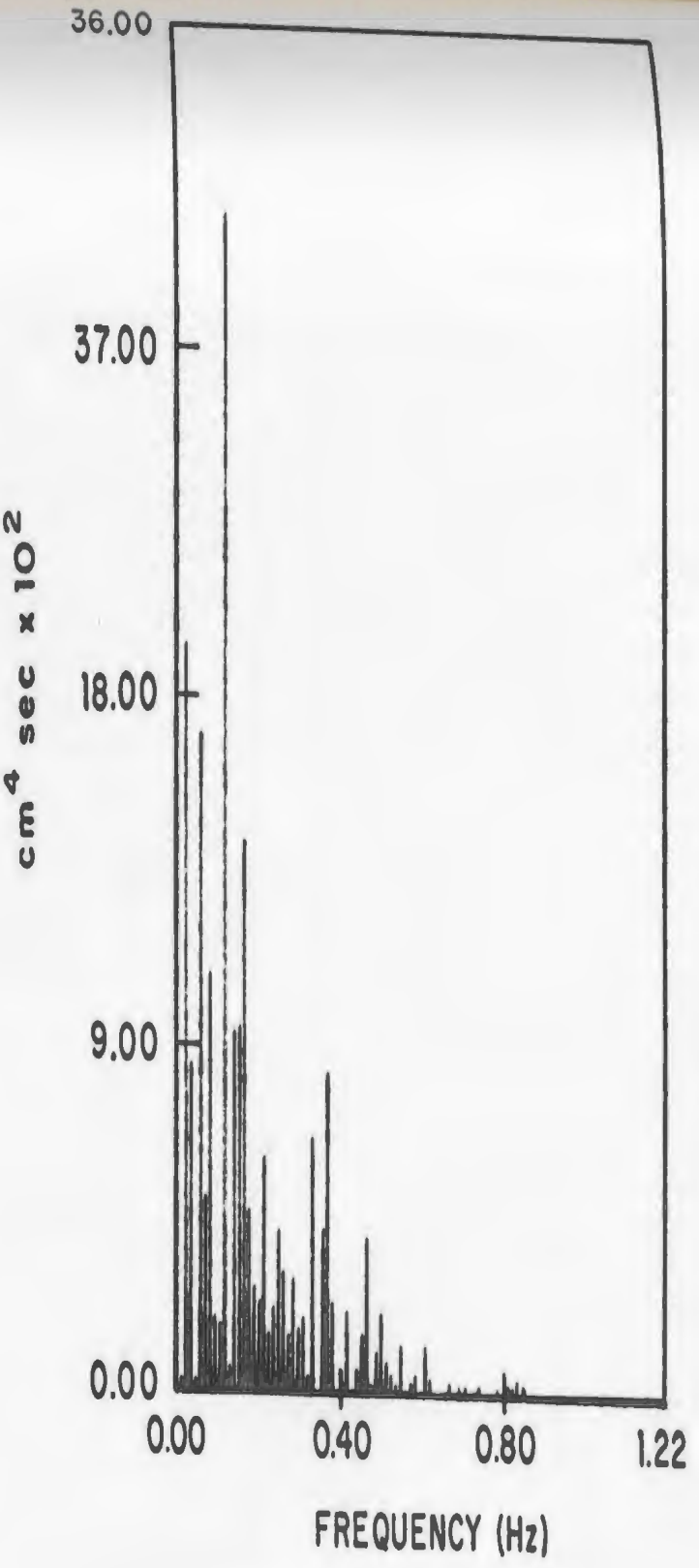

SIWEH SPECTRAL DENSITY

FIG. 5.13 WAVE AND SIWEH SPECTRAL DENSITIES FOR SPECTRUM 12

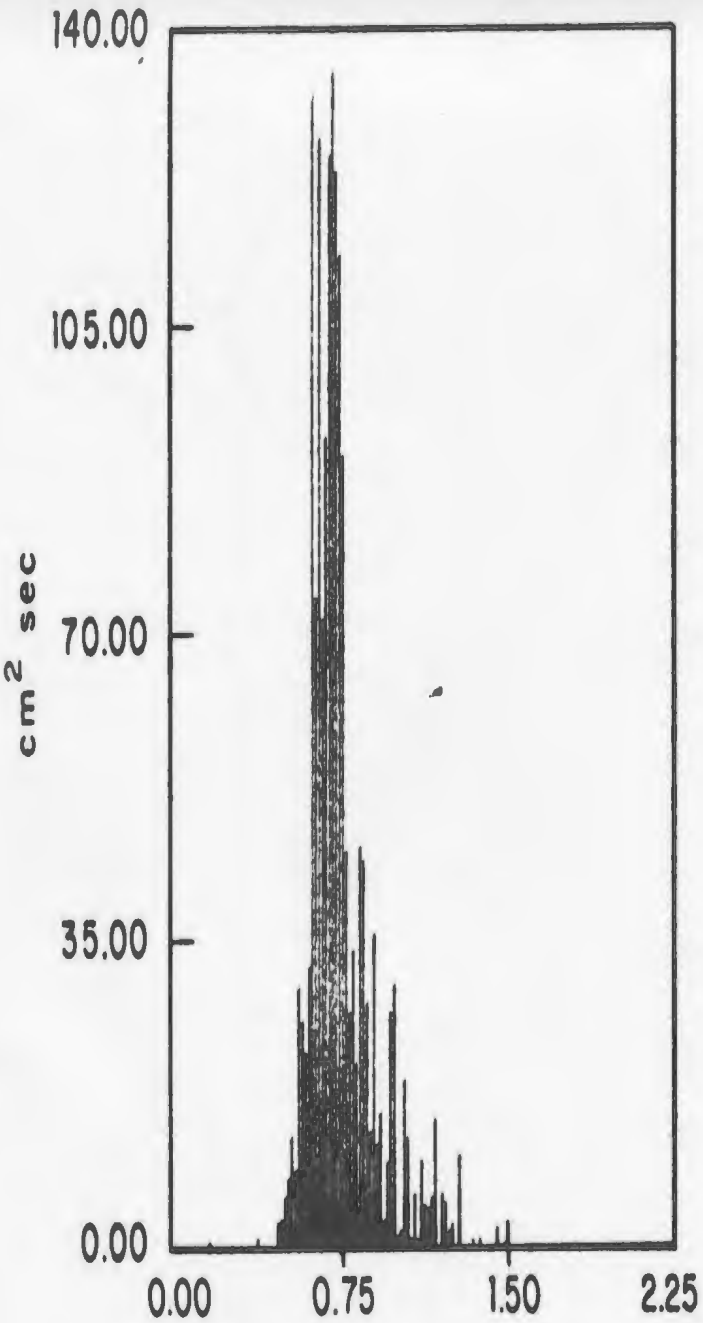

WAVE SPECTRAL DENSITY

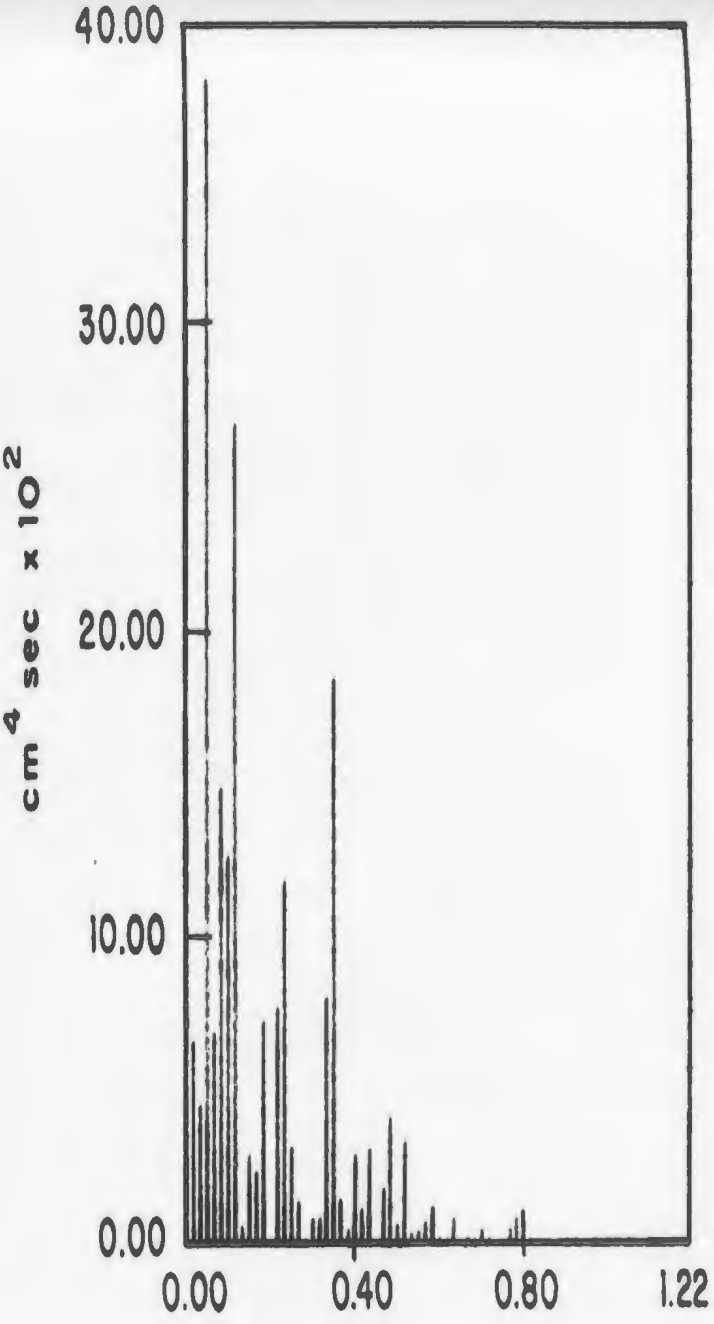

SIWEH SPECTRAL DENSITY

FIG. 5.14 WAVE AND SIWEH SPECTRAL DENSITIES FOR SPECTRUM 14

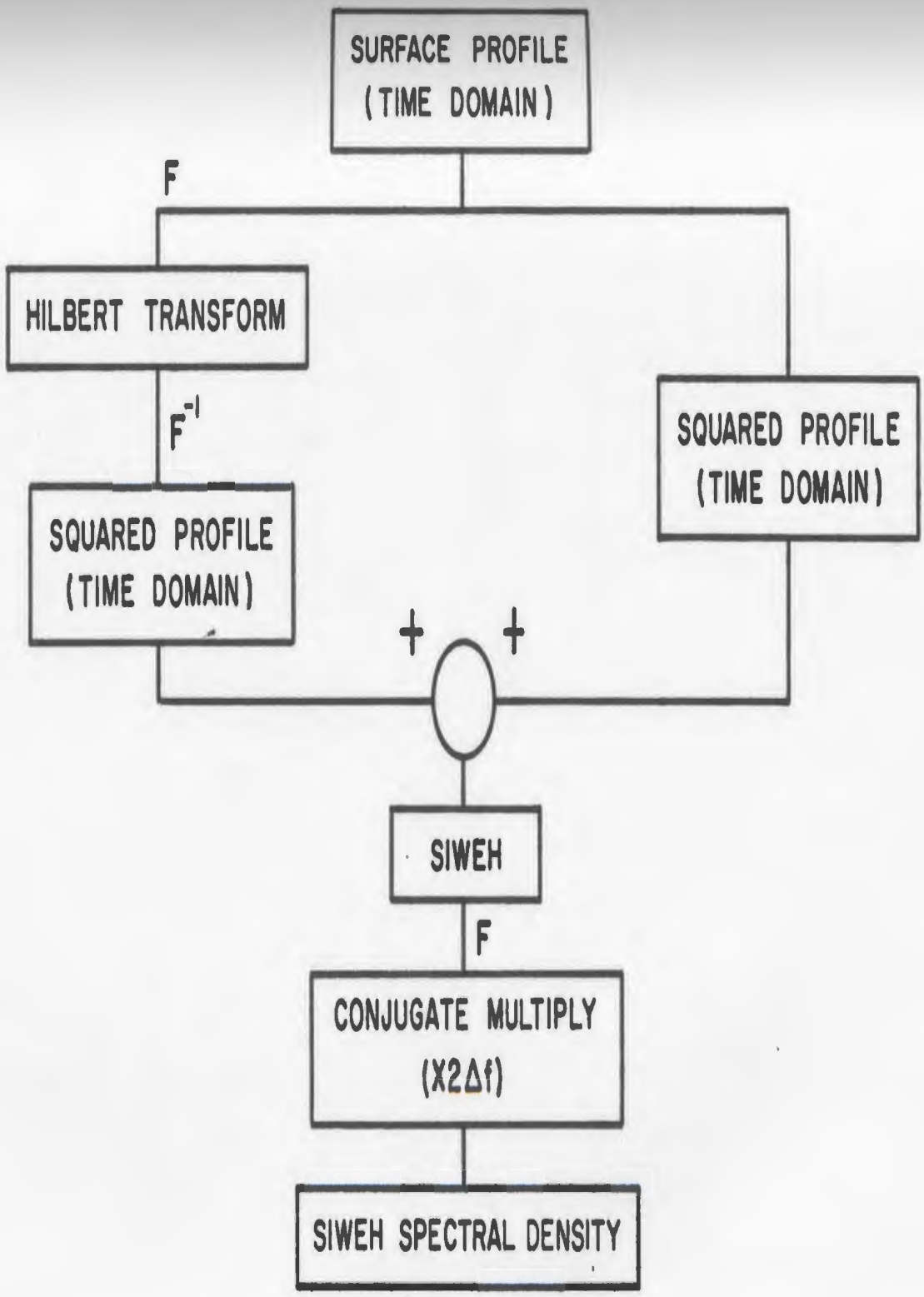

FIG. 5.15 METHOD TO DETERMINE SIWEH SPECTRAL DENSITY

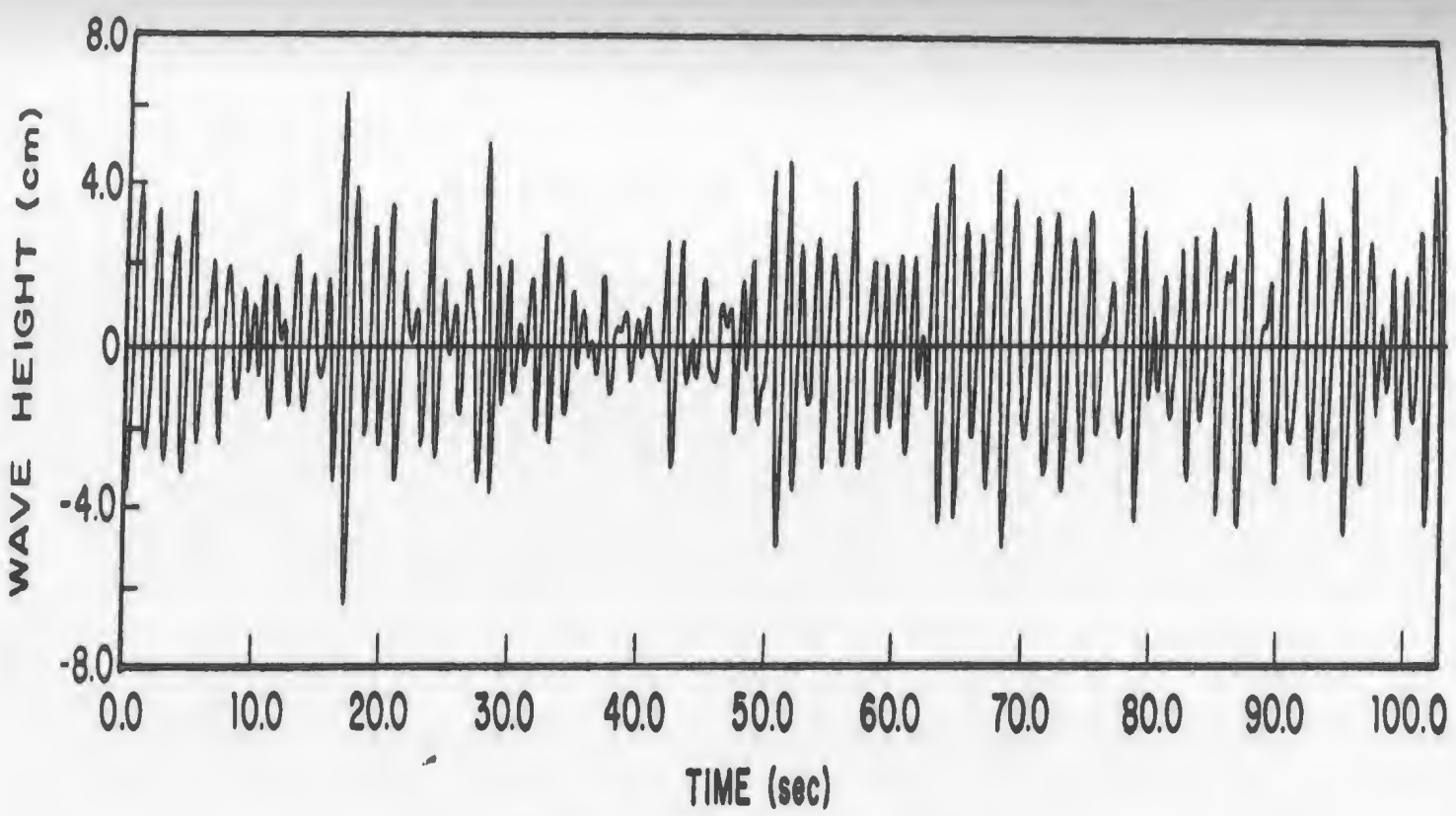

TARGET PROFILE OF SPECTRUM 10

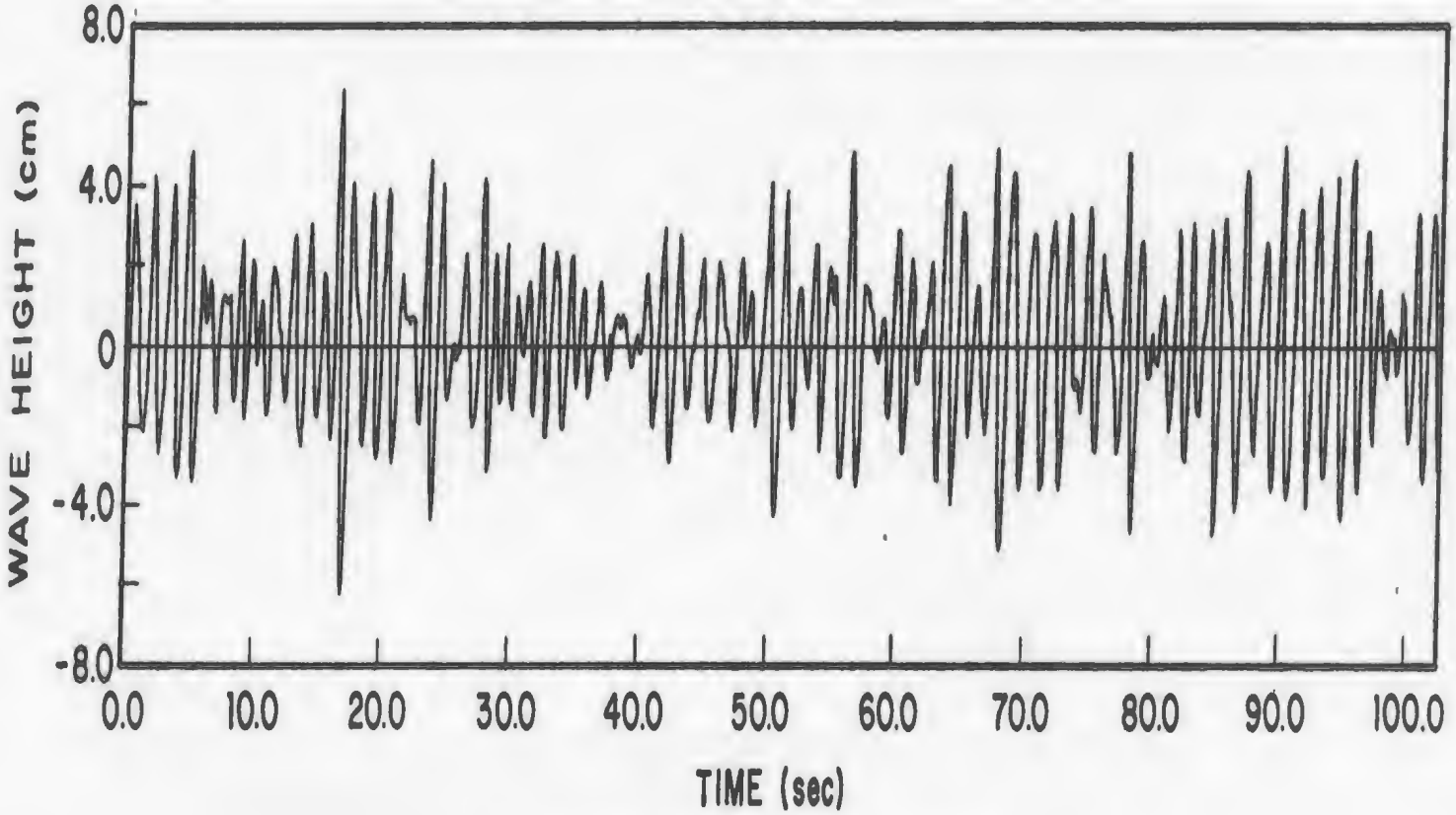

MEASURED PROFILE OF SPECTRUM 10

FIG. 5.16 TARGET AND MEASURED PROFILES OF GROUP 10

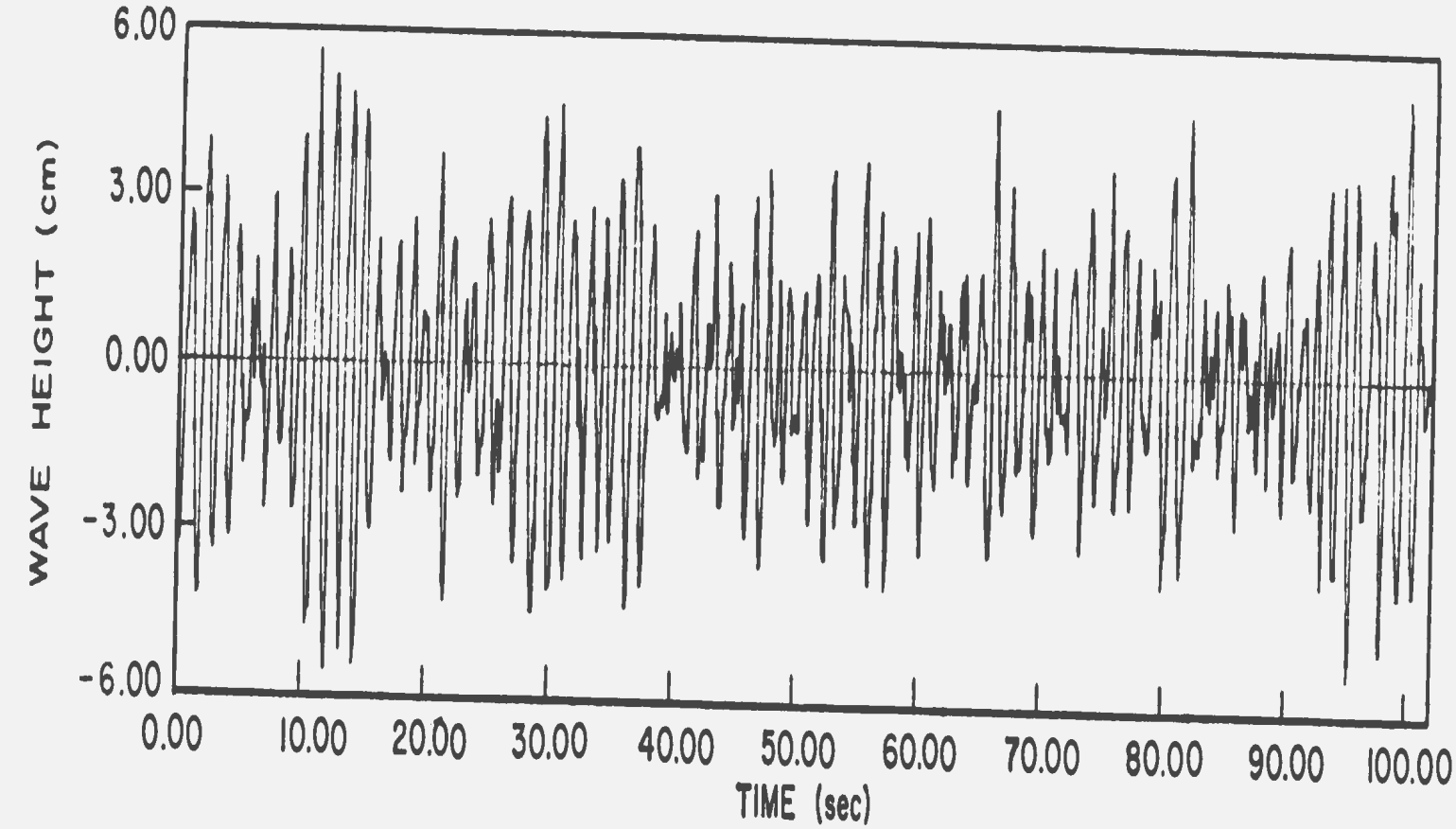

TARGET PROFILE OF SPECTRUM 2

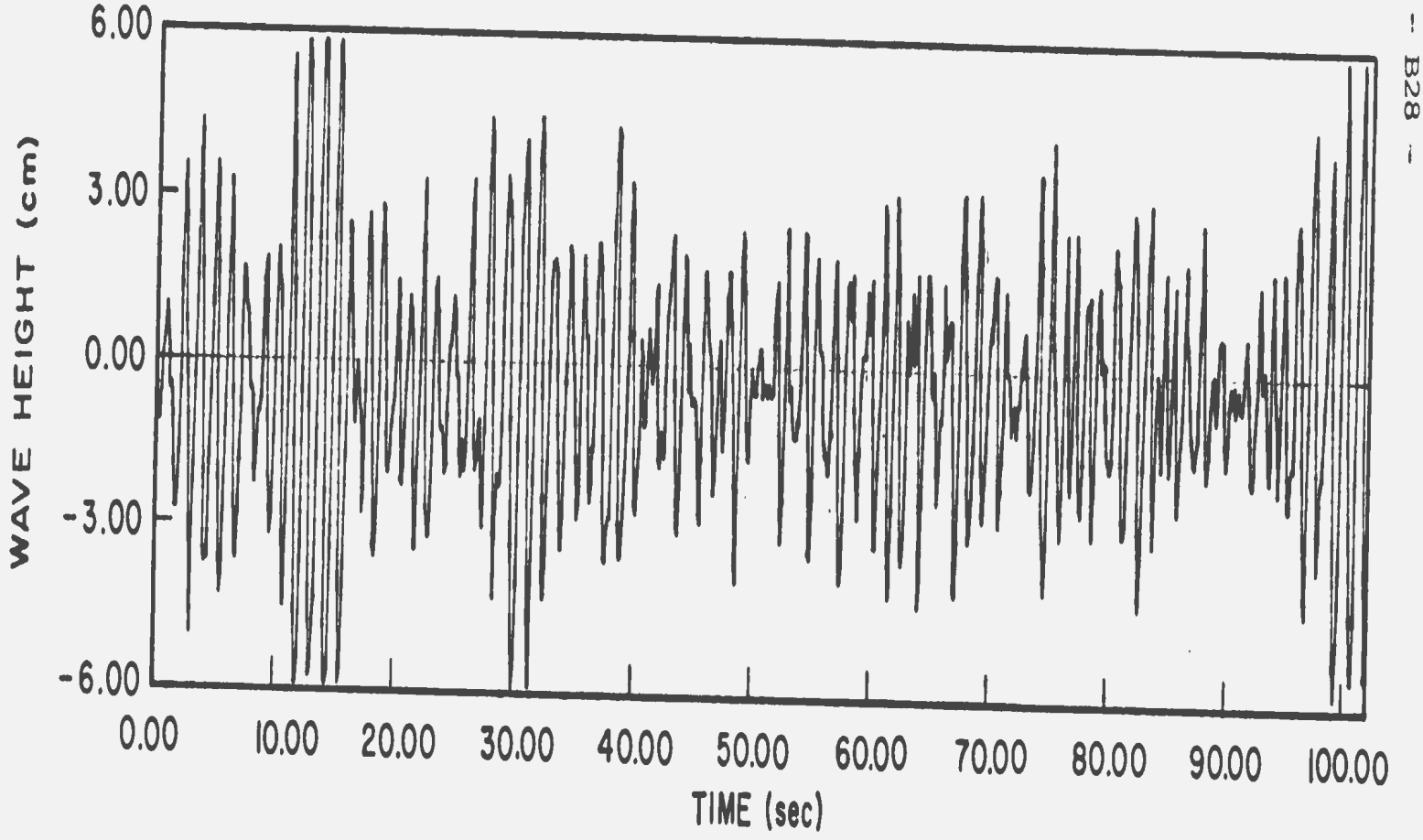

MEASURED PROFILE OF SPECTRUM 2

FIG. 5.17 TARGET AND MEASURED PROFILES OF GROUP 2

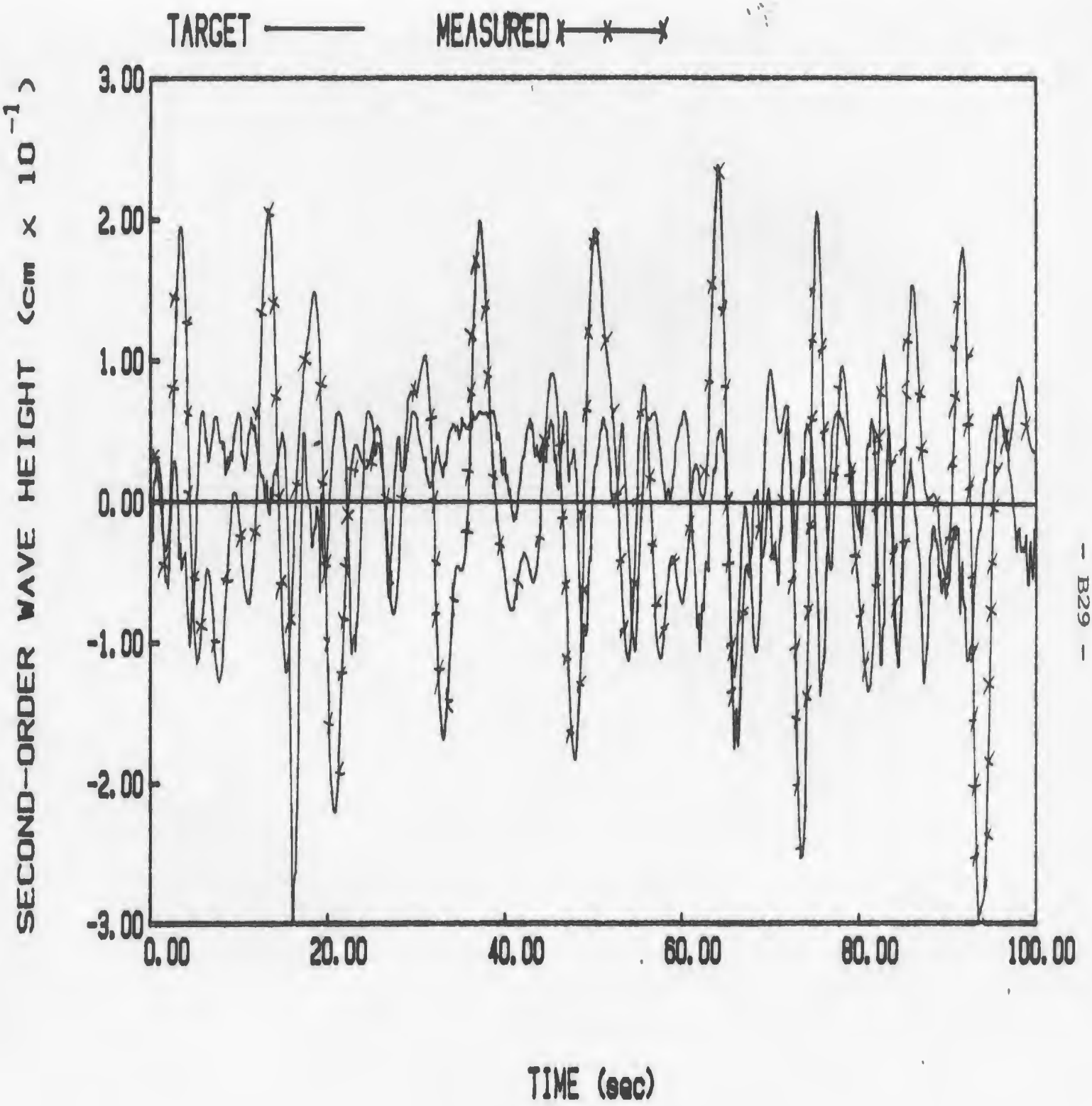

FIG. 5.18 TARGET AND MEASURED SECOND-ORDER PROFILES OF GROUP 10

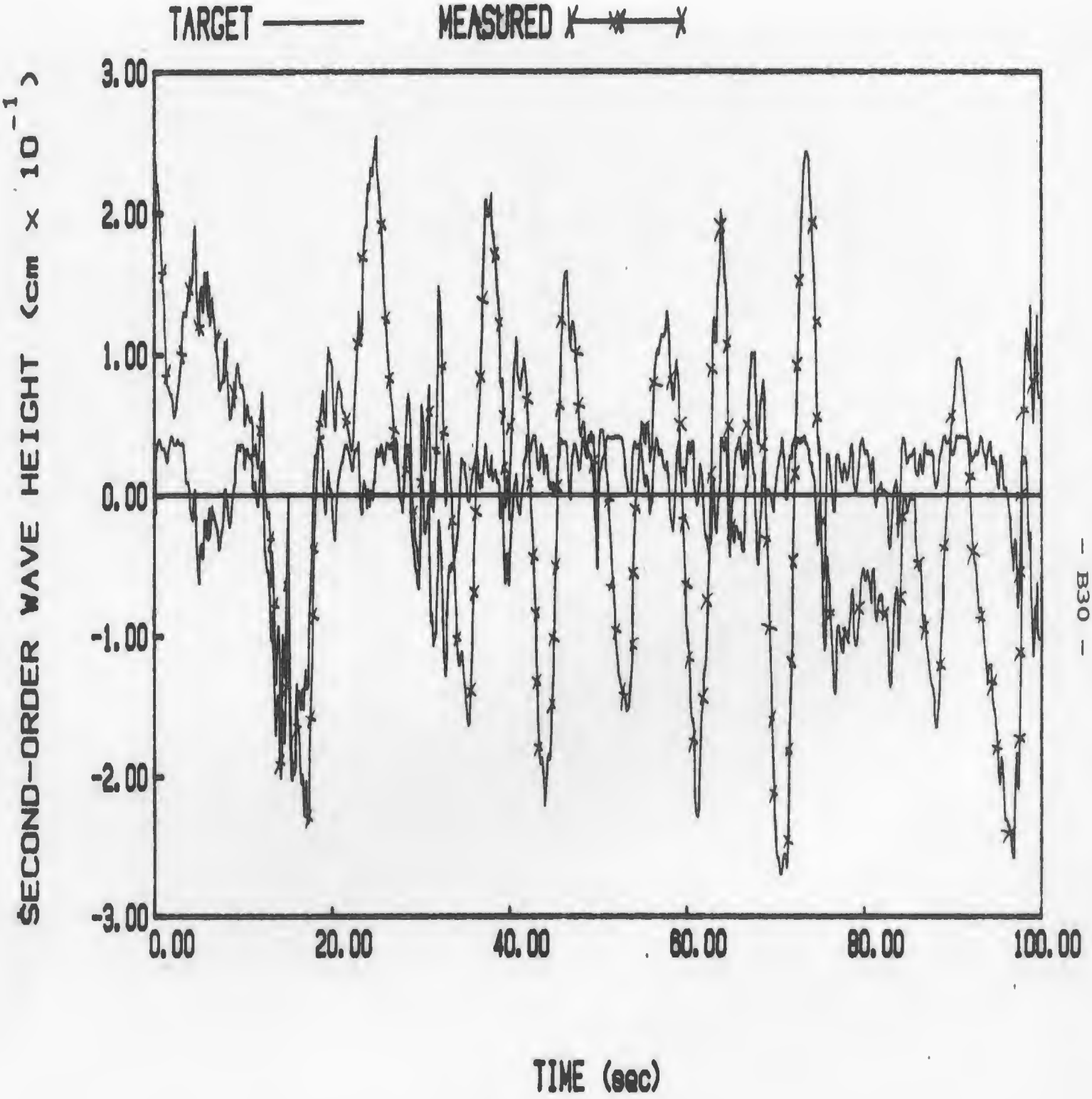

FIG. 5.19 TARGET AND MEASURED SECOND-ORDER PROFILES OF GROUP 2

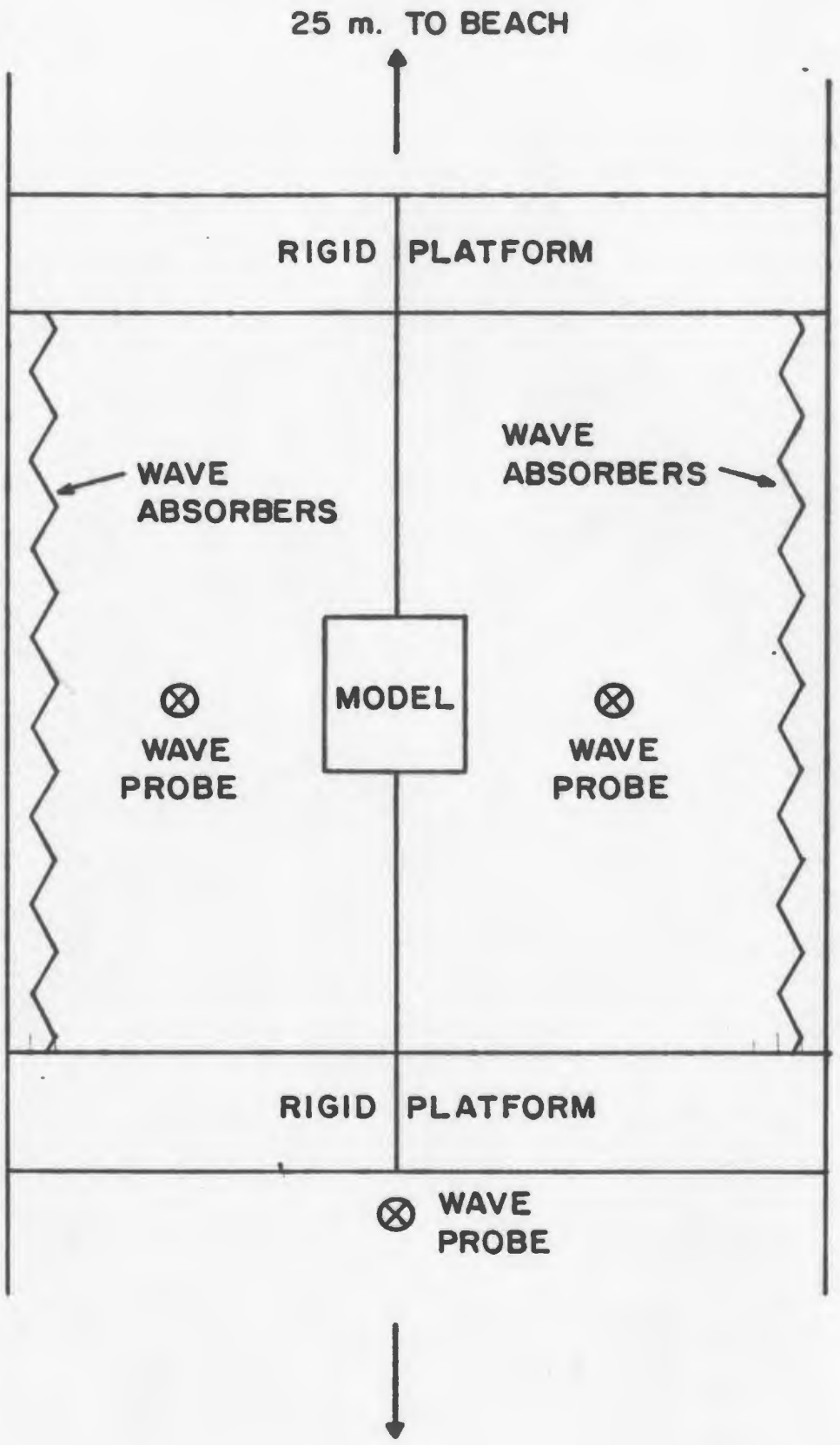

FIG. 5.20 RECTANGULAR BARGE IN MOORED POSITION
PLAN VIEW

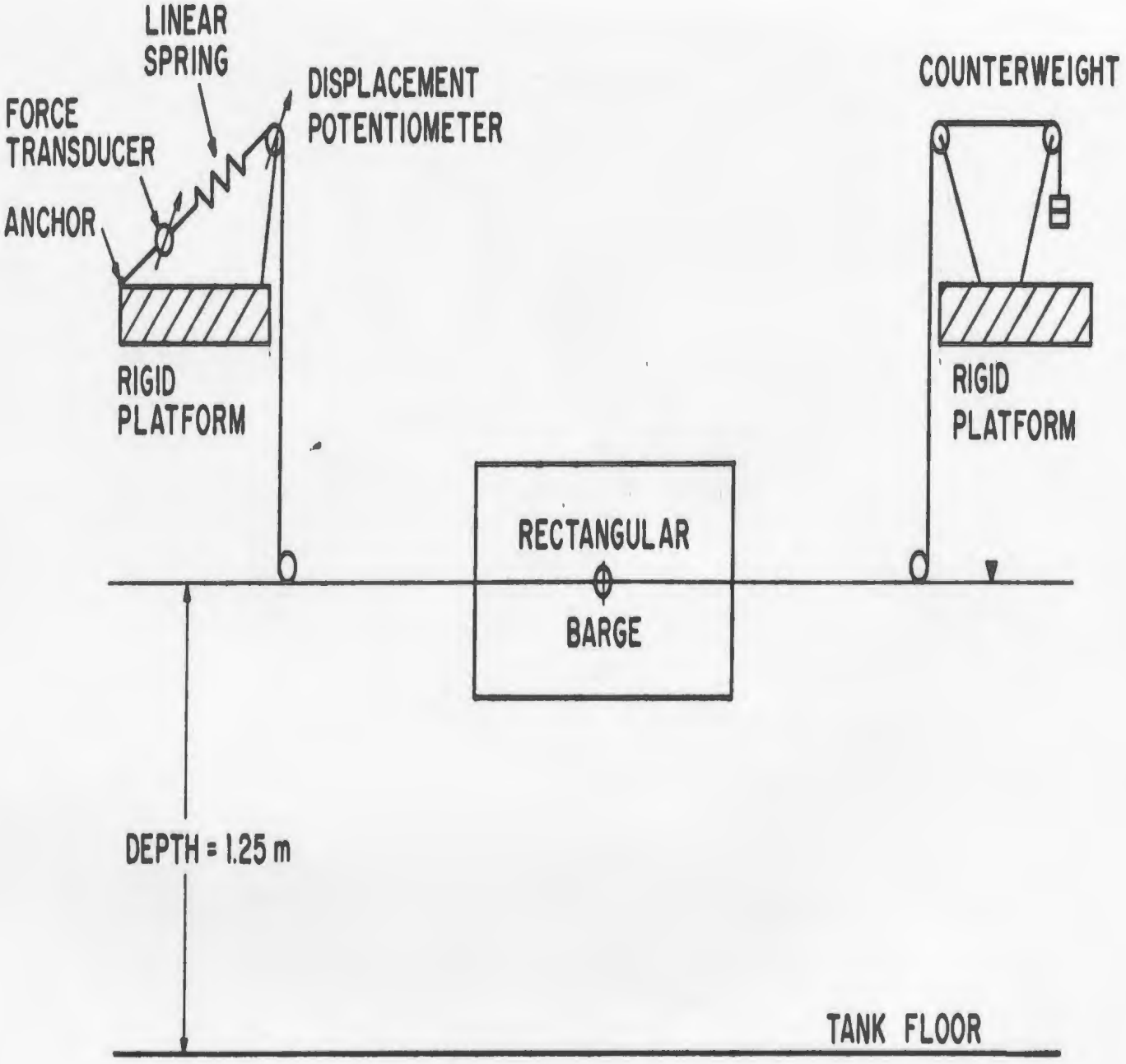

FIG. 5.21 RECTANGULAR BARGE MODEL MOORED IN POSITION, SIDE VIEW

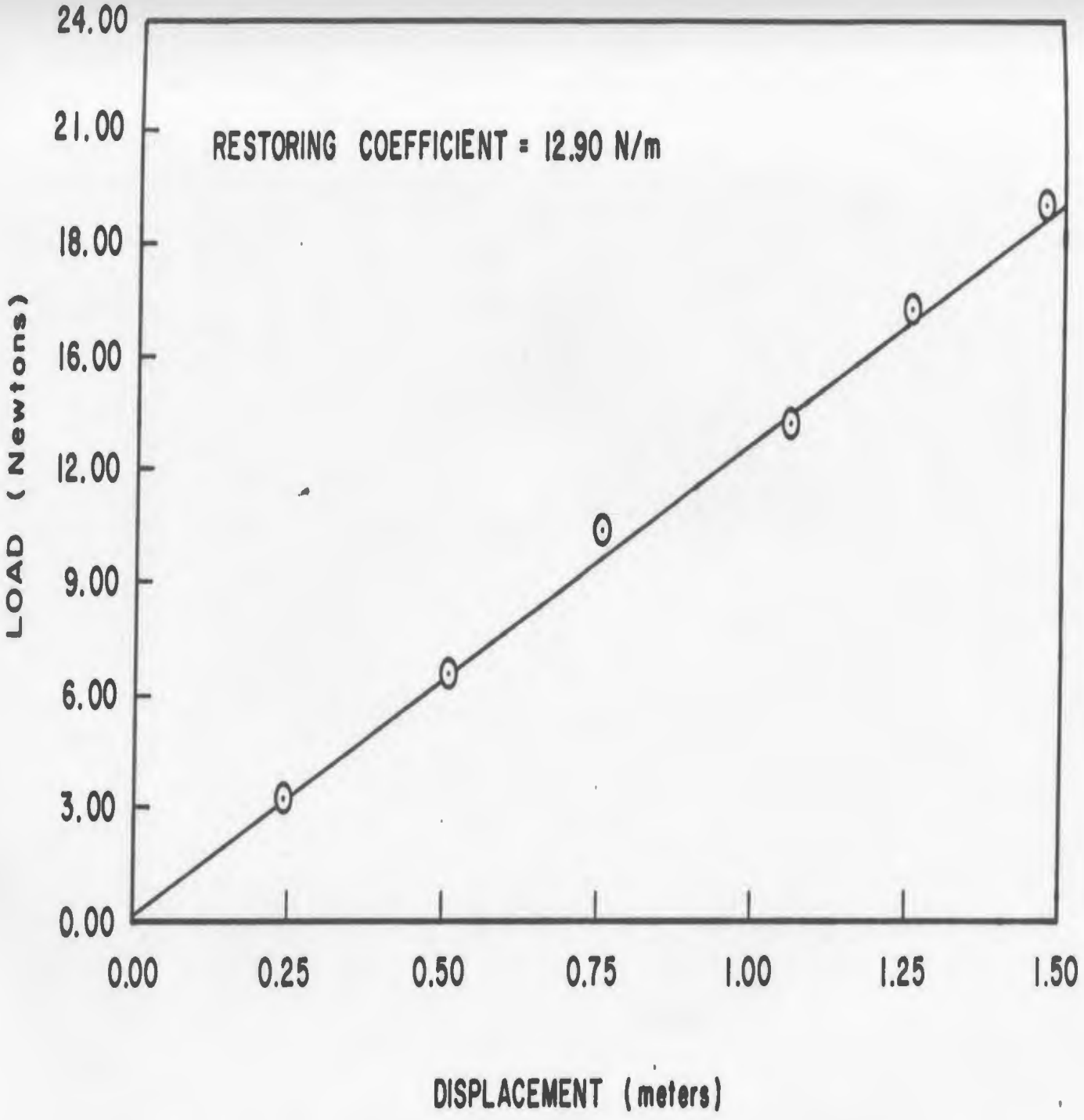

FIG. 5.22 TOTAL RESTORING COEFFICIENT OF BARGE IN MOORED CONDITION

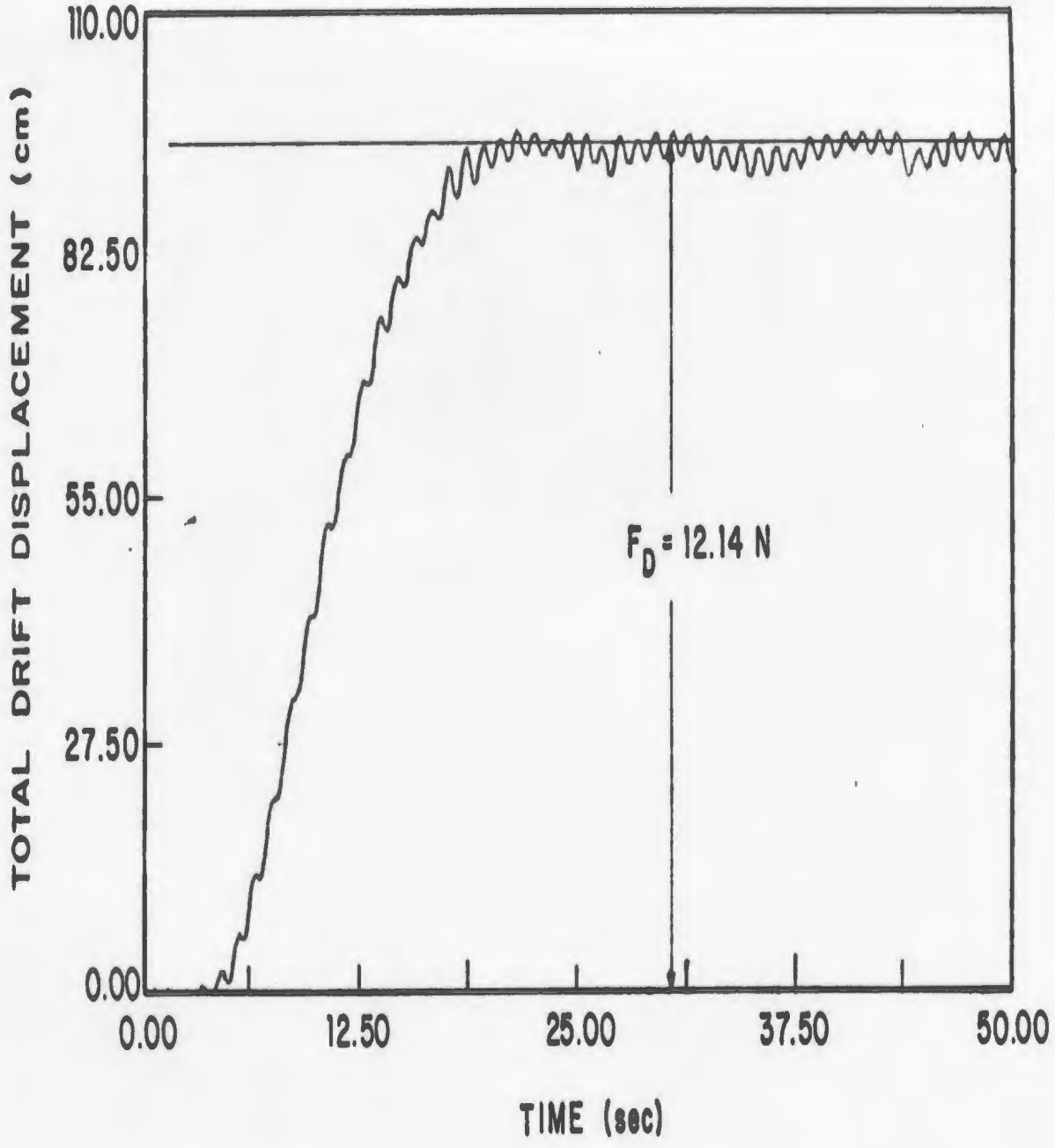

FIG. 5.23 SAMPLE OF STEADY DRIFT RESPONSE OF BARGE IN REGULAR WAVES

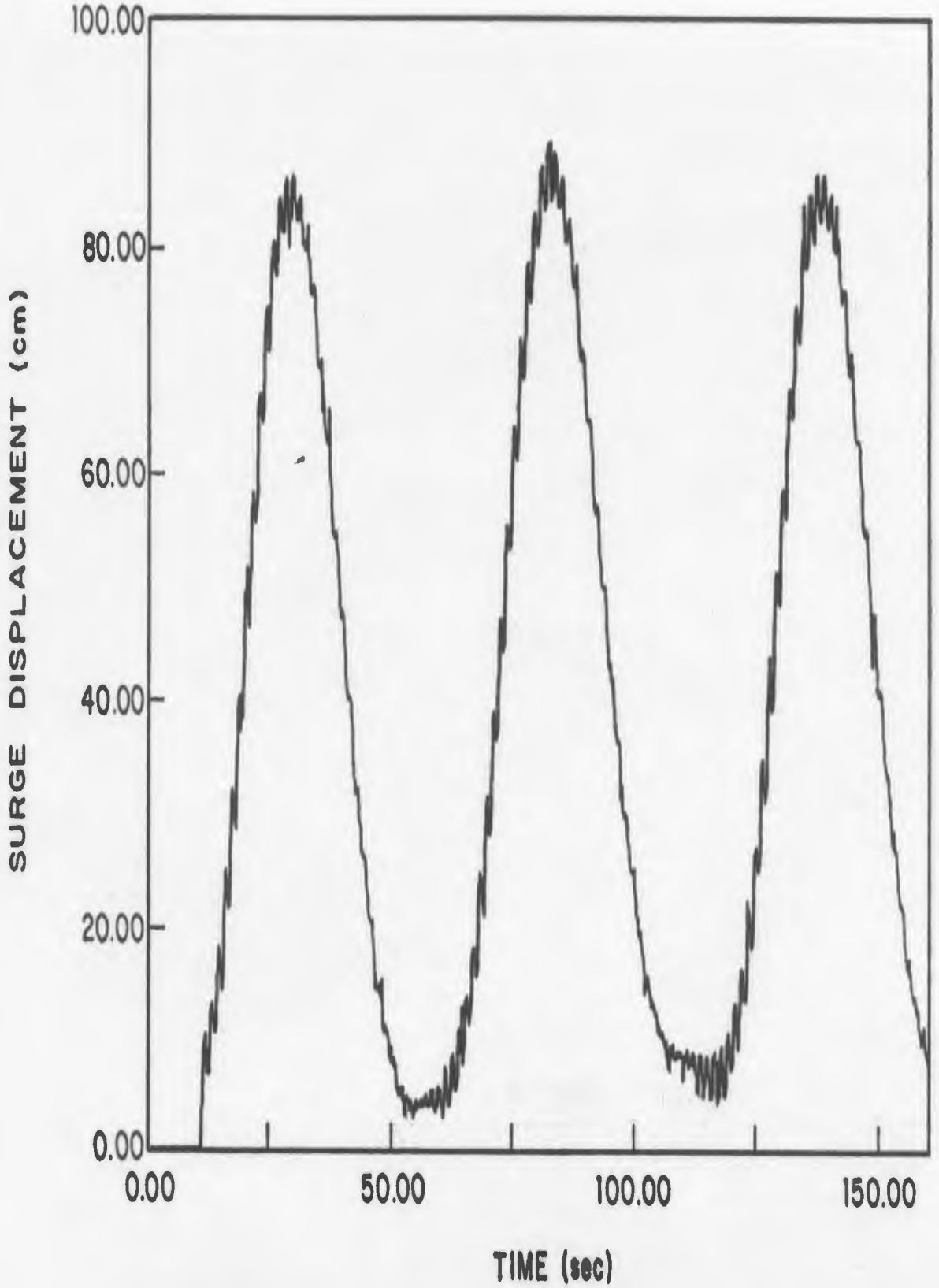

FIG. 5.24 SAMPLE OF SLOW — DRIFT RESPONSE OF BARGE IN REGULAR WAVE GROUP

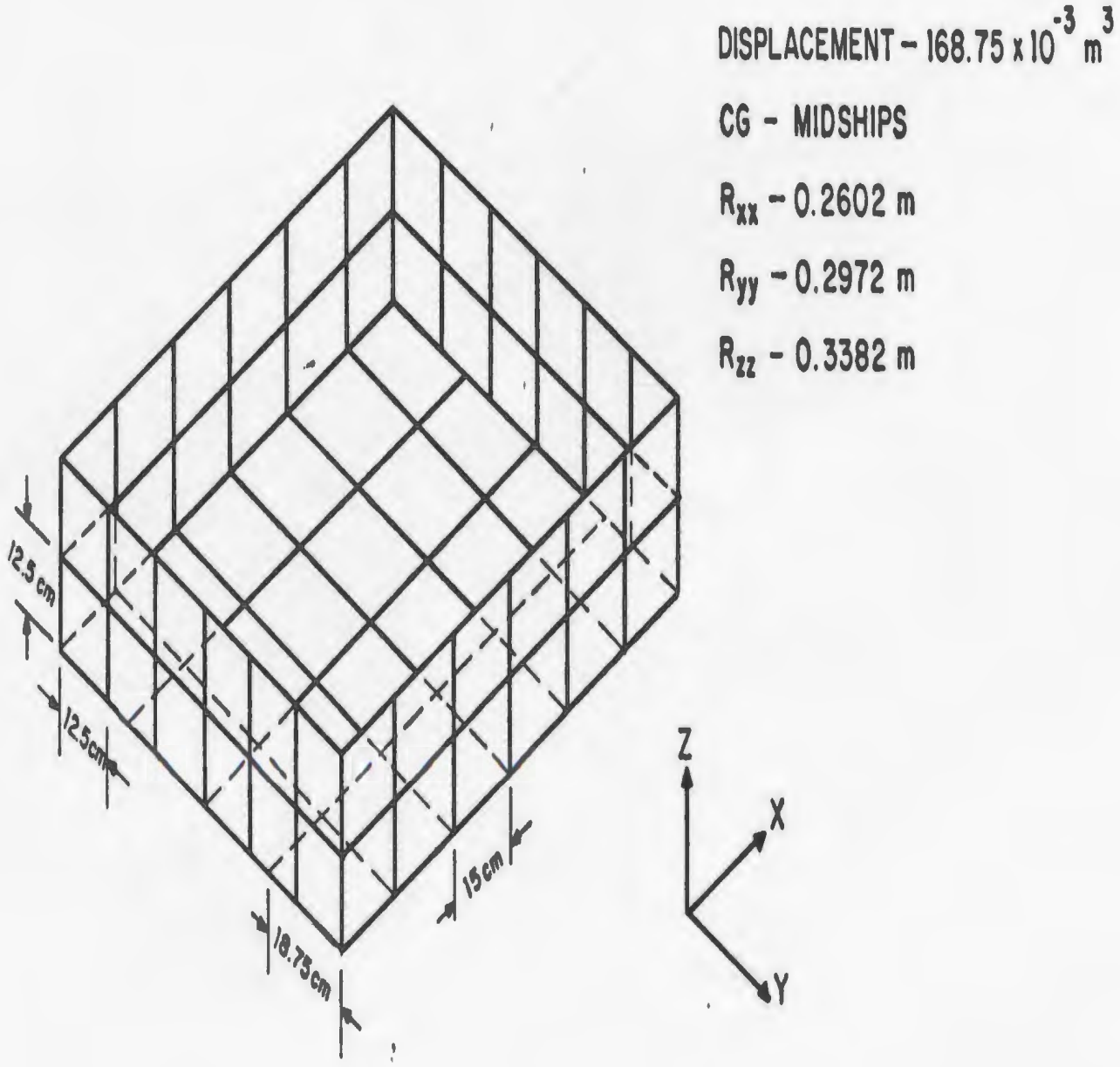

FIG. 6.1 RECTANGULAR BARGE USED IN MODEL TESTS

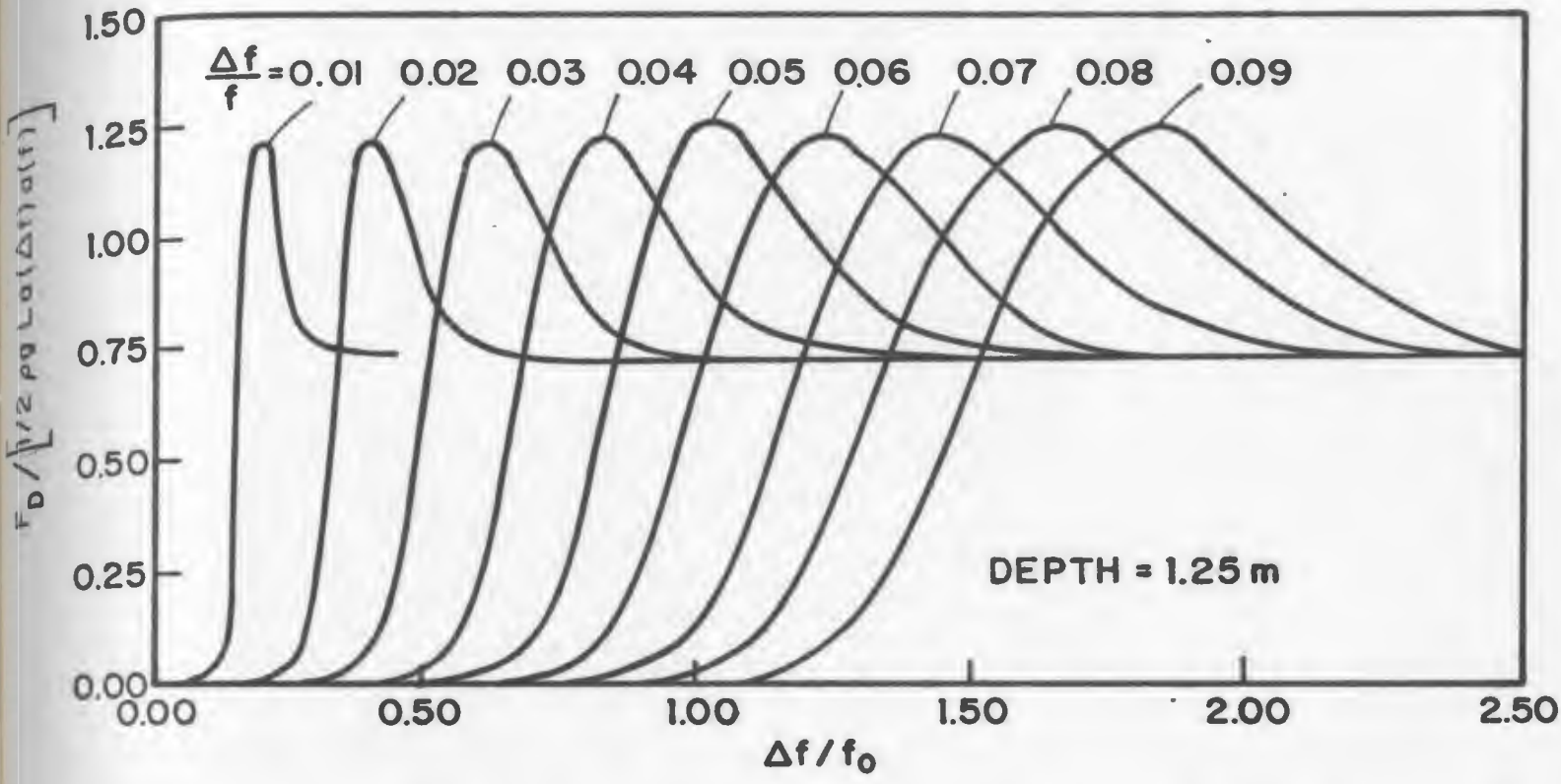

CONTRIBUTIONS OF FIRST ORDER WAVES TO SLOW DRIFT FORCE

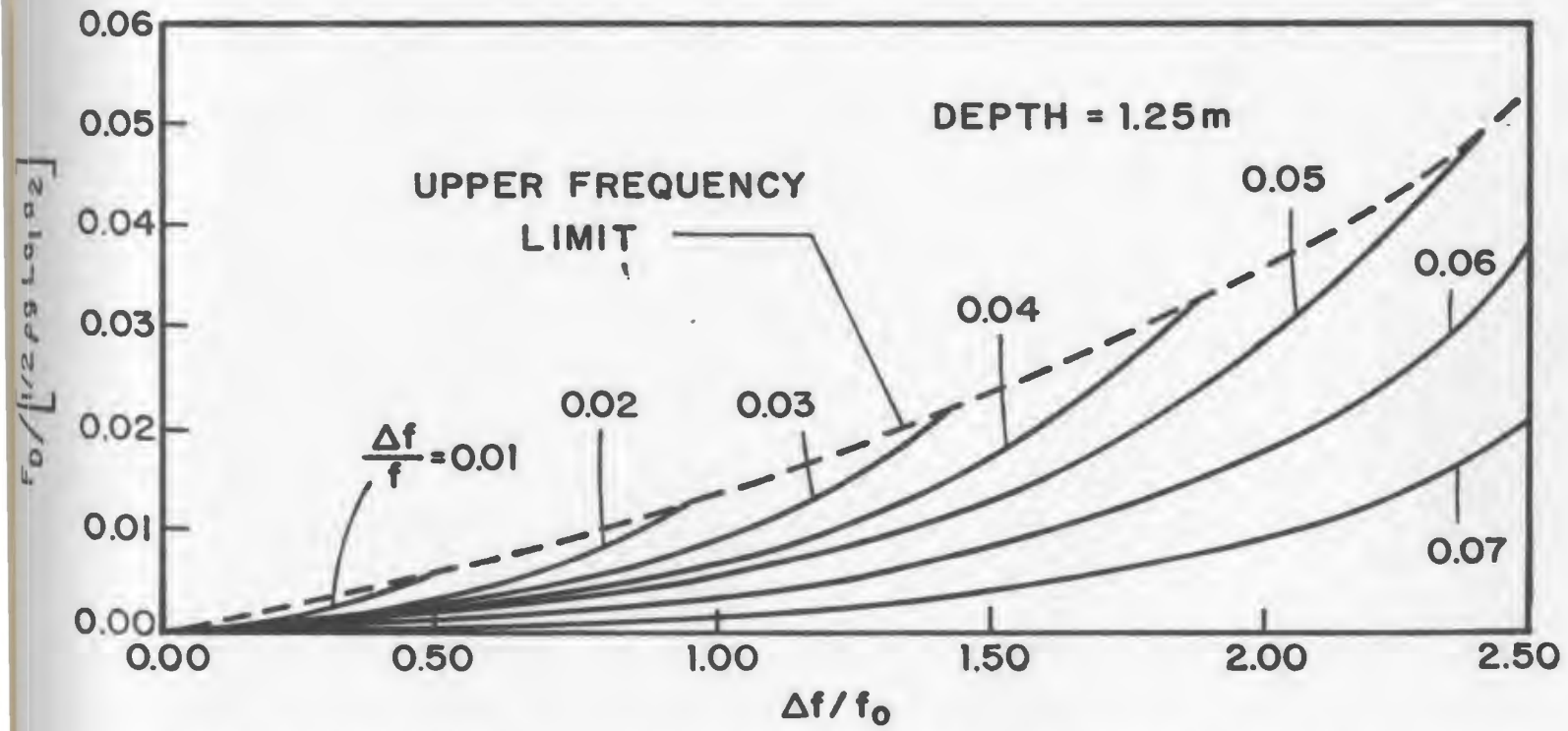

CONTRIBUTIONS OF SETDOWN WAVES TO SLOW DRIFT FORCE

FIG. 6.2 CONTRIBUTIONS TO SLOW DRIFT FORCE

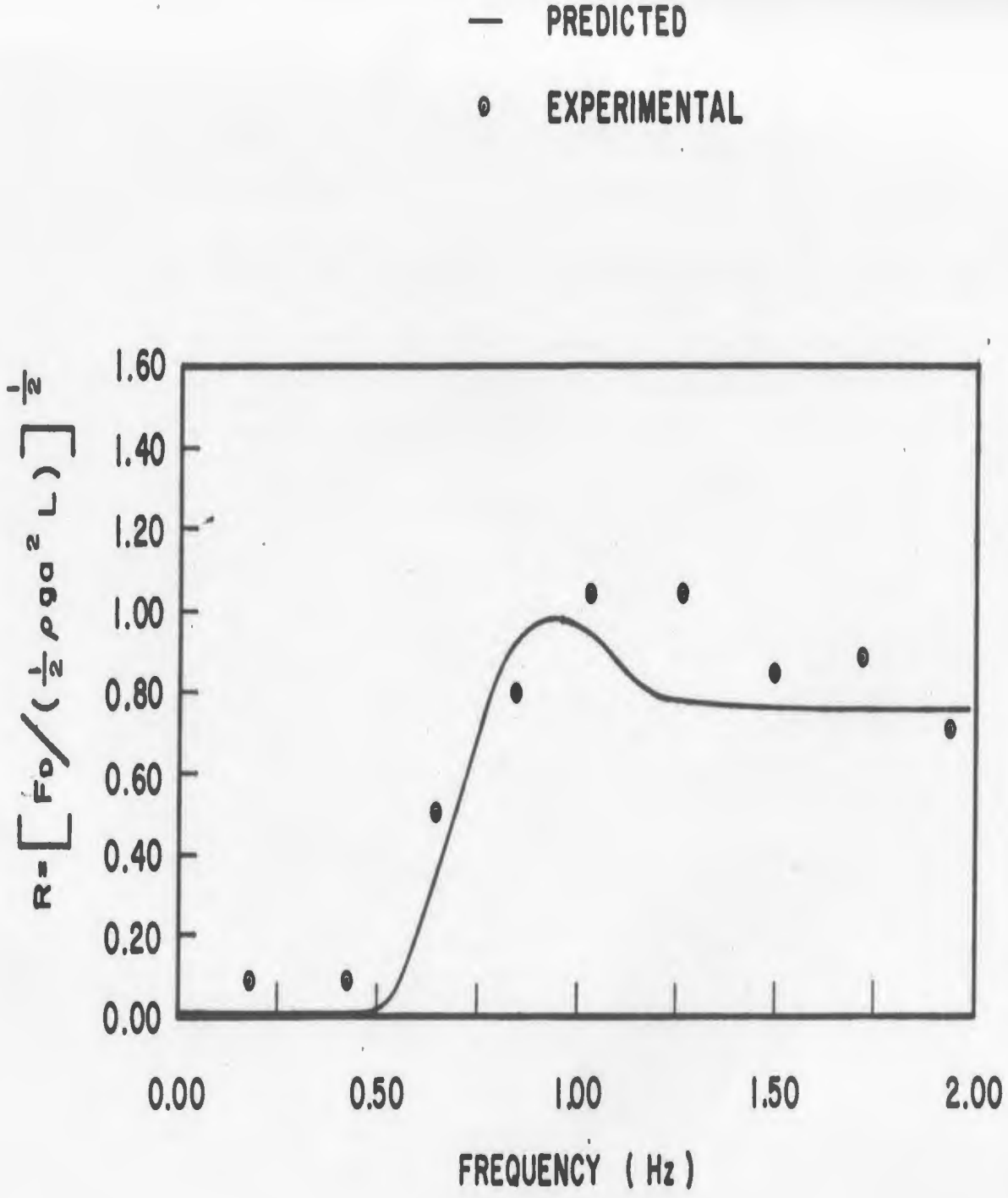

FIG. 6.3 STEADY DRIFT COEFFICIENTS OF RECTANGULAR BARGE IN REGULAR WAVES

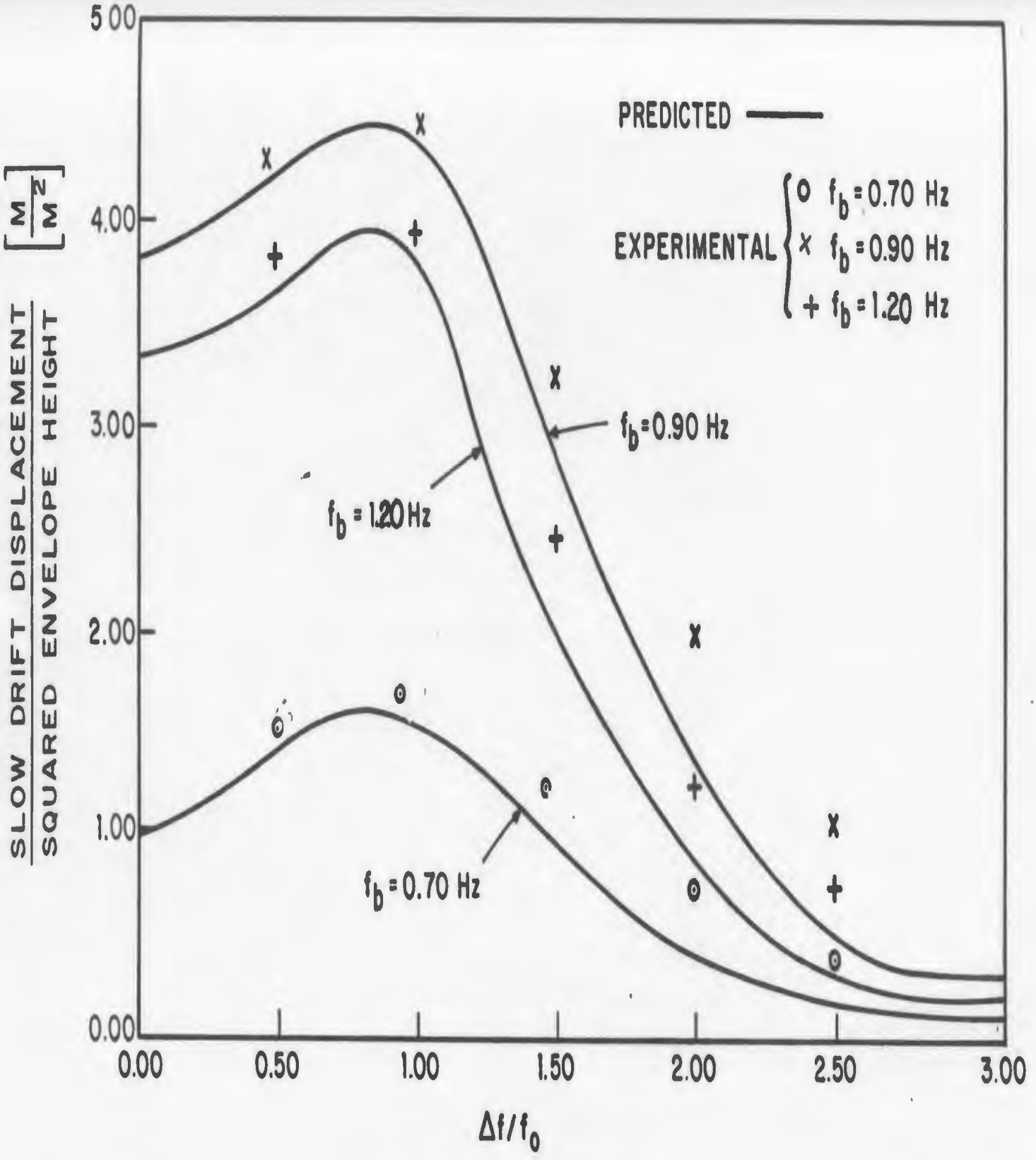

FIG. 6.4 RESPONSE OF RECTANGULAR BARGE TO REGULAR WAVE GROUPS

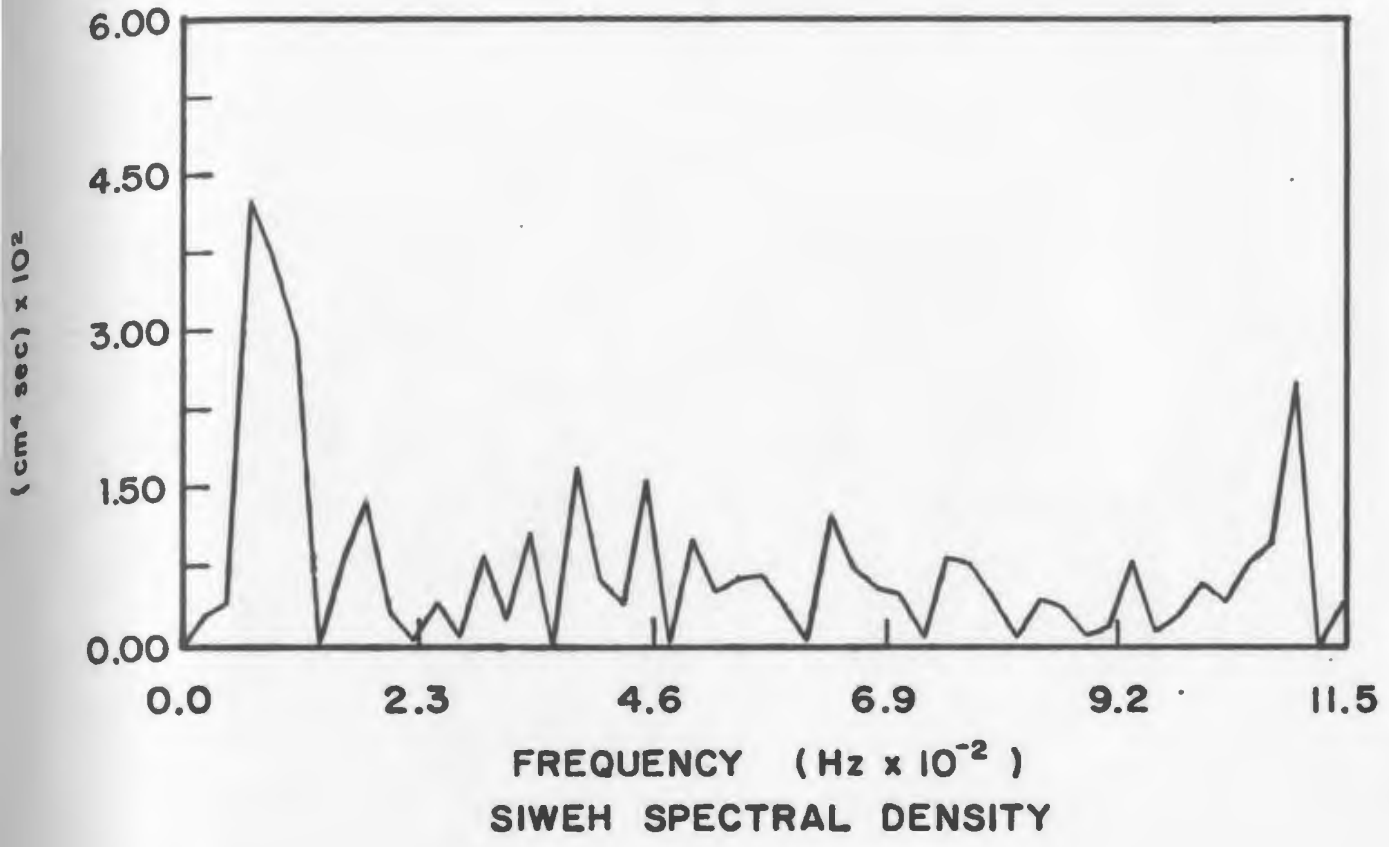

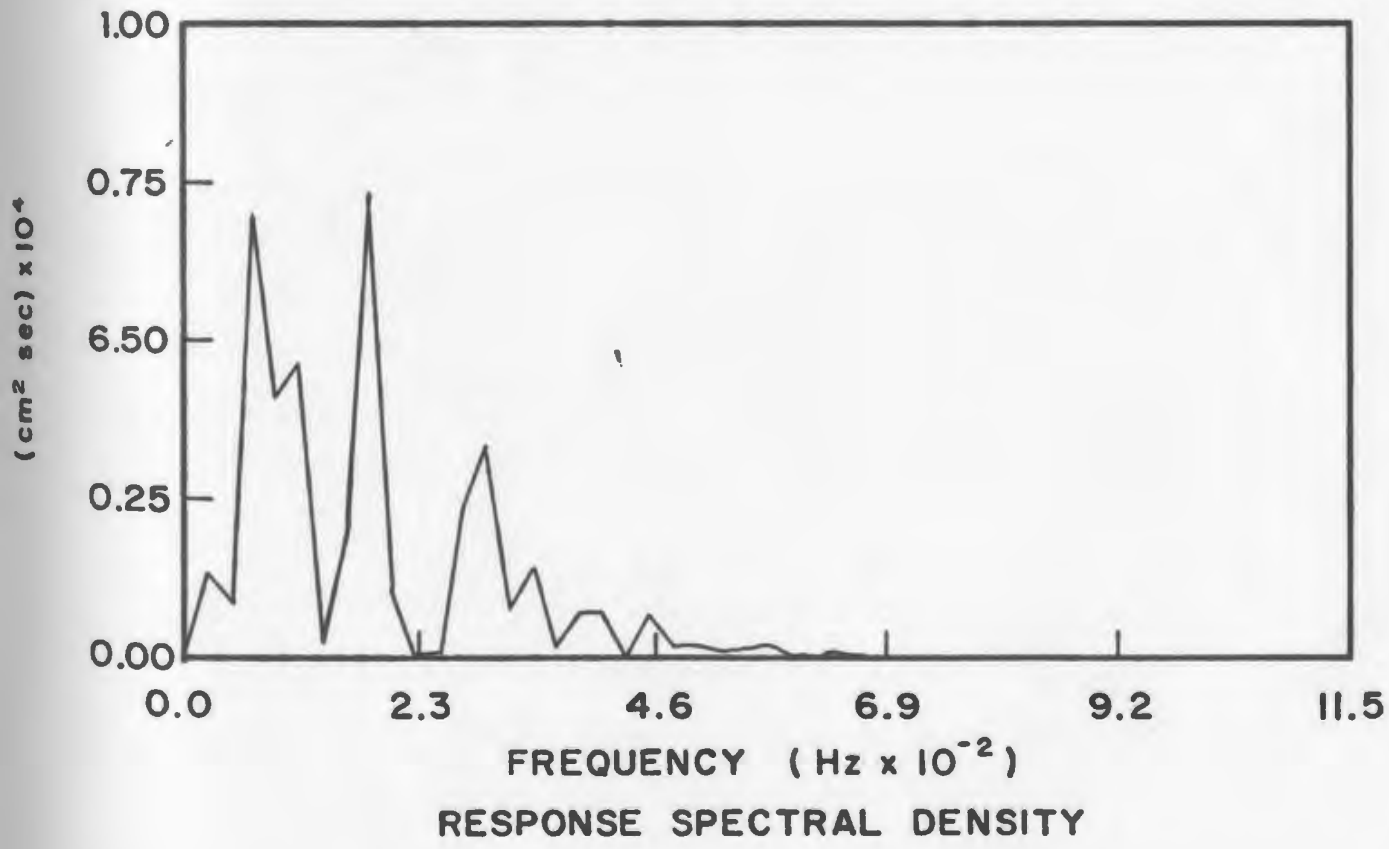

FIG. 6.5 SIWEH AND RESPONSE SPECTRAL DENSITIES FOR SPECTRUM 1.

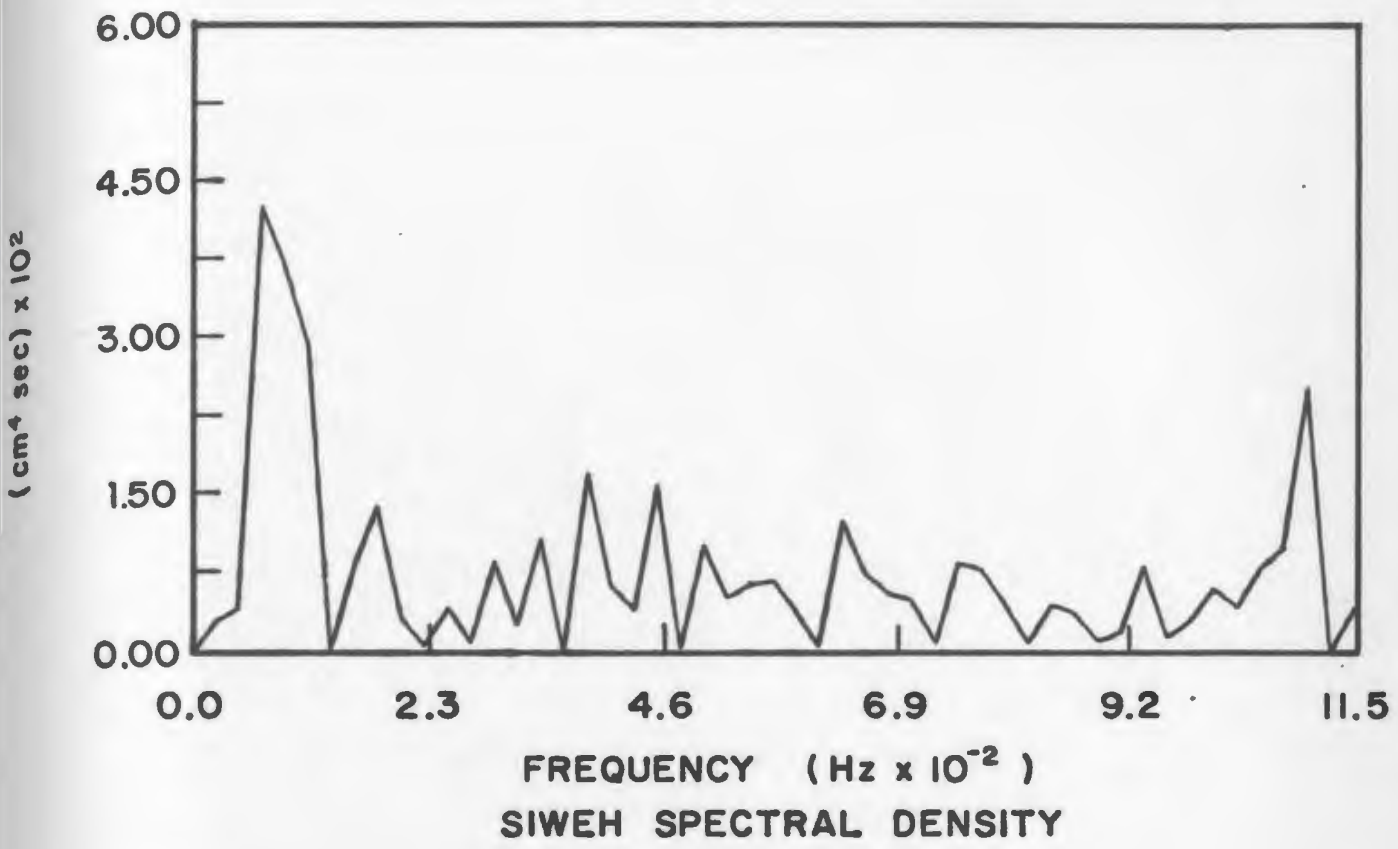

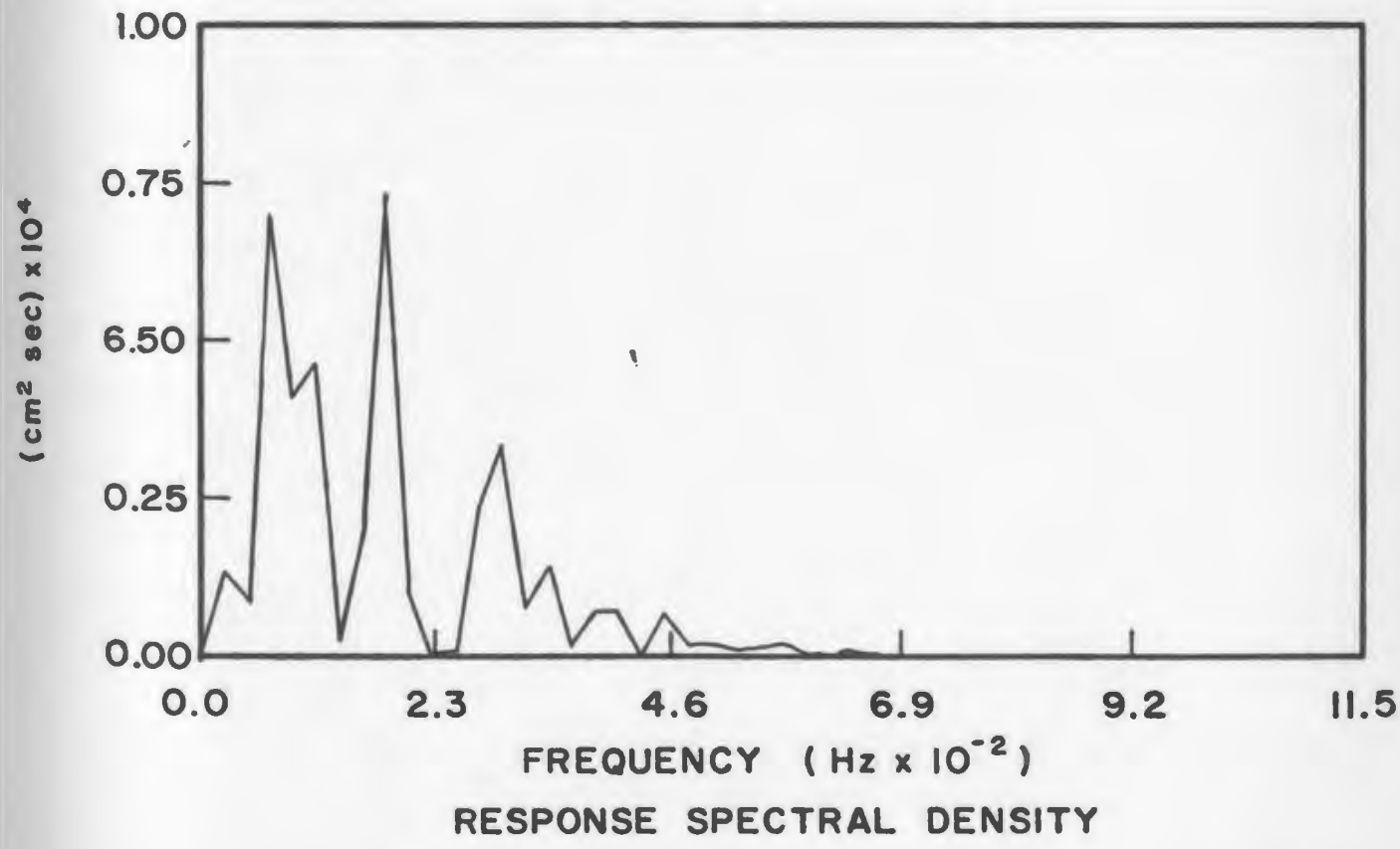

FIG. 6.5 SIWEH AND RESPONSE SPECTRAL DENSITIES FOR SPECTRUM 1.

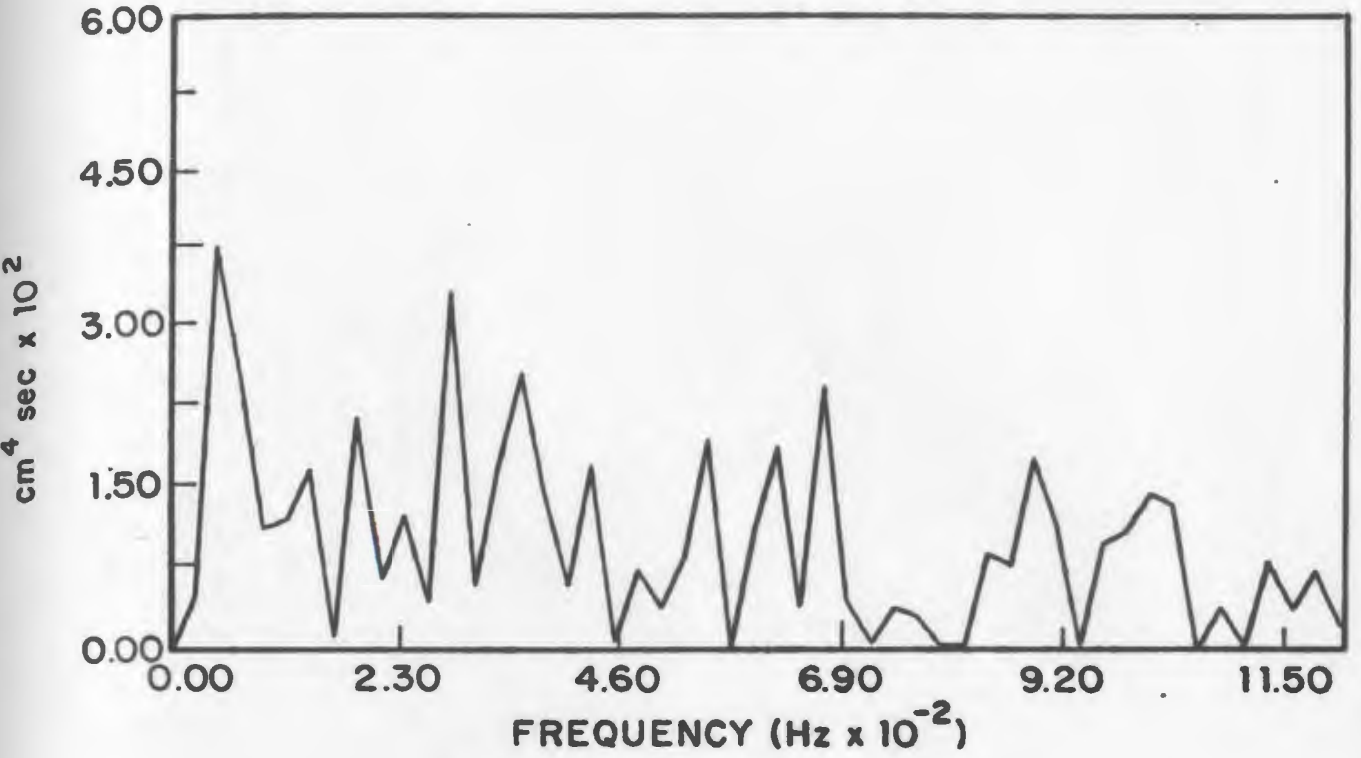

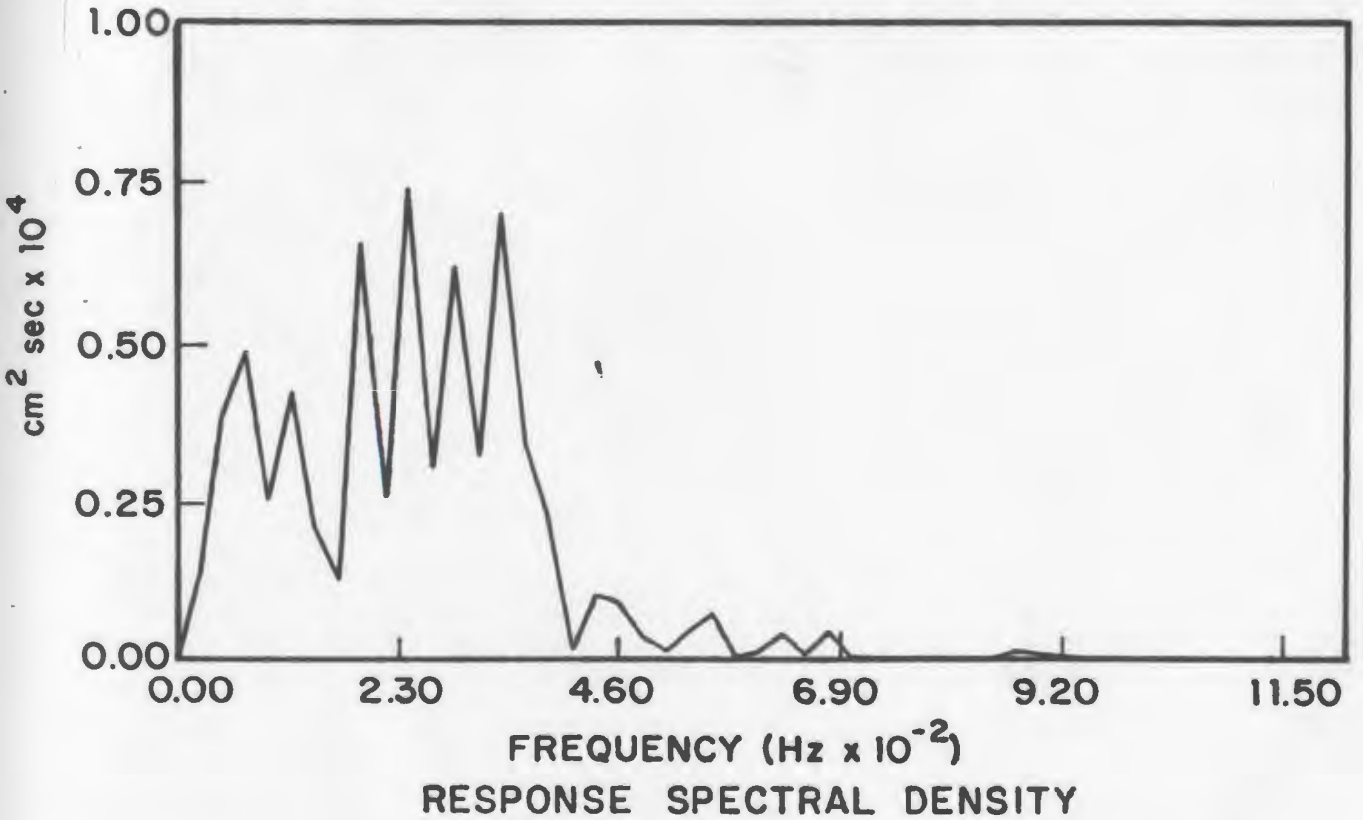

FIG. 6.6 SIWEH AND RESPONSE SPECTRAL DENSITIES FOR SPECTRUM 2.

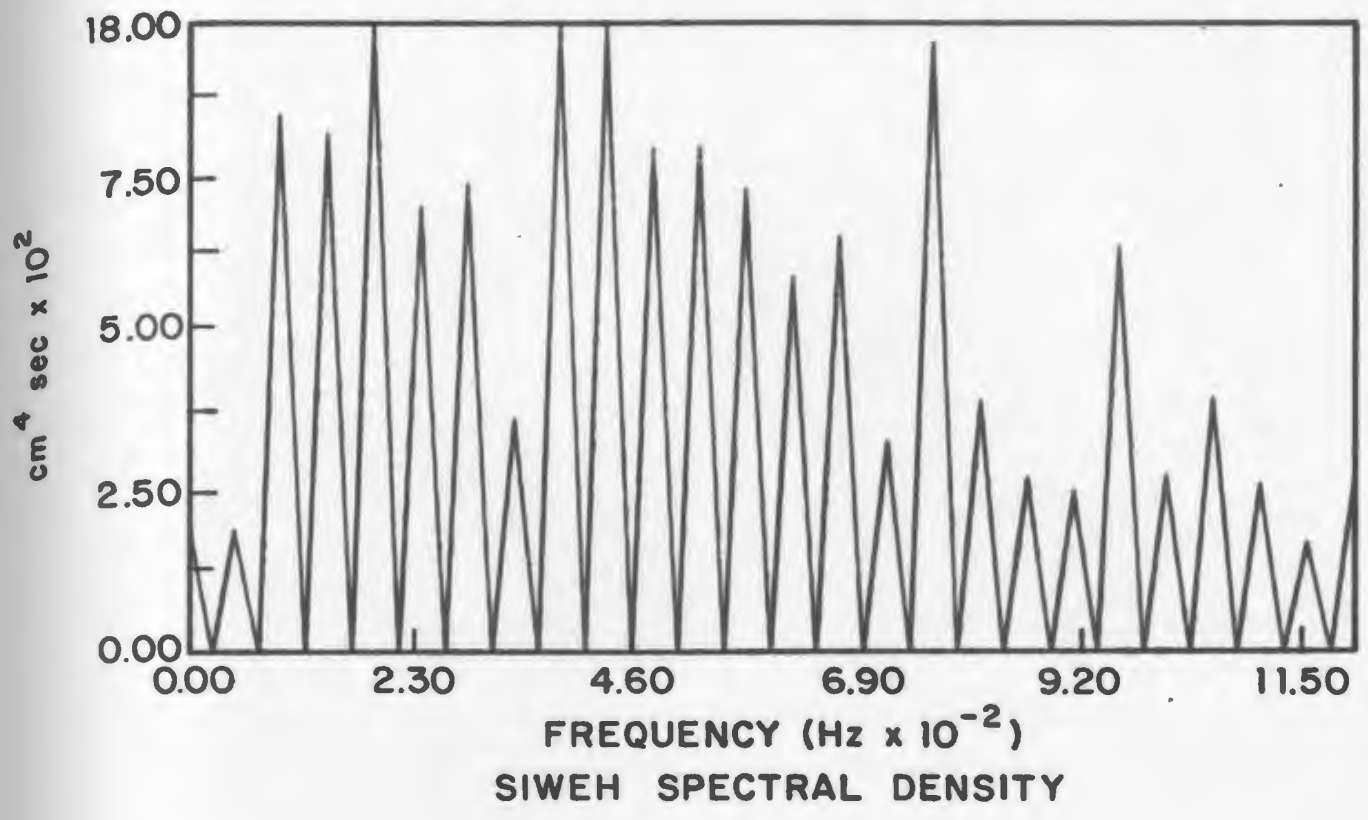

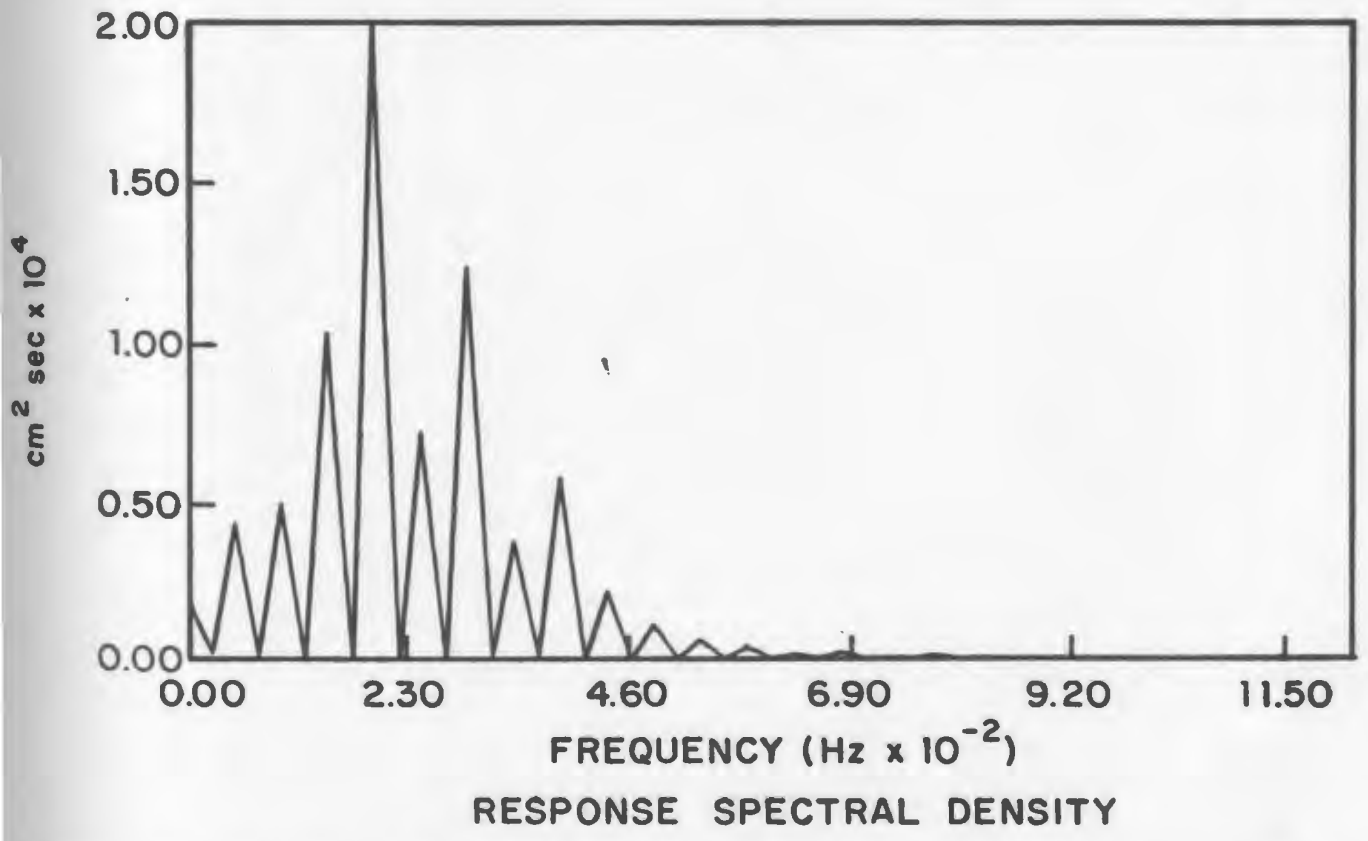

FIG. 6.7 SIWEH AND RESPONSE SPECTRAL DENSITIES FOR SPECTRUM 6.

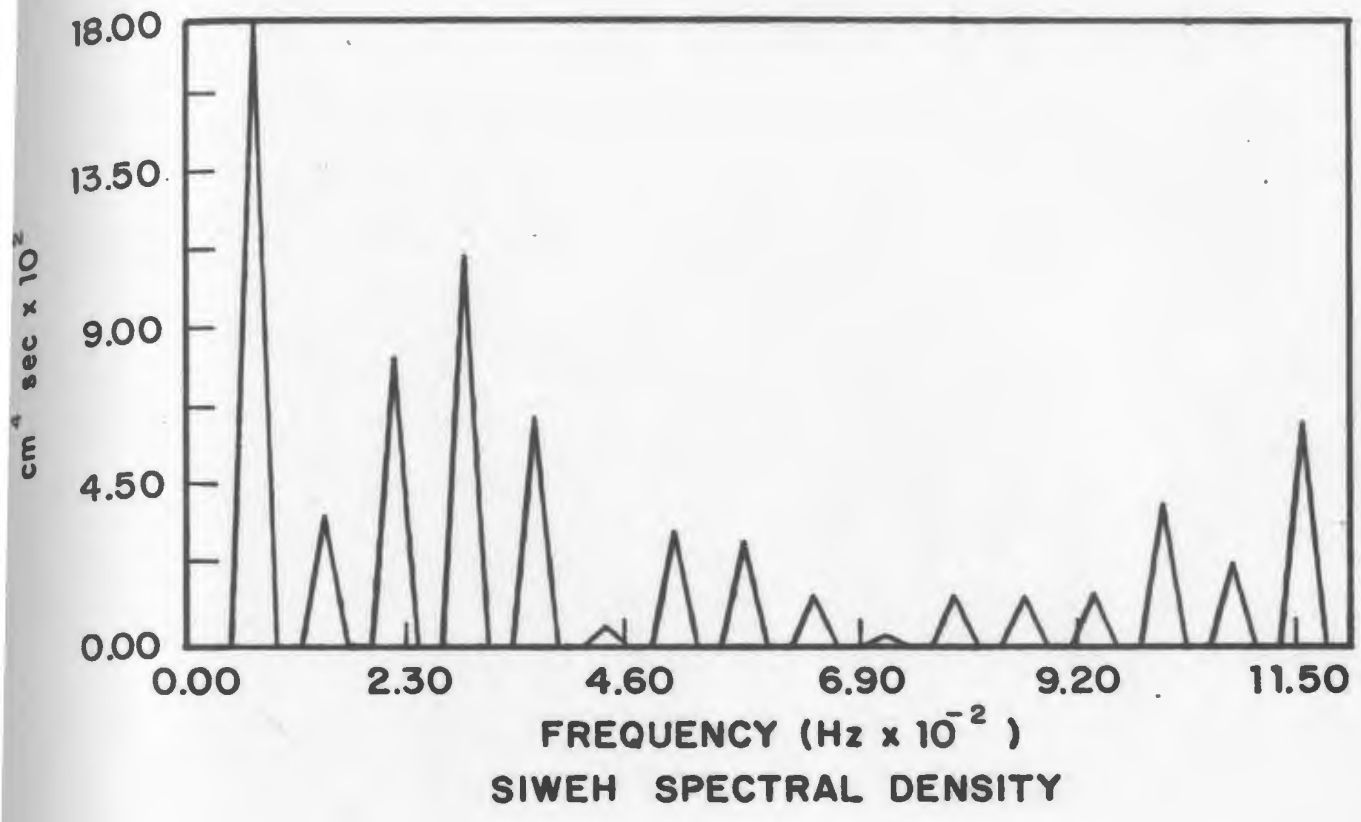

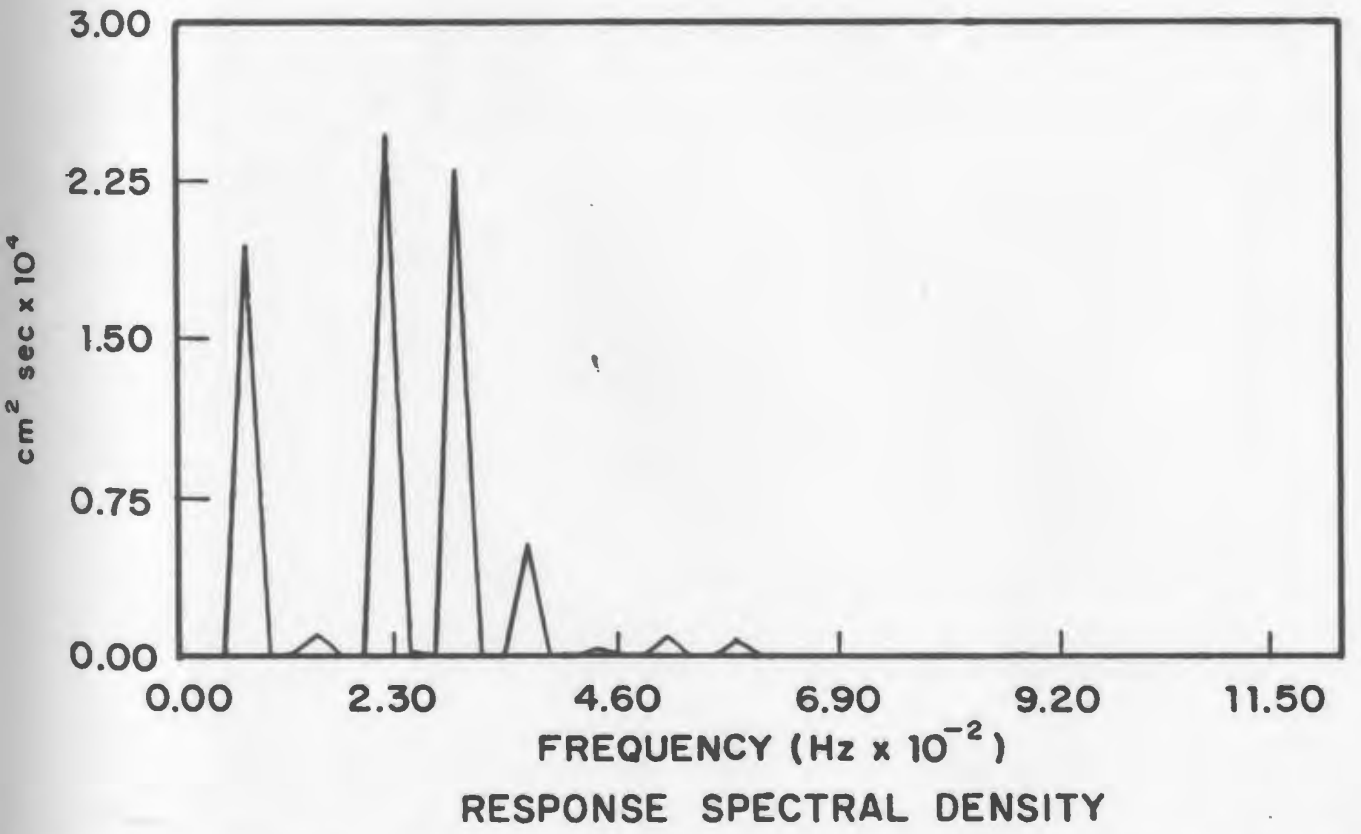

FIG. 6.8 SIWEH AND RESPONSE SPECTRAL DENSITIES FOR SPECTRUM 8.

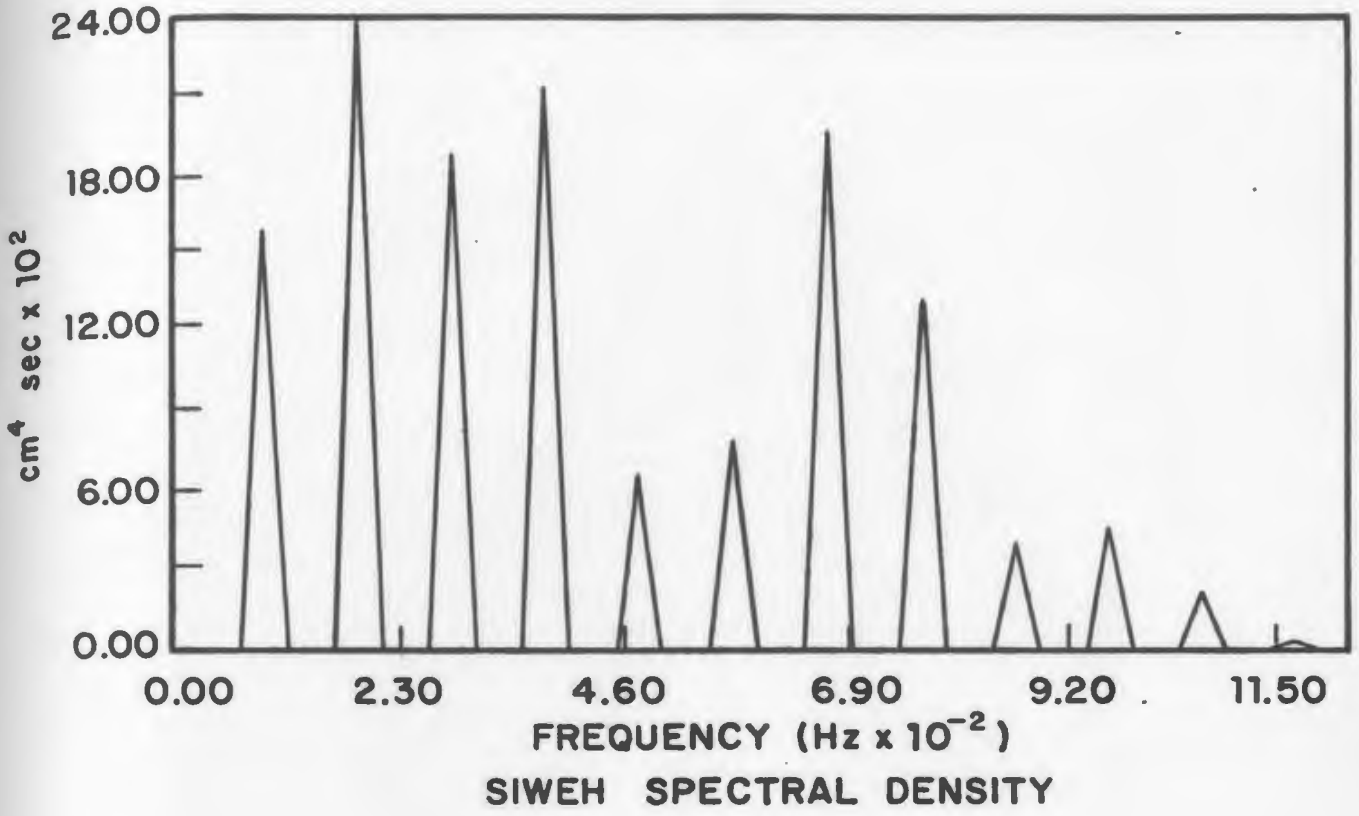

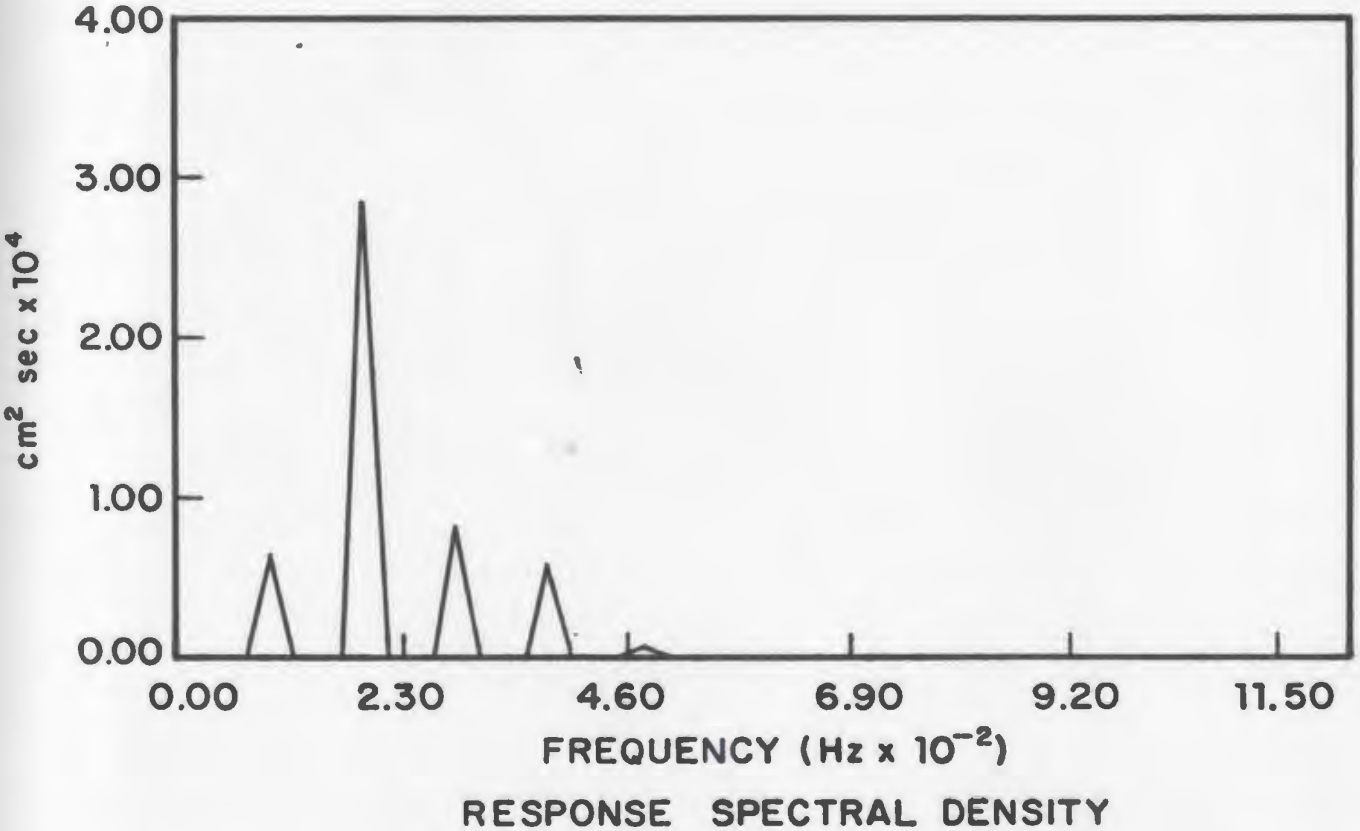

FIG. 6.9 SIWEH AND RESPONSE SPECTRAL DENSITIES FOR SPECTRUM 10.

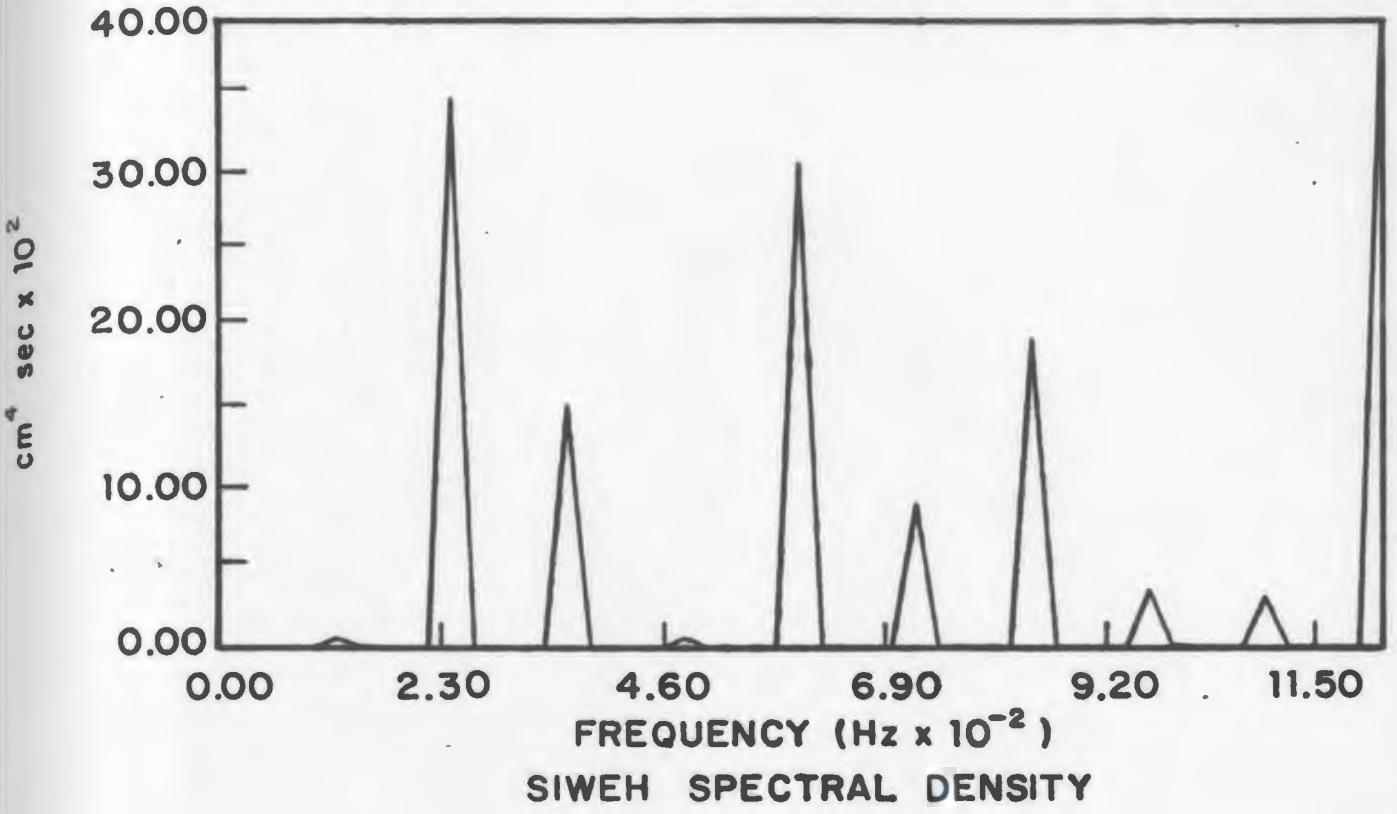

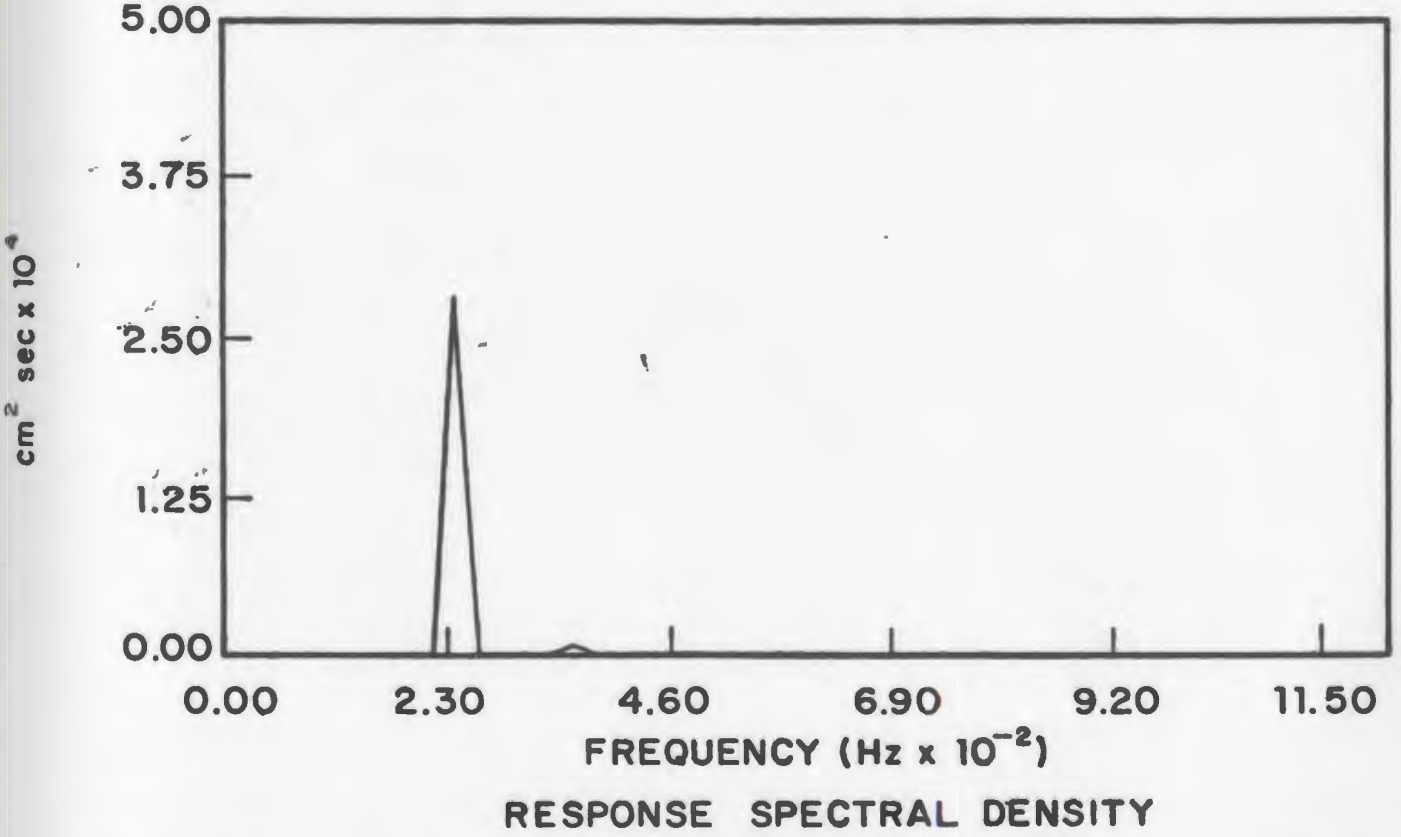

FIG. 6.10 SIWEH AND RESPONSE SPECTRAL DENSITIES FOR SPECTRUM 12 .

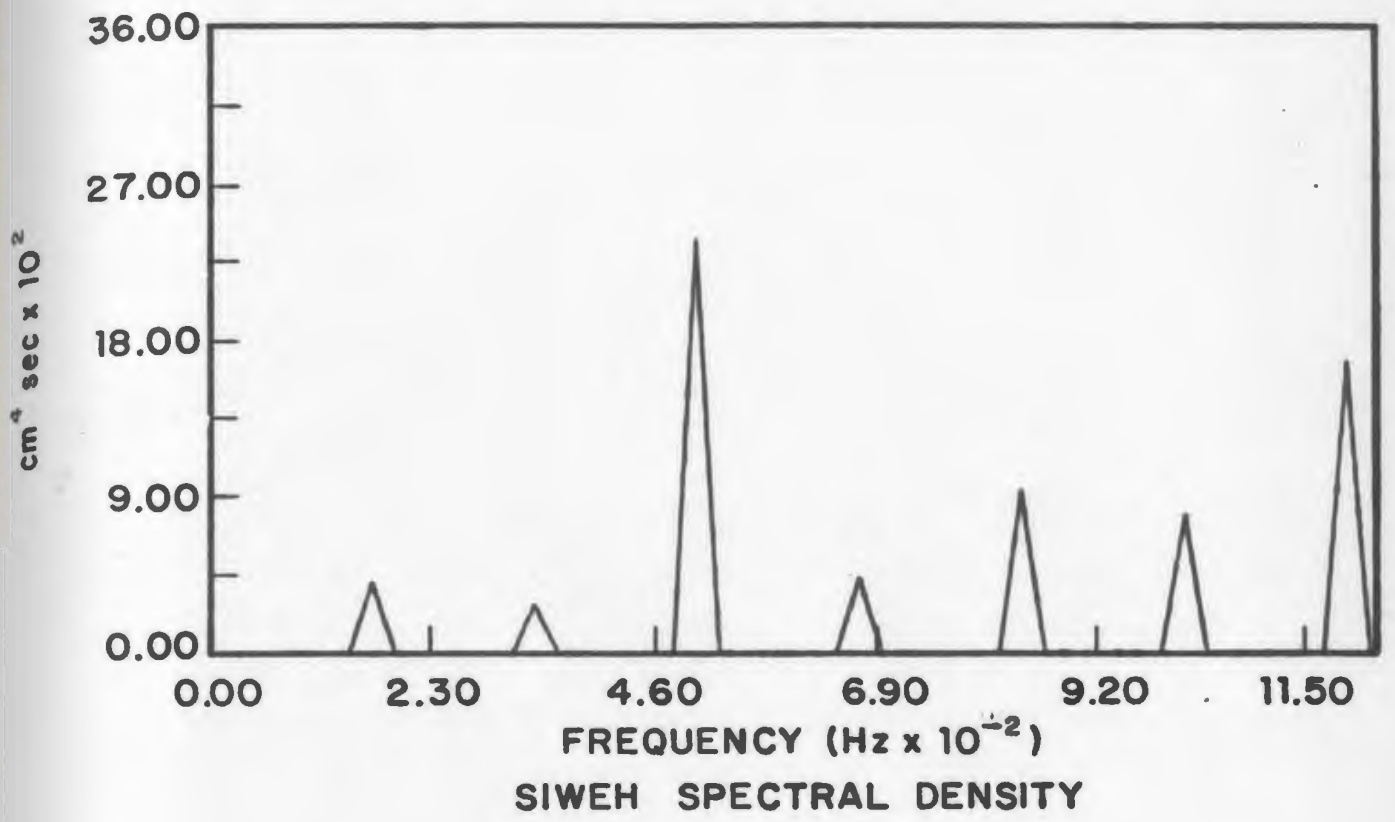

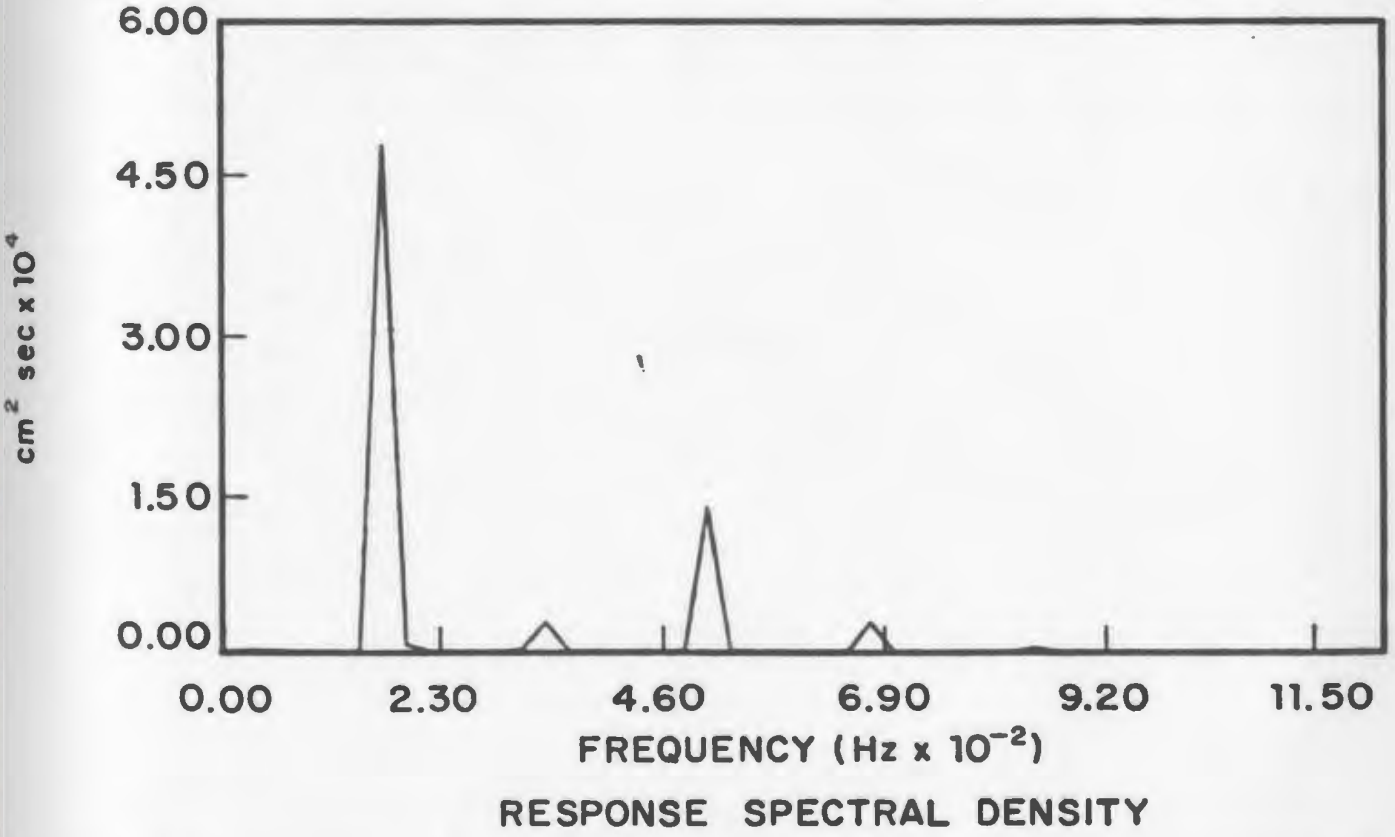

FIG. 6.11 SIWEH AND RESPONSE SPECTRAL DENSITIES FOR SPECTRUM 14.

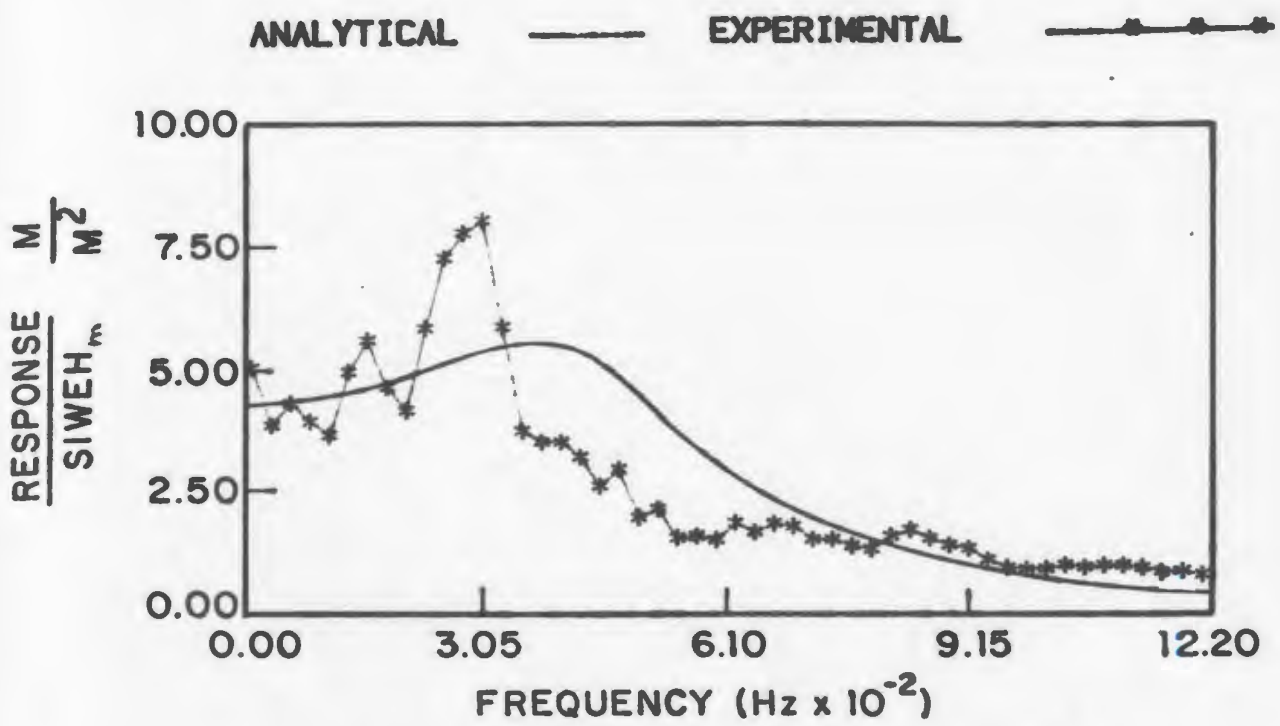

MAGNITUDE OF TRANSFER FUNCTION
FOR SPECTRUM

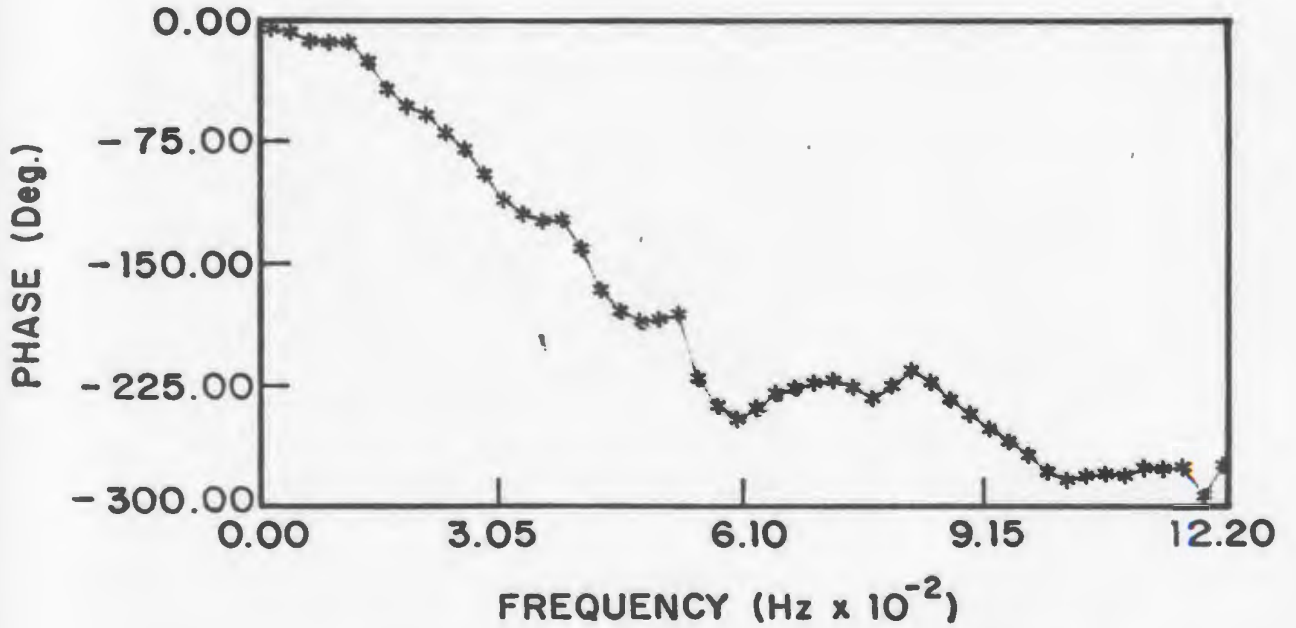

PHASE OF TRANSFER FUNCTION
FOR SPECTRUM

FIG. 6.12 TRANSFER FUNCTION FOR SPECTRUM 1.

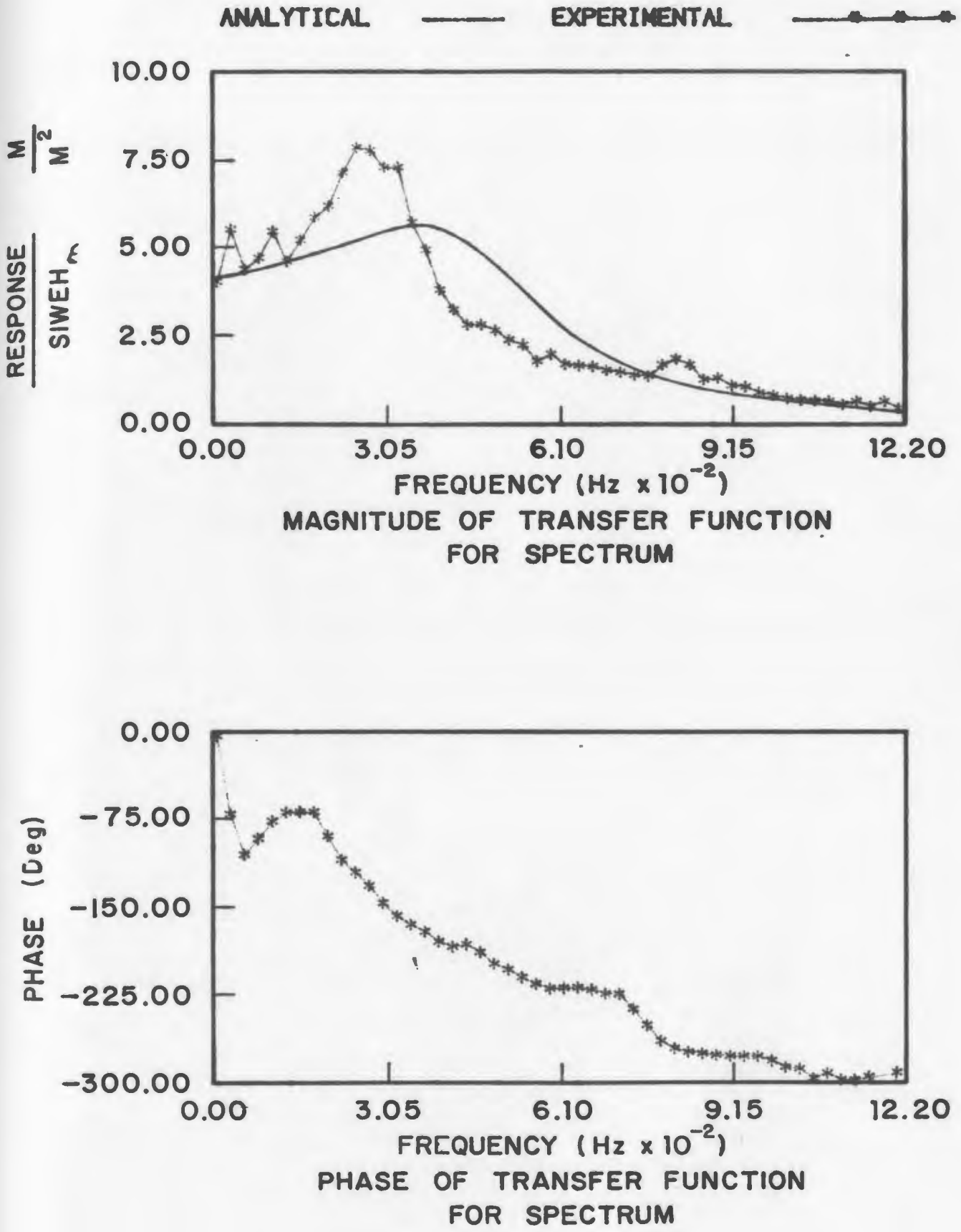

FIG. 6.13 TRANSFER FUNCTION FOR SPECTRUM 2.

ANALYTICAL ——— EXPERIMENTAL —•—•—

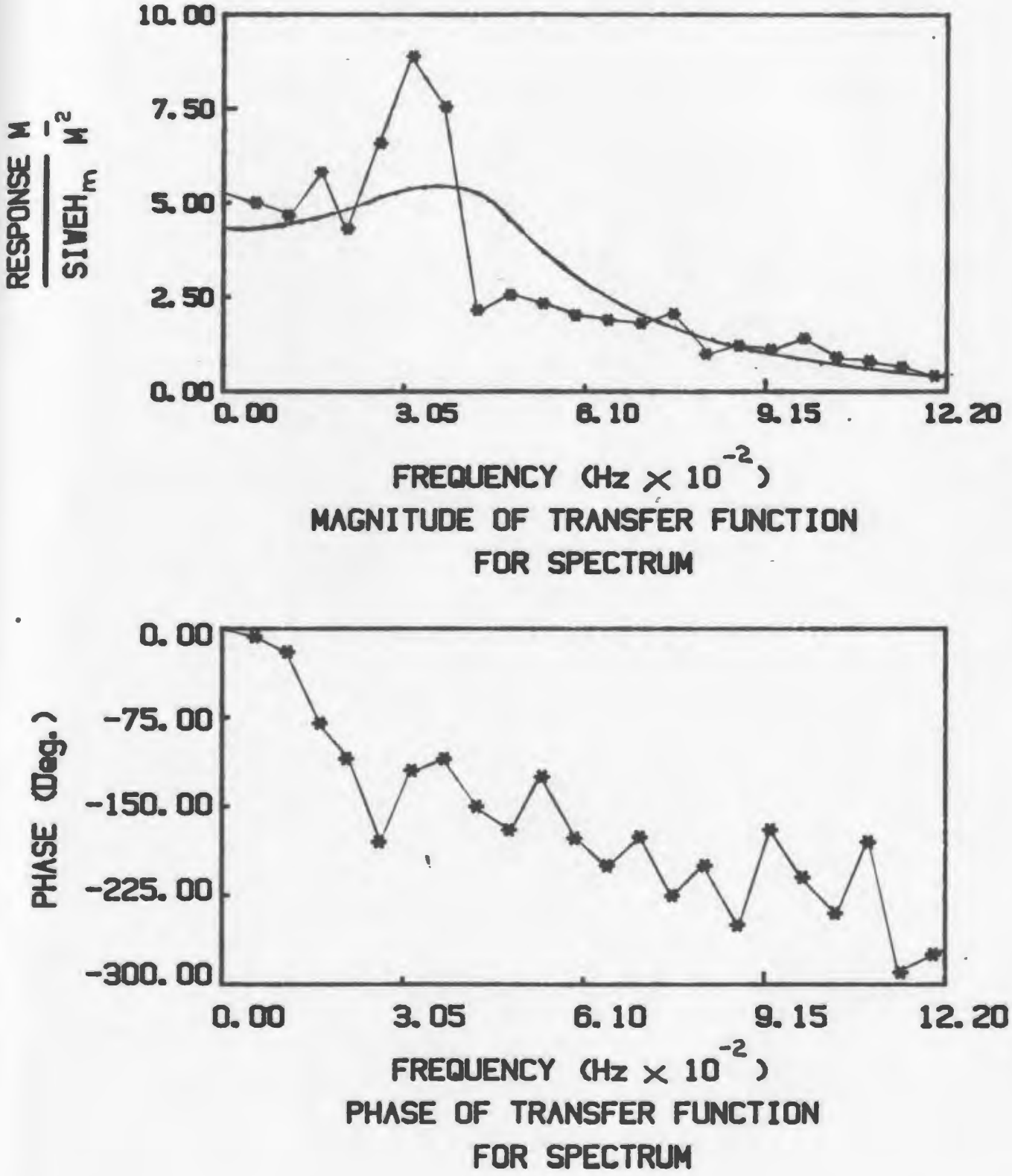

FIG. 6.14 TRANSFER FUNCTION FOR SPECTRUM 6

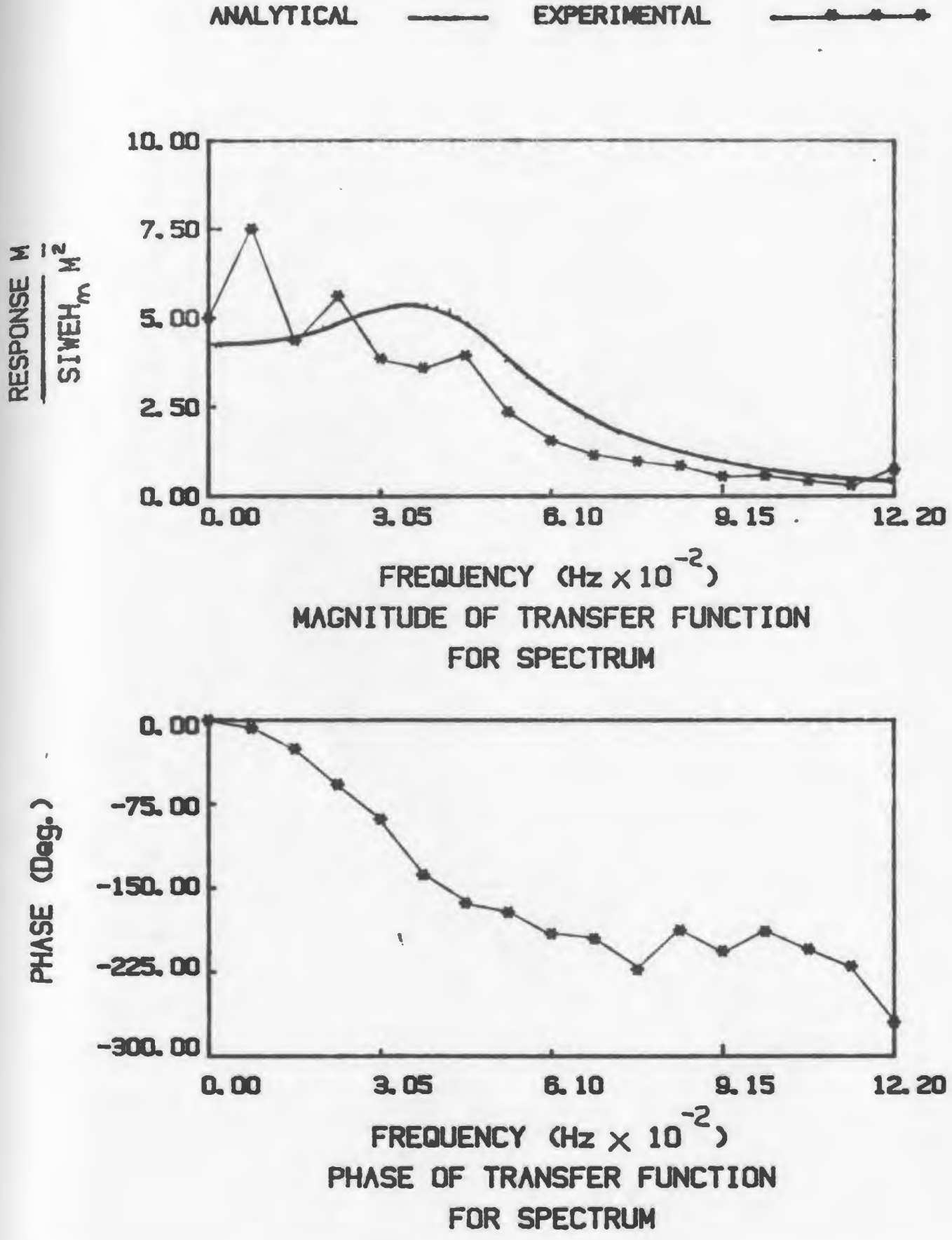

FIG. 6.15 TRANSFER FUNCTION FOR SPECTRUM 8

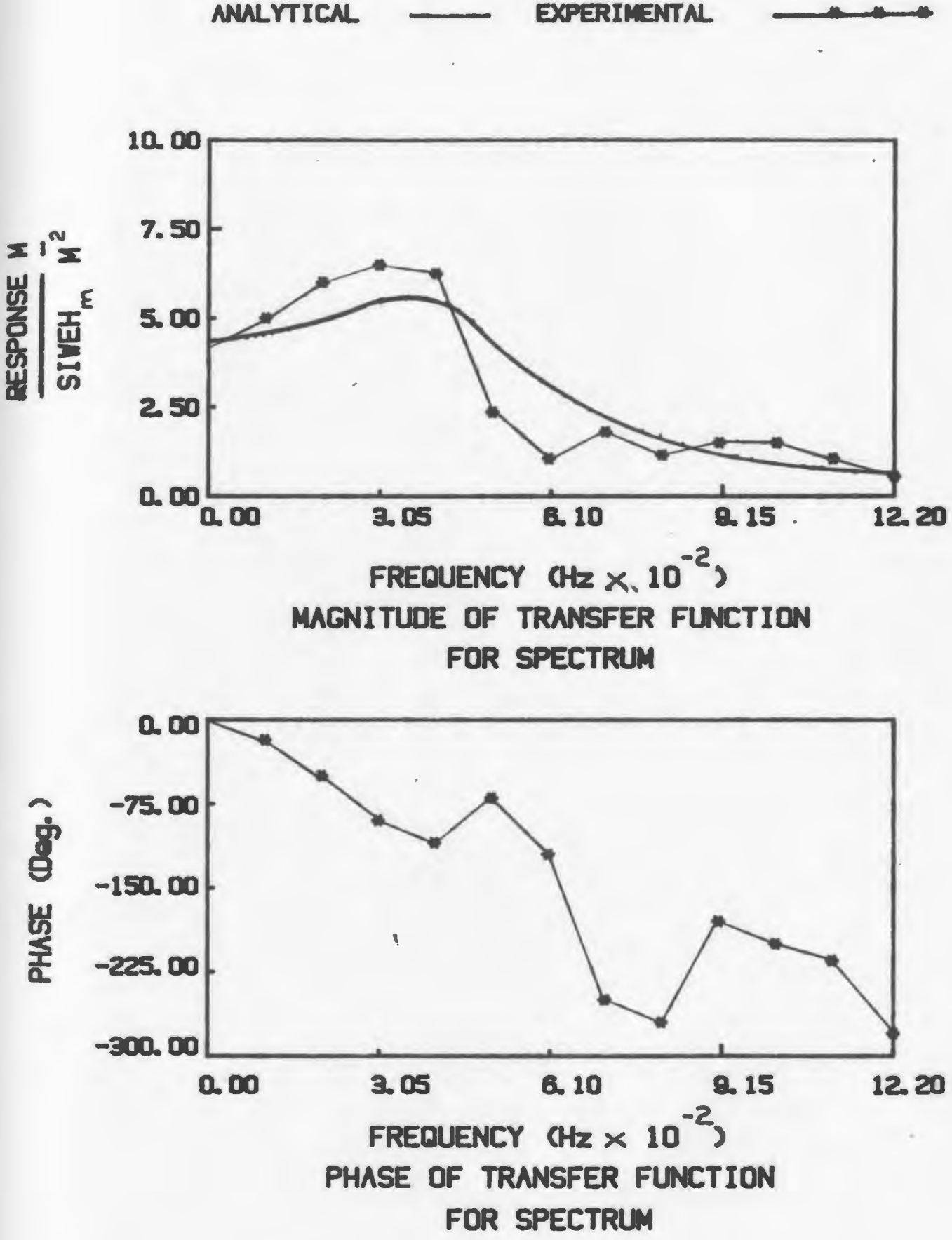

FIG. 6.16 TRANSFER FUNCTION FOR SPECTRUM 10

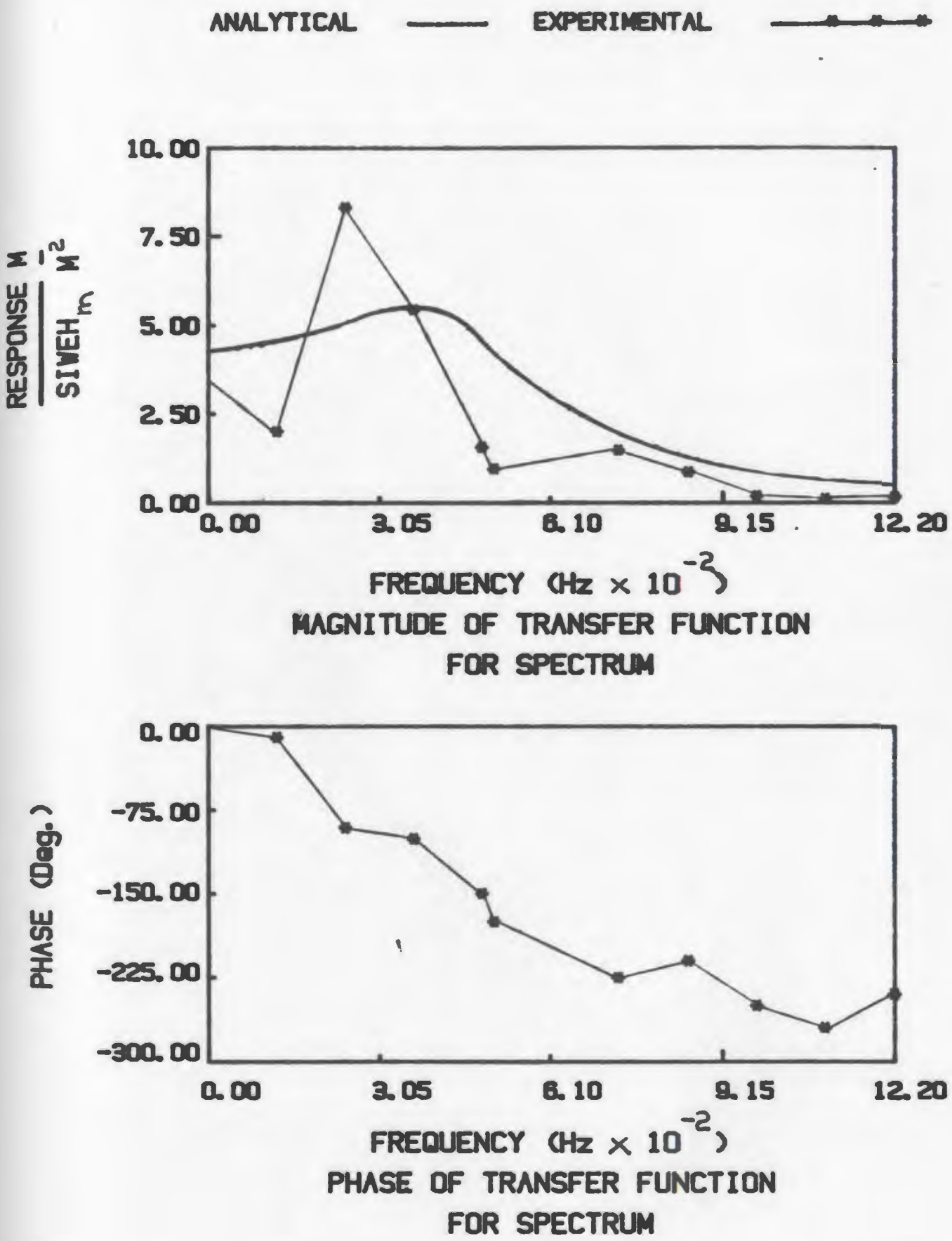

FIG. 6.17 TRANSFER FUNCTION FOR SPECTRUM 12

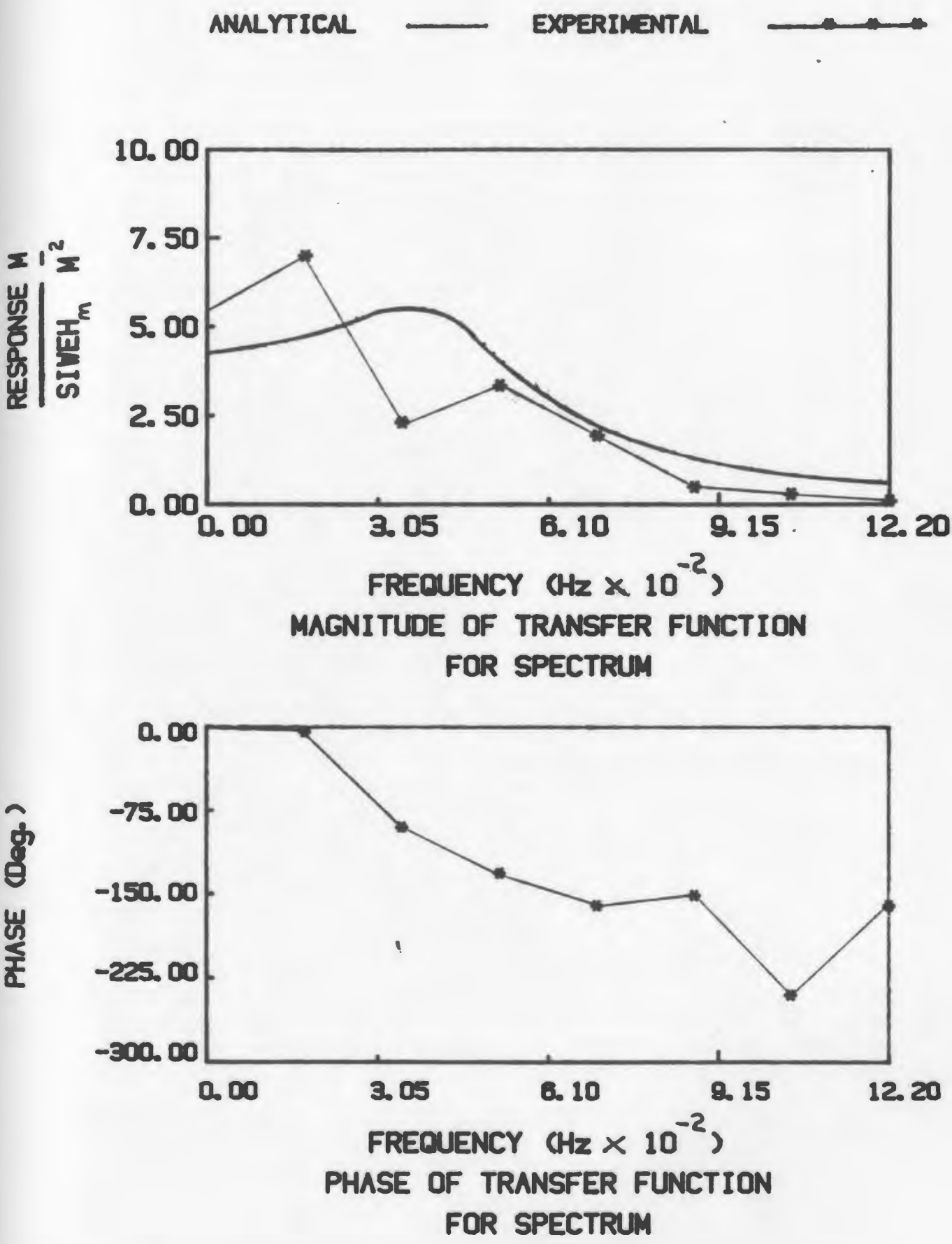

FIG. 6.18 TRANSFER FUNCTION FOR SPECTRUM 14

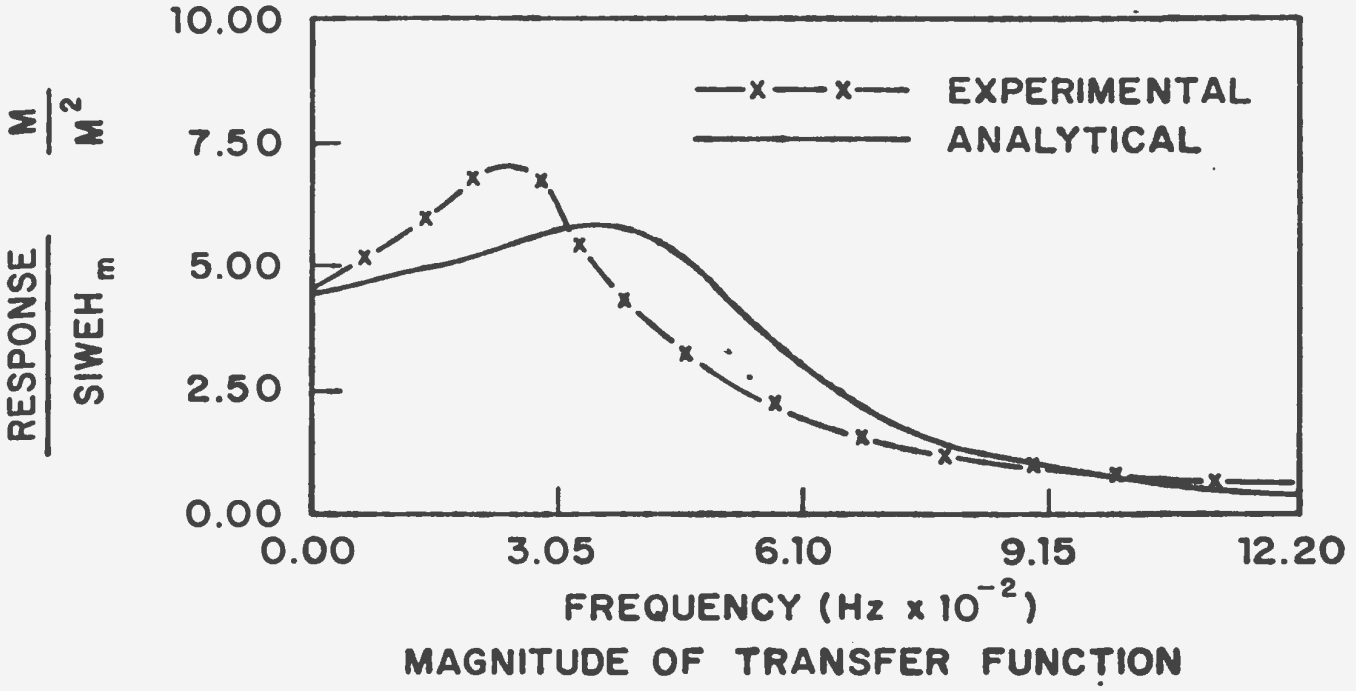

MAGNITUDE OF TRANSFER FUNCTION

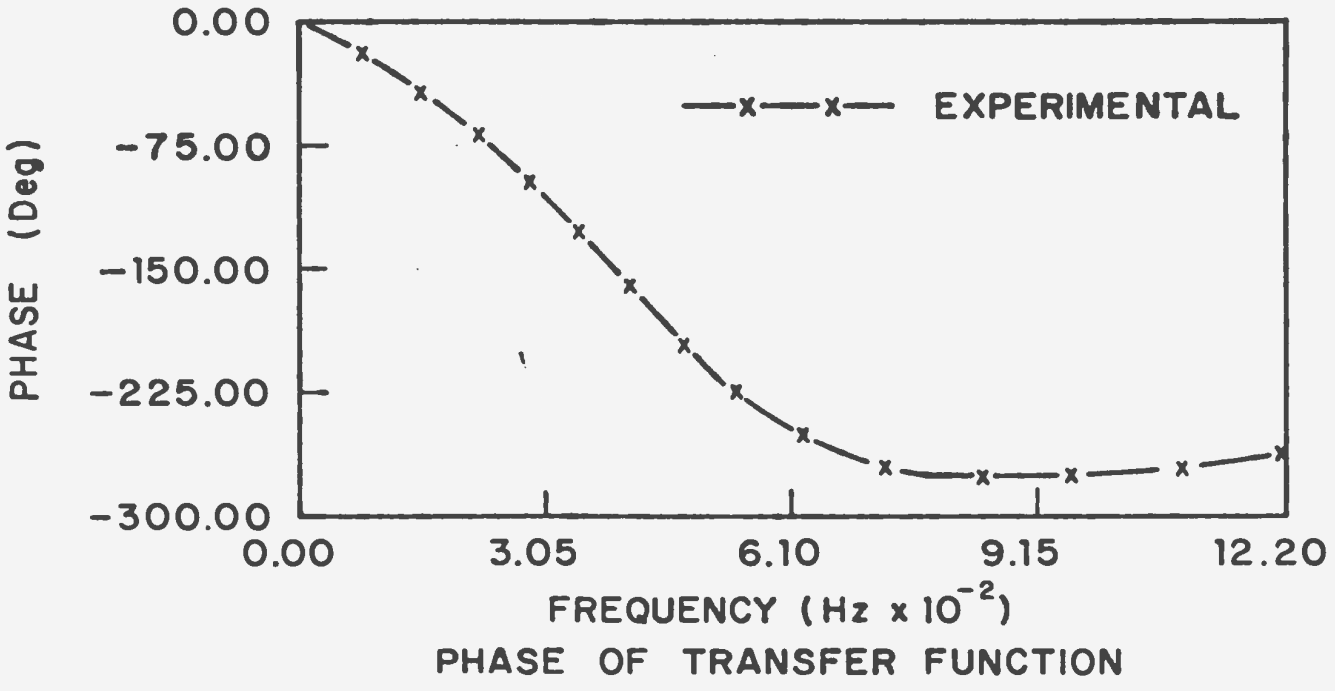

PHASE OF TRANSFER FUNCTION

FIG. 6.19 COMPARISON BETWEEN ANAYTICAL AND EXPERIMENTAL TRANSFER FUNCTIONS

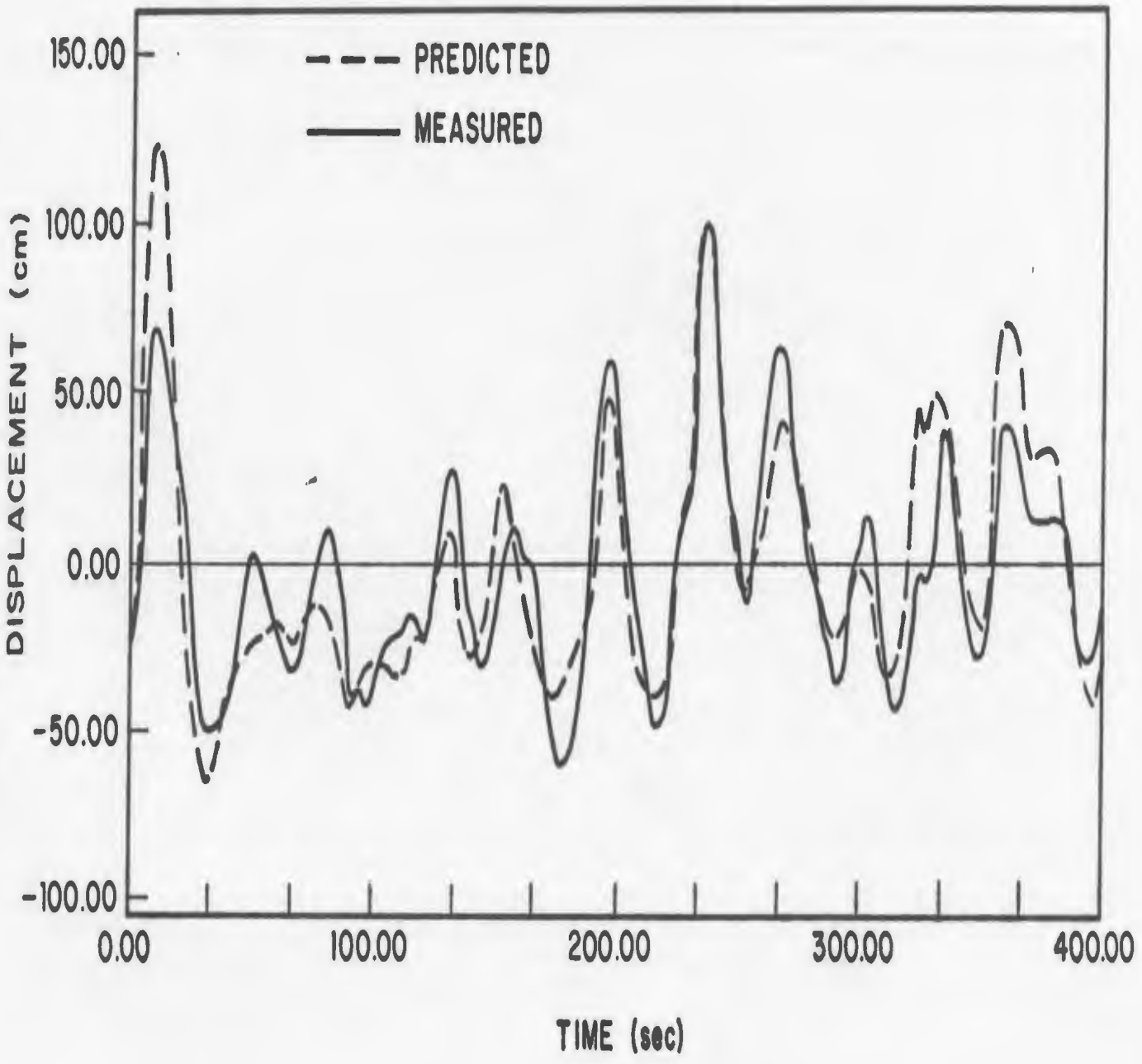

FIG. 6.20 COMPARISON BETWEEN PREDICTED AND MEASURED SLOW DRIFT DISPLACEMENT FOR SPECTRUM 1a.

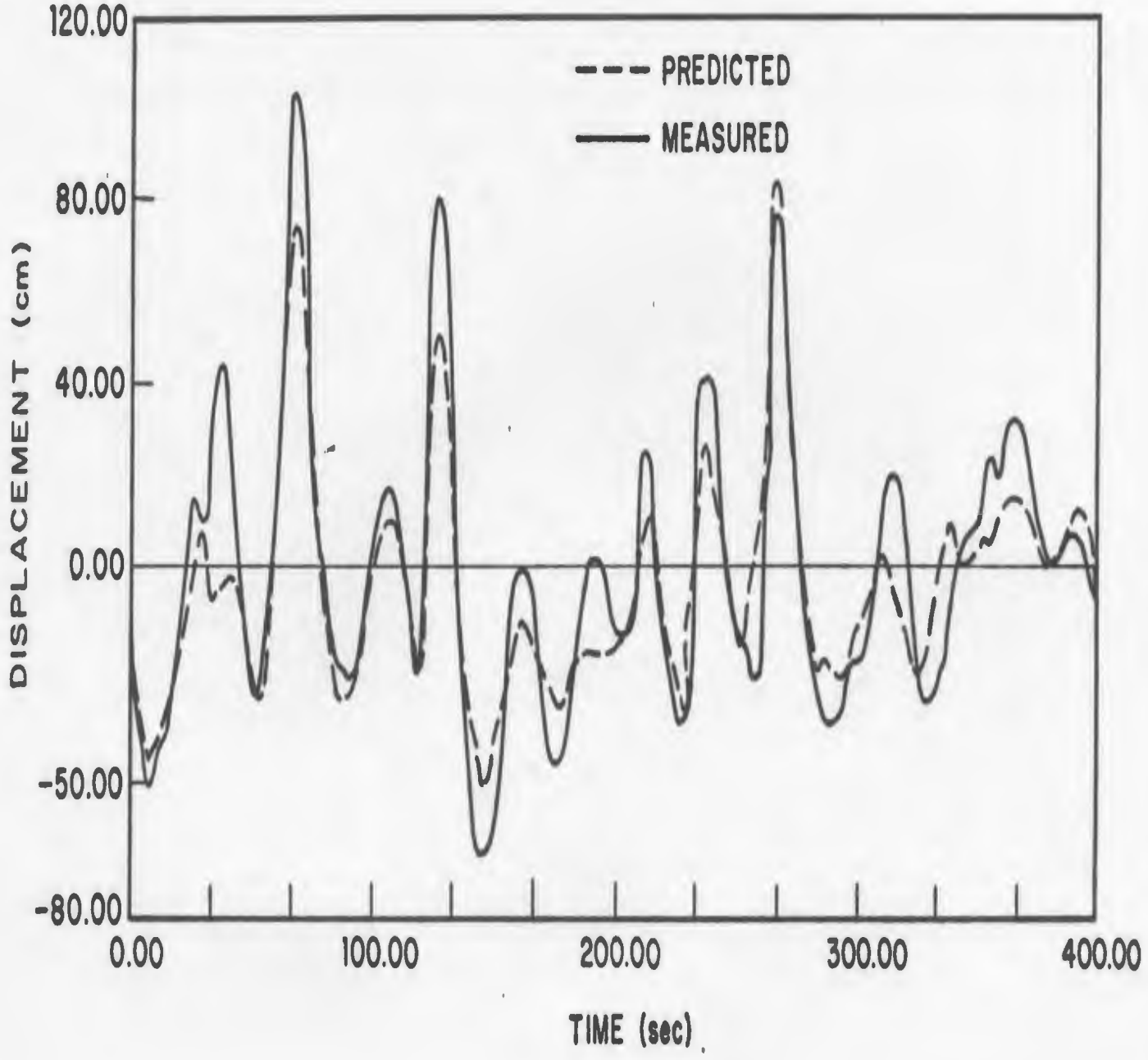

FIG. 6.21 COMPARISON BETWEEN PREDICTED AND MEASURED SLOW DRIFT DISPLACEMENT FOR SPECTRUM 2a

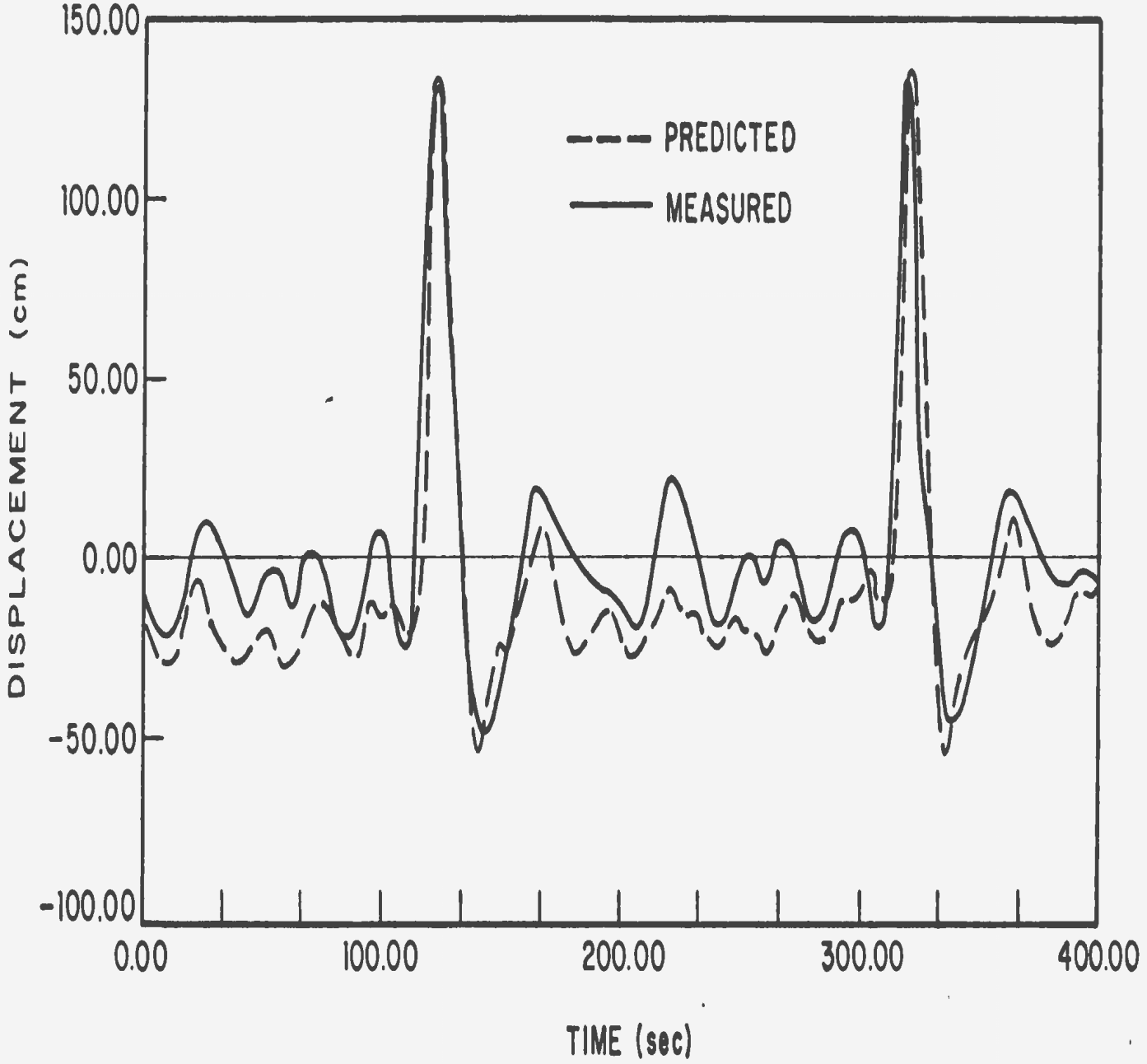

FIG. 6.22 COMPARISON BETWEEN PREDICTED AND MEASURED SLOW DRIFT DISPLACEMENT FOR SPECTRUM 3a.

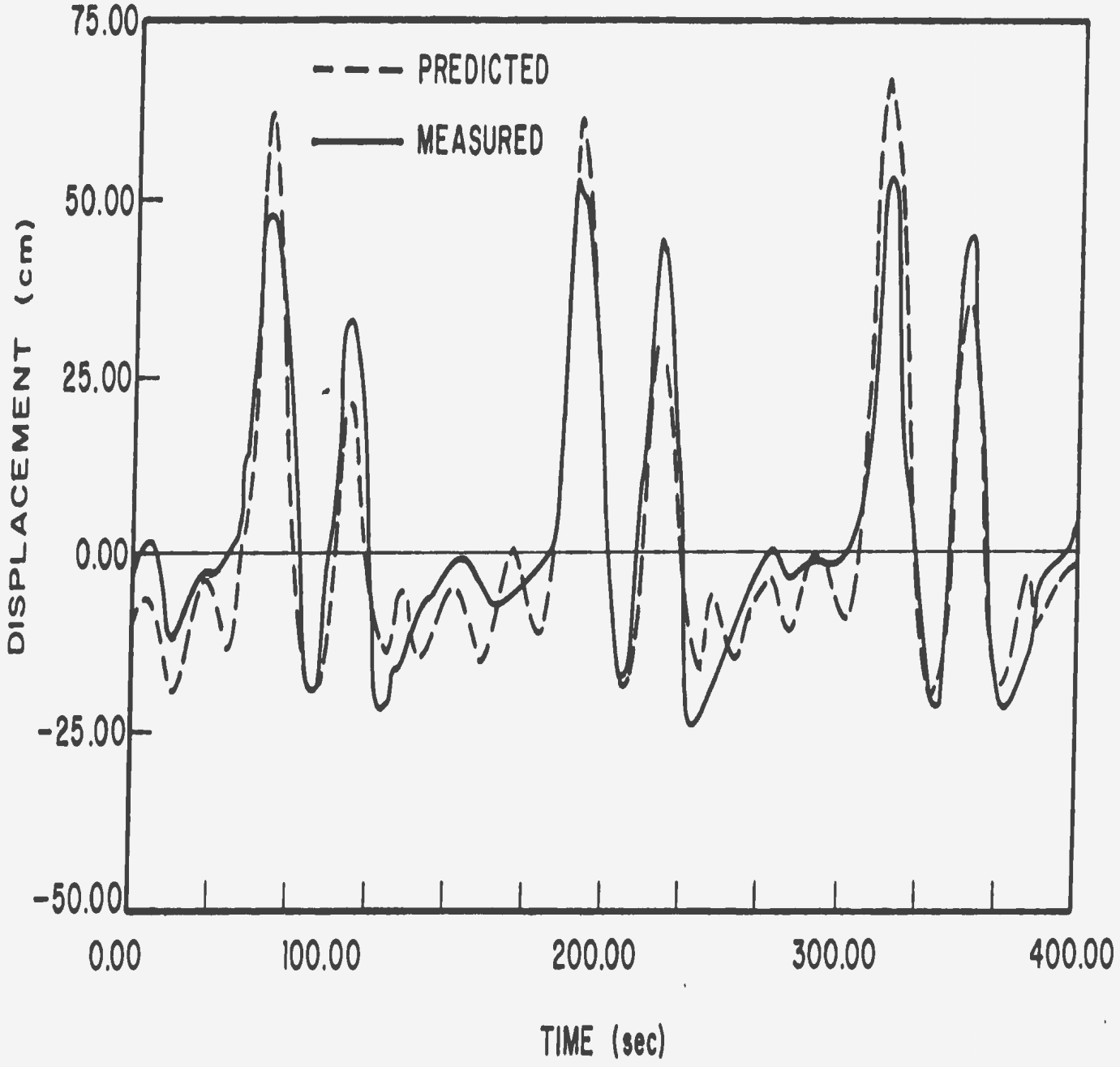

FIG. 6.23 COMPARISON BETWEEN PREDICTED AND MEASURED SLOW DRIFT DISPLACEMENT FOR SPECTRUM 4a.

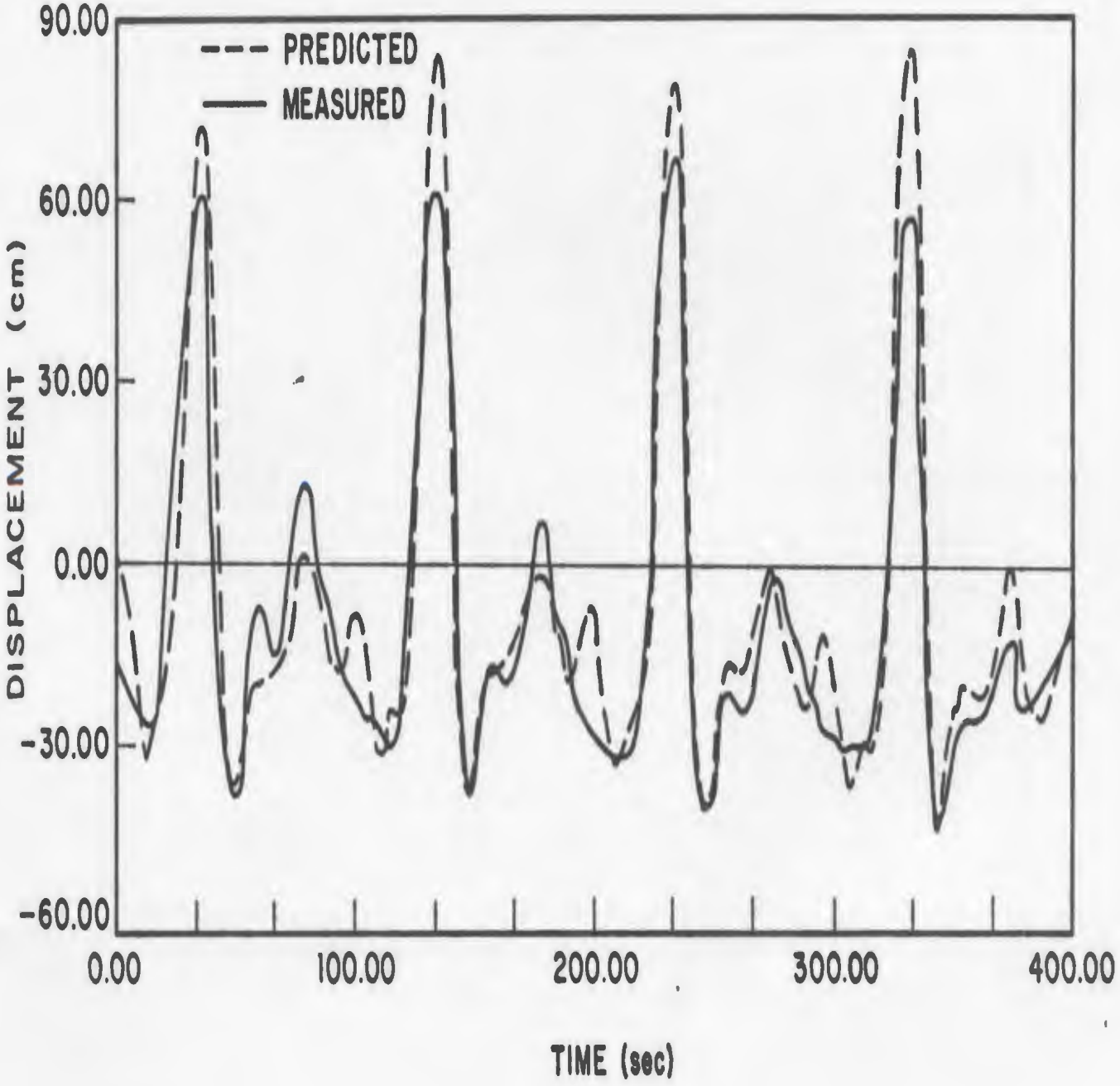

FIG. 6.24 COMPARISON BETWEEN PREDICTED AND MEASURED SLOW DRIFT DISPLACEMENT FOR SPECTRUM 5a.

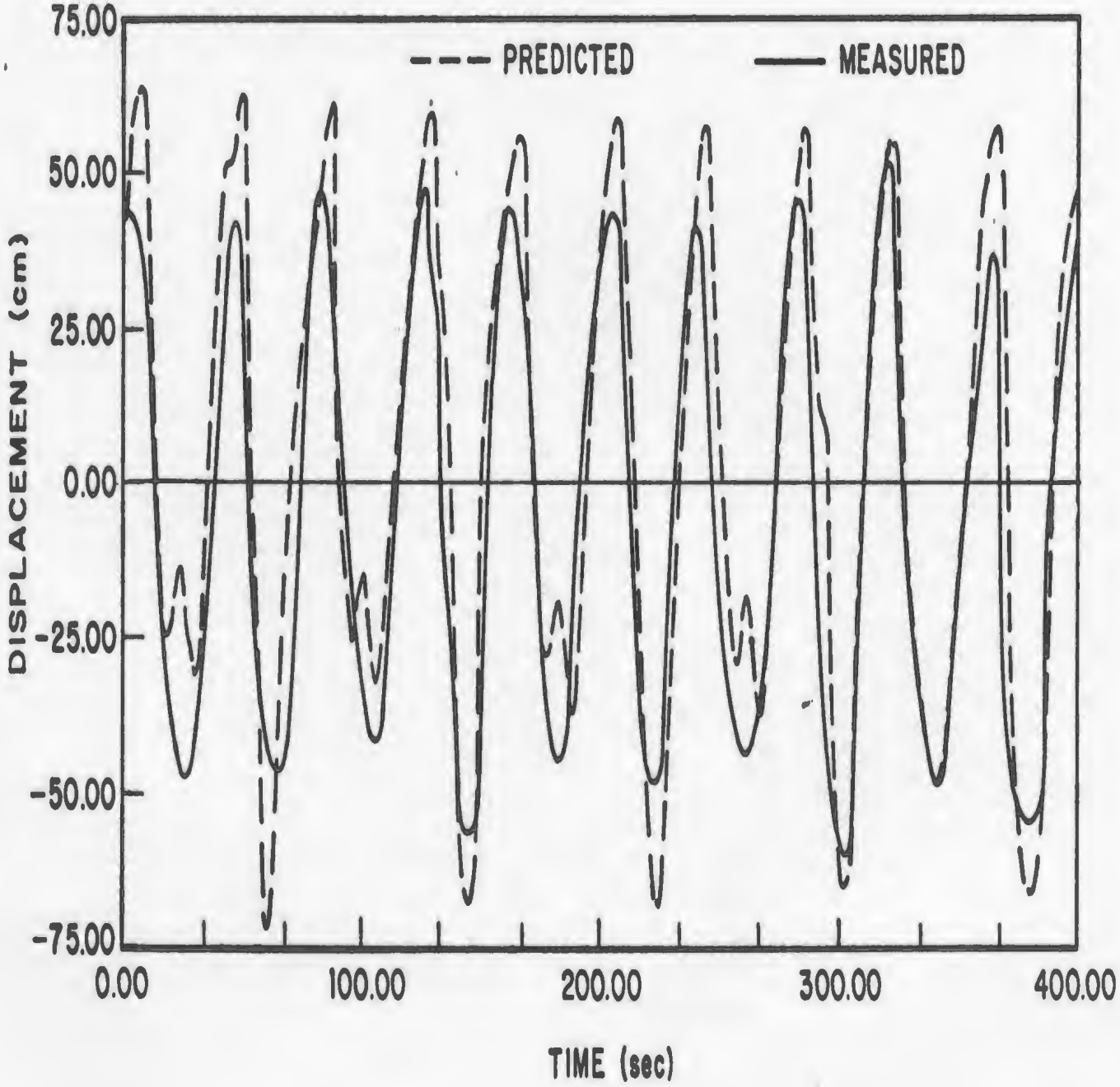

FIG. 6.25 COMPARISON BETWEEN PREDICTED AND MEASURED SLOW DRIFT DISPLACEMENT FOR SPECTRUM 6a.

APPENDIX C

HYDRODYNAMIC TERMS

APPENDIX C

The slowly varying second-order wave force which results from the nonlinear interactions between adjacent portions of the wave spectrum is determined under the postulation that the hydrodynamic force is due to the presence of two simultaneous waves and thus the wave system can be represented by a discrete spectrum. The presence of more than one frequency, in water of constant depth, will cause a non-uniformity in the wave amplitude and consequently cause long period fluctuations in the mass transport which are proportional to the square of the wave amplitudes. These low frequency mass-transport currents fluctuate more rapidly than the currents produced by steady wave trains of uniform amplitude which are largely effected by viscosity and therefore the two effects may be considered independently.

C.1 The Stokes Approximation

The Stokes method of approximation is used to solve the field equations and boundary conditions as far as second order, limiting the second order approximation to the different frequencies. The rectangular coordinate system (x,y,z) defined with the x axis horizontal and in the direction of the wave propagation and the z axis vertical. The flow field equations to be satisfied are,

$$\bar{u} = \nabla\phi \tag{C.1a}$$

$$\nabla^2\phi = 0 \tag{C.1b}$$

$$\frac{P}{\rho} + gz + \frac{1}{2}\bar{u}^2 + \frac{\partial\phi}{\partial t} = 0 \tag{C.1c}$$

where ϕ = velocity potential

$\bar{u}$ = velocity vector (u,v,w)

p = pressure

g = gravitational acceleration

ρ = density

with the boundary conditions,

$$(\bar{n} \cdot \nabla\phi)_{z=-h} = 0 \qquad \text{(C.2a)}$$

$$p_{z = \zeta_a} = 0 \qquad \text{(C.2b)}$$

$$\left[\left(\frac{\partial}{\partial t} + \bar{u}.\nabla\right)(z-\zeta_a)\right]_{z=\zeta_a} = 0 \qquad \text{(C.2c)}$$

where $z = -h$ is the bottom boundary condition and ζ_a = free surface elevation.

The Stokes method of approximation takes the form,

$$\bar{u} = \bar{u}^{(1)} + \bar{u}^{(2)} + \ldots. \qquad \text{(C.3a)}$$

$$\phi = \phi^{(1)} + \phi^{(2)} + \ldots. \qquad \text{(C.3b)}$$

$$\zeta_a = \zeta_a^{(1)} + \zeta_a^{(2)} + \ldots.. \qquad \text{(C.3c)}$$

$$p + \rho g z = p^{(1)} + p^{(2)} + \ldots. \qquad \text{(C.3d)}$$

First order quantities satisfy the linearized equations and boundary conditions. The equations of $\phi^{(1)}$ are

$$\nabla^2 \phi^{(1)} = 0 \qquad \text{(C.4a)}$$

$$\left[\frac{\partial \phi^{(1)}}{\partial z}\right]_{z=-h} = 0 \qquad \text{(C.4b)}$$

$$\left[\frac{\partial^2 \phi^{(1)}}{\partial t^2} + g\frac{\partial \phi^{(1)}}{\partial z}\right]_{z=0} = 0 \qquad \text{(C.4c)}$$

and

$$\bar{u}^{(1)} = \nabla\phi^{(1)} \tag{C.5a}$$

$$\frac{p^{(1)}}{\rho} = -\frac{\partial\phi^{(1)}}{\partial t} \tag{C.5b}$$

$$g\zeta_a^{(1)} = -\left[\frac{\partial\phi^{(1)}}{\partial t}\right]_{z=0} = 0 \tag{C.5c}$$

Furthermore, it is assumed that the mean values of $\bar{u}^{(1)}$ and $\bar{\zeta}^{(1)}$ are zero.

The equations for the second approximation $\phi^{(2)}$ are,

$$\nabla^2\phi^{(2)} = 0 \tag{C.6a}$$

$$\left[\frac{\partial\phi^{(2)}}{\partial z}\right]_{z=-h}=0 \tag{C.6b}$$

$$\left[\frac{\partial^2\phi^{(2)}}{\partial t^2} + g\frac{\partial\phi^{(2)}}{\partial z}\right]_{z=0} = -\left[\frac{\partial}{\partial t}(\bar{u}^{(1)2}) + \zeta_a^{(1)}\frac{\partial}{\partial z}\left(\frac{\partial^2\phi^{(1)}}{\partial t^2} + g\frac{\partial\phi^{(1)}}{\partial z}\right)\right]_{z=0} \tag{C.6c}$$

then $\bar{u}^{(2)}$, $p^{(2)}$ and $\zeta_a^{(2)}$ may be found from the relations,

$$\bar{u}^{(2)} = \nabla\phi^{(2)} \tag{C.7a}$$

$$\frac{p^{(2)}}{\rho} = -\left[\frac{\partial\phi^{(2)}}{\partial t} + \frac{1}{2}\bar{u}^{(1)2}\right] \tag{C.7b}$$

$$g\zeta_a^{(2)} = -\left[\frac{\partial\phi^2}{\partial t} + \frac{1}{2}\bar{u}^{(1)2} + \zeta_a^{(1)}\frac{\partial^2\phi^{(1)}}{\partial z\,\partial t}\right]_{z=0} \tag{C.7c}$$

3.2 Solution of First-Order and Second-Order Potentials

Solution of equations 3.4 yields the classical first-order solution for the velocity potential of a wave of uniform amplitude, a, frequency, ω, and wave number, k, as,

$$\phi^{(1)} = \frac{a\omega \cosh(k\ (z-h))}{k \sinh(kh)} \sin\ (kx-\omega t) \qquad (C.8)$$

Other relationships are;

$$\zeta_a^{(1)} = a \cos\ (kx-\omega t)$$

and, $\omega^2 = gk \tanh\ (kh)$

The phase velocity, C, and group velocity, C_g, are expressed as

$$C = \frac{\omega}{k} = (gh)^{1/2}\left(\frac{\tanh)kh)}{kh}\right)^{1/2}$$

and

$$C_g = \frac{1}{2}\, C\ (1 + \frac{2kh}{\sinh(2kh)})$$

A solution for the second-order velocity potential is found using a perturbation technique. First it is assumed that the group consists of a narrow band of n discrete wave frequencies such that the free surface is given to first order as,

$$\zeta_a^{(1)}(t) = \sum_n a_n \cos\ (k_n x-\omega_n t + \epsilon_n) \qquad (C.9)$$

The frequency and wave number for each are related by,

$$\omega_n^2 = gk_n \tanh(k_n h) \qquad (C.10)$$

The first-order potential corresponding to equation 3.6 may be rewritten as

$$\phi^{(1)} = \sum_{n} \frac{a_n \omega_n \cosh(k_n(z+h))}{k_n \sinh k_n h} \sin(k_n x - \omega_n t + \varepsilon_n) \qquad (C.11)$$

The corresponding relationships for the second-order approximation are Equations (C.6). Since the right hand side of these equations is expressed totally in terms of first- order terms, they may be given as sums of terms of wave numbers $(k_n + k_m)$ and $(k_n - k_m)$ respectively. Retaining differences only,

$$\bar{u}^{(1)2} = \sum_{n=1}^{N} \sum_{m=1}^{N} \frac{a_n a_m \omega_n \omega_m \cosh((k_n + k_m)h)}{2 \sinh(k_n h)\sinh(k_m h)} \cos\{\Delta k x_{nm} - \Delta\omega t_{nm} + \Delta\varepsilon_m\} \qquad (C.12)$$

where $k_n - k_m = \Delta k_{nm}$

$\omega_n - \omega_n = \Delta\omega_{nm}$

$\varepsilon_n - \varepsilon_m = \Delta\varepsilon_{nm}$

Assuming small differences in frequencies

$$\frac{\partial u^{(1)2}}{\partial t} = \sum_{n=1}^{N} \sum_{m=1}^{N} \frac{a_m a_n \Delta\omega_{nm} \cosh(2kh)}{2 \sinh^2(kh)} \sin(\Delta k_{nm} x - \Delta\omega_{nm} t + \Delta\varepsilon_{nm}) \qquad (C.13)$$

(Using the relationship of Equations C.5c and C.6c)

$$\zeta^{(1)} \frac{\partial}{\partial t}\left(\frac{\partial^2\phi^{(1)}}{\partial t^2} + g \frac{\partial\phi^{(1)}}{\partial z}\right)_{z=0} = \sum_{n=1}^{N} \sum_{m=1}^{N} \frac{a_n a_m \omega_n^3}{2 \sinh^2(k_n h)} \sin(\Delta k_{nm} - \Delta\omega_{nm} t + \Delta\varepsilon_{nm}) \qquad (C.14)$$

Retaining diferences only, Equation (C.6c) will take the form,

$$\left(\frac{\partial^2\phi^{(2)}}{\partial t^2} + g \frac{\partial\phi^{(2)}}{\partial z}\right)_{z=0} = \sum_{n=1}^{N} \sum_{m=1}^{N} \kappa\, a_m a_n \sin(\Delta k_{nm} x - \Delta\omega_{nm} t + \Delta\varepsilon_{nm}) \qquad (C.15)$$

where

$$\kappa = \frac{\omega_n \cosh(2kh + \omega_n^3)}{2 \sinh^2(kh)}$$

Bowers (1975) gives solution to this Equation (retaining differences only) as,

$$\phi^{(2)} = \sum_{m=1}^{N-1} \sum_{n=m+1}^{N} d_{mn} \cosh(\Delta k_{nm}(z+h)) \sin(\Delta\omega_{nm} t + \Delta k_{nm} x + \Delta\varepsilon_{nm}) \qquad \text{(C.16a)}$$

where

$$d_{mn} = \frac{1}{2} a_n a_m g^2 \frac{e_{nm} + 2k_n k_m \Delta\omega_{nm}(1+\tanh k_m h)\tanh(k_n h))/\omega_m \omega_n}{(\Delta\omega_{nm})^2 \cosh(\Delta k_{nm} h - g\Delta k_{nm}) \sinh(\Delta k_{nm} h)} \qquad \text{(C.16b)}$$

and

a_n is the amplitude of the wave component of frequency ω_n,

Also

$$e_{nm} = \frac{k_n^2}{\omega_n \cosh^2(k_n h)} - \frac{k_m^2}{\omega_n \cosh^2(k_m h)} \qquad \text{(C.16c)}$$

APPENDIX D

COMPARISON BETWEEN METHODS TO DETERMINE WAVE DRIFT FORCES AND VALIDATION OF PRESENT PROGRAMS FOR SAME CALCULATIONS

There are a number of procedures for predicting the second-order behaviour of a structure in waves. These procedures can be separated into two main techniques known as the "far field" and "near field" approaches. The former is based on considerations of momentum of the incident, diffracted and radiated waves far from the structure, while the near field approach makes a direct calculation of the forces on the structure itself. The far field approach requires relatively less computational effort since only the mean components of horizontal force and overturning moments are being considered. Although the near field method is more demanding in computational effort, it can be used to calculate vertical forces and moments and can also be used to calculate the low frequency forces.

In this Appendix the far field method presented by Faltinsen and Michelsen (1974) is described as well as the near field approach of Pinkster (1977) and results generated by both methods are compared using data from published literature. Furthermore, data generated from the program to be used in the present analysis is also compared. This existing program is based on the method of Faltinsen and Michelsen (1974).

D.1 Wave Drift Forces and Moments - Far Field Approach

Newman (1967) derived an exact expression for the mean horizontal and mean transverse components $\bar{F}_x$, $\bar{F}_y$ and the mean overturning moment $\bar{M}_z$ based on changes of momentum in each degree of freedom considered.

The equations are given as,

$$\bar{F}_x = -\overline{\iint_{S_\infty} [P \cos\theta + \rho V_R (V_R \cos\theta - V_\theta \sin\theta)] R \, d\theta \, dz} \qquad (D.1a)$$

$$\bar{F}_y = -\overline{\iint_{S_\infty} [P \sin\theta + \rho V_R (V_R \sin\theta + V_\theta \cos\theta)] R \, d\theta \, dz} \qquad (D.1b)$$

$$\bar{M}_z = -\overline{\iint_{S_\infty} V_R \, V_\theta \, R^2 d\theta \, dz} \qquad (D.1c)$$

Integration is over a large cylindrical control surface S_∞ of radius R that is extending from the free surface down to z=-h. The fluid velocity is defined as V with radial and tangential components V_R, V_θ, respectively, and P is the dynamic pressure.

Faltinsen and Michelsen (1974) showed that these formulae are valid for water of finite depth. Assuming the body motions to be small the boundary conditions for the motion of the body and wave motions at the free surface were linearized. Since the second-order potential makes no contribution to the mean drift force, (Ref: Standing et al (1981)) the problem can be formulated in terms of first order potentials. The total velocity potential, ϕ_T, is written as,

$$\phi_T = \phi_o e^{-i\omega t} + \phi_7 e^{-i\omega t} + \sum_{j=1}^{6} \phi_j e^{-i\omega t} \qquad (D.2)$$

where ϕ_o is the velocity potential of the incident wave defined as,

$$\phi_o e^{-i\omega t} = \frac{g\zeta_a}{\omega} \frac{\cosh k(z+h)}{\cosh kh} e^{i(kx \cos\beta + ky \sin\beta - \omega t)} \qquad (D.3)$$

$\phi_7 e^{i\omega t}$ is the diffraction potential for the restrained body and ϕ_j, $j = 1,6$ is the contribution to the velocity potential from the jth mode

of motion. The solution of ϕ is found using the Green's Function and singularity distribution method by first expressing ϕ_j (j=1...7) as,

$$\phi_j = \iint_S Q_j(\varepsilon,\eta,\zeta)\, G\,(x,y,z,;\ \xi,\ \eta,\ \zeta)ds \tag{D.4}$$

where Q_j is the unknown source density function and $G(x,y,z;\ \xi,\ \eta,\ \zeta)$ is the Green's function for the problem for ϕ_j.

The kernel function $G(x,y,z;\ \xi,\eta,\zeta)$ can be written according to Wehausen and Laitone (1965) in integeral form as,

$$G(x,y,z;\ \xi,\eta,\zeta) = \frac{1}{R} + \frac{1}{R'}$$

$$+ 2\ PV\int_0^\infty (\mu+\nu)e^{-\mu h}\ \frac{\cosh\,[\mu\ (\zeta+h)].\cosh\,[\mu\ (z+h)]}{\mu\ \sinh\ (\mu h)\ -\ \nu\ \cosh\ (\mu h)}\ .J_o(\mu r')d\mu$$

$$+ i\frac{2\pi(k^2-\nu^2)}{k^2h-\nu^2h+\nu}.\ \cosh\,[k(\zeta+h)].\cosh\,[k(z+h)].J_o(\mu r') \tag{D.5}$$

and the "series form":

$$G\ (x,y,z;\ \xi,\eta,\zeta)$$

$$= \frac{2\pi\ (\nu^2-k^2)}{k^2h\ -\ \nu^2h\ +\ \nu}\ .\cosh\,[k\ (\zeta+h)].\cosh\,[k\ (z+h)].[Y_o(kr')\ -J_o(kr')]$$

$$+ 4\sum_{j=1}^{\infty}\frac{(\mu_j^2\ +\ \nu^2)}{\mu_j^2h\ +\ \nu^2h\ -\ \nu}.\cos[\mu_j(\eta+h)].\cosh[\mu_j(z+h)].K_o(\mu_j r') \tag{D.6}$$

where

$$\nu = \frac{\omega^2}{g} = k\ \tanh\ kh \tag{D.7a}$$

$$R = [(x-\xi)^2 + (y-\eta)^2 + (z-\zeta)^2]^{1/2} \tag{D.7b}$$

$$R' = [(x-\xi)^2 + (y-\eta)^2\ (z+2h+\zeta)^2]^{1/2} \tag{D.7c}$$

$$r' = [(x-\xi)^2 + (y-\eta)^2]^{1/2} \tag{D.7d}$$

J_o and Y_o denote, respectively, the Bessel function of the first kind and the second kind of order zero, and K_o denotes the modified Bessel

function of the second kind of order zero. PV in Equation (D.4) indicates the principal value of the integral; μ_j in Equation (D.7) are the real positive roots of the equation:

$$\mu_j \tan(\mu_j h) + \nu = 0 \tag{D.8}$$

Since Equation (D.3) is also valid for $\bar{x}$ as a point on the body boundary, taking the normal directional derivative of ϕ_j in Equation (D.3) yields the following integral equation for Q_j.

The solution to this boundary value problem takes the form,

$$2\pi Q_j(x,y,z) + \iint_S Q_j(\xi,\eta,\zeta)\frac{\partial G}{\partial n}(x,y,z;\xi,\eta,\zeta)ds = -\frac{\partial \phi_o}{\partial n}; \text{ for } j = 7$$

$$= \frac{\partial \phi_j}{\partial n}, \text{ for } j = 1,\ldots,6 \tag{D.9}$$

providing the following conditions are satisfied.

In the fluid domain,

$$\nabla^2 \phi_j = 0; \text{ for } j = 1, \ldots,7 \tag{D.10a}$$

The kinemetic conditions at the ocean floor boundary,

$$\frac{\partial \phi_j}{\partial z} = 0 \text{ for } z = -h \quad j = 1,\ldots,7 \tag{D.10b}$$

The kinematic and dynamic conditions at the mean free surface,

$$\frac{\partial \phi_j}{\partial z} - \frac{\omega^2}{g}\phi_j = 0 \text{ at } z = 0, \text{ for } j = 1,\ldots,7 \tag{D.10c}$$

Also on the mean position of the wetted surface of the immersed body,

$$\frac{\partial \phi_j}{\partial n} = n_j, \text{ for } j = 1,\ldots,6 \tag{D.10d}$$

and,

$$\frac{\partial \phi_7}{\partial n} = - \frac{\partial \phi_o}{\partial n} \text{ for } j = 7 \qquad \text{(D.10e)}$$

Equation D.9 is now solved by approximating the body surface into a number of quadrilateral panels assuming the same density, Q_j to be constant over any given panel. Therefore, the Equation, represented as a set of intergals, may be approximated by summations.

Using equations (D.1), (D.2) and (D.3) the asymptotic expansion of the Green's function (D.4), the far field expression for the first order potential was found,

$$\phi - \frac{g\zeta_a \cosh k(z+h)}{\omega \cosh kh} . e^{i(kx \cos \beta + ky \sin \beta - \omega t)} + T(\theta)\, e^{i\tau(\theta)} \cosh(k(z+h)) \sqrt{\frac{1}{r}}\, e^{-(kr-\omega t)} \qquad \text{(D.11)}$$

where $T(\theta)$ and $\tau(\theta)$ are real functions of θ, and $T(\theta).e^{i\tau(\theta)}$ is given by:

$$T(\theta).e^{i\tau(\theta)} = \frac{2\pi(\nu^2 - k^2)}{k^2 h - \nu^2 h + \nu} \sqrt{\frac{2}{\pi k}}\, e^{-i3\pi/4} \cdot \iint_S \{Q(\xi,\eta,\zeta) \cosh[k(\zeta + h)]\, e^{-i(k\xi \cos\theta + k\eta \sin\theta)}\} ds \qquad \text{(D.12)}$$

where $Q(\bar{\xi})$ is the "total source" density:

$$Q(\xi,\eta,\zeta) = Q_7 + \sum_{j=1}^{6} Q_j(i\omega)\, \bar{\eta}_j ,$$

where $\eta_j = \bar{\eta}_j e^{-i\omega t}$

If only contributions up to second-order terms of ϕ_T are retained, for the computation of forces, then the drift forces and moment can be written in terms of the first-order far field potential as,

$$(\bar{F}_x) = -\frac{\rho}{2}\frac{\omega\zeta_a}{\sinh kh}\frac{2\pi}{k}\left[\frac{1}{4}\sinh 2kh + \frac{kh}{2}\right] 2T(\beta)\cos[\tau(\beta) + \pi/4]\cos\beta$$

$$- \frac{\rho k}{2}\left[\frac{1}{4}\sinh 2kh + \frac{kh}{2}\right]\int_0^{2\pi} T^2(\theta).\cos\theta\, d\theta \qquad (D.13)$$

$$(\bar{F}_y) = -\frac{\rho}{2}\frac{\omega\,\zeta_a}{\sinh kh}\frac{2\pi}{k}\left[\frac{1}{4}\sinh 2kh + \frac{kh}{2}\right] 2T(\beta)\cos\left[\tau(\beta) + \frac{\pi}{4}\right]$$

$$\sin\beta - \frac{\rho k}{2}\left[\frac{1}{4}\sinh 2kh + \frac{kh}{2}\right]\int_0^{2\pi} T^2(\theta)\sin\theta\, d\theta \qquad (D.14)$$

$$(\bar{M}_z) = \left(\frac{\sinh 2kh}{4k} + \frac{h}{2}\right)\left[-\frac{\rho\omega\zeta_a}{\sinh kh}\sqrt{2\pi/k}.T'(\beta).\sin[\tau(\beta) + \pi/4]\right.$$

$$\left. - \frac{\rho\omega\zeta_a}{\sinh kh}\cdot\frac{2\pi}{k}\tau'(\beta)\cos[\tau(\beta) + \pi/4]\right] \qquad (D.15)$$

$$- \frac{\rho k}{2}\int_0^{2\pi} T^2(\theta)\,\tau'(\theta)\, d\theta$$

where, $T'(\beta)$ and $(\tau'(\beta))$ is interpreted as $\frac{dT}{d\theta}$ and $(\frac{d\tau}{d\theta})$ respectively and evaluated at $\theta=\beta$.

The working formulae (D.13) - (D.15) are used in a computer program developed to evaluate the steady horizontal drift forces and vertical moment. The detail of the derivation is rather complicated and lengthy. It can be found in Faltinsen and Michelsen (1974), and hence is omitted here.

D.2 Wave Drift Forces and Moments - Near Field Approach

The following analysis follows that of Pinkster et al (1977). The response motions of the structure are related to a system of three co-ordinate axes as illustrated in Figure D.1. The first system, attached to the body, is defined by $G - x_1 - x_2 - x_3$ with its origin fixed to the center of gravity of the body. A second system of

co-ordinate axes, fixed with its origin at the mean free surface, is defined as $0 - X_1 - X_2 - X_3$. The third system of co-ordinate axes is defined as $G - X_1' - X_2' - X_3'$, has its origin at the center of gravity of the body and is always parallel to the axes of the fixed system $0 - X_1 - X_2 - X_3$.

As the body moves due to first-order and second-order wave forces, a point on the surface is positioned relative to the fixed system of $0 - X_1 - X_2 - X_3$ as,

$$\bar{X} = \bar{X}^{(0)} + \varepsilon\bar{X}^{(1)} + \varepsilon^2\bar{X}^{(2)} \tag{D.16}$$

where

$$\bar{X}^{(0)} = \bar{X}g^{(0)} + \bar{x} \tag{D.17}$$

i.e. the mean position vector and $\bar{X}^{(1)}$ is the first-order oscillatory motion defined as

$$\bar{X}^{(1)} = \bar{X}g^{(1)} + \bar{\alpha}^{(1)} \times \bar{x} \tag{D.18}$$

where $\alpha^{(1)}$ represents the first-order rotations $x_4^{(1)}$, $x_5^{(1)}$ and $x_6^{(1)}$ which represent roll, pitch and yaw respectively. The term $\bar{x}$ is the vector to a point on the surface. The orientation of a surface element on the body is denoted by the outward normal vector $\bar{n}$. This vector is related to the coordinate system $0 - X_1 - X_2 - X_3$ and $0 - X_1' - X_2' - X_3'$ by,

$$\bar{N} = \bar{N}^{(0)} + \varepsilon\bar{N}^{(1)} + \varepsilon^2\bar{N}^{(2)} \tag{D.19a}$$

where,

$$\bar{N}^{(0)} = \bar{n} \tag{D.19b}$$

$$\bar{N}^{(1)} = \bar{\alpha}^{(1)} \times \bar{n} \tag{D.19c}$$

$$\bar{N}^{(2)} = \bar{\alpha}^{(2)} \times \bar{n} \tag{D.19d}$$

The potentials in this expression are defined relative to the $0 - X_1 - X_2 - X_3$ axes with,

$$\phi_T = \phi_T(\bar{X}, t) \tag{D.24}$$

where t indicates time and $\bar{X}$ the position vector of the point under consideration. This fluid is bounded by the free surface, the sea floor and the body surface and thus must satisfy conditions at each of these boundaries. The free surface and sea floor boundary conditions are Equations (C.4) for the first-order potential, $\phi^{(1)}$, and Equations (C.6) for the second-order potential, $\phi^{(2)}$. The boundary condition on the body surface is that the relative velocity between the fluid and the body in the direction of the normal to the body is zero, i.e. no fluid passes through the hull. This boundary condition has to be satisfied at the instantaneous position of the body surface element and is written as,

$$\nabla \phi_T \bar{N} = \bar{V} \cdot \bar{N} \tag{D.25}$$

where $\bar{V}$ is the velocity vector of the surface relative to the fixed $0 - X_1 - X_2 - X_3$ and $\bar{N}$ is defined by Equation (D.19a). The $\phi^{(1)}$ term in Equation (P.24) is represented as three components expressed as,

$$\phi^{(1)} = \phi_w^{(1)} + \phi_d^{(1)} + \phi_b^{(1)} \tag{D.26}$$

where $\phi_w^{(1)}$ represents the potential of the undisturbed incoming waves and $\phi_d^{(1)}$ represents the diffraction potential. It is from these two components that the first-order wave exciting forces are found. The body motion potential $\phi_b^{(1)}$ is used to determine the hydrodynamic reaction forces known as added mass and damping. The second-order

velocity potential is expressed as

$$\phi^{(2)} = \phi_w^{(2)} + \phi_d^{(2)} + \phi_b^{(2)} \tag{D.27}$$

where $\phi_w^{(2)}$ can be considered as the undisturbed second-order wave which must satisfy the free surface boundary condition defined by Equation (C.6c) whereas the second-order diffraction potential, $\phi_d^{(2)}$, and the second order body potential $\phi_b^{(2)}$satisfy the linearized free surface equation given by Equation (C.4c). The solution of the second-order diffraction potential, $\phi_d^{(2)}$, and the undisturbed second-order potential $\phi_w^{(2)}$ provides the low frequency second-order wave exciting forces. The second-order body potential $\phi_b^{(2)}$ satisfies the same boundary conditions as the first-order body potential and is expressed in terms of added mass and damping.

D.2.1 Second-order Wave Force

The second-order forces which induce slow drift motions of the structure are the only components considered here. The wave drift forces are determined along the G - X_1' - X_2' - X_3' axis of the co-ordinate system.

Equation (D.20) is expanded by substituting equations (D.22) and (D.19) into (D.21). Therefore,

$$\bar{F}_T = -\iint_{S_o} (p^{(0)} + \varepsilon p^{(1)} + \varepsilon^2 p^{(2)}) (\bar{n} + \varepsilon \bar{N}^{(1)} + \varepsilon^2 \bar{N}^{(2)}) \, dS$$

$$- \iint_{S} (p^{(0)} + \varepsilon p^{(1)} + \varepsilon^2 p^{(2)}) (\bar{n} + \varepsilon \bar{N} + \varepsilon^2 \bar{N}^{(2)}) \, dS \tag{D.28}$$

The second-order force is determined by integration of all products of pressures, p_T, and normal vectors, $\bar{N}$, which give

second-order force contributions over the constant part, S_o, of the wetted surface and by integration of first-order pressures over the oscillating surface s,

$$\bar{F}_T^{(2)} = \iint_{S_o} (p^{(1)} \bar{N}^{(1)} + p^{(2)} \bar{n} + p^{(0)} \bar{N}^{(2)}) dS + \iint_{S} p^{(1)} \bar{n} \, dS \qquad (D.29)$$

Using Equation (D.19c)

$$- \iint_{S_o} (p^{(1)} \bar{N}^{(1)}) \, dS = \bar{\alpha}^{(1)} \times - \iint_{S_o} p^{(1)} \bar{n} \, dS \qquad (D.30)$$

The gravity force on the structure must also be accounted for in this expression. The force along the $0 - X_1' - X_2' - X_3'$ axis caused by gravity can be written as,

$$\bar{F}^{(2)}_{gravity} = \bar{\alpha}^{(1)} \times (0, 0, \rho g \Psi) \qquad (D.31)$$

where is the structure displacement. Therefore Equation D.30 can be written as,

$$\iint_{S_o} (p^{(1)} \bar{N}^{(1)} dS = \bar{\alpha}^{(1)} \times \{ - \iint_{S_o} p^{(1)} \bar{n} \, dS + \bar{\alpha}^{(1)} x (0, 0, \rho g \Psi) \} \qquad (D.32)$$

This gravity effect is the result of a rotation of the structure in response to first-order loading and is expressed as,

$$\bar{\alpha}^{(1)} \times \bar{F}_T^{(1)} = \bar{\alpha}^{(1)} \times (M \ddot{\bar{X}}_g^{(1)}) \qquad (D.33)$$

where, M = mass of structure

$\ddot{\bar{X}}_g$ = acceleration due to gravity.

The second part of Equation (D.29) is essentially the integration of the pressure, $p^{(2)}$, described by Equation (D.22c).

Finally, the second integral in Equation (D.29) is on the wetted oscillating part of the structure between the static waterline on the body surface, WL, and the wave profile along the body, $\zeta_a^{(1)}$,

This integral becomes

$$-\int_{WL} \frac{1}{2} \rho g \, \zeta_r^{(1)2} \cdot \bar{n} \cdot d\ell \qquad (D.34)$$

where $\zeta_r^{(1)}$ is the relative wave amplitude and $d\ell$ is the line element of the waterline.

The above analysis has indicated that there are several components contributing to the second order forces on a structure. They are summarized, following Pinkster (1980) as follows:

I. Relative wave height contribution,

$$-\frac{1}{2} \rho g \int_{WL} \zeta_r^{(1)2} \cdot \bar{n} \cdot d\ell \qquad (D.35a)$$

II. Pressure drop due to velocity squared term,

$$\frac{1}{2} \rho \iint_{S_o} \left| \nabla \Phi^{(1)} \right|^2 \cdot \bar{n} \cdot ds \qquad (D.35b)$$

III. Pressure drop due to product of gradient of first-order pressure and first-order motion,

$$-\rho \iint_{So} \{ \frac{\partial \nabla \Phi^{(1)}}{\partial t} \cdot \bar{X}^{(1)} \} \cdot \bar{n} \cdot ds \qquad (D.35c)$$

IV. The effects of first-order rotations and inertia forces

$$\bar{\alpha}^{(1)} \times (M \ddot{\bar{X}}_g^{(1)}) \qquad (D.35d)$$

V. The effects of second-order waves.

$$-\rho \iint_{So} \frac{\partial \Phi^{(2)}}{\partial t} \bar{n} \, ds \qquad (D.35e)$$

VI. A complex term representing second-order motions of the structure's center of buoyancy and water plane area.

D.3 Sample Calculations

Figure D.3 compares the results given by the present program, which is based on Equation (D.13), to the near field results of Pinkster (1980) and Standing et al (1981) for the barge shown in Figure D.2. Also included in the comparison are the results of the far field approach presented by Standing et al (1981). The near field results given by Standing et al (1981) are based on the method of Pinkster (1980) and the far field results given by the same reference are based on the method of Faltinsen and Michelsen (1975). As indicated in the Figure, there is very good agreement between the results generated by the program used in the present analysis and those presented by Standing et al (1981). There is however a considerable discrepancy between the results presented by Pinkster (1981) and those presented by Standing et al (1981) which are presumably based on the same method. Further investigations were conducted by Standing et al (1981) to determine the cause of this disagreement. Figure D.4 illustrates the individual contributions of Equations (D.35) to the total drift force. As can be seen in the Figure, there is a considerable difference in the contribution made by equation (D.35a). Standing attributes this disagreement to the manner in which the waterline was modelled for the two cases. The Standing method uses twice as many points as the number of sources in the row of panels nearest the waterline than does Pinkster (1981), presumably giving a more accurate result.

The contribution of the second-order wave referred to as "setdown" is also investigated for the barge shown in Figure D.2. The results obtained from Equation (3.15) are compared to those presented by Pinkster (1980) and Standing et al (1981) for the same wave conditions in Table D1. As indicated in this table, good agreement was found for the range tested.

i = Pinkster (1980)

ii = Standing et al (1981)

iii = Present Program

$$\frac{\text{Force}}{a(\omega_n)a(\omega_m)}\left[\frac{\text{Tonnes}}{2_m}\right]$$

ω_m (rad/sec)	ω_n = 0.50	0.60	0.70	0.80	0.90	1.00
0.50	i 0 ii 0 iii 0					
0.60	6 5 6	0 0 0				
0.70	4 7 8	6 8 6	0 0 0			
0.80	11 8 10	5 6 6	6 4 6	0 0 0		
0.90	14 15 15	8 3 8	6 6 5	8 3 6	0 0 0	
1.00	17 16 17	15 13 17	5 4 7	6 2 4	6 7 8	0 0 0

Table 3 Comparison Among Present Computed Analysis and Published Data For Second-order Wave Effects on a Rectangular Barge

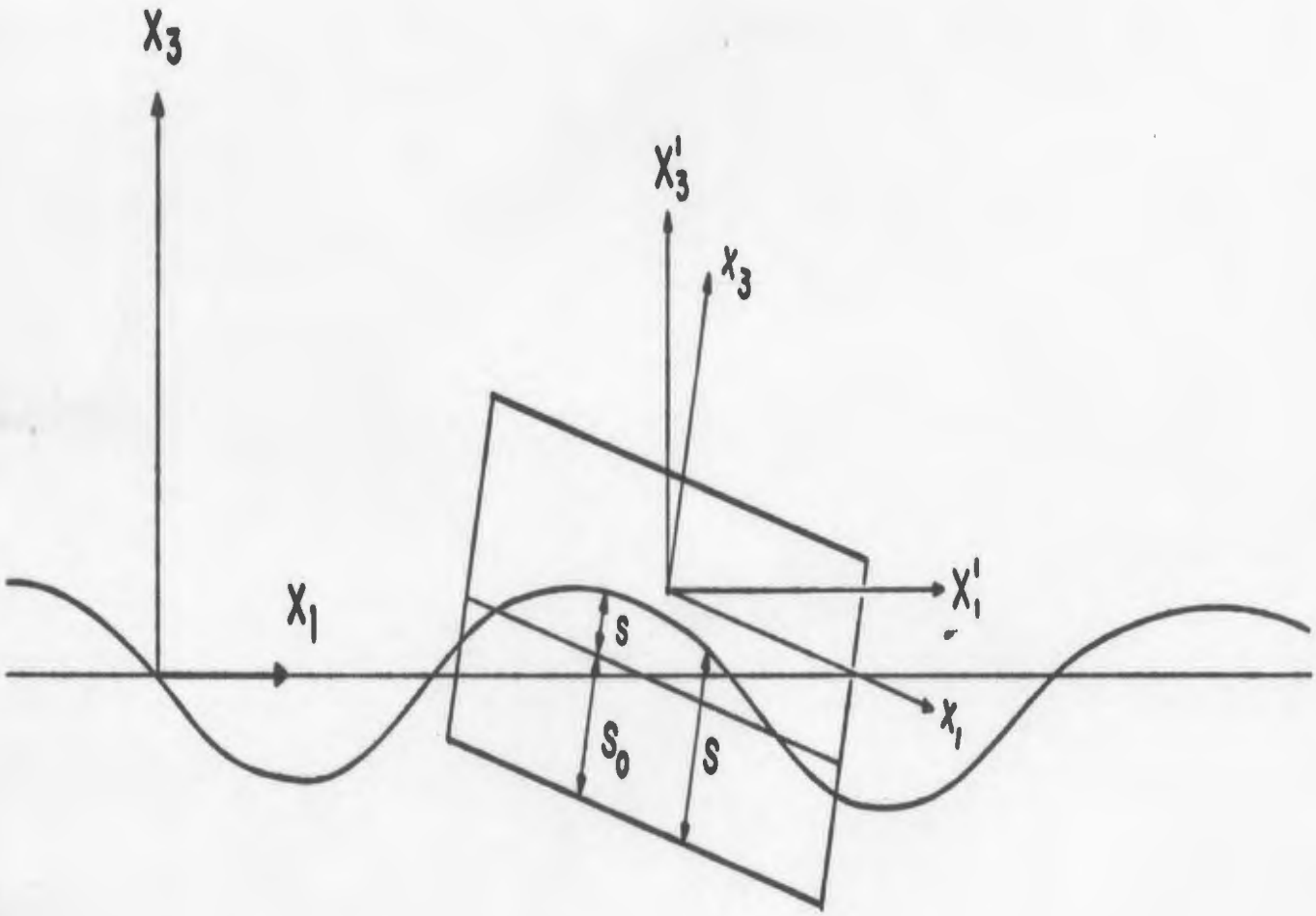

FIG. D.1 COORDINATE SYSTEM FOR NEAR FIELD APPROACH.

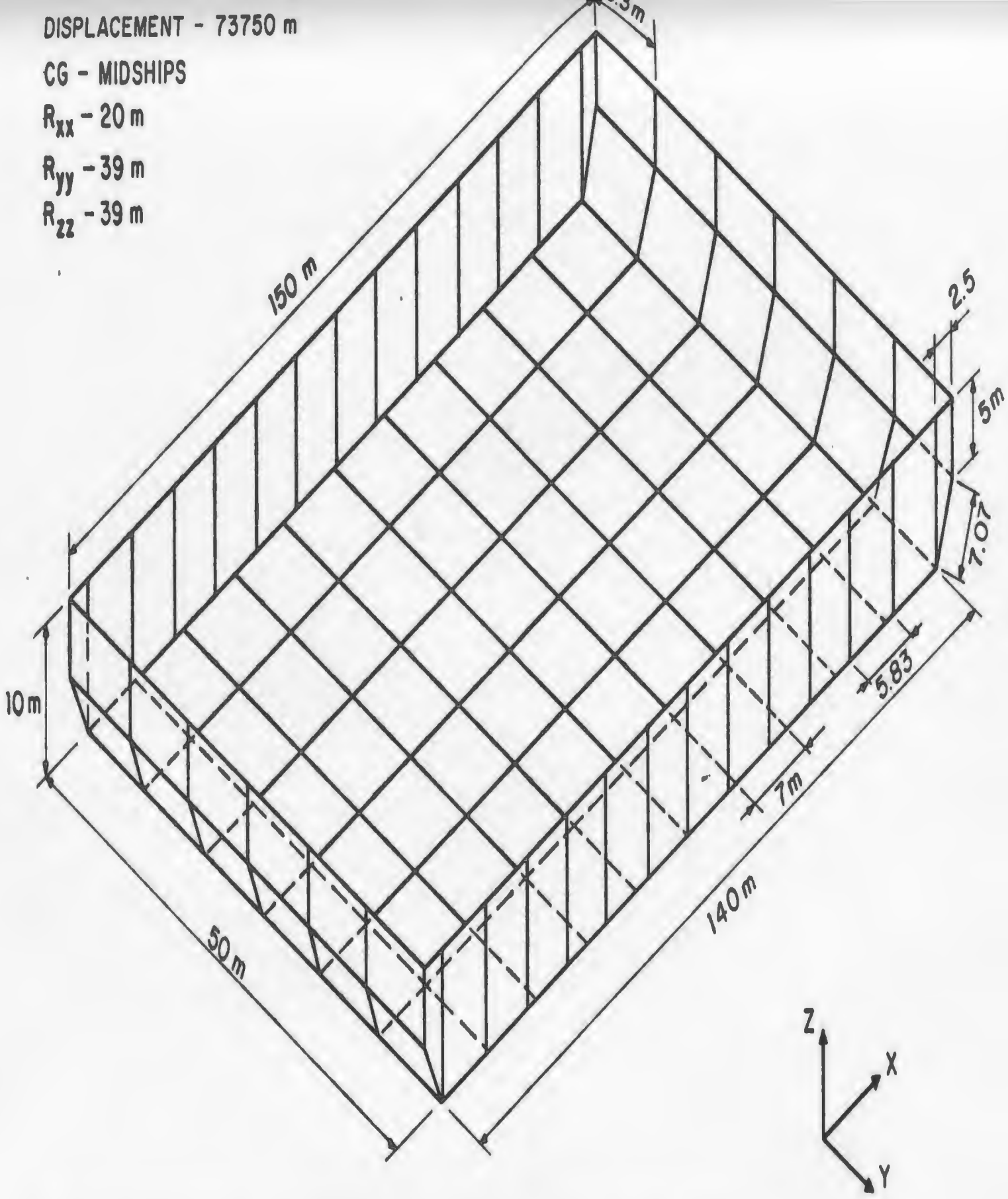

FIG. D.2 RECTANGULAR BARGE USED TO COMPARE NEAR AND FAR FIELD APPROACHES

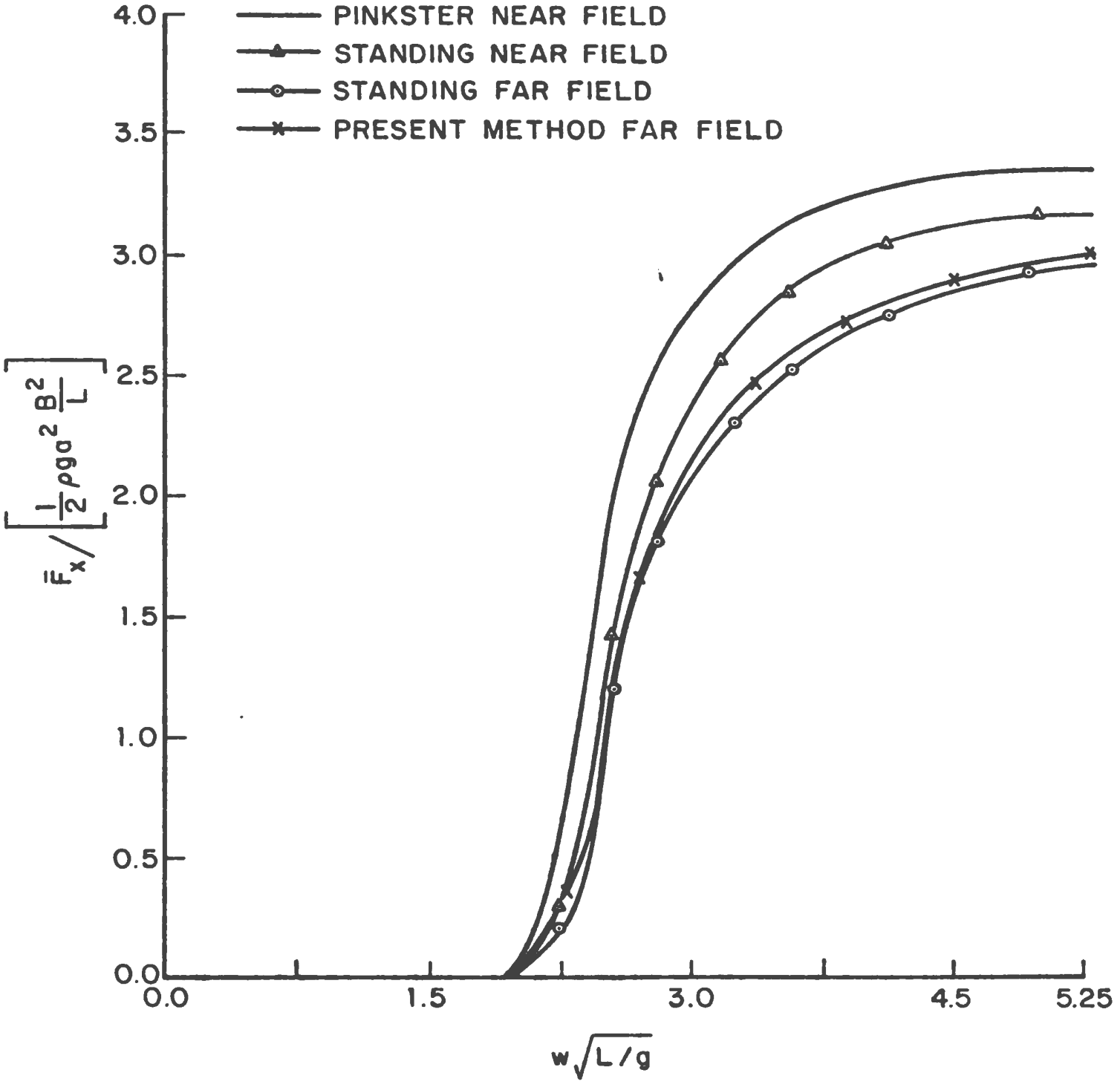

FIG. D.3 MEAN DRIFT FORCE COEFFICIENTS IN HEAD SEAS FOR RECTANGULAR BARGE SHOWN IN FIG. D.2.

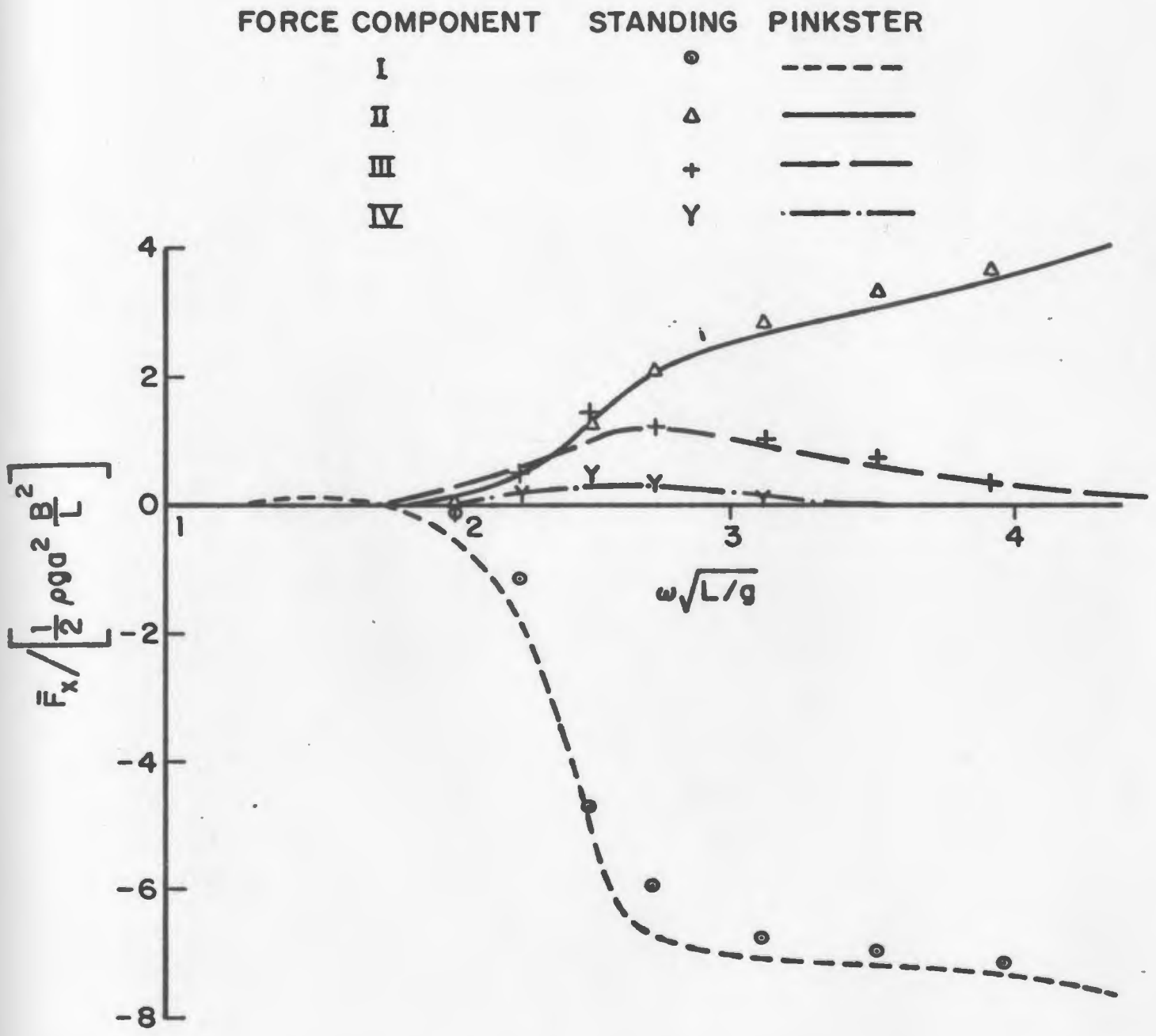

FIG. D.4 COMPARISON AMONG COMPONENTS CONTRIBUTING TO THE NEAR FIELD APPROACH IN FIG. D. 3

APPENDIX E

SECOND ORDER CONTROL SIGNALS

In first-order wave generation undesirable long waves are produced which may and the result in erroneous response spectra of the model under investigation due to incorrect representation of second-order waves. Considerable attention has been recently given to this second-order problem by Ottesen Hansen (1978) and Sand (1982). Sand (1982) has presented the second-order control signals for second-order generation. These second-order signals are unique to the type of generator system being used. A variety of wave generator types can be found in hydraulic laboratories throughout the world, most of which are of the piston or flap type or a combination of both.

Ottesen-Hansen (1978) has presented transfer functions which relate first-order waves in a wave group to natural second-order long waves. These transfer functions, G_{nm}, relate the wave elevations $\zeta_n(t)$ and $\zeta_m(t)$ generated at frequencies f_n and f_m respectively, to the second-order long wave, $\xi_{nm}(t)$ by the relationship,

$$\frac{\xi_{nm}(t)}{h} = G_{nm}h \left[\left(\frac{a_n a_m + b_n b_m}{h^2} \right) \cos(\Delta\omega_{nm} t - \Delta k_{nm} x_1) + \left(\frac{a_m b_n - a_n b_m}{h^2} \right) \sin(\Delta\omega_{nm} t - \Delta k_{nm} x_1) \right] \qquad \text{(E.1a)}$$

where,

$$G_{nm}h = \frac{G1_{nm}h + G2_{nm}h - G3_{nm}h}{G4_{nm}h} \qquad \text{(E.1b)}$$

$$G1_{nm}h = \left[\frac{4\pi^2 D_n D_m \Delta k_{nm} h \cos h(\Delta k_{nm} h)}{\cosh(k_n h + k_m h) - \cosh(\Delta k_{nm} h)} \right] \qquad \text{(E.1c)}$$

$$G2_{nm}h = \frac{\Delta k_{nm} h (D_n - D_m)(k_n h D_m + k_m h D_n) \coth(\Delta k_{nm} h)}{2 D_n D_m} \qquad \text{(E.1d)}$$

$$G3_{nm}h = 2\pi^2(D_n - D_m)^2 \Delta k_{nm}h \qquad (E.1e)$$

$$G4_{nm}h = 4\pi^2(D_n - D_m)^2 \coth(\Delta k_{nm}h) - \Delta k_{nm}h \qquad (E.1f)$$

$$D_i = (h/g)^{1/2} f_i \qquad (E.1g)$$

and, h = water depth

Curves of these $G_{nm}h$ values are shown in Figure E.2 for a range of frequency differences and water depths. It is evident from this graph that the long wave amplitude is greatly amplified in shallow water.

Sand (1982) has included these equations of G_{nm} in a second-order control signal to produce correct second-order piston positions for the correct group induced long wave. The second order piston position is defined in time as,

$$X^{(2)}t = \sum_{n-m=1}^{\infty} \sum_{m=m^*}^{\infty} X^2_{nm}(t) \qquad (E.2a)$$

where, $m^* = \frac{f^*}{f_o}$, f^* = lowest frequency.

The solution to the second-order equation is given by Sand (1982) as,

$$\frac{X^{(2)}(t)}{h} = \left[\left(\frac{a_n b_m - a_m b_n}{h^2}\right) F_1 h + \left(\frac{a_n a_m + b_n b_m}{h^2}\right) F_{23} h\right] \cos \Delta\omega_{nm} t$$

$$+ \left[\left(\frac{a_n a_m + b_n b_m}{h^2}\right) F_1 h + \left(\frac{a_m b_n - a_n b_m}{h^2}\right) F_{23} h\right] \sin \Delta\omega_{nm} t \qquad (E.2b)$$

In this expression,

$$F_1 h = F_{11} h + F_{12} h \qquad (E.2c)$$

where,

$$F_{11}h=\frac{G_{nm}h\Delta k_f h[(\Delta k_{nm}h-\Delta k_f h)\sinh(\Delta k_{nm}h+\Delta k_f h)+(\Delta k_{nm}h+\Delta k_f h)\sinh(\Delta k_{nm}h-\Delta k_f h)]}{2(\Delta k^2_{nm}h^2-\Delta k_f{}^2h^2)\sinh(\Delta k_{nm}h)\sinh(\Delta k_f h)} \tag{E.2d}$$

and

$$F_{12}h = \frac{f_m\Delta k_f h k_m h(1+G_n)[\delta k_m^- h\ \sinh(\delta k_m^+ h) + \delta k_m^+ h\ \sinh(\delta k_m^- h)]}{\Delta f 8(k_m^2h^2-\Delta k_f^2h^2)\ \sinh\ (\Delta k_f h)\ \sinh\ (k_m h)\ \tanh\ k_n h)}$$

$$+ \frac{f_n\Delta k_f h k_n h(1+G_m)[\delta k_n^- h\ \sinh(\delta k_n^+ h) + \delta k_n^+ h\ \sinh(\delta k_n^- h)]}{\Delta f 8(k_n^2h^2 - \Delta k_f^2h^2)\sinh(\Delta k_f h)\sinh(k_n h)\tanh(k_m h)} \tag{E.2e}$$

also, Δf is determined from

$$(\Delta\omega_{nm})^2 = g\ \Delta k_f\ \tanh\ (\Delta k_f h) \tag{E.2f}$$

and, $\delta K_m = km \pm \Delta k_f$

Finally the last transfer function in Equation (E.2b) is,

$$F_{23}h = F_2h(F_{3,m} - F_{3,n}) \tag{E.2g}$$

where

$$F_2h = \frac{\Delta k_j h(1+G_n)(1+G_m)}{8\ \tanh\ (k_n h)\ \tanh\ (k_m h)}\ ;\quad G_m = \frac{2k_m h}{\sinh(2k_m h)} \tag{E.2h}$$

and

$$F_{3,m} = \frac{f_m}{\Delta f}\sum_{j=1}^{\infty}\frac{2k_j h\ \sin(k_j h)[k_j h\ \sin(k_j h)\coth(\Delta k_f h) + \Delta k_f h\ \cos(k_j h)]}{(k_j^2h^2 + \Delta k_f^2h^2)[\sin(k_j h)\cos(k_j h) + k_j h]} \tag{E.2i}$$

in which $k_j h$ is determined from the expression,

$$\frac{4\pi^2hf^2}{g}{}_m = -k_j h\ \tan(k_j h),\ \text{with}\ (j - \tfrac{1}{2})\ \pi < k_j h < j\pi$$

In the previous Equation $F_{11}h$ is the contribution to the second-order piston position $X^{(2)}_{nm}(t)$ for the natural second-order wave $\xi_{nm}(t)$, $F_{12}h$ is the contribution used to eliminate the errors caused by the wave board displacement and F_{23} contributes to eliminate the free second-order waves generated by first-order local disturbances. The contribution of $F_{23}h$ is negligible compared to the other two and therefore will not be discussed further.

Curves of F_1h are presented in Figure E.1. It can be seen from the Figure that there are certain conditions where the second-order control signal makes no adjustment to the first order wave board displacement. This means that below this point the purpose of the second-order displacement is to enhance the generated group bounded waves while in the deeper water situation the signal's purpose is to supress the second-order wave effect. Barthel et al (1983) has shown these second-order control signals to be very effective in generating correct group bounded waves in shallow water conditions for a piston type generator.

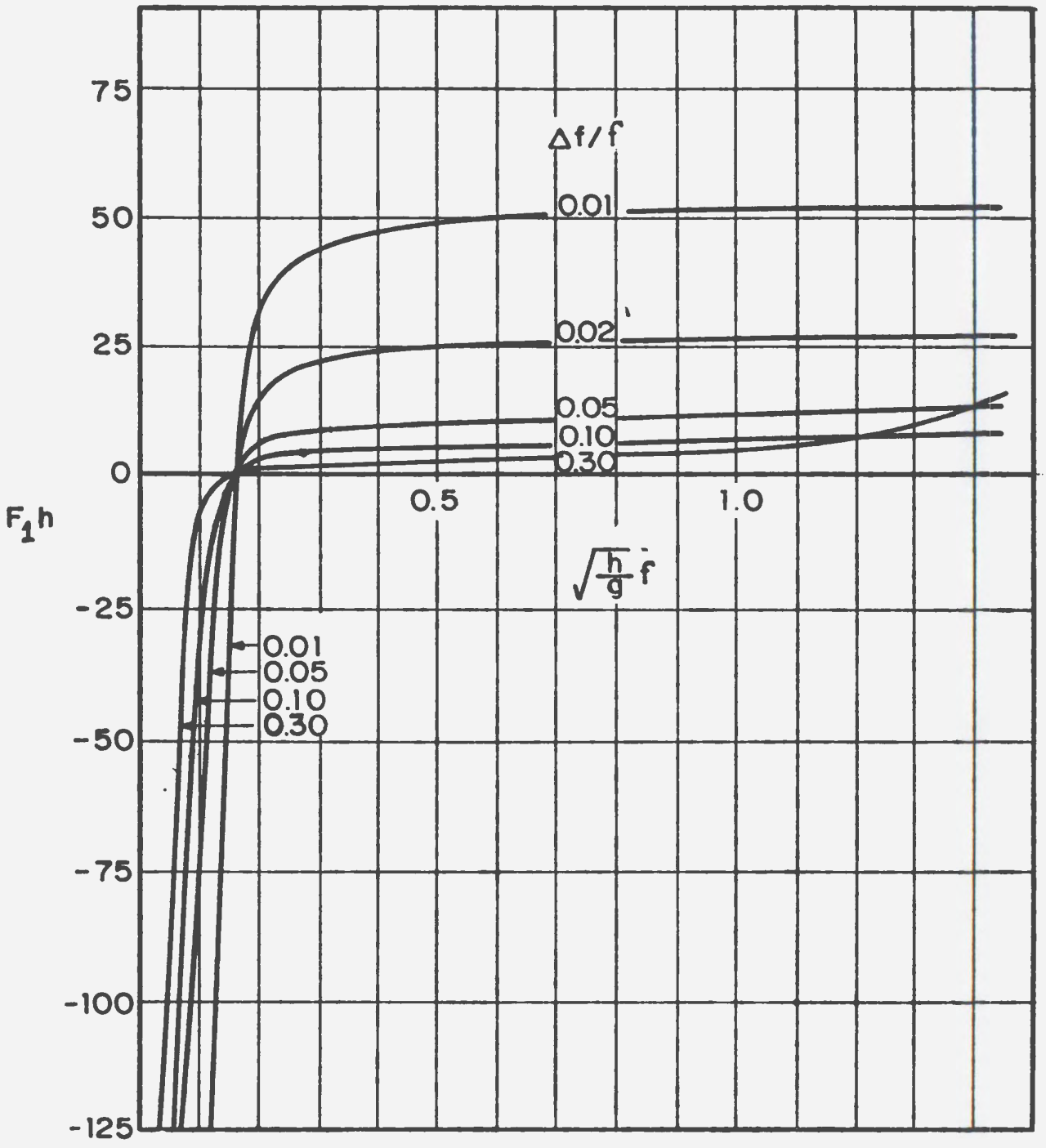

FIG. E.1 TRANSFER FUNCTION FOR SECOND-ORDER PISTON CONTROL SIGNALS FOR VIABLE GROUP GENERATION (SAND 1982)

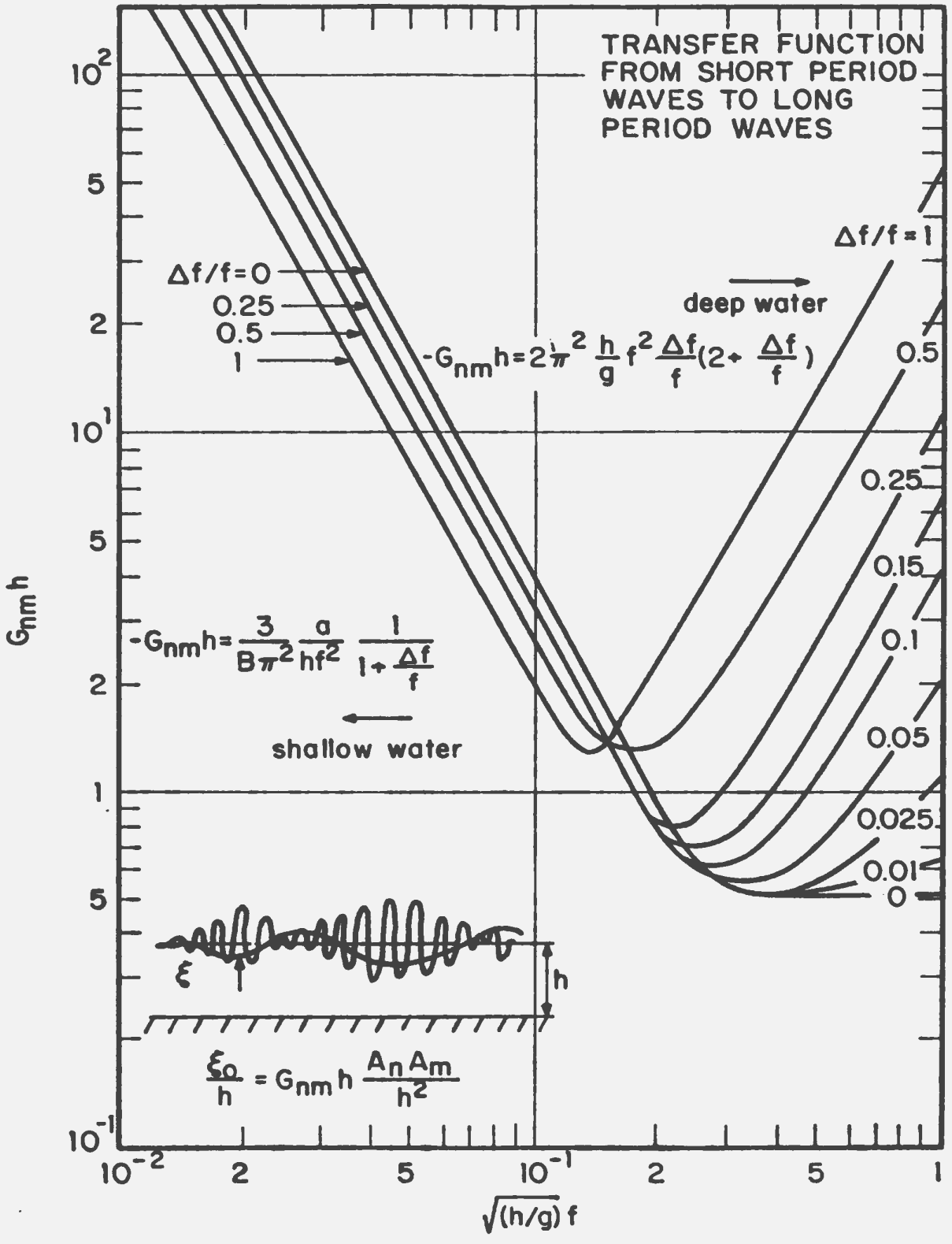

FIG. E.2 TRANSFER FUNCTION, $G_{nm}h$, FOR WAVE GROUPS SAND (1982)